STRUCTURAL AND THEORETICAL STUDIES OF COMPLEXES OF URANYL(VI) AND PALLADIUM(II) IONS HAVING SOFT AND HARD DONOR LIGANDS

By

DEBASISH DAS
CHEM01201104007

Bhabha Atomic Research Centre,
Mumbai 400085, India

A thesis submitted to the
Board of studies in Chemical Sciences
in partial fulfillment of the requirements
for the degree of

Doctor of Philosophy
of
Homi Bhabha National Institute

March, 2018

HOMI BHABHA NATIONAL INSTITUTE

Recommendations of the Viva Voce Committee

As members of the Viva Voce Committee, we certify that we have read the dissertation prepared by **Shri D. Das** entitled "**Structural and theoretical studies of complexes of uranyl (VI) and palladium (II) ions having soft and hard donor ligands**" and recommend that it may be accepted as fulfilling the thesis requirement for the award of Degree of Doctor of Philosophy.

Chairman: Prof. D. Das	D Das. 16/3/18
Ph.D. Guide : Prof. S. Kannan	16-3-18
Examiner: Prof. M.S. Balakrishna	16/3/18
Member 1: Dr. V.K. Jain	Vimal Jain 16/03/2018
Member 2: Dr. P.K. Mohapatra	16/3/2018
Co-Guide: Dr. S.K. Ghosh	Ghosh 16/3/2018

Final approval and acceptance of this thesis is contingent upon the candidate's submission of the final copies of the thesis to HBNI.

I/We hereby certify that I/We have read this thesis prepared under my direction and recommend that it may be accepted as fulfilling the thesis requirement.

Date: 16/03/18

Place: Mumbai

Guide/ Convener

STATEMENT BY AUTHOR

This dissertation has been submitted in partial fulfillment of requirements for an advanced degree at Homi Bhabha National Institute (HBNI) and is deposited in the library to be made available to borrowers under rules of the HBNI.

Brief quotations from this dissertation are allowable without special permission, provided that accurate acknowledgement of source is made. Requests for permission for extended quotation from or reproduction of this manuscript in whole or in part may be granted by the competent authority of HBNI when in his or her judgment the proposed use of the material is in the interests of scholarship. In all other instances, however, permission must be obtained from the author.

Debasish Das

Debasish Das

DECLARATION

I, hereby declare that the investigation presented in the thesis has been carried out by me. The work is original and has not been submitted earlier as a whole or in part for a degree/ diploma at this or any other Institution / University.

Debasish Das
Debasish Das

Dedicated

to

My beloved family

List of Publications

Journal

1. Steric effects on uranyl complexation: synthetic, structural, and theoretical studies of carbamoyl pyrazole compounds of the uranyl(VI) ion; **Debasish Das**, Shanmugaperumal Kannan, Dilip K. Maity, Michael G. B. Drew, Inorg. Chem. 51 (2012) 4869−4876.

2. Steric effects in pyrazole palladium(II) compounds: synthetic, structural, and theoretical studies of a highly distorted octahedral palladium(II) pyrazole compound; **Debasish Das**, Bal Govind Vats, Shanmugaperumal Kannan, Dilip K. Maity, Michael G.B. Drew, Polyhedron 54 (2013) 104–109.

3. Synthetic and structural studies of piperidine carboxamide uranyl ion complexes; **D. Das**, B.G. Vats, S. Kannan, Mukesh Kumar, M.K. Sureshkumar, Polyhedron 81 (2014) 39–44.

4. Selective recognition of uranyl ions from bulk of thorium(IV) and lanthanide(III) ions by tetraalkyl urea: a combined experimental and quantum chemical study; Bal Govind Vats, **Debasish Das**, Biswajit Sadhu, S. Kannan, I. C. Pius, D. M. Noronha, Mahesh Sundararajan, Mukesh Kumar, Dalton Trans. 45 (2016) 10319-10325.

5. Coordination diversity in palladium(II) picolinamide ligand complexes: structural and quantum chemical studies; **Debasish Das**, Amsaveni Muruganantham, S. Kannan, Mukesh Kumar, Mahesh Sundararajan, M.K. Sureshkumar, J. Coord. Chem. 70 (2017) 1548-1553.

Conferences/Symposium

1. Synthesis and structural studies of N-oxo picolinamide based ligands with uranyl and lanthanide nitrates - An evaluation of CONO based ligands; **Debasish Das**, S. Kannan, Mukesh Kumar, M.K. Sureshkumar, J.S. Yadav, P.M. Gandhi; 6th DAE-BRNS Interdisciplinary Symposium on Materials Chemistry (ISMC 2016), Page No. 248.

2. Synthesis and structural diversity in some U(VI) and Pd(II) complexes derived from picolinamide ligands with different alkyl groups; **Debasish Das**, S. Kannan, Mukesh Kumar, M.K. Sureshkumar, J.S. Yadav, P.M. Gandhi; 6th DAE-BRNS Interdisciplinary Symposium on Materials Chemistry (ISMC 2016), Page No. 250.

Acknowledgments

I wish to express my sincere gratitude to my guide **Prof. S. Kannan** for his continuous guidance, encouragement and constant supervision during the progress of my research work. I am highly indebted to him for introducing me to experimental aspects of coordination chemistry of lanthanides and actinides. I feel highly privileged to work under his invaluable guidance.

I am grateful to my co-guide **Prof. Sunil K. Ghosh** for his continuous support of my work and providing guidelines for synthesizing new organic ligands. He also supported to get the NMR spectra of my synthesized compounds from Bio Organic Division.

I would also like to thank members of the doctoral committee: **Prof. D. Das (Chairman)**, **Prof. V. K. Jain (Member)** and **Prof. P. K. Mohapatra (Member)**, for their valuable advice, encouragement and insightful comments, valuable suggestions and extensive discussions on my research work.

I would like to express my sincere gratitude to **Dr. M. K. Sureshkumar** for supporting me in the research work and giving time to time suggestion to improve myself. Moreover during my PhD period, I got excellent cooperation and support from all senior and junior colleagues in Plutonium Plant.

I specially thank **Dr. Raghunath Chowdhury, Dr. Liladhar Kumbhare, Dr. Rekha Singh, Shri Trilochan Gadly, Shri Adish Tyagi, Shri Manojkumar Pal** and **Dr. Nisha Kushwah** for recording the NMR spectra of my compounds at various stages of my PhD programme. I also want to thank **Dr. R.K. Singhal** for recording the FTIR spectra of my compounds whenever required.

I am specially thankful to my collaborators **Dr. Mukesh Kumar, Dr. Dilip K. Maity, Dr. Mahesh Sunderarajan** for sharing their expert skill in my research work.

I would like to express my heartiest gratitude to my parents **Shri Felu Ranjan Das and Smt. Rekha Das** for their endless love, motivation and blessings which helped me to keep focus on my life goal. My special thanks to my wife **Sumita** for being with me with patience and make me confident enough to pursue my dreams. I would also like to express my love to my little son, **Aryan** whom I have ignored a lot during my PhD days.

Last but not the least: I thank the beautiful and soulful presence of almighty God in my life for everything.

Debasish Das
Debasish Das

Table of Contents

Chapter 5: Synthesis, structural and theoretical Studies of picolinamide complexes with palladium(II) and uranyl (VI) ions *143*

SYNOPSIS

There is always a high demand for suitable solvents which can be used to separate particular metal ion or group of metal ions according to the need. As nuclear industries are concern, separation of actinides from high level liquid waste is the important step which not only helps to close the nuclear fuel cycle but also take part in environmental remediation [1-2]. To design and synthesize suitable solvents for metal ions, the molecular level understanding of the metal ligand interaction is a prerequisite factor. The coordination chemistry is the basic tool for solving this factor.

The selective separation of uranium-233 from the mixture of thorium and other fission products is an important step in the advanced water reactor (AHWR) technology of the Indian Atomic Energy programme [3-4]. Many new extractants have been studied for the selective recognition and separation of uranyl ion from various media in recent years [5-7]. In past, we have carried out the systematic structural studies on *iso*butyramide uranyl complexes and explained the stability and selectivity on the basis of strong bonding between the amide oxygen and uranyl group [7(a)]. Inspired by the results obtained, we studied the coordination and separation studies of few urea based ligands with uranyl nitrate, chloride and bromide by expecting even more strong bonding due to increased electron density on the O-atom of the ligands by mesomeric effects of two N-atoms placed both side of C=O group.

Steric effect is the common phenomenon observed in the uranium complexes and this is one of the controlling factors for metal ligand stoichiometry, geometry and stability. Uranium forms stable complexes with ligands consist of hard donor atoms like O, N, etc, which often form five or six membered cyclic chelates. From the previous studies, it is observed that five membered chelates are sterically more controlled than the other types [8].

Separation of palladium from high active liquid waste is getting recent attention due to many applications like catalysis, photoluminescence, medicine etc. Till date a number of extractants containing hard and/or soft donor atoms were tested for their efficacy for the separation and recovery of palladium from simulated and actual high level liquid waste [9-13]. Although these studies produced some satisfactory results, all of them have their own limitations such as selectivity, use of non-ideal diluents, non suitable acidity range, hydrolytic and radiolytic stability of the solvents etc. This demand more research on finding suitable solvent which can satisfy all characteristics of an ideal solvent. With this in mind, we have explored the complex chemistry pyrazole and picolinamide based ligands with palladium (II) ion.

N-oxide based ligands are expected to form strong complexes with lanthanides well as actinides due to highly polar nature of the N-O bond in these ligands. Till date various N-oxide based ligands were studied for their complexation reaction with uranyl and lanthanide ions in the solid state [14-16]. But their application in the solvent extraction processes especially in the back end of the nuclear fuel cycle is very limited [17]. In the solid state, it is observed that, for multifunctional N-oxide ligands, there is various mode of bonding with the metal ions. In few cases, the N-oxide group takes part in the bonding with the metal ions while in other cases, the ligand is bonded through other functional group and N-oxide group is free, often attached with the solvent molecules or form intra/inter molecular hydrogen bonds. In view of the above observation, we report herein the synthesis of N-oxo picolinamide ligands and study their coordination chemistry with lanthanides and actinides which can help to explore the use of this type of ligands for the separation studies.

The thesis consists of five chapters and the details are given below.

Chapter 1

Introduction

This chapter deals with a brief introduction to coordination chemistry of uranium, lanthanide and palladium ions and the factors affect the coordination number and geometry around the metal ions. It also deals with different types of ligands used in the different stages of the nuclear fuel cycle and the structural studies of uranyl and lanthanide ions with these ligands with latest literature information. A brief discussion on the characterization techniques like infrared spectroscopy (IR), nuclear magnetic resonance (NMR) and single crystal X-ray diffraction (XRD) employed in this work is also presented. Finally, the scope of the present work is discussed.

Chapter 2

Synthesis, structural and solvent extraction studies of piperidine urea and tetraalkyl urea with uranyl ions

This chapter deals with the synthesis, complexation and separation studies of piperidine urea and tetraalkyl urea based ligands with uranyl ion.

2.1 Synthesis of ligands

The general reaction for the synthesis of ligands can be represented by the following equation.

Piperidine urea ligands

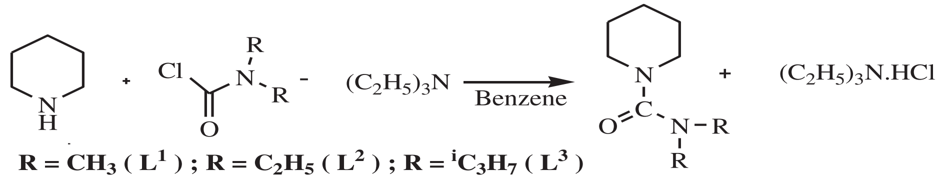

R = CH_3 (L^1) ; R = C_2H_5 (L^2) ; R = $^iC_3H_7$ (L^3)

Tetraalkyl urea ligands

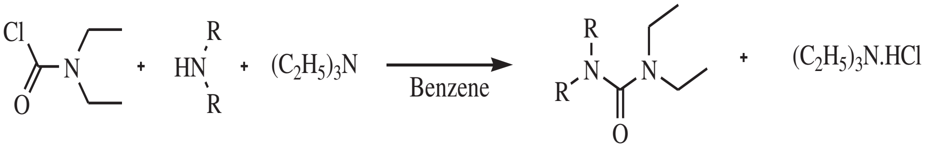

R = $^iC_4H_9$ (L^4) ; R = n-C_8H_{17} (L^5)

2.2 Synthesis of uranyl complexes

The synthesis of metal complexes are given in the following reactions

Piperidine urea ligand complexes

$$[UO_2(NO_3)_2.6H_2O] \quad + \quad 2L \xrightarrow{\qquad} [UO_2(NO_3)_2L_2] \quad (L = L^1, L^2, L^3)$$

$$[UO_2(DBM)_2.2H_2O] \quad + \quad L \xrightarrow{\qquad} [UO_2(DBM)_2.L] \quad (L = L^1, L^2, L^3)$$

(DBM = Dibenzoyl methanate)

$$[UO_2(TTA)_2.2H_2O] \quad + \quad L \xrightarrow{\qquad} [UO_2(TTA)_2.L] \quad (L = L^1, L^2, L^3)$$

(TTA = Thenoyl trifluroacetonate)

$$[UO_2X_2,\ nH_2O] \quad + \quad 2L \xrightarrow{\qquad} UO_2X_2L_2 \quad (L = L^1, L^2, L^3)$$

(X = Cl, Br)

Tetraalkyl urea ligand complexes

$$[UO_2(NO_3)_2.\ 6H_2O] \quad + \quad 2L \xrightarrow{\qquad} [UO_2(NO_3)_2L_2] \quad (L = L^4)$$

$$[UO_2X_2.\ nH_2O] \quad + \quad 2L \xrightarrow{\qquad} UO_2X_2L_2 \quad (L = L^4)$$

(X = Cl, Br)

2.3 Results and discussion

The ligands L^1-L^4 and their compounds of uranyl nitrate, uranyl halide (halide = chloride, bromide) and uranyl bis(β-diketonate) (β-diketonate = dibenzoylmethanate, thenoyltrifluoroacetonate) were characterized by CHN analysis, IR and NMR techniques. The IR spectra of all complexes indicate that the carbamoyl group is bonded to the uranyl group directly. The ^1H NMR spectra of the compounds confirm the bonding between the carbamoyl oxygen and uranyl group in solution. The structures of L^3 ligand with uranyl nitrate, uranyl chloride, uranyl bromide and uranyl bis(thenoyltrifluoroacetonate) are shown in Figures 1, 2, 3 and 4 respectively and with L^4 with uranyl nitrate, chloride and bromide are shown in 5, 6 and 7 respectively.

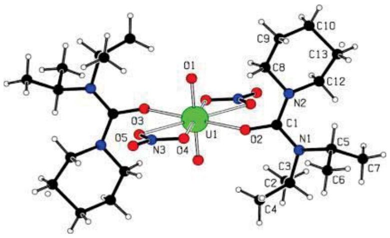

Fig. 1. Molecular structure of $[UO_2(NO_3)_2\{C_5H_{10}NCON(^iC_3H_7)_2\}_2]$

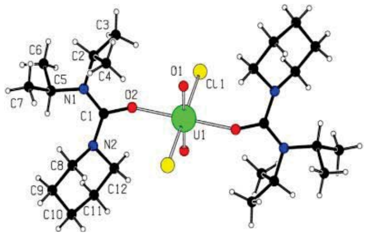

Fig. 2. Molecular structure of $[UO_2Cl_2\{C_5H_{10}NCON(^iC_3H_7)_2\}_2]$

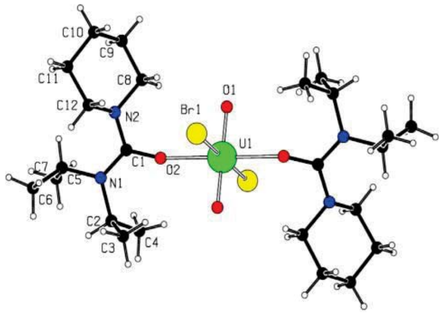

Fig. 3. Molecular structure of $[UO_2Br_2\{C_5H_{10}NCON(^iC_3H_7)_2\}_2]$

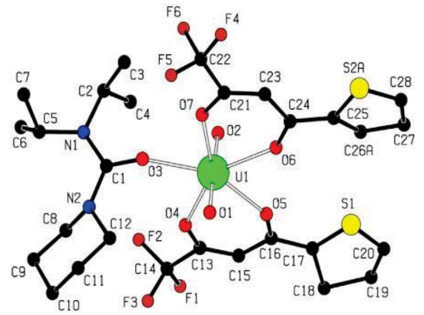

Fig. 4. Molecular structure of $[UO_2(C_4H_3SCOCHCOCF_3)_2\{C_5H_{10}NCON(^iC_3H_7)_2\}]$

The figures show that both the ligands are bonded to the uranyl group in monodentate fashion through the urea oxygen atom. The geometry of the uranyl nitrate, uranyl halide and uranyl bis(thenoyltrifluoroacetonate) complexes with the ligands are hexagonal bi-pyramidal, octahedral and pentagonal bipyramidal respectively.

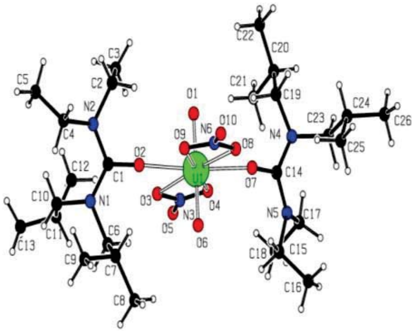

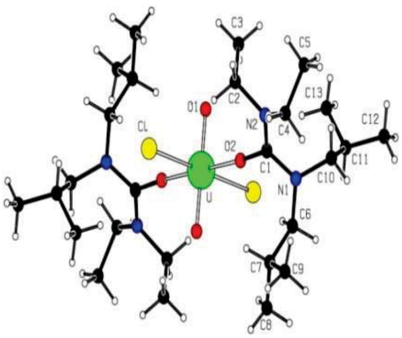

Fig. 5. Molecular structure of $[UO_2(NO_3)_2\{C_4H_{10}NCON(^iC_4H_9)_2\}_2]$

Fig. 6. Molecular structure of $[UO_2Cl_2\{C_4H_{10}NCON(^iC_4H_9)_2\}_2]$

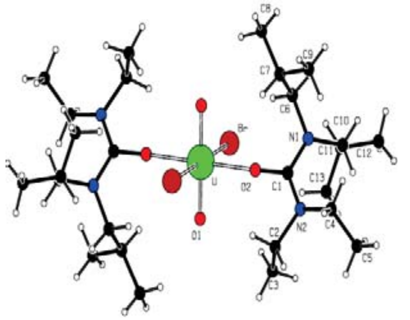

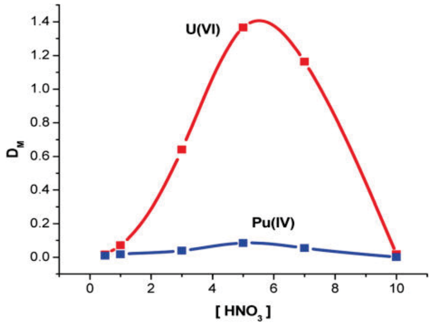

Fig. 7. Molecular structure of $[UO_2Br_2\{C_4H_{10}NCON(^iC_4H_9)_2\}_2]$

Fig. 8. The D_M values of UO_2^{2+} and Pu(IV) at different nitric acid concentration

When the ligand L^4 is layered over a 3M HNO_3 solution of uranyl nitrates containing large excess of thorium(IV), lanthanum(III), samarium(III) and europium(III) nitrates, selectively precipitate yellow crystalline solid of $[UO_2(NO_3)_2 \cdot 2L^4]$. Moreover solvent extraction studies of ligand L^5 in dodecane with uranyl(VI) and plutonium(IV) ions from a nitric acid medium show that uranyl ion is selectively extracted over plutonium(IV) ion (Fig. 8).

Based on electronic structure calculations at the DFT level of theory, we report the preferential binding to uranyl compared to Th is modulated by both steric and electronic factors.

2.4 Conclusions

The coordination chemistry of piperidine urea and tetra alkyl urea ligands with uranyl nitrate and uranyl halides reveal that the ligands act as monodentate ligands and bond through the C=O groups to uranyl ion. Density functional theory study revealed that the steric effect plays a crucial role for the uranyl selectivity by the ligands.

Chapter 3

Synthesis, structural and coordination studies of N-oxo picolinamide complexes with uranyl and lanthanide ions

This chapter deals with the synthesis and structural studies of N-oxo picolinamide complexes of uranyl nitrate and lanthanide nitrates.

3.1 Synthesis of ligands

The ligands were synthesized according to following reaction.

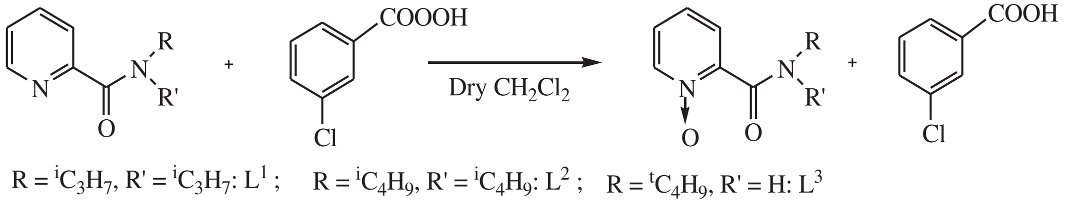

R = $^iC_3H_7$, R' = $^iC_3H_7$: L^1 ; R = $^iC_4H_9$, R' = $^iC_4H_9$: L^2 ; R = $^tC_4H_9$, R' = H: L^3

3.2 Synthesis of metal complexes

The metal complexes were synthesized by following reactions.

$$[UO_2(NO_3)_2.\ 6H_2O] \quad + \quad L \longrightarrow [UO_2(NO_3)_2L]$$

$(L = L^1 :1), (L = L^2 :2), (L = L^3 :3)$

$$[Ln(NO_3)_3.\ 6H_2O] \quad + \quad 2L \longrightarrow [Ln(NO_3)_3.H_2O.L_2]$$

For Ln = La and $(L = L^1 :4), (L = L^2 :5), (L = L^3 :6)$

For Ln = Sm and $(L = L^1 :7), (L = L^2 :8), (L = L^3 :9)$

For Ln = Eu and $(L = L^1 :10), (L = L^2 :11), (L = L^3 :12)$

3.3 Results and discussion

All ligands and their compounds with uranyl nitrate and lanthanide nitrates (where, lanthanide = lanthanum, samarium, europium) were characterized by elemental analysis followed by IR and NMR spectroscopic techniques. IR spectra of the compounds indicate the bonding of amide and N-oxo groups of the ligands with uranyl ions in complexes 1-3, where as only the N-O groups of the ligands are bonded with the metal ions in complexes 4-12. The ^1H NMR spectra of all the complexes show that the coordination of the ligands to the metal ions persists in solution. The structures of the two compounds $[UO_2(NO_3)_2\{C_5H_4NCONH(^tC_4H_9)\}]$ (3) and $[Eu(NO_3)_3\{C_5H_4NOCON(^iC_3H_7)_2\}_2.H_2O]$ (10) were characterized by single crystal XRD and are shown in the Fig. 9-10.

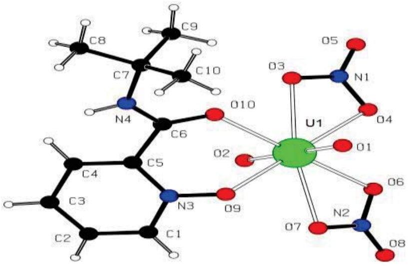

Fig. 9. Molecular structure of $[UO_2(NO_3)_2\{C_5H_4NOCONH(^tC_4H_9)\}]$

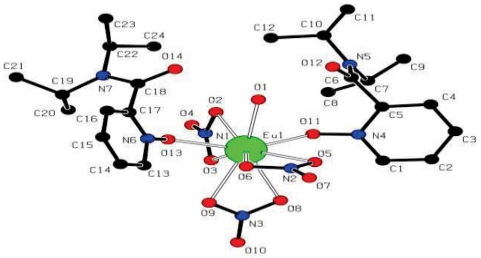

Fig. 10. Molecular structure of $[Eu(NO_3)_3(H_2O)\{C_5H_4NOCON(^iC_3H_7)_2\}_2]$

The molecular structure of (**1**) and (**3**) show that the uranium atom is surrounded by eight oxygen atoms in a hexagonal bi-pyramidal geometry. The ligands act as bidentate chelating ligand and bond through both N-oxo group and amide oxygen atoms to uranyl group. The molecular structure of (**10**) shows that the ligand is bonded with europium ion through N-oxo group in a monodentate mode and Eu(III) ion is surrounded by nine oxygen atoms.

3.4 Conclusions

Structure of N-oxo picolinamide with uranyl nitrate shows bidentate chelating mode of bonding, where as it shows monodentate mode of bonding with lanthanide ions through N-oxo group only.

Chapter 4

Synthesis, structural and theoretical studies of carbamoyl pyrazole compounds of the uranyl(VI) and Pd(II) ions

This chapter deals with the synthesis, coordination, structural and theoretical studies of carbamoyl pyrazole ligands with uranyl and Pd(II) ions.

4.1 Synthesis of ligands

The general reaction for the synthesis of ligands can be represented by the following equation.

R = H, R' = Me: (L^1); R = H, R' = Et: (L^2); R = H, R' = ^{i}Pr: (L^3); R = Me, R' = Me: (L^4); R = Me, R' = Et: (L^5); R = Me, R' = ^{i}Pr: (L^6)

4.2 Synthesis of the metal complexes

4.2.1 Synthesis of complexes with uranyl ion

These ligands have been used for the synthesis of uranyl complexes and reactions are given below:

$$[UO_2(NO_3)_2.6H_2O] + L \longrightarrow [UO_2(NO_3)_2L]$$

$(L = L^1 :1), (L = L^2 :2), (L = L^3 :3)$

$$[UO_2(NO_3)_2.6H_2O] + 2L \longrightarrow [UO_2(NO_3)_2(H_2O)_2(L)_2]$$

$(L = L^4 :4), (L = L^5 :5), (L = L^6 :6)$

$$[UO_2(DBM)_2.2H_2O] + L \longrightarrow [UO_2(DBM)_2.L]$$

(DBM = Dibenzoylmethanate)

$(L = L^1 :7), (L = L^2 :8)$

$$[UO_2(DBM)_2.2H_2O] + L \longrightarrow \text{No Reaction} \quad (L = L^4, L^5, L^6)$$

4.2.2 Synthesis of complexes with palladium(II) ion

These ligands have been used for the synthesis of palladium(II) complexes and reactions are given below:

$$PdCl_2 + 2L \xrightarrow[CH_3CN]{} [PdCl_2L_2]$$

$L = L^1$ (9); $L = L^2$ (10); $L = L^3$ (11); $L = L^4$ (12); $L = L^5$ (13); $L = L^6$ (14)

4.3 Results and discussion

All ligands and their compounds of uranyl nitrate and uranyl dibenzoylmethanate were characterized by elemental analysis followed by IR and NMR spectroscopic techniques. IR spectra of **1-3** indicate the strong bonding between carbamoyl groups of the ligands with uranyl ion. On the other hand, IR spectra of **4-6** signify that the ligands are uncoordinated in the complexes. The observed ^1H NMR spectra of **1-3** and **7−8** show that the pyrazolyl protons is deshielded w.r.t to free ligands, indicating that the bonding persist in solution also. The molecular structures of three compounds $[UO_2(NO_3)_2\{C_3H_3N_2CON(C_2H_5)_2\}]$ **(2)**, $[UO_2(NO_3)_2(H_2O)_2\{C_5H_7N_2CON(C_2H_5)_2\}_2]$ **(5)** and $[UO_2(C_6H_5COCHCOC_6H_5)_2\{C_3H_3N_2CON(C_2H_5)_2\}]$ **(8)** are characterized by single crystal XRD and shown in the Fig. 11, Fig. 12 and Fig. 13, which confirm the spectral observations.

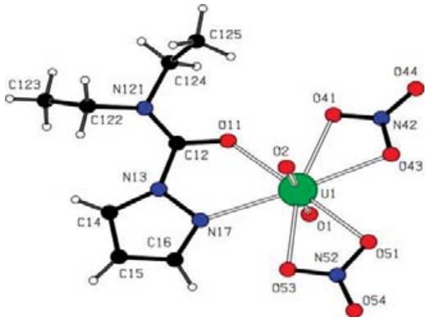

Fig. 11 Molecular Structure of $[UO_2(NO_3)_2\{C_3H_3N_2CON(C_2H_5)_2\}]$

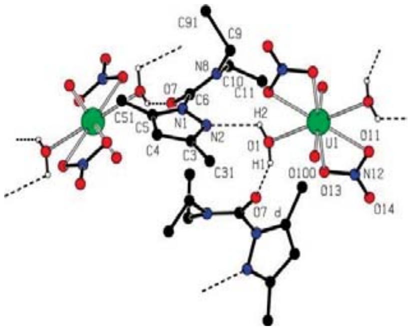

Fig. 12 Molecular Structure of $[UO_2(NO_3)_2(H_2O)_2\{C_5H_7N_2CON(C_2H_5)_2\}_2]$

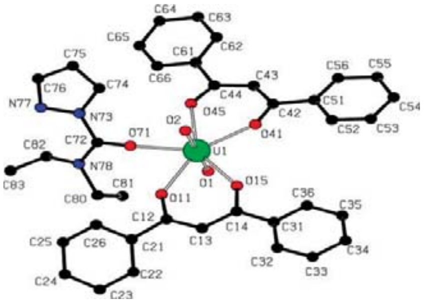

Fig. 13 Molecular Structure of $[UO_2(C_6H_5COCHCOC_6H_5)_2\{C_3H_3N_2CON(C_2H_5)_2\}]$

The structure of **2** shows that the uranium atom is surrounded by one nitrogen and seven oxygen atoms in a hexagonal bipyramidal geometry. On the other hand, the structure of **5** consists of centrosymmetric $[UO_2(NO_3)_2 \cdot 2H_2O]$ groups, bridged by carbamoyl dimethyl pyrazole ligand via O−H···O and O−H···N hydrogen bonds. The structure shows that there is no direct bonding between ligand and the uranyl ion and the uranium(VI) ion are surrounded by eight oxygen atoms to give hexagonal bipyramidal geometry. In compound **8**, the pyrazole ligand acts as a monodentate ligand and is bonded through the carbamoyl oxygen atom to the uranyl group.

The CHN analyses revealed that the ratio of metal to ligand is 1:2 in all the palladium compounds **9-14**. The IR spectra of **9-14** signify that the carbamoyl group is un-coordinated in all the compounds and the ligands are bonded through the pyrazole nitrogen atom to the metal centres. The ^{1}H NMR spectra of the compounds show that the pyrazole protons are deshielded with respect to the free ligands proving further evidence for the coordination of the ligand to the metal ion. The structures for compounds **10** (Fig. 14) and **13** (Fig. 15) confirm our interpretation of the spectral data.

Theoretical studies revealed that the steric effect play an important role in deciding the bonding of pyrazole based ligands with uranyl nitrate and palladium (II) chloride.

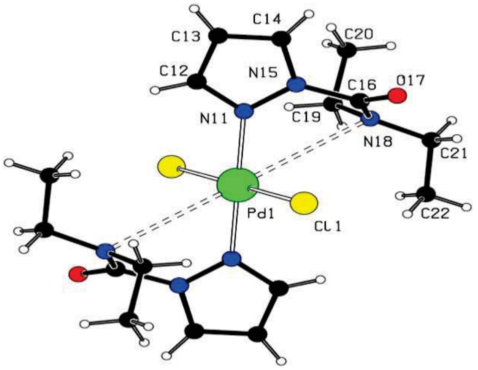

Fig. 14. Molecular Structure of $[PdCl_2\{C_5H_7N_2CON(C_2H_5)_2\}_2]$

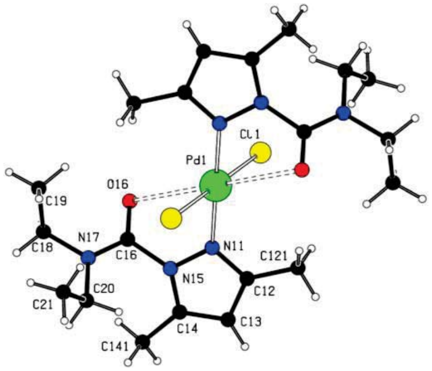

Fig. 15. Molecular Structure of $[PdCl_2\{C_5H_7N_2CON(C_2H_5)_2\}_2]$

4.4 Conclusions

Pyrazole based ligands form 1:1 complex with uranyl nitrate and uranyl bis(dibenzoylmethanate), and dimethyl pyrazole based ligands form second sphere complexes with uranyl nitrate with metal to ligand ratio of 1:2. Both pyrazole and dimethyl pyrazole ligands form 1:2 complexes with palladium(II) chloride and bond through the pyrazolyl nitrogen atom only. Theoretical study explains the steric effect plays the important role behind the structural difference between carbamoyl pyrazole and dimethyl carbamoyl pyrazole complexes with uranyl and palladium ion.

Chapter 5

Synthesis, structural and theoretical studies of picolinamide complexes with palladium and uranyl ions

This chapter deals with the synthesis and structural studies of picolinamide complexes of palladium chloride and uranyl nitrate.

5.1 Synthesis of ligands

The ligands were synthesized according to following reaction.

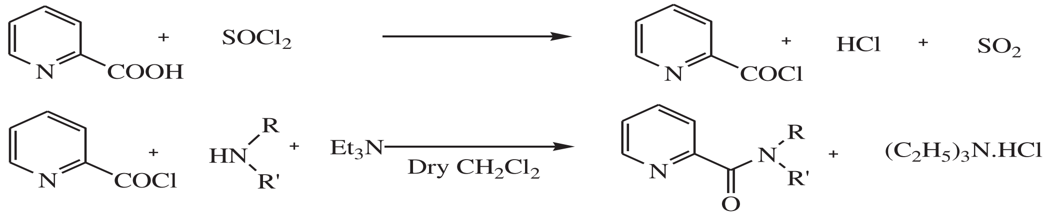

$R = {}^{i}C_3H_7$, $R' = {}^{i}C_3H_7$: L^1 ; $R = {}^{i}C_4H_9$, $R' = {}^{i}C_4H_9$: L^2 ; $R = {}^{t}C_4H_9$, $R' = H$: L^3

5.2 Synthesis of metal complexes

The metal complexes were synthesized by following reactions.

$$[UO_2(NO_3)_2.\ 6H_2O] + L \longrightarrow [UO_2(NO_3)_2L]$$

$(L = L^1 : 1)$, $(L = L^2 : 2)$, $(L = L^3 : 3)$

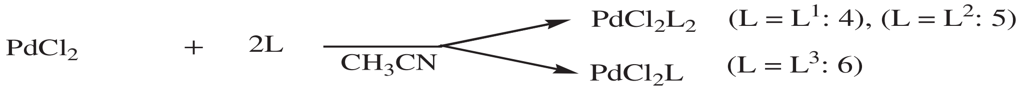

$$PdCl_2 + 2L \xrightarrow[CH_3CN]{} \begin{cases} PdCl_2L_2 & (L = L^1: 4), (L = L^2: 5) \\ PdCl_2L & (L = L^3: 6) \end{cases}$$

5.3 Results and discussion

All ligands and their compounds with uranyl nitrate and palladium chloride were characterized by elemental analysis followed by IR and NMR spectroscopic techniques. IR spectra of **1-3** show that absorption frequency for the C=O is 34-55 cm^{-1} lower as compared to that of free ligands, indicating a direct bonding between the amide group and uranyl ion. On the other hand, while the IR spectra of **4-5** show that absorption frequency for the C=O is unchanged and is red shifted by 56 cm^{-1} for compound **6**. This indicates that in complex **6** the C=O is bonded with the metal ion and is free in **4-5.** The ^1H NMR spectra of all compounds of uranium and palladium show that the pyridyl protons are deshielded with respect to the free ligands proving further evidence for the coordination of the ligands to the metal ion. The structures of compounds $[UO_2(NO_3)_2\{C_5H_4NCON({}^{i}C_3H_7)_2\}]$ (1), $[PdCl_2\{C_5H_4NCON({}^{i}C_3H_7)_2\}_2]$ (4) and $[PdCl_2\{C_5H_4NCONH({}^{t}C_4H_9)\}]$ (6) were characterized by single crystal XRD and are shown in the Figures 16-18.

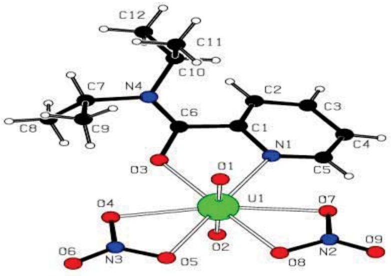

Fig. 16. Molecular structure of $[UO_2(NO_3)_2\{C_5H_4NCON(^iC_3H_7)_2\}]$

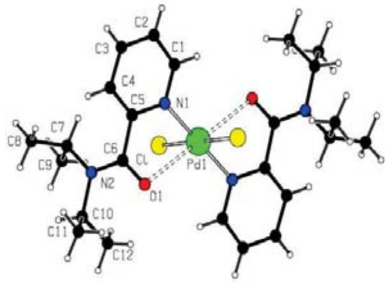

Fig. 17. Molecular structure of $[PdCl_2\{C_5H_4NCON(^iC_3H_7)_2\}_2]$

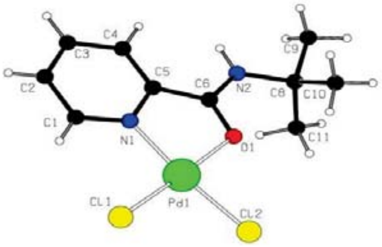

Fig. 18. Molecular structure of $[PdCl_2\{C_5H_4NCONH(^tC_4H_9)\}]$

The molecular structure of (1) shows that the uranium atom is surrounded by seven oxygen atoms and one nitrogen atom in a hexagonal bi-pyramidal geometry. The molecular structure of (4) shows that two ligands are bonded with palladium in a monodentate mode and Pd(II) ion is surrounded by two nitrogen and two chlorine atoms in a trans square planar geometry. On the other hand, the molecular structure of (6) shows that the ligand is bonded with palladium in a bidentate mode and Pd(II) ion is surrounded by one nitrogen, one oxygen and two chlorine atoms in a cis square planar geometry. DFT study indicates that steric hindrance between 3-pyridyl H atom and N-substituted alkyl groups inside the ligands are the reason behind this kind of coordination diversity in palladium complexes.

Theoretical studies revealed that the steric effect is the reason behind the coordination diversity observed in picolinamide complexes with palladium (II) chloride.

5.4 Conclusions

The structures of picolinamide compounds show that the ligands show coordination diversiry with the two selected metal ions. DFT studies clearly revealed that the steric effects play an important role for deciding the coordination mode of the ligands.

Overall conclusions

Study of basic coordination chemistry of organic ligands having different functionalities with the specific metal ion can provide the ideas about the stability, bonding, stoichiometry of the complexes formed due to their mutual interaction. These ideas could be very helpful to design suitable molecules by synthetic organic chemists and their deployment in the field of separation science.

We have synthesized total five types of mono and bidentate ligands with different functionality and studied their coordination chemistry with uranyl(VI), palladium(II) and few lanthanide(III) ions, viz. La^{3+}, Sm^{3+}, Eu^{3+} in order to understand their mode of bonding, structural variation, stoichiometry etc. It helps us to make a layout of best solvent system for the separation of different metal ions especially in the field of back end of nuclear fuel cycle.

While both the monodentate ligands, piperidine carboxamide and tetraalkyl urea form 1:2 complexes with uranyl nitrate and uranyl dihalides, they form 1:1 complexes with uranyl β-diketonates. They form very strong complexes with the uranyl compounds which is confirmed by the short U-O(amide) bond length observed in X-ray crystallography and lower vibrational frequency of both $C{=}O_{str}$ and $U{=}O_{asy}$ bonds observed in IR spectroscopy. N,N-di- n-Octyl tetraalkyl urea showed very high selectivity towards ^{233}U from the simulated AHWR fuel dissolver solution.

In case of, N-Oxo picolinamide complexes of uranyl and lanthanide (La, Sm, Eu) nitrates variation in bonding and structure was observed in the solid state. While the ligands act as bidentate chelating ligands with uranyl nitrate, they act as monodentate ligands with lanthanide nitrates through the O(N-Oxo)-metal bonding. The metal:ligand stoichiometry in the uranyl nitrate and lanthanide nitrates complexes is found to be 1:1 and 1:2 respectively.

Carbamoyl pyrazole ligands form stable complexes with uranyl nitrate and uranyl β-diketonates and act as bidentate chelating and monodentate ligand respectively. On the other hand, carbamoyl 1,3-dimethyl pyrazole ligands form second sphere complexes with uranyl nitrate and do not form any complex with uranyl β-diketonates. This type of variation in reactivity of these two ligand systems was successfully explained (by density functional theory calculation) on the basis of steric effect provided by the later when approaches towards the identical metal system. Both the type of ligands form 1:2 complexes with palladium chloride and bonded through pyrazoyl N-atom. Here they act as monodentate ligands.

Pyridine carboxamide ligands form stable complexes with uranyl nitrate and act as bidentate chelating ligands. The metal:ligand stoichiometry of these complexes was found to be 1:1. But it was observed that with variation in the alkyl group, the ligands show structural variety with palladium chloride. While the isopropyl and isobutyl based ligands form 1:2 complexes and act as monodentate ligands, the mono substituted tertiary butyl based ligand form 1:1 complex and act as bidentate chelating ligand.

From the above observation it can be concluded that with changing the electronic and steric property of the ligands the reactivity and bonding mode of these ligands can be tuned. The donor strength of the ligands is the combination of basicity of the donor atoms and steric hindrance provided by the ligands towards the metal system.

Future perspectives

Nuclear waste management is the most important and challenging task in the nuclear fuel cycle, not only to recover the valuables from the waste even to protect the environment as well. Nuclear waste solution after dissolution of spent fuel comprises of a varieties of metal ions, like alkali and alkaline earth metal ions, transition metal ions even lanthanides and actinides. Solution chemistry of theses metal ions are different and they present in various oxidation states, especially transition metal ions. Speciation data of these metal ions in 3-4 M HNO_3 medium is not fully known till date. So, it is really very difficult to achieve selectivity of their separation from complex mixture solution like high level liquid waste (HLLW). We got partial achievement to selectivity separate ^{233}U from simulated AHWR high level liquid waste using one of our synthesized ligands. This may show a new direction for the development of thoria based fuel cycle.

In future there is huge scope to develop suitable solvent system for separation of other metal ions from various waste streams. Apart from their high donor strength and favourable steric property, they should also have other suitable properties to get a global acceptance like, viscosity, radiolytic and hydrolytic stability, solubility in commonly used diluents etc. For this doctoral work, we have synthesized some simple mono and bidentate ligands with preferably amide functional group and studied their coordination chemistry with uranyl, palladium and lanthanide compounds. However complex molecules with more number of functional groups could be synthesized and tested for separating rather difficult and intractable metal ion system.

References

1. K.L. Nash, J.C. Braley, Challenges for Actinide Separations in Advanced Nuclear Fuel Cycles, ACS Symposium Series, 1046 (2010) 19 (Chapter 3).
2. Dominique Warin, IOP Conf. Series: Materials Science and Engineering 9 (2010) 012063.
3. S. Kant, Int. J. Nucl. Ener. Sci. Tech. 1 (2005) 204.
4. R. K. Sinha, A. Kakodkar, Nucl. Eng. Des. 236 (2006) 683.
5. (a) G. Szigethy, K.N. Raymond, Chem. Eur. J. 17 (2011) 1818−1827. (b) C. Ni, D.K. Shuh, K.N. Raymond, Chem. Commun. 47 (2011) 6392−6394. (c) G. Szigethy, K.N.

Raymond, Inorg. Chem. 49 (2010) 6755−6767. (d) G. Szigethy, K.N. Raymond, J. Am. Chem. Soc. 133 (2011) 7942−7956. (e) A.E.V. Gorden, J. Xu, K.N. Raymond, P. Durbin, Chem. Rev. 103 (2003) 4207−4282. (f) C. Drouza, V. Gramlich, M.P. Sigalas, I. Pashalidis, A.D. Keramidas, Inorg. Chem. 43 (2004) 8336−8345.

6. A.C. Sather, O.B. Berryman, J. Jr. Rebek, J. Am. Chem. Soc. 132 (2010) 13572−13574.
7. (a) S. Kannan, S.B. Deb, J.S. Gamare, M.G.B. Drew, Polyhedron 27 (2008) 2557−2562. (b) P.N. Pathak, D.R. Prabhu, R.B. Ruikar, V.K. Manchanda, Solvent Extr. Ion Exch. 20 (2002) 293−311.
8. (a) R.D. Hancock, A.E. Martell, Chem. Rev. 89 (1989) 1875−1914. (b) A.E. Martell, R.D. Hancock, Metal complexes in aqueous solution; Plenum Press: New York, 1996.
9. Z. Zhu, Y. Sasaki, H. Suzuki, S. Suzuki, T. Kimura, Anal. Chim. Acta 527 (2004) 163.
10. Y. Sasaki, Y. Morita, Y. Kitatsuji, T. Kimura, Solv. Extr. Ion Exch. 28 (2010) 335.
11. N.T. Hung, M. Watanabe, T. Kimura, Solv. Extr. Ion. Exch. 25 (2007) 407.
12. E.A. Mezhov, A.V. Kuchmunov, V.V. Druzhenkov, Radiochemistry 44 (2002) 135.
13. A. Dakshinamoorthy, P.S. Dhami, P.W. Naik, N.L. Dudwadkar, S.K. Munshi, P.K. Dey, V. Venugopal, Desalination 232 (2008) 26.
14. Bal Govind Vats, Jayashree S. Gamare, S. Kannan, I.C. Pius, D.M. Noronha, M. Kumar, Inorg. Chim. Acta 467 (2017) 1–6.
15. Sylvie Pailloux, Iris Binyamin, Lorraine M. Deck, Benjamin P. Hay, Eileen N. Duesler, Lev N. Zakharov, W. Scott Kassel, Arnold L. Rheingold, Robert T. Pain, Polyhedron 28 (2009) 3979–3984.
16. Hai-Jun Zhang, Ru-Hu Gou, Lan Yan, Ru-Dong Yang, Spectrochim. Acta, Part A 66 (2007) 289–294.
17. M. Ejaz, Sep. Sci. 10 (1975) 425-446.

Abbreviations

An = Actinide

AHWR = Advanced heavy water reactor

BE = Binding energy

Bipy = Bipyridyl

CCD = Charge-coupled device

CMP = Carbamoyl methyl phosphonates

CMPO = Carbamoyl methyl phosphine oxides

CMSO = Carbamoyl methyl sulfoxide

DBA = Dibenzylidineacetone

DBM = Dibenzoylmethanate

DCM = Dichloromethane

Dcpe = Dicyclohexylphosphino ethane

DEHPA = Di-(2-ethylhexyl) phosphoric acid

DFT = Density functional theory

DIAMEX = Diamide Extraction

DIDPA = Di-isodecyl phosphoric acid

DMDBTDMA = Dimethyl-dibutyl-tetradecylmalonamide

DMDOHEMA = N,N′-dimethyl-N,N′-dioctylhexylethoxymalonamide

DMF = Dimethylformamide

Dmpz = Dimethyl pyrazole

DMSO = Dimethyl sulfoxide

Dppe = Diphenylphosphinomethane

DNPPA = Di-nonylphenyl phosphoric acid

DOPPA = Di-octylphenyl phosphoric acid

DU = Depleted uranium

EDA = Energy decomposition analysis

EDXRF = Energy dispersive X-Ray Fluorescence

ESIMS = Elctrospray ionization mass spectrometry

FMO = Frontier molecular orbital

FTIR = Fourier transform infrared

HDEHP = Di-(2-ethylhexyl) phosphoric acid

Ln = Lanthanide

MPA = Mülliken population analysis

NLMO = Natural localized molecular orbital

NMR = Nuclear magnetic resonance

ORTEP = Oak Ridge Thermal Ellipsoid Plot

PCM = Polarizable continuum model

PGM = Platinum group metals

PUREX = Plutonium uranium extraction

Pz = Pyrazole

RE = Rare earth

RI = Resolution of Identity

SC-ECP = small-core effective core potential

Tacn = 1,4,7-triazacyclononane

TBP= Tri-butyl phosphate

THF = Tetrahydrofuran

TRUEX = Transuranic extraction

Ttcn = 1,4,7-trithiacyclononane

TTA = Theonyltrifluoroacetonate

TXRF = Total Reflection X-Ray Fluorescence

UV = Ultra violet

XRD = X-ray diffraction

ZORA = Zeroth Order Regular Approximation

Table of Contents

Chapter 4: Synthesis, structural and theoretical studies of carbamoyl pyrazole compounds of the uranyl(VI) and Pd(II) ions 104

Thesis Highlight

Name of the Student Debasish Das
Name of the CI/OCC BARC, Mumbai **Enrolment No.** CHEM01201104007
Thesis Title Structural and theoretical studies of complexes of uranyl(VI) and palladium(II) ions having soft and hard donor ligands
Discipline: Chemical Sciences **Sub-Area of Discipline:** Inorganic Chemistry
Date of viva voce: 16/03/2018

Study of basic coordination chemistry of organic ligands having different functional groups with specific metal ions can provide the ideas about the stability, bonding and stoichiometry of the complexes formed due to their mutual interaction.These ideas could be very helpful to designsuitable molecules for selective separation of metal ions in the field of hydrometallurgy.

In present work, five types of mono and bidentate ligands with different functional groups were synthesized and their coordination chemistry with uranyl(VI), palladium(II) and few lanthanide(III) ions, viz. La^{3+}, Sm^{3+}, Eu^{3+} were explored to understand their mode of bonding, structural variation, stoichiometry etc.It helps us to make a layout of best ligand system for the separation of metal ions relevant to the back end nuclear fuel cycle.

The steric effects playimportant role for the selective separation of uranyl ion from bulk of thorium and lanthanide ions. The structure of carbamoylpyrazole-uranylnitrate complex shows that the ligand forms inner-sphere complex while the carbamoyl3,5-dimethyl pyrazole forms outer sphere complex (Fig. 1a &1b). Theoretical studies clearly revealed that the steric effect is the deciding factor during complexation. This idea promoted us to synthesis stericallybulky N,N,N′,N′-tetraalkyl urea type ligands, which show high selectivity for uranyl ion over throium and lanthanide ions.

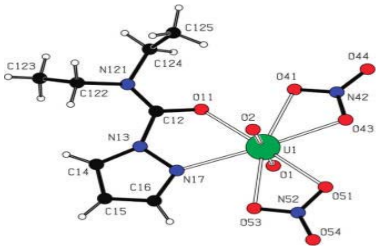

Fig. 1a crystal structure of N,N-diethyl carbamoylpyrazole-uranyl nitrate complex

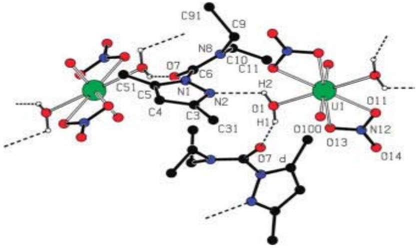

Fig. 1b crystal structure of N,N-diethyl carbamoyl3,5-dimethyl pyrazole-uranyl nitrate complex

Chemistry of pyrazole amide ligands with palladium(II) ion show that they acts as monodentate ligands and bond through the soft nitrogen atom to palladium(II) centre. However, when pyridylcarboxamide based ligands were used, they act either as monodentate or bidendate chelate depending upon the group attached to the amidic nitrogen atom (Fig. 2a&2b).

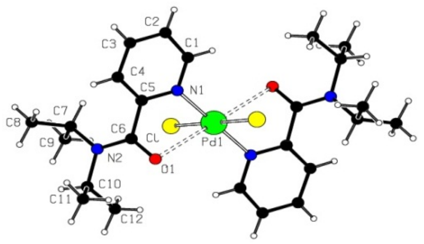

Fig. 2a crystal structure of N,N-diisopropylpyridyl2-carboxamide-palladium(II) chloride complex

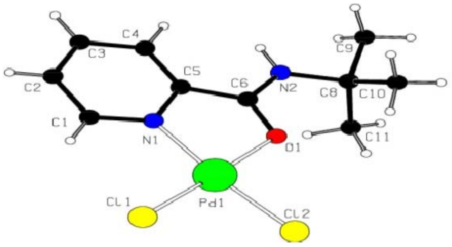

Fig. 2b crystal structure of N-tert-butylpyridyl 2-carboxamide-palladium(II) chloride complex

CHAPTER 1

General introduction to chemistry of uranyl(VI), palladium(II) and lanthanide(III) ions and methods and materials used in present investigation

CHAPTER – 1

1.1 Introduction

From front end to the back end, the complete nuclear fuel cycle deals with variety of actinides, and the safe processing and management of actinides are very challenging to the nuclear scientists [1-3]. The study of actinide coordination chemistry is highly instrumental in solving this problem. It provides the information about the molecular level interaction of metal ions with various types of ligands. This can be done by investigating the structure, stoichiometry and nature of the complexes which are formed during the solvent extraction separation of metal by the ligands in the organic phase. This in turn helps to develop suitable extractant which can be used to selectively separate one particularly metal ion of sufficient purity or a group of metal ions from complex mixture.

Interest in the organometallic chemistry of the actinide elements dates back to the Manhattan project and to the search for volatile compounds to be agents for uranium isotope separation. Since then to date, continuous efforts have been given to study the basic coordination chemistry of the actinides for solving different problems. One of those problems is the selective separation of uranium-233 from the mixture of thorium [4] and other fission products in the advanced heavy water reactor (AHWR) technology of the Indian Atomic Energy programme [5]. Separation of uranium from other metal ions and complex media is also important in seawater, environmental and biological samples [6-7]. Selective separation of uranyl ion (UO_2^{2+}) from different conditions is reported for many years by designing suitable sterically demanding ligands. Raymond et al, have shown that the ligand with stereognostic coordination platform forming an intramolecular hydrogen bond with the oxo groups of uranyl group selectively separate this ion from complex media [8]. It is reported that the biological proteins forming intramolecular hydrogen bonding interaction with uranyl oxygen atoms selectively recognise the uranyl ion upto femtomolar concentration from other ions [9]. Sather et. al. reported that the tripodal carboxylate based ligand with equatorial coordination groups required for uranyl ion bonding and stereognostic hydrogen bonding interactions to uranyl oxo group selectively binds to uranyl ion [10]. It is also reported that the isobutyramide based ligands show selectivity for uranyl in the presence of large excess of thorium and lanthanide ions [11]. Structural and theoretical studies on the complexes of isobutyramide based ligands with uranyl ion clearly show that in addition to steric effects, a strong interaction between the oxygen atom of amide group and uranyl ion with shorter U-O(amide) bond distances and near linear U-O-C bond angle is responsible for the selectivity [12]. These studies further show that no intramolecular hydrogen bonding interaction between the uranyl oxygen atoms with any groups of the isobutyramide based ligands for their selectivity towards uranyl ion.

Palladium is one of the major fission products, which are produced during the burn up of nuclear fuel in the reactor and present in the acidic high level liquid waste after reprocessing of the spent fuel [13-15]. Palladium is a member of platinum group metals, which are very rarely found in earth. The abundance of palladium in the earth's crust is ~6.3×10^{-7} %. Due to low abundance and high application of this metal in various fields, there is a need to look for alternative sources. Nuclear fuel reprocessing and their selective separation from the acidic high level liquid waste is such kind of source which can be adopted to balance the day to day increasing need of this precious metal.

In order to design a ligand for selective separation of this metal ion from acidic waste, the basic understanding of coordination chemistry is very important. This chapter will give a brief introduction to basic chemistry and coordination chemistry of uranyl and palladium(II) ions with reference to separation chemistry.

1.2 Uranium chemistry

1.2.1 An overview

Uranium was discovered by Martin Heinrich Klaproth in 1789, around 100 years ago of the discovery of radioactivity by Henri Becquerel in 1896. The usage of uranium compounds as colourants for ceramics and glass has been documented since roman times however the element was not recognised in its pureform until the 1840s when Péligot succeeded in preparing metallic uranium by reduction of UCl_4 with potassium. The crucial importance of uranium to mankind was not established until 1939 upon the discovery of the nuclear fission of the element by Hahn and Strassman. Since then, the chemistry of uranium has occupied a central position in the field of nuclear energy, studied alongside the materials science and physics of the element with the primary aim of improving the safety and effectiveness of the many nuclear process in which uranium is now employed [16]. An early actinide often associated with radioactivity and nuclear fuel, uranium is a naturally occurring element with unique reactivity [17]. Among the actinides, uranium is the second most abundant element in the earth crust after thorium. The main uranium ore is U_3O_8 and is known as pitchblende, because it occurs in black, pitch-like masses. Uranium is mined primarily as part of an ore, occurring with an average crustal abundance of ~2 ppm but up to ~4 ppm in granitic ores, where most of the uranium is found in oxide form or as part of a mineral phase. It is also found in seawater at a concentration of ~0.003 ppm, which, although low, represents a significant reserve, which may one day be economically recoverable. Uranium extracted from the earth consists of three isotopes: ^{238}U, ^{235}U, and ^{234}U, with ^{238}U being the most abundant at a weight percentage of 99.27% and with a half-life of around 4.5 billion years [18]. Usage in the nuclear fuel industry requires enrichment of natural uranium to obtain a higher percentage abundance of fissile ^{235}U, producing depleted uranium (DU, containing typically between

0.2-0.4% ^{235}U) as a side product. Current uses for DU include ammunition, airplane counterbalances, radiation shields and drilling equipment [19]. ^{238}U is a weak alpha-emitter, and this coupled with its long half-life means that DU can be safely handled in a laboratory environment as long as sufficient care is taken not to ingest or inhale any material.

1.2.2 Chemical behaviour

The chemical behaviour of uranium differs from lanthanides, transition metals, and even from the later half of the actinide series, resulting in new forms of reactivity. Actinides possess 5f orbitals that are less shielded by 6s and 6p electrons, incomparison to the greater shielding of the lanthanide 4f orbitals by the 5s and 5p electrons [20]**.** Whilst bonding models of the f-block elements have mainly been classed as electrostatic, the diffuse nature of the 5f orbitals in uranium and the other early-actinides (Th to Np) allows some participation in covalent bonding, in comparison to the more ionic bonding of the lanthanides and later actinides. The more radially-extended 5f electrons also mean that π-back bonding is possible, hence multiple bonding is available for uranium as well as early-actinides [21]. For all these reasons, the early actinides are amongst the most synthetically attractive elements at the frontier of the periodic table, with uranium being the most readily available, easiest to manipulate and perhaps of greatest relevance to nuclear science.

Uranium has an electronic configuration of $[Rn]5f^3 6d^1 7s^2$ and can access oxidation states U(III) to U(VI), with U(IV) and U(VI) being the most common. It is a highly electropositive and oxophilic element and these characteristics along with its large ionic radii and potential for high coordination numbers result in it possessing some unique chemistry. For compounds of uranium in the +4 and +6 oxidation states, uranium oxides are ubiquitous in both the natural environment and the nuclear fuel cycle and it is for this reason that the physiochemical properties of such compounds have been studied in great detail [22].

1.2.3 Scope of synthetic uranium chemistry

Though it is true that in some instances it behaves like a transition metal, engaging in redox chemistry spanning multiple oxidation states, and in other times like a main group metal, displaying high lewis acidity and coordination number, it is on the rare occasion when the uranium ion exhibits a previously unknown reaction pathway or coordination mode that makes this metal so exciting to the modern synthetic chemist. The study of the coordination chemistry and reactivity of uranium is not purely an academic pursuit by any means, as fundamental principles revealed by these investigations are directly relevant to development of nuclear fuels, nuclear waste management and remediation, extraction of uranium from complex mixtures, and the development of depleted uranium as a catalyst.

New developments in synthetic uranium chemistry have leveraged the many available oxidation states of the uranium ion. In coordination complexes, uranium is known to adopt oxidation states ranging from 2+ to 6+ [23-27]. The majority of hexavalent uranium complexes that have been investigated contain the $U^{VI}O_2^{2+}$cation. The basic coordination chemistry of the uranium(VI) ion with simple ligand types including alkoxides [28], amides [29], ketimides [30] and alkyls [31], demonstrating the stability of the 6+ oxidation state in the absence of a uranium-ligand multiple bond was explained. In general, the U=O multiple bond lends incredible stability to the high valent state, shifting the U(VI/V) reduction potential over a 2 V range [32]. Uranium(VI) complexes typically appear diamagnetic by NMR spectroscopy, but are known to exhibit temperature independent paramagnetism [33] Much of the recent work on uranium(VI) complexes has focused on the preparation of novel uranium-ligand multiple bonds [34] with interest in understanding the role of covalency and the ability for the 5f and 6d orbitals to engage in bonding.

1.2.4 Extraction and Purification of Uranium

Uranium is deposited widely in the earth's crust, hence it has few ores, notably the oxides uraninite and pitchblende. The ores are leached with H_2SO_4 in the presence of an oxidizing agent such as $NaClO_3$ or MnO_2, to oxidize all the uranium to the (+6) state as a sulfate or chloride complex. On neutralization with ammonia a precipitate of 'yellow cake', a yellow solid with the approximate composition $(NH_4)_2U_2O_7$ is formed [35-36]. This is converted into UO_3 on ignition at 300 ^{o}C. This can be purified further by conversion into uranyl nitrate, followed by solvent extraction using tributyl phosphate in kerosene as the extractant.

1.2.5 Uranium Isotope Separation

Having purified the uranium, it is then treated to separate the ^{235}U and ^{238}U isotopes for nuclear fuel purposes (any uranium compounds purchased commercially are already depleted in ^{235}U) [37-38]. In practice, nuclear fuel requires enrichment from the natural abundance of 0.71% ^{235}U to around 5%, so what follows details a degree of enrichment not usually required. The uranium compound usually used is UF_6. It is chosen on account of its volatility (sublimes at 56.5 ^{o}C) and low molecular mass (M_r), despite its extreme sensitivity to moisture (and toxicity of the HF produced) requiring the use of scrupulously sealed and water-free conditions, as well as fluorine-resistant materials.

1.3 Compounds of uranium

1.3.1 Uranium halides

These form a large and interesting series of substances, in oxidation states ranging form +3 to +6, illustrating principles of structure and property. The structures of the uranium halides are shown in Table 1.1.

Table 1.1 Coordination polyhedra in the uranium halides [39].

Oxidation state	F	Cl	Br	I
6	Octahedron	Octahedron	-	-
5	Octahedron Pentagonal bipyramid	Octahedron dimer	Octahedron dimer	-
4	Sq. antiprism	Dodecahedron	Pentagonal bipyramid	Octahedron (chain)
3	Fully capped trigonal prism	Tricapped trigonal prism	Tricapped trigonal prism	Bicapped trigonal prism

1.3.1.1 Uranium(III) halides

Because of the ease of oxidation of the U^{3+} ion, these are all made under reducing conditions.

$$2\,UF_4 + H_2 \rightarrow 2\,UF_3 + 2\,HF\ (950\ ^oC)$$

$$2\,UH_3 + 6\,HCl \rightarrow 2\,UCl_3 + 3\,H_2\ (350\ ^oC)$$

$$2\,UH_3 + 6\,HBr \rightarrow 2\,UBr_3 + 3\,H_2\ (300\ ^oC)$$

$$2\,UH_3 + 3\,HI \rightarrow 2\,UI_3 + 3\,H_2\ (300\ ^oC)$$

These compounds have structures typical of the actinide trihalides. Green UF_3 has the 11-coordinate LaF_3 structure whilst UCl_3 and UBr_3, both red, have the tricapped trigonal prismatic 'UCl_3' structure. Nine iodide ions cannot pack round uranium, so black UI_3 adopts the 8-coordinate $PuBr_3$ structure [40].

1.3.1.2 Uranium (IV) halides

In normal laboratory work, these are the most important uranium halides, especially UCl_4.

$$UO_2 + 4\,HF \rightarrow UF_4 + 2\,H_2O\ (550\ ^oC)$$

$$UO_2 + 2\,CCl_4 \rightarrow UCl_4 + 2\,COCl_2\ (250\ ^oC)$$

$$U_3O_8 + C_3Cl_6 \rightarrow 3\,UCl_4 + Cl_2C{=}CClCOCl \text{ etc. (reflux)}$$

$$U + 2\,Br_2 \rightarrow UBr_4\ (He/Br_2;\ 650\ ^oC)$$

$$U + 2\,I_2 \rightarrow UI_4\ (I_2;\ 500\ ^oC,\ 20\ kPa)$$

HF is used in the synthesis of the tetrafluoride since obviously the use of fluorine in this reaction would tend to produce UF_6. Although Peligot first prepared UCl_4 in 1842 by the reaction of uranium oxide with chlorine and charcoal, nowadays it is conveniently made by refluxing the oxide with organochlorine compounds such as hexachloropropene and CCl_4 [41-42]. U^{4+} does not have reducing tendencies, and UI_4 is stable, though not to hydrolysis.

Table 1.2 lists some properties of these compounds. As usual in the lower oxidation states, the fluorides have significantly lower volatilities. In fact, like the other MF_4 and MCl_4, UF_4 vapourizes as MF_4 molecules. As usual, the coordination number C.N. of the metal decreases as the halogen gets larger whilst the bond lengths increase.

Table 1.2 Uranium(IV) halides

	UF_4	UCl_4	UBr_4	UI_4
Description	Air-stable green solid	Deliquescent green solid	Deliquescent brown solid	Deliquescent black solid
Mp (^oC)	1036	590	519	506
Bp (^oC)		789	761	
Solubility		H_2O and most org.solvents	H_2O and most org.solvents	H_2O and most org.solvents
Coordination geometry	Square antiprism	Dodecahedron	Pentagonal bipyramid	Octahedron
C.N. of uranium	8	8	7	6
U–X distance (A°)	2.25–2.32	2.64–2.87	2.61 (term.) 2.78–2.95 (bridge)	2.92(term.) 3.08–3.11 (bridge)

1.3.1.3 Uranium(V) halides

These are among the best characterized compounds in this somewhat rare oxidation state, although they do tend to be unstable (see the preparation of UCl_6) and UI_5 does not exist.

$$2\ UF_6 + 2\ HBr \rightarrow 2\ UF_5 + Br_2 + 2\ HF$$

$$2\ UO_3 + 6\ CCl_4 \rightarrow 2\ UCl_5 + 6\ COCl_2 + Cl_2\ (20\ \text{atm.}, 160\ ^oC)$$

$$2\ UBr_4 + Br_2 \rightarrow 2\ UBr_5\ (\text{Soxhlet extraction; brown solid})$$

Grey UF_5 has a polymeric structure with 6- and 7-coordinate uranium, whilst red-brown UCl_5 and brown UBr_5 have a dimeric structure in which two octahedra share an edge.

1.3.1.4 Uranium(VI) halides

UF_6 and UCl_6 are two remarkable substances, the former on account of its application in isotopic enrichment of uranium [43-44]; the latter as the only actinide hexachloride. Colourless UF_6 can be made by a wide variety of routes, including:

$$UF_4 + F_2 \rightarrow UF_6 \ (250\text{–}400\ ^\circ C)$$

$$3UF_4 + 2ClF_3 \rightarrow 3UF_6 + Cl_2$$

$$2UF_4 + O_2 \rightarrow UF_6 + UO_2F_2 \ (600\text{–}900\ ^\circ C)$$

Dark green, hygroscopic, UCl_6 may be synthesized by halogen exchange or disproportionation:

$$UF_6 + 2\ BCl_3 \rightarrow UCl_6 + 2\ BF_3 \ (-107\ ^\circ C)$$

$$2\ UCl_5 \rightarrow UCl_4 + UCl_6 \ (120\ ^\circ C)$$

Both have octahedral molecular structures (U–F = 1.994 A° in UF_6) and are volatile under reduced pressure at temperatures below 100 ^oC.

1.3.2 Uranium Oxides

The uranium–oxygen phase diagram is very complicated, with some of the 14 reported phases not being genuine and several phases showing variable composition. The important phases are UO_2, U_4O_9, U_3O_8, and UO_3. Brown-black UO_2 has the fluorite structure. It is best made by reduction of higher uranium oxides (e.g. UO_3 with H_2 or CO at 300–600 ^oC). Additional oxygen can be incorporated into interstitial sites in the basic fluorite structure until the composition reaches U_4O_9 (black $UO_{2.25}$). Green-black U_3O_8 is the result of heating uranyl salts at around 650–800 ^oC; above 800 ^oC, it tends to lose oxygen.

$$3\ UO_2(NO_3)_2 \rightarrow U_3O_8 + 6\ NO_2 + 2\ O_2$$

This is a mixed-valence compound with pentagonal bipyramidal coordination of uranium. Addition of more oxygen eventually results in orange-yellow UO_3. This has several crystalline forms, most of which contain uranyl groups in 2 + 4 coordination, and can be made by heating, e.g., $(NH_4)_2U_2O_7$ or $UO_2(NO_3)_2$ at 400–600 °C (above which temperature, oxygen loss to U_3O_8 tends to occur). When uranium oxides are heated with M_2CO_3 or $M'CO_3$ (M, M' are group I or II metals), uranates with formulae such as Na_2UO_4 or $K_2U_2O_7$ result [45]; unlike d-block metal compounds with similar formulae, these contain UO_6 polyhedra.

1.3.3 Oxyhalides

The most important oxyhalides, though, are the uranium compounds. Yellow UO_2F_2 and UO_2Cl_2, and red UO_2Br_2, have been known for a long while, but the existence of beige UO_2I_2 was doubted for many years, only being confirmed in 2004 by Berthet *et al* [46].

$$UO_3 \rightarrow UO_2F_2\ (HF;\ 400\ ^{o}C)$$

$$U_3O_8 \rightarrow UO_2Cl_2.2\ H_2O\ (HCl/H_2O_2)$$

$$UO_2Cl_2.\ 2H_2O \rightarrow UO_2Cl_2\ (Cl_2/HCl;\ 450\ ^{o}C)$$

$$UCl_4 \rightarrow UO_2Cl_2\ (O_2;\ 350\ ^{o}C)$$

$$UBr_4 \rightarrow UO_2Br_2\ (O_2;\ 170\ ^{o}C)$$

$$UO_2(OTf)_2 \rightarrow UO_2I_2\ (Me_3SiI;\ OTf = CF_3SO_3)$$

In the solid state, UO_2F_2 has a structure in which a uranyl unit is bound to six fluorides (all bridging); whilst in UO_2Cl_2 uranium is bound to the two 'oxo' oxygens, four chlorines, and another oxygen, from another uranyl unit. UO_2I_2 has not been obtained in crystalline form.

A number of adducts of the oxyhalides are well characterized, such as *all-trans*-$[UO_2X_2L_2]$ [X = Cl, L = Ph_3PO; X = Br, L = $(Me_2N)_3PO$; X = I, L = $(Me_2N)_3PO$, Ph_3PO, Ph_3AsO]. Others are anionic, containing ions such as $[UO_2F_5]^{3-}$ and $[UO_2X_4]^{2-}$ (X = Cl, Br).

1.3.4 Uranyl Chemistry

1.3.4.1 Uranyl complexes

The great majority of uranium(VI) compounds contain the UO_2 group and are known as uranyl compounds; exceptions are a few molecular compounds, such as the halides UOF_4, UF_6, and UCl_6, and some alkoxides such as $U(OMe)_6$. Uranyl compounds result eventually from exposure of compounds of uranium in other oxidation states to air. They characteristically have a yellow fluorescence under UV light.

Uranyl complexes can be thought of as derivatives of the UO_2^{2+}ion. There is a very wide range of them; they may be cationic, such as $[UO_2(OH_2)_5]^{2+}$ions; neutral, e.g. $[UO_2(OPPh_3)_2Cl_2]$; or anionic, such as $[UO_2Cl_4]^{2-}$, yet all feature a *trans*-UO_2 grouping with the characteristic short U–O bonds (1.7–1.9 A°). The presence of the uranyl group can readily be detected in the IR spectrum of a uranium compound through the presence of a strong band in the region 920–980 cm^{-1} caused by the asymmetric O–U–O stretching vibration; a corresponding band around 860 cm^{-1} caused by the symmetric O–U–O stretching vibration is seen in the Raman spectrum. Fine structure due to symmetric uranyl stretching vibrations can be seen on an absorption peak in the spectrum of uranyl complexes around 450 nm. The essentially linear geometry of the UO_2 unit is an invariable feature of uranyl complexes; no other atoms can approach the uranium nearer than ~2.2 A°. Uranium d–p and f–p π bonding have both been invoked to explain the bonding [47] (Fig. 1.1).

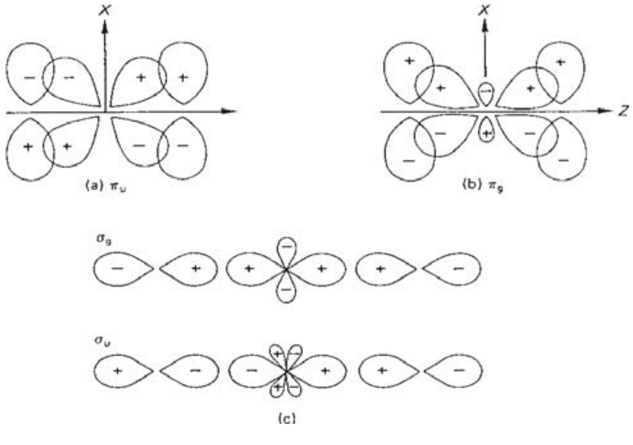

Fig. 1.1 π-bonding in the uranyl, $[UO_2]^{2+}$ ion: (a) d_{xz}–p_x overlap; (b) f_{xz^2}–p_x overlap; (c) σ-bonding in the uranyl ion.

The uranium(V) species UO_2^+exists, but is less stable than UO_2^{2+}, possibly owing to weaker overlap; it readily decomposes by disproportionation:

$$2\ UO_2^+(aq) + 4\ H^+(aq) \rightarrow UO_2^{2+}(aq) + U^{4+}(aq) + 2\ H_2O(l)$$

1.3.4.2 Molecular orbital description of uranyl complexes

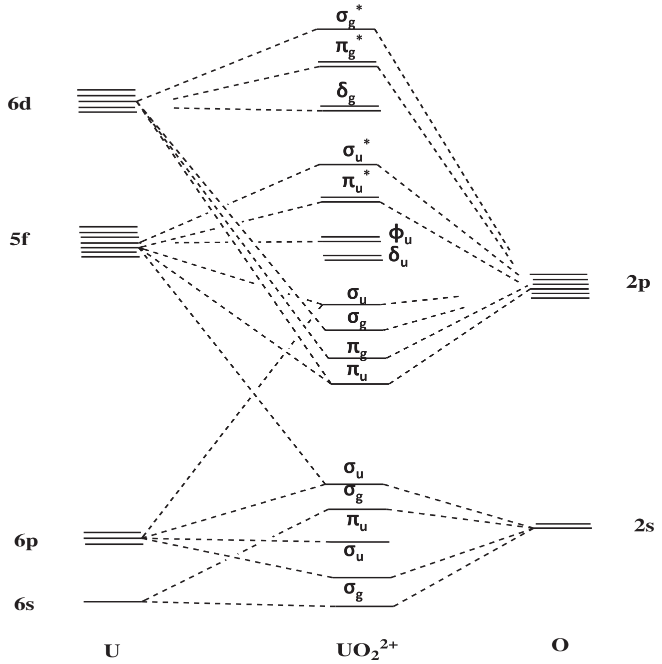

Fig. 1.2 Molecular orbital diagram of uranyl complexes

An energy level diagram for the uranyl ion is shown in Figure 1.2. An electron count takes 6 electrons from uranium, four from each oxygen, deducting two for the positive charges; alternatively, if the uranyl ion is thought of as a combination of U^{6+} and two O^{2-} , taking six electrons from each oxide and none from U^{6+} , again giving 12. These completely occupy the six σ_u , σ_g , π_u , and π_g molecular orbitals ($\sigma_u^2\ \sigma_g^2\ \pi_u^4\ \pi_g^4$). The overlap of the atomic orbitals results in the formation of a formal U≡O triple bond. It has been suggested that repulsion (antibonding overlap) between oxygen p orbitals and occupied uranium 6d and 5f orbitals may destabilize the bonding σ molecular orbitals, causing them to be higher in energy than the π bonding orbitals, as shown. Addition of further electrons puts them in the essentially non-bonding δ_u and φ_u orbitals, accounting for the existence of the rather less stable MO_2^{2+} (M = Np, Pu, Am) ions. Ligand donor atoms can take part bonding with this linear $O{=}U{=}O^{2+}$ species only from the equatorial position due to matching symmetry of δ_u, φ_u orbitals and donor atomic orbitals.

1.3.4.3 Absorption and emission spectra

The ground state of the uranyl ion has a closed-shell electron configuration. There is a characteristic absorption ~25 000 cm^{-1} (400 nm) which frequently gives uranyl compounds a yellow colour (though other colours like orange and red are not infrequent). This absorption band often exhibits fine structure due to progressions in symmetric O=U=O vibrations in the excited state, sometimes very well resolved, sometimes not.

It should also be remarked that uranyl complexes tend to emit a bright green fluorescence under UV irradiation, from the first excited state. This is used by geologists both to identify and to assay uranium-bearing minerals in deposits of uranium ores.

1.3.4.4 Coordination numbers and geometries in uranyl complexes

An extensive range of uranyl complexes has been prepared and had their structures determined. Their structure can be summarized as a uranyl ion surrounded by a 'girdle' of 4, 5, or 6 donor atoms round its waist (a rare example of 2 + 3 coordination is known for a complex of the uranyl ion with a calixarene ligand [48]; another is the amide complex $[K(thf)_2]\ [UO_2\{N(SiMe_3)_2\}_3]$ [49]). If the ligands are monodentate donors, there are usually 4 of them, unless they are small, like F or NCS, when five can be accommodated. When bidentate ligands with small steric demands like NO_3, CH_3COO, and CO_3 can be accommodated, six donor atoms can surround the uranyl group. Table 1.3 shows examples of uranium complexes for 5-, 6-, 7-, and 8-coordination.

Table 1.3 Uranyl complexes

5-coordinate (2 + 3)	6-coordinate (2 + 4)	7-coordinate (2 + 5)	8-coordinate (2 + 6)
$[UO_2\{N(SiMe_3)_2\}_3]^-$	$Cs_2[UO_2Cl_4]$ $(Me_4N)_2[UO_2Br_4]$ $MgUO_4$ $BaUO_4$	UO_2Cl_2 UO_2(superphthalocyanine) $[UO_2(NO_3)_2(Ph_3PO)]$ $[UO_2(L)_5]^{2+}$ (L, e.g., H_2O, DMSO, urea)	UO_2F_2 UO_2CO_3 $[UO_2(NO_3)_2(H_2O)_2]$ $CaUO_4$ $SrUO_4$ $Rb[UO_2(NO_3)_3]$

The uranium(VI) aqua ion is now firmly established as the pentagonal bipyramidal $[UO_2(OH_2)_5]^{2+}$; it has been found in crystals of the salt $[UO_2(OH_2)_5]$ $(ClO_4)_2.2H_2O$ (U=O 1.702 A° , U–OH_2 2.421 A°) and also found in solutions by X-ray diffraction studies. Similar $[UO_2(L)_5]^{2+}$ions (L = urea, Me_2SO, $HCONMe_2$) also exist. Uranyl nitrate forms complexes with phosphine oxides of the type $[UO_2(NO_3)_2(R_3PO)_2]$; similar phosphate complexes $[UO_2(NO_3)_2\{(RO)_3PO\}_2]$ are important in the extraction of uranium in nuclear waste processing (Fig. 1.3).

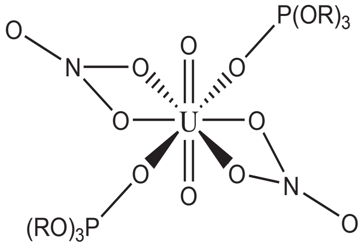

Fig. 1.3 Structure of $UO_2(NO_3)_2[(RO)_3PO]_2$

1.3.4.5 Some Other Complexes

Uranyl carbonate complexes have attracted considerable interest in recent years as they are intermediates in the processing of mixed oxide reactor fuels and in extraction of uranium from certain ores using carbonate leaching [50]; more topically they can be formed when uranyl ores react with carbonate or bicarbonate ions underground, and can be present in relatively high amounts in groundwaters [51-52]. The main complex formed in carbonate leaching of uranyl ores is 8 coordinate $[UO_2(CO_3)_3]^{3-}$, but around pH 6 a cyclic trimer $[(UO_2)_3(CO_3)_6]^{6-}$ has been identified.

UO_3 dissolves in acetic acid to form yellow uranyl acetate, $UO_2(CH_3COO)_2.2H_2O$. It formerly found use in analysis since, in the presence of M^{2+} (M = Mg or Zn), it precipitates sodium ions as $NaM[UO_2(CH_3COO)_3]_3.6H_2O$.

1.3.4.6 Uranyl nitrate and its complexes; their role in processing nuclear waste

Reaction of uranium oxide with nitric acid results in the formation of nitrates $UO_2(NO_3)_2 \cdot xH_2O$ (x = 2, 3, 6); the value of x depends upon the acid concentration [53]. All contain $[UO_2(NO_3)_2(H_2O)_2]$ molecules; the nitrate groups are bidentate, so that uranium is 8 coordinate (Fig. 1.4). Its most important property lies in its high solubility in a range of organic solvents in addition to water, which is an important factor in the processing of nuclear waste.

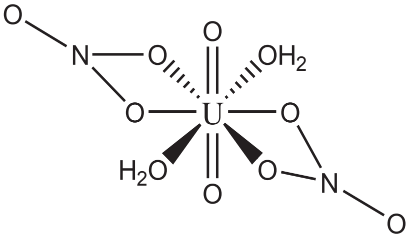

Fig. 1.4 Structure of $UO_2(NO_3)_2(H_2O)_2$

By adding metal nitrates as 'salting out' agents, the solubility of uranyl nitrate in water can be decreased to favour its extraction from aqueous solution into the organic layer. Tributyl phosphate [TBP; $(C_4H_9O)_3P{=}O$] acts as a complexing agent and also as solvent, with no salting out agent being needed. In practice, a solution of TBP in kerosene is used to give better separation, as pure TBP is too viscous and also has a rather similar density to that of water [54].

1.3.4.7 Uranyl Beta-diketonates

Numbers of acidic extractants were employed for the separation of actinide ions from the acidic media and the well studied extractants are β-diketonates [55-56]. These extractants are having ionisable protons and could be easily dissociated to form complexes with the metal ions. These complexes are organic soluble and could be extracted in to the organic phases. Complexes responsible for the extraction in many of the cases were isolated in the solid state and characterized by using the well known spectroscopic techniques, like IR, ^{1}H, ^{19}F NMR.

The structure of $[UO_2(TTA)_2. 2H_2O]$ (where, HTTA = Thenoyltrifluoroacetone) [57] shows that the uranyl group is bonded to two of the TTA units and one of the water molecule in the primary coordination sphere. The coordination number and geometry around the uranium(VI) is seven and pentagonal bi-pyramidal. The second water molecule is present in the second coordination sphere and hydrogen bonded to the first water molecule. The structures for the tetravalent metal β-diketonate complexes $[M(OO)_4]$ (M = Th, U or Pu) (OO = β-diketonate anion) [58] show that the metal ion is surrounded by four β-diketonate anions in a square anti-prismatic geometry.

1.3.5 Complexes of the uranium(IV)

1.3.5.1 Nitrate complexes

Uranium forms complexes in the +4 state that are generally similar to those of thorium.

$$Cs_2U(NO_3)_6 + 2\ Ph_3PO \rightarrow U(NO_3)_4(OPPh_3)_2 + 2\ CsNO_3$$

The reaction is carried out in a polar solvent like propanone; precipitated caesium nitrate is filtered off and green (the most characteristic colour of U^{IV} complexes) crystals of the nitrate complex are obtained on concentrating the solution. $U(NO_3)_4(OPPh_3)_2$ has a 10-coordinate structure (Fig. 1.5) with phosphine oxide ligands *trans* to each other, and bidentate nitrates.

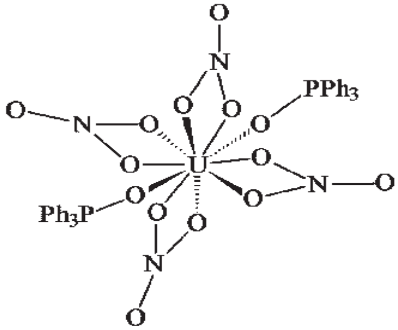

Fig. 1.5 Structure of $U(NO_3)_4(Ph_3PO)_2$.

1.3.5.2 Halide complexes

A large number of these have been synthesized, usually by reaction of the halides with the ligand in a polar solvent like MeCN or acetone, which will form a labile complex such as $[UCl_4(MeCN)_4]$ that will undergo ready substitution by a stronger donor:

$$UCl_4 + 2\ (Me_2N)_3PO \rightarrow UCl_4[(Me_2N)_3PO]_2\ \text{(in } Me_2CO\text{)}$$

Although sometimes direct reaction with a liquid ligand is possible:

$$UCl_4 + 3\ THF \rightarrow UCl_4(thf)_3$$

$$UCl_4 + 2\ Me_3N \rightarrow UCl_4(Me_3N)_2$$

Relatively few UI_4 complexes have been made. They can often be synthesized by reaction in a solvent like MeCN and, whilst relatively stable thermally, undergo ready oxidation to uranyl complexes in (moist) air. The structures of many of these compounds have been determined, such as UCl_4L_2 [L = Ph_3PO, $(Me_2N)_3PO$, Et_3AsO, $(Me_2N)_2PhPO$] and UBr_4L_2 [L = Ph_3PO, $(Me_2N)_3PO$] and $UX_4[(Me_2N)_2CO]_2$(X = Cl, Br, I). Both the 2:1 stoichiometry and *trans*-UX_4L_2 geometry are very common, but there are exceptions. $UCl_4(Me_2SO)_3$ is $[UCl_2(Me_2SO)_6]UCl_6$ and $UCl_4(Me_3PO)_6$ is $[UCl(Me_3PO)_6]Cl_3$; although no X-ray study has been carried out, $UI_4(Ph_3AsO)_2$ is almost certainly $[UI_2(Ph_3AsO)_4]\ UI_6$.

The only complete family of UX_4 complexes (X = Cl, Br, I) that has been examined crystallographically is that with tetramethylurea, $UX_4[(Me_2N)_2CO]_2$.

1.3.5.3 Thiocyanates

As the anhydrous actinide thiocyanates are not known {only hydrated $[M(NCS)_4(H_2O)_4]$}, thiocyanate complexes are prepared metathetically.

$$UCl_4(Ph_3PO)_2 + 4\ KNCS + 2\ Ph_3PO \rightarrow U(NCS)_4(Ph_3PO)_4 + 4\ KCl\ \text{(in } Me_2CO\text{)}$$

The precipitate of insoluble KCl is filtered off and the solution concentrated to obtain the actinide complex. The structure of $U(NCS)_4(L)_4$ [L=Ph_3PO, $(Me_2N)_3PO$, Me_3PO] are all square antiprismatic.

Some complexes are known where thiocyanate is the only ligand bound to uranium. The geometry of $(Et_4N)_4[U(NCS)_8]$ is cubic, whilst $Cs_4[U(NCS)_8]$ is square antiprismatic.

1.4. Palladium

1.4.1 General introduction

Palladium is a chemical element with symbol Pd and atomic number 46. It was discovered in 1803 by William Hyde Wollaston. He named it after the asteroid Pallas, which was itself named after the epithet of the Greek goddess Athena, acquired by her when she slew Pallas. Palladium is a soft silver-white metal that resembles platinum. It is soft and ductile when annealed and is greatly increased in strength and hardness when cold-worked. Palladium does not tarnish in air. It dissolves slowly in concentrated nitric acid, in hot, concentrated sulfuric acid, and when finely ground, in hydrochloric acid [59]. It dissolves readily at room temperature in aqua regia. Palladium, platinum, rhodium, ruthenium, iridium and osmium form a group of elements referred to as the platinum group metals (PGMs). These have similar chemical properties, but palladium has the lowest melting point and is the least dense of them. Palladium belongs to group 10 in the periodic table, but the configuration in the outermost electron shells is atypical for group 10. Palladium compounds primarily exist in the 0 and +2 oxidation state. Other less common states are also recognized. The largest use of palladium today is in catalytic converters [60-61]. Hydrogen readily diffuses through heated palladium, so this method is often used to purify the gas. Palladium is also used in jewellery, dentistry, watch making, blood sugar test strips, aircraft spark plugs, surgical instruments, and electrical contacts [62-64]. Palladium is a key component of fuel cells, which react hydrogen with oxygen to produce electricity, heat, and water. ^{103}Pd, a radioactive isotope of palladium (half-life 17 days), has been used in the treatment of prostate and breast cancer [65-66]. Naturally occurring palladium is composed of seven isotopes, six of which are stable. The most stable radioisotopes are ^{107}Pd with a half-life of 6.5 million years (found in nature), ^{103}Pd with 17 days, and ^{100}Pd with 3.63 days. Eighteen other radioisotopes have been characterized with atomic weights ranging from 90.94948(64) u (^{91}Pd) to 122.93426(64) u

(^{123}Pd). These have half-lives of less than thirty minutes, except ^{101}Pd (half-life: 8.47 hours), ^{109}Pd (half-life: 13.7 hours), and ^{112}Pd (half-life: 21 hours).

Table 1.4 Some parameters of elemental palladium.

Parameter	
Atomic symbol	Pd
Atomic number	46
Atomic weight/g mol^{-1}	106.42
Electronic configuration	[Kr] 4d^{10}
Density(20°C)/g cm^{-3}	12.023
Melting point/°C	1,554.9
Boiling point/°C	2,963
ΔH_{fus}/ kJ mol^{-1}	16.74
ΔH_{vap}/ kJ mol^{-1}	358
Molar heat capacity J mol^{-1}K^{-1}	25.98
Electronegativity (Pauling Scale)	2.20
Electrical resistivity (20°C)/μ-cm	105.4
Number of stable isotopes	9
Effective ionic radius (6-coordinated) (in pm)	75.5 (Pd^{4+} ion)
	90 (Pd^{3+} ion)
	78 (Pd^{4+} ion)
Effective ionic radius (4-coordinated) (in pm)	100 (Pd^{4+} ion)

1.4.2 Oxidation states

Although palladium can exist in a number of different oxidation states, the most stable oxidation states are Pd(0) and Pd(II) [67], although few Pd(IV) [68] compounds have been reported. There are relatively few known compounds with palladium unambiguously in the

+3 oxidation state, though such compounds have been proposed as intermediates in many palladium-catalyzed cross coupling reactions [69]. In 2002, palladium(VI) was first reported [70]. The increased stability of the even-numbered oxidation states (e.g., 0, +2, +4) can be rationalized by the low tendency of palladium to undergo one-electron or radical processes; conversely, it readily participates in two-electron oxidation or reduction. Palladium's ability to undergo facile and reversible two-electron operations has contributed to its widespread use as a catalyst, since each oxidation state can yield different chemistry. Reactions such as cross couplings and olefin hydrogenation are common to the Pd(0) platform, while transformations such as alcohol oxidation and cyclo-isomerization can be achieved using Pd(II).

1.4.3 Compounds of palladium

Palladium generally prefers low oxidation states. Elemental palladium reacts with chlorine to give palladium(II) chloride; it dissolves in nitric acid and precipitates palladium(II) acetate on addition of acetic acid. These two compounds and the bromide are reactive and relatively inexpensive, making them convenient entry points to palladium chemistry [71-72]. All three are not monomeric; the chloride and bromide often must be refluxed in acetonitrile to obtain the more reactive acetonitrile complex monomers. Palladium(II) chloride is used to prepare heterogeneous palladium catalysts: palladium on barium sulfate, palladium on carbon, and palladium chloride on carbon. It reacts with triphenylphosphine in coordinating solvents to give bis(triphenylphosphine)palladium(II) dichloride, a useful catalyst. The great many reactions in which palladium compounds serve as catalysts are collectively known as palladium-catalyzed coupling reactions. Prominent examples include the Heck, Suzuki and Stille reactions.

Zero valent $4d^{10}$ complexes of palladium generally contain tertiary phosphine donor ligands, and are often prepared by reduction of an appropriate palladium(II) complex. Phosphine free zerovalent complexes of palladium are also known, for example, $[Pd(AsPh_3)_4]$, and the dibenzylidineacetone complex [Pd(dba)$_2$]. A number of dinuclear Pd(0) complexes containing bridging ligands have also been characterised, examples include [Pd$_2$(dcpe)$_2$] [73], [Pd$_2$(dppm)$_3$] [74] and [Pd$_2$(dba)$_3$] [75]. It should be noted that palladium, like platinum, does not form any simple carbonyl complexes analogous to [Ni(CO)$_4$], but more stable mixed phosphine-carbonyl complexes are known, e.g. [Pd(CO)(PPh$_3$)$_3$] [75]. Zero valent cluster compounds have also been reported, such as [Pd$_3$(CNCy)$_6$] [76] which contains a triangle of Pd(0) atoms. An enormous number of palladium(0) carbonyl-phosphine clusters of varying nuclearity with the general formula [Pd$_n$(CO)$_x$(PR$_3$)$_y$] are known, in which n can take values from 3 to 145 [77-78].

By far, the most common oxidation state of palladium is divalent (4d^8) and is a typical Class B (soft) metal ion, hence prefers to bind with elements of higher atomic number in a given group of the periodic table. For example, the affinity of palladium(II) to form complexes with halides decreases in the order $I^- > Br^- > Cl^- > F^-$; similarly the observed order of ligand binding affinities are $SR_2 > OR_2$ and $PR_3 > NR_3$ [**79].** A large number of cationic, neutral and anionic complexes of palladium(II) are known [**75],** and the metal centre is generally fourcoordinate, adopting square planar geometry, as is observed in [Pd(NH$_3$)$_4$][Pd(SCN)$_4$] [80], Vauquelin's salt [Pd(NH$_3$)$_4$][PdCl$_4$] [76], [Pd(NH$_3$)$_4$]Cl$_2$ [75] and (Ph$_4$P)$_2$[Pd$_2$(SPh)$_6$] [81]. Higher coordination numbers are also possible with strong σ-donor ligands; [PdCl(diars)$_2$]$^+$ [75] and [PdCl$_2$(PMe$_2$Ph)$_3$] [82] are examples of five-coordinate trigonal bipyramidal and square pyramidal complexes, respectively.

Mononuclear trivalent 4d^7 palladium complexes are relatively uncommon, although examples of these paramagnetic species containing an unpaired electron have been reported. In general, they contain large, electron-rich macrocyclic ligands capable of shielding the metal centre (hence unpaired electron) from electron pairing, preventing the formation of dinuclear diamagnetic species containing a formal metal-metal bond. Careful electrochemical oxidation of the divalent palladium complexes $[Pd(ttcn)_2][PF_6]_2$ and $[Pd(tacn)_2][PF_6]_2$ (ttcn = 1,4,7-trithiacyclononane, tacn = 1,4,7-triazacyclononane) gave the trivalent species $[Pd(ttcn)_2][PF_6]_3$ [83] and $[Pd(tacn)_2][PF_6]_3$ [84] respectively.

Tetravalent $4d^6$ palladium complexes generally adopt octahedral geometry about the metal centre, however, unlike their platinum analogues, this oxidation state is much less accessible, owing to the higher ionisation potential required to form Pd^{4+}. The highly reactive PdF_4 is the only known simple halide of palladium(IV) and has been shown by neutron powder diffraction to contain octahedrally coordinated palladium atoms bound to four bridging and two terminal fluorine atoms [85]. Palladium(IV) complexes are usually prepared by oxidative addition procedures, although the products are often labile towards reductive elimination. Complexes of the type $[PdCl_4L_2]$ (L = NMe_3, py, Pn Pr_3; L_2 = bipy) and trans-$[PdCl_2L_2][ClO_4]_2$ [L_2 = $Me_2PCH_2CH_2PMe_2$, o-$C_6H_4(AsMe_2)_2$] [86,87] have been prepared. Several palladium(IV) complexes containing a tridentate N,N′,C-ligand, derived by C−H activation of a neutral bipyridylamide ligand, that are more resistant to reductive elimination have also been reported [88].

1.4.4 Molecular orbital description of palladium(II) square planar complexes

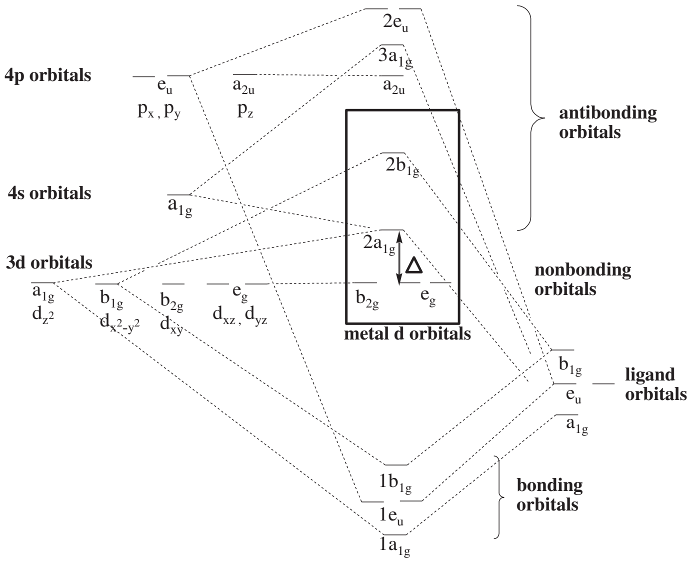

Fig. 1.6 Molecular orbital diagram of palladium(II) square planar complexes

An energy level diagram for a square planar Pd(II) ion is shown in Figure 1.6. In this type of complex with square planar geometry in the xy plane, having four identical ligands oriented along the x and y axes (D_{4h} symmetry), the σ-orbitals of Pd(II) are those directed along the x and y axes, including the spherical 5s and the $4d_{z2}$ which has its collar around the xy plane. Thus we have the following Pd(II) orbitals with their symmetry lebels:

5s : a_{1g}
$5p_x$, $5p_y$: e_u $5p_z$: a_{2u}
$4d_{z2}$: a_{1g} $5d_{xz}$, $5d_{yz}$: e_g
$5d_{xy}$: b_{2g} $5d_{x2-y2}$: b_{1g}

The a_{2u}, e_g and the b_{2g} orbitals do not make any net σ-overlap in the xy plane and remain nonbonding in a σ-only system. The four ligands give rise to LGO-s of a_{1g}, b_{1g} and e_u symmetry which interact with Pd(II) orbitals of the same symmetry. Eight 4d electrons of Pd(II) ion and eight electrons from four ligands together form molecular orbital of total 16 electrons. These may be assigned just to fill all the bonding m.o-s and all anti-bonding molecular orbitals are vacant. Thus we may infer that square planar Pd(II) complexes is most stable four coordinated complexes.

1.5 Structural studies on the compounds of lanthanides relevant to separation process

As the coordination chemistry of trivalent actinides is similar to the trivalent lanthanides, we have synthesized and studied the complex chemistry of some lanthanide nitrate complexes with few previously unexplored ligands.

1.5.1 Nitrate compounds

Lanthanide nitrates dissolve easily in polar solvents such as water, alcohols, esters or nitriles. Lanthanide nitrates usually have the formula $[RE(NO_3)_3 \cdot nH_2O]$, where $n = 6$ for the lighter rare earth nitrates (lanthanum to neodymium) and $n = 5$ for the heavier rare earth nitrate (europium to lutetium) and this is due to lanthanide contraction. In lanthanide nitrates, the nitrate groups usually behaves as a bidentate chelating ligand similar to reported in $[Ce(NO_3)_3(C_5H_7N_2CH_2CONBu_2)_2]$ [89].

1.5.2 Monodentate neutral ligand lanthanide nitrate compounds

Lanthanide nitrates form weak complexes with monoamides, sulfoxides and phosphates [90-92]. In general, these ligands show very poor extractions for lanthanides from HNO_3 medium due to poor complexing ability of these ligands with lanthanide ions. However, the phosphine oxides show appreciable extraction for these ions from nitric acid medium [93] and larger number of phosphine oxide compounds are isolated in solid state and structurally characterized. The phosphine oxides form either $[Ln(NO_3)_3(OPR_3)_3]$ [94] or $[Ln(NO_3)_3(OPR_3)_4]$ [95] types of complexes with coordination number varies between 9 and 10.

1.5.3 Bidentate neutral ligand lanthanide nitrate compounds

Many bi-functional ligands such as carbamoyl methyl phosphonates, carbamoyl methyl phosphine oxides, carbamoyl methyl sulfoxide ligands show excellent extraction for lanthanide and actinide ions from nitric acid medium [96-99]. Numbers of compounds are isolated in solid state and are structurally characterized. All these ligands form 2:1 complexes with lanthanide nitrates with the formula $[Ln(NO_3)_3.2L]$ (where, L = malonamides, carbamoyl methyl phosphonates, carbamoyl methyl phosphine oxides, carbamoyl methyl sulfoxide). In all cases, the ligands act as bidentate chelating ligands and bond through both the donor groups (Fig. 1.7). The coordination number and geometry are 10 and bi-capped square antiprism, respectively.

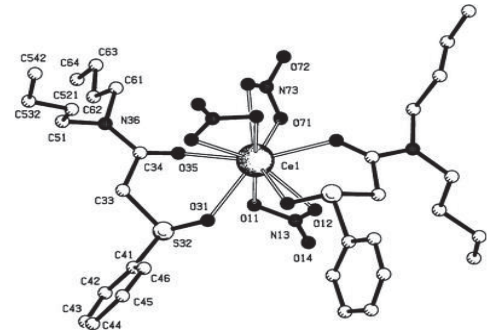

Fig. 1.7 Structure of $[Ce(NO_3)_3(PhSOCH_2CON^iBu_2)_2]$

1.5.4 Tridentate neutral ligand lanthanide nitrate compounds

In recent years, tri-functional chelating ligands of diglycolamide type show excellent extractions for the trivalent lanthanides and actinides from nitric acid medium [100]. For some of the cases, the lanthanide complexes are isolated and structurally characterized. In all cases, the ligand act as tridentate chelating ligand and bond through both the carbamoyl and ethereal oxygen atoms to the metal centre. These ligand form 3:1 complexes of the formula $[LnL_3](NO_3)_3$ with lanthanide nitrates, in which the nitrate ions are outside the coordination sphere [101]. Tri-functional ligands containing nitrogen donor centres are also show good extraction for trivalent actinide ions over lanthanide ions [102-103] and for some cases, the species responsible for the separation have been structurally characterized [102]. In most of the cases, the ligand act as tridentate ligands and bond through all nitrogen atoms to metal centre (Fig.1.8).

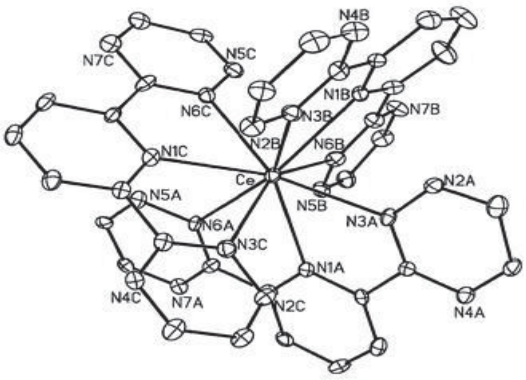

Fig. 1.8 Structure of $[Ce(Mebtp)_3]^{3+}$

1.6. Materials and methods

1.6.1 Glassware

Glassware fitted with interchangeable standard ground joints were used. Special types ofglassware with appropriate joints were used for synthesis and storage of compounds. Precipitates formed during the reaction were filtered through G-3 and G-2 sintered disks. All the glassware were immersed overnight in an alkali bath [5% NaOH in ethanol-water(1:1 v/v) mixture], washed thoroughly with water, rinsed with distilled water followed byacetone and dried at 120-130 °C overnight prior to experiment. Synthesized air and moisture sensitive compounds were storedinside desiccator containing either silica gel beads or fused $CaCl_2$.

1.6.2 Solvents and Chemicals

All solvents used were of AR grade and dried by standard procedures [104]. Benzene and toluene were dehydrated and purified by refluxing them with sodium metal and benzophenone. Dichloromethane and acetonitrile were dried over P_2O_5 followed by distillation. Methanol was refluxed over magnesium methoxide (prepared from magnesium turnings and methanol inpresence of catalytic amount of iodine) for 2 h and distilled under nitrogen atmosphere.

The starting compounds $[UO_2(NO_3)_2.6H_2O]$, UO_2Cl_2. xH_2O and UO_2Br_2. xH_2O were prepared from UO_3 and lanthanide nitrates were obtained from Indian Rare Earths Ltd, Mumbai. $PdCl_2$ used as palladium precursor was purchased from SRL, Mumbai.

1.7 Analytical techniques

1.7.1 Infrared Spectroscopy

The IR spectra were recorded as Nujol mulls between CsI (200-4000 cm^{-1})/KBr (400-400 cm^{-1}) plates on a Jasco (model FT-IR-6100) FT-IR spectrometer with a resolution of 4 cm^{-1}. The spectra were calibrated using a polystyrene film.

1.7.2 Nuclear magnetic spectroscopy

The ^1H and ^{13}C NMR spectra were recorded on a Bruker 500 and 200MHz NMR spectrometer. Chemical shifts are reported in ppm from internal chloroform peak at 7.26 ppm for ^1H and 77.0 ppm for ^{13}C unless otherwise stated, all the spectra were recorded at room temperature.

1.7.3 X-Ray Crystallography

The single crystal X-ray structure analyses of the synthesized compounds were carriedout on an Agilent SuperNova system equipped with a Titan CCD detector at 293(2) K using CuK_α radiation (λ = 1.5418 Å). The crystals were directly mounted on diffractometer after examining the quality of the crystal underpolarizing microscope. Sometimes crystals were cut to the desired size before mounting.All the crystals were mounted at ambient temperature. The crystals were positioned at 101mm from the Image Plate. Data analysis was carried out with the CRYSALIS program [105]. The structures were solved using direct methods with the SHELXS97 program [106]. All non-hydrogen atoms in these structures were refined with anisotropic thermal parameters. The hydrogen atoms bonded to carbon atoms were included in the geometric positions and given thermal parameters equivalent to 1.2 times those of the atoms to which they attached. Empirical absorption corrections were carried out using the ABSPACK program [107]. The structures were refined to convergence on F^2 using SHELXL97 [108].

1.7.4 Total Reflection X-Ray Fluorescence analysis

Elemental compositions in some of the selected compounds and supernatant solutions were analyzed via an ITAL-TXRF instrument. An ITAL Structures TXRF spectrometer TX 2000 having Mo–W dual target X-ray tube was used for all TXRF measurements. The X-ray generator was operated at 50 kV and 10 mA. The W–C multilayer having a 2θ value of 49.4 A° was used to select the desired narrow energy part of the continuum ofthe tube spectrum (with an intensity maxima at around 30 keV) for efficient excitation. The desired energy band was selected by changing the incidence angle of the primarybeam on the multilayer and the total reflection condition on the quartz sample supportwas obtained by adjusting the X-ray tube housing inclination in such a manner that thenarrow energy band of X-rays from the multilayer fall at sample support at an angel lessthan the critical angel for the support. While doing this adjustment for TXRF conditions, the angle between multilayer and X-ray beam incident on it was kept constant in theearlier optimized position. All the necessary multilayer and tube inclination movements were done by motors controlled by TXRF32 program, provided with the instrument. Thefulfilment of the TXRF condition was checked by measuring the intensity of characteristic X-ray line of a suitable single element standard (e.g. Ga) at differentinclination values of tube housing. The tube housing inclination giving maximumintensity of the single element standard X-ray line indicates that the TXRF conditions aresatisfied. This position is used for TXRF measurements. The X-rays were detected andmeasured using a Si(Li) detector having a resolution of 139 eV (FWHM) at Mn Kα (5.9keV). For TXRF measurements, a life time of 1000 was used.

1.7.5 Electrospray ionization mass spectrometric analysis

ESI–MS detection of positive ions was recorded in $CH_2Cl_2/CH_3OH/CH_3CN$ using aMicromass-Q-TOFMICRO instrument. The sample was introduced into the source witha syringe pump. Nitrogen was employed as both the drying and spraying gas with a source temperature of 900^oC. The cone voltage was set to 30 V, the voltage applied on thecapillary was 1162 kV and the sample solution flow rate was 5 mL min^{-1}. Spectrum was recorded from m/z of 100–1000.

1.8 Scope of the present work

Considering the above facts and the importance of the actinide complexes of nitrogen-oxygen donor atoms based ligands in the field of nuclear fuel cycle, different series of ligands having carbamoyl groups (piperidine carboxamide and teraalkyl urea based ligands), nitrogen, carbamoyl groups (pyrazole carboxamide, picolinamide based ligands) and N-oxide, carbamoyl groups (N-oxo picolinamide based ligands) have been synthesized and their complex chemistry with uranyl and palldium(II) ions is explored. All the ligands and the complexes have been characterized with the help of microanalytical, physico-chemical and spectroscopic tools. The structures of some of the selected metal complexes have been determined by X-ray diffraction method.

For clarity the present work is subdivided as follows:

a) Synthesis, structural and solvent extraction studies of piperidine urea and tetraalkyl urea with uranyl(VI) ions

b) Synthesis, structural and coordination studies of N-oxo picolinamide complexes with uranyl(VI) and lanthanide(III) ions

c) Synthesis, structural and theoretical studies of carbamoyl pyrazole compounds of the uranyl(VI) and Pd(II) ions

d) Synthesis, structural and theoretical studies of picolinamide complexes with palladium(II) and uranyl (VI) ions.

1.9 References

1. L.R. Morss, N.M. Edelstein, J. Fuger, J.J. Katz, 'The Chemistry of the Actinide and Transactinide Elements, Springer', Netherlands (2006).
2. C.J. Burns, M.P. Neu, H. Boukhalfa, K.E. Gutowshi, N.J. Bridges, R.D. Rogers, J.A. McCleverty, T.J. Meyer, G.F.R. Parkin, (Eds.), 'Comprehensive Coordination Chemistry II', Elsevier, Oxford, 3 (2004) 189.
3. M. Ephritikhine, Dalton Trans. (2006) 2501.
4. S. Kant, Int. J. Nucl. Ener. Sci. Tech. 1 (2005) 204.
5. R.K. Sinha, A. Kakodkar, Nucl. Eng. Des. 236 (2006) 683-700.
6. (a) G. Szigethy, K.N. Raymond, Chem. Eur. J. 17 (2011) 1818−1827. (b) C. Ni, D.K. Shuh, K.N. Raymond, Chem. Commun. 47 (2011) 6392−6394. (c) G. Szigethy, K.N. Raymond, Inorg. Chem. 49 (2010) 6755−6767. (d) G. Szigethy, K.N. Raymond, J. Am. Chem. Soc. 133 (2011) 7942−7956. (e) A.E.V. Gorden, J. Xu, K.N. Raymond, P. Durbin, Chem. Rev. 103 (2003) 4207−4282. (f) C. Drouza, V. Gramlich, M.P. Sigalas, I. Pashalidis, A.D. Keramidas, Inorg. Chem. 43 (2004) 8336−8345.
7. A.C. Sather, O.B. Berryman, Jr. J. Rebek, J. Am. Chem. Soc. 132 (2010) 13572−13574.
8. Thaddeus S. Franczyk, Kenneth R. Czerwinski, Kenneth N. Raymond, J. Am. Chem. Soc. 114 (1992) 8138–8146.

9. Lu Zhou, Mike Bosscher, Changsheng Zhang, Salih Ozcubukcu, Liang Zhang, Wen Zhang, Charles J. Li, Jianzhao Liu, Mark P. Jensen, Luhua Lai, Chuan He, Nat. Chem. 6 (2014) 236–241.
10. Aaron C. Sather, Orion B. Berryman, Jr. Julius Rebek, J. Am. Chem. Soc. 132 (2010) 13572–13574.
11. P.N. Pathak, D.R. Prabhu, R.B. Ruikar, V.K. Manchanda, Solvent Extr. Ion Exch. 20 (2002) 293−311.
12. S. Kannan, S.B. Deb, J.S. Gamare, M.G.B. Drew, Polyhedron 27 (2008) 2557−2562.
13. R. Ruhela, A.K. Singh, B.S. Tomar, R.C. Hubli, RSC Adv. 4 (2014) 24344-24350.
14. A. Dakshinamoorthy, P.S. Dhami, P.W. Naik, N.L. Dudwadkar, S.K. Munshi, P.K. Dey, V. Venugopal, Desalination 232 (2008) 26-36.
15. G.H. Rizvi, J.N. Mathur, M.S. Murali, R.H. Iyer, Sep. Sci. Technol. 31 (1996) 1805-1816.
16. I. Grenthe, J. Drożdżyński, T. Fujino, E.C. Buck, T.E. Albrecht-Schmitt, S.F. Wolf, in The chemistry of the actinide and trans actinide elements, Vol. 1, 3rd ed. (Eds.: L. R. Morss, N. M. Edelstein, J. Fuger, J. J. Katz), Springer, 2006.
17. L.L. Quill, Chem. Rev. 23 (1938) 87–155.
18. D.R. Lide, Ed., CRC Handbook of Chemistry and Physics: 86th Edition, Taylor & Francis, 86th edn., 2005.
19. Department of Health (2007), Understanding Radiation: Depleted Uranium, available at: https://www.gov.uk/depleted-uranium-du-general-information-andtoxicology (Accessed: April 2014).
20. T.J. Marks, Science 217 (1982) 989–997.
21. S.A. Cotton, Lanthanide and Actinide Chemistry, John Wiley & Sons, Ltd, Chichester, First Edit., 2006.
22. N. Kaltsoyannis, P. Scott, The f elements, Oxford University Press, 1999.
23. M.R. MacDonald, M.E. Fieser, J.E. Bates, J.W. Ziller, F. Furche, W.J. Evans, J. Am. Chem. Soc. 135 (2013) 13310.
24. I. Korobkov, S. Gambarotta, Trivalent Uranium: A Versatile Species for Molecular Activation. In Prog. Inorg. Chem., John Wiley & Sons, Inc. (2005) 321.
25. M. Ephritikhine, Organometallics 32 (2013) 2464.
26. C.R. Graves, J.L. Kiplinger, Chem. Commun. (2009) 3831.
27. R.J. Baker, Chem. Eur. J. 18 (2012) 16258.
28. S. Fortier, G. Wu, T.W. Hayton, Inorg. Chem. 47 (2008) 4752.

29. L.A. Seaman, S. Fortier, G. Wu, T.W. Hayton, Inorg. Chem. 50 (2011) 636.
30. L.A. Seaman, G. Wu, N. Edelstein, W.W. Lukens, N. Magnani, T.W. Hayton, J. Am. Chem. Soc. 134 (2012) 4931.
31. S. Fortier, J.R. Walensky, G. Wu, T.W. Hayton, J. Am. Chem. Soc. 133 (2011) 11732.
32. S. Fortier, T.W. Hayton, Coord. Chem. Rev. 254 (2010) 197.
33. E.A. Cuellar, T.J. Marks, Inorg. Chem. 20 (1981) 2129.
34. T.W. Hayton, Dalton Trans. 39 (2010) 1145.
35. Hurd W. Safford, A. Kuebel, J. Chem. Educ. 20 (1943) 88.
36. Department of Energy, Decommissioning of U.S. Uranium Production Facilities, February 1995.
37. J.H. Hill, J.W. Parks, "Uranium Enrichment in the United States," U.S. Energy Research and Development Administration, CONF-750324-7, 5 Mar 75.
38. S. Nazare, J. Nucl. Mat. 124 (1984) 14.
39. J.C. Taylor, Coord. Chem. Rev. 20 (1976) 203.
40. A.F. Wells, Structural Inorganic Chemistry, Clarendon Press, Oxford (3rd edn, 1962).
41. Tetsuhiko Yoshimura, Chie Miyake, Shosuke Imoto, J. Nucl. Sci. Technol. 8 (1971) 498-502.
42. Dipti Patel, Ashley J. Wooles, Emtithal Hashem, Harrison Omorodion, Robert J. Baker, Stephen T. Liddle, New J. Chem. 39 (2015) 7559-7562.
43. A.S. Krass, Laser enrichement of uranium: The proliferation connection, Science 196 (1977) 721-731.
44. J. Boureston, C.D. Ferguson, Separation anxiety, Bull. Atomic Scientists 61 (2005) 14-18.
45. Trevor R. Griffiths, Vladimir A. Volkovich, J. Nucl. Mater. 274 (1999) 229-251.
46. Jean-Claude Berthet, Martine Nierlich, Michel Ephritikhine, Chem. Commun. (2004) 870–871.
47. S.A. Cotton, Lanthanides and Actinides, Macmillan, 1991.
48. Pierre Thuéry, Martine Nierlich, Bernardo Masci, Zouhair Asfari, Jacques Vicens, J. Chem. Soc., Dalton Trans. (1999) 3151–3152.
49. Carol J. Burns, David L. Clark, Robert J. Donohoe, Paul B. Duval, Brian L. Scott, C. Drew Tait, Inorg. Chem. 39 (2000) 5464-5468.
50. Y.S. Kim, ed., Uranium Mining Technology: Proceedings of a First Conference (U. of Nevada, 1977).
51. Y. Kopylova, N. Guseva, A. Shestakova, A. Khvaschevskaya, K. Arakchaa, Earth Environ. Sci. Trans. 27 (2015) 12034.

52. M.P. Elless, S.Y. Lee, Water Air Soil Pollut. 107 (1998) 147–162.
53. J.R. Lacher, J.D. Salzman, J.D. Park, Ind. Eng. Chem. 53 (1961) 282–284.
54. C.J. Hardy, D. Fairhurst, H.A.C. McKay, A.M. Willson, Trans. Faraday Soc. 60 (1964) 1626-1636.
55. E.V. Fedoseev, M.I. Aizenberg, A.V. Davydov, B.F. Myasoedov, J. Radioanal. Nucl. Chem. 136 (1989) 395.
56. L.L. Shcherbakova, V.Yu. Mishin, E.M. Rubtsov, Soviet Radiokhim. 26 (1984) 698.
57. Y. Baskin, J.R. Ferraro, J. Inorg. Nucl. Chem. 30 (1968) 241.
58. Y. Baskin, N.S.K. Prasad, J. Inorg. Nucl. Chem. 25 (1963) 1011.
59. F.E. Beamish, W.A.E. Mcbryde, Anal. Chem. 25 (1953) 1613-1617.
60. F. Bonet, S. Grugeon, R. Herrera Urbina, K. Tekaia-Elhsissen, J.M. Tarascon, Solid State Sci. 4 (2002) 665–670.
61. K.C. Taylor, Stud. Surf. Sci. Catal. 30 (1987) 97-116.
62. Christopher W. Corti, Platinum Met. Rev. 53 (2009) 198–202.
63. J.C. Wataha, C.T. Hanks, J. Oral Rehabil. 23 (1996) 309-320.
64. Morton Antler, Platinum Met. Rev. 26 (1982) 106-117.
65. Christopher R. King, Int. J. Radiat. Oncol. Biol. Phys. 47 (2000) 1165–1167.
66. N. Miksys, J.E. Cygler, J.M. Caudrelier, R.M. Thomson, Phys. Med. Biol. 61 (2016) 2705–2729.
67. C.J. Elsevier, Coord. Chem. Rev. 185/186 (1999) 809.
68. P.K. Byers, A.J. Canty, B.W. Skelton, A.H. White, J. Chem. Soc. Chem. Commun. (1986) 1722.
69. R. Uson, J. Fornies, R. Navarro, J. Organomet. Chem. 96 (1975) 307.
70. A.A. Timakov, V.N. Prusakov, Y.V. Drobyshevskii, Russ. J. Inorg. Chem. 27 (1982) 1704.
71. David E. Berry, Philippa Carrie, Kelli L. Fawkes, Bruce Rebner, Yao (Shirley) Xing, J. Chem. Educ. 87 (2010) 533–534.
72. Barbara Milani, Anna Anzilutti, Lidia Vicentini, Andrea Sessanta o Santi, Ennio Zangrando, Silvano Geremia, Giovanni Mestroni, Organometallics 16 (1997) 5064–5075.
73. Y. Pan, J.T. Mague, M.J. Fink, J. Am. Chem. Soc. 115 (1993) 3842.
74. R.U. Kirss, R. Eisenberg, Inorg. Chem. 28 (1989) 3372.
75. F.A. Cotton, G. Wilkinson, C.A. Murillo, M. Bochmann, Advanced Inorganic Chemistry; 6h Edition; John Wiley & Sons: New York, 1999.

76. S.A. Cotton, Ed.; Chemistry of Precious Metals; Springer, 1997.
77. E.G. Mednikov, L.F. Dahl, Phil. Trans. R. Soc. A 368 (2010) 1301 and references cited therein.
78. K.R. Dixon, A. Dixon, Comprehensive Organometallics Chemistry II; Elsevier. 8 (1995) 200 and references cited therein.
79. (a) J.H. Duffus, Pure Appl. Chem. 74 (2002) 793. (b) S. Ahrland, J. Chatt, N.R. Davies, Quart. Rev. 12 (1958) 265. (c) R.G. Pearson, J. Chem. Educ. 45 (1968) 581. (d) R.G. Pearson, J. Chem. Educ. 45 (1968) 643.
80. F.A. Cotton, G. Wilkinson, P.L. Gaus, Basic Inorganic Chemistry; 3rd Edition, Wiley, 1994.
81. I. Nakanishi, K.Matsumoto, S. Ooi, Acta Crystallogr. Sect. C 47 (1991) 2073.
82. W.J. Louw, D.J.A. DeWaal, G.J. Kruger, J. Chem. Soc., Dalton Trans. (1976) 2365.
83. A.J. Blake, A.J. Holder, T.I. Hyde, M. Schröder, J. Chem. Soc., Chem. Commun. (1987) 987.
84. A.J. Blake, A.J. Holder, T.I. Hyde, Y.V. Roberts, A.J. Lavery, M. Schröder, J. Organomet. Chem. 323 (1987) 261.
85. A.F. Wright, B.E.F. Fender, N. Bartlett, K. Leary, Inorg. Chem. 17 (1978) 748.
86. D.J. Gulliver, W. Levason, J. Chem. Soc., Dalton Trans. (1982) 1895.
87. L.R. Gray, D.J. Gulliver, W. Levason, M. Webster, J. Chem. Soc., Dalton Trans. (1983) 133.
88. A. Maleckis, M.S. Sanford, Organometallics 30 (2011) 6617.
89. S. Kannan, J.S. Gamare, K.V. Chetty, M.G.B. Drew, Polyhedron 26 (2007) 3810.
90. L. Nigond, C. Musikas, C.C. Cullerdier, Solv. Extr. Ion Exch. 12 (1994) 261.
91. M.S. Subramanian, J. Radioanal. Nucl. Chem. Lett. 187 (1994) 91.
92. S.S Biswas, P.S. Murty, A. Sethumadhavan, R. Kaimal, A.V. Sankaran, Anal. Lett. 24 (1991) 887.
93. J. Chen, J.C. Wang, Prog. Chem. 23 (2011) 1366.
94. M. Bosson, W. Levason, T. Patel, M.C. Popham, M. Webster, Polyhedron 20 (2001) 2055.
95. W. Levason, E.H. Newman, M. Webster, Polyhedron 19 (2000) 2697.
96. M.J. Hudson, F.W. Lewis, L.M. Harwood, ‘Strategies and Tactics in Organic Synthesis’ 9 (2013) 177.
97. M.S. Nagar, P.B. Ruikar, J.N. Mathur, R.H. Iyer, Syn. React. Inorg. Met. 28 (1998) 621.

98. Y. Kulyako, D. Malikova, T. Trofimova, M. Chmutovaa, B. Myasoedova, J. Nucl. Sci. Technol. 39 (2002) 302.
99. S. Kannan, K.V. Chetty, V. Venugopal, M.G.B. Drew, Dalton Trans. (2004) 3604.
100. Y. Sasakia, Y. Sugoa, S. Suzukia, S. Tachimoria, Solvent Extr. Ion Exch. 19 (2001) 91.
101. S. Kannan, M.A. Moody, C.L. Barnes, P.B. Duval, Inorg. Chem. 47 (2008) 4691.
102. J.C. Berthet, Y. Miquel, P.B. Iveson, M. Nierlich, P. Thuéry, C. Madic, M. Ephritikhine, J. Chem. Soc., Dalton Trans. (2002) 3265.
103. P.J. Panak, A. Ge, Chem. Rev. 113 (2013) 1199.
104. A.I. Vogel, ‘Textbook of Practical Organic Chemistry’, 4th Ed., English Language Book Society, Longman, London (1987).
105. CRYSALIS program, Oxford Diffraction Ltd., 2005.
106. G.M. Sheldrick, SHELXS, Program for Crystal Structure Solution, University of Gottingen, Gottingen, Germany, 1997.
107. ABSPACK Program, Oxford Diffraction Ltd., 2005.
108. G.M. Sheldrick, SHELXL, Program for Crystal Structure Refinement, University of Gottingen, Gottingen, Germany, 1997.

CHAPTER 2

Synthesis, structural and separation studies of piperidine carboxamide and tetraalkyl urea with uranyl ions

CHAPTER-2

2.1 Introduction

The coordination chemistry of actinides plays very important role for the development of new methods concerning the processing of irradiated nuclear fuel and their storage [1–3]. The selective separation of uranium-233 from the mixture of thorium and other fission products is an important step [4] in the advanced heavy water reactor (AHWR) technology [5] of the Indian atomic energy program, where upon the thorium oxide is used as a fuel material. In recent years, incinerable organic amide based extractants have proved to be of particular interest in the process chemistry of lanthanides and actinides from the nitric acid medium [6-12]. It is reported that the N,N'-2-ethylhexyl iso-butyramide shows selective extraction property for the uranium(VI) ion from a mixture containing thorium(IV) or plutonium(IV) ion [13-15]. The solvent extraction method needs many steps such as: extraction, stripping, precipitation and purification during the reprocessing of fuel materials. The neutral N-cyclohexyl-2-pyrrolidone ligand shows selective precipitation of uranium(VI) ion (up to 68%) from the mixture containing various other ions [16] and with this ligand only two steps are required namely precipitation and purification. It has also been reported recently that isobutyramide based amide ligands show an excellent coordination property towards the uranyl group and form air and moisture stable halide and thiolato complexes [17-18]. The stability of these complexes was explained on the basis of very strong bonding between the amide and uranyl group. The observed bond distances in these complexes are much shorter in length compared to those of any of the uranyl-amide [19–21], uranyl-phosphine oxide [22-26] and uranyl-pyrrolidone [27-28] complexes reported. Inspired by the results obtained, we report herein the synthesis, characterization and the coordination chemistry of some urea based ligands with uranyl nitrate, chloride, bromide and uranyl bis(β-diketonates) by expecting even more strong bonding due to increased electron density on the O-atom of the ligands by the mesomeric effect of two N-atoms placed both sides of C=O group.

2.2 Experimental

2.2.1 General Considerations

All uranyl bis(β-diketonates) were prepared according to the reported methods [29].

2.2.2 Synthesis of the ligands (Scheme 1)

2.2.2.1 Piperidine carboxamide ligands

*2.2.2.1.1 Synthesis of $C_5H_{10}NCON(CH_3)_2$ (**L^1**)*

To a solution of N,N-dimethyl carbamoyl chloride (10.75 g, 0.1 mol) in (50 mL) benzene, a solution of piperidine (8.52 g, 0.1 mol) and triethyl amine (12.1 g, 0.12 mol) in benzene (50 mL) was added slowly with stirring. The reaction mixture was refluxed for 2 h and treated with 100 ml. of 5% HCl solution. The organic layer was separated, dried over anhydrous sodium sulfate and filtered. The solution on evaporation yielded a colorless liquid. Yield: 62%. Anal. Calc. for $C_8H_{16}N_2O$: C, 61.5; H, 10.25; N, 17.9. Found: C, 60.5; H, 10.1; N, 17.5%. ^1H NMR ($CDCl_3$, 25°C) δ: 2.85 (br, 4H, 2,6-piperidyl CH_2), 2.50 (s, 6H, $N(CH_3)_2$), 1.26 (br, 6H, piperidyl CH_2). IR (cm^{-1}) ν: 1653 (C=O).

*2.2.2.1.2 Synthesis of $C_5H_{10}NCON(C_2H_5)_2$ (**L^2**)*

This was prepared similarly to L^1 in 76% yield by taking N,N-diethyl carbamoyl chloride. Anal. Calc. for $C_{10}H_{20}N_2O$: C, 65.2; H, 10.9; N, 15.2. Found: C, 64.5; H, 10.3; N, 15.5%. ^1H NMR ($CDCl_3$, 25 °C) δ: 3.15 (8H, 2,6-piperidyl CH_2 and $N(C_2H_5)_2$ CH_2), 1.55 (br, 6H, 3,4,5-piperidyl CH_2), 1.09 (t, J = 7.0 Hz, 6H, $N(C_2H_5)_2$ CH_3). IR (cm^{-1}) ν: 1622 (C=O).

*2.2.2.1.3 Synthesis of $C_5H_{10}NCON(^iC_3H_9)_2$ (**L^3**)*

This was prepared similarly to L^1 in 94% yield by taking N,N-diisoproyl carbamoyl chloride. Anal. Calc. for $C_{12}H_{24}N_2O$: C, 67.9; H, 11.3; N, 13.2. Found: C, 66.6; H, 10.7; N, 13.0%. ^1H NMR ($CDCl_3$, 25 °C) δ: 3.48 (m, 2H, $N(iPr_2)$ CH), 2.91 (br, 4H, 2,6-piperidyl CH_2), 1.44 (br, 6H, 3,4,5-piperidyl CH_2), 1.15 (d, J = 6.6 Hz, 12H, $N(iPr_2)$ CH_3). IR (cm^{-1}) ν: 1651 (C=O).

2.2.2.2 Tetraalkyl urea ligands

*2.2.2.2.1 Synthesis of $C_4H_{10}NCON({}^iC_4H_9)_2$ (**L^4**)*

Diisobutyl amine (1.290 g, 10mmol) and triethyl amine (1.01g, 10mmol) were taken in benzene. A solution of N,N-diethyl carbamoyl chloride (1.35g, 10mmol) in benzene was added dropwise over the period of half an hour. Immediately white precipitate was formed. Solution was stirred for 5 hours. Washed with 10% HCl. Dried over Na_2SO_4. After evaporation of solvent, a yellow oily product was obtained. Yield (81%). ^1H NMR ($CDCl_3$): $\delta = 0.783$ (d, 12H, CH_3, ^iBu), 1.033 (t, 6H, CH_3, Et), 1.829 (m, 2H, -CH-, ^iBu), 2.915 (d, 2H, -CH_2N-, ^iBu), 3.095 (q, 4H, -CH_2N-, Et), IR (cm^{-1}): $\nu = 1646$ (C=O).

*2.2.2.2.2 Synthesis of $C_4H_{10}NCON(n\text{-}C_8H_{17})_2$ (**L^5**)*

Synthesized similar to Ligand L^4 by taking N,N-dioctyl carbamoyl chloride instead of N,N-diethyl carbamoyl chloride. Yield (75%). ^1H NMR: ($CDCl_3$): $\delta = 0.822$ (t, 6H, CH_3, octyl), 1.046 (t, 6H, CH_3, Et), 1.211 (br, 20H, -$(CH_2)_5$-, octyl), 1.439 (m, 4H, -CH_2-, octyl), 3.026-3.133 (m, 8H, -CH_2N-, Et and octyl), IR (cm^{-1}): $\nu = 1649$ (C=O).

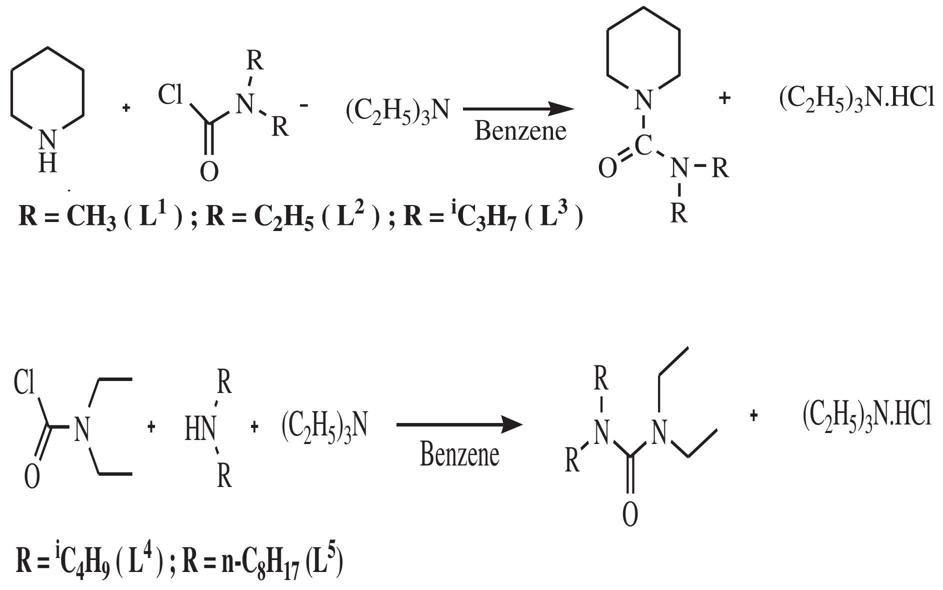

Scheme 1. Synthesis of the ligands.

$$[\mathrm{UO_2(NO_3)_2.6H_2O}] + 2\mathrm{L} \longrightarrow [\mathrm{UO_2(NO_3)_2L_2}] \quad (\mathrm{L} = \mathrm{L}^1, \mathrm{L}^2, \mathrm{L}^3)$$

$$[\mathrm{UO_2(DBM)_2.2H_2O}] + \mathrm{L} \longrightarrow [\mathrm{UO_2(DBM)_2.L}] \quad (\mathrm{L} = \mathrm{L}^1, \mathrm{L}^2, \mathrm{L}^3)$$

(DBM = Dibenzoyl methanate)

$$[\mathrm{UO_2(TTA)_2.2H_2O}] + \mathrm{L} \longrightarrow [\mathrm{UO_2(TTA)_2.L}] \quad (\mathrm{L} = \mathrm{L}^1, \mathrm{L}^2, \mathrm{L}^3)$$

(TTA = Thenoyl trifluroacetonate)

$$[\mathrm{UO_2X_2,\ nH_2O}] + 2\mathrm{L} \longrightarrow \mathrm{UO_2X_2L_2} \quad (\mathrm{L} = \mathrm{L}^1, \mathrm{L}^2, \mathrm{L}^3)$$

(X = Cl, Br)

$$[\mathrm{UO_2(NO_3)_2.\ 6H_2O}] + 2\mathrm{L} \longrightarrow [\mathrm{UO_2(NO_3)_2L_2}] \quad (\mathrm{L} = \mathrm{L}^4)$$

$$[\mathrm{UO_2X_2.\ nH_2O}] + 2\mathrm{L} \longrightarrow \mathrm{UO_2X_2L_2} \quad (\mathrm{L} = \mathrm{L}^4)$$

(X = Cl, Br)

Scheme 2. Synthesis of the uranyl compounds.

2.2.3 Synthesis of the compounds (Scheme 2)

*2.2.3.1 Synthesis of $[UO_2(NO_3)_2\{C_5H_{10}NCON(CH_3)_2\}_2]$ (**1**)*

To a solution of N,N-dimethylpiperidine-1-carboxamide (200 mg, 1.29 mmol) in chloroform, solid $UO_2(NO_3)_2.6H_2O$ (300 mg, 0.59 mmol) was added with stirring. The solution was allowed to stir until the entire uranyl nitrate dissolved to give a clear solution. This solution was filtered and layered with isooctane. This solution on slow evaporation yielded a yellow crystalline solid. This was filtered, washed with hexane and air dried. Yield: 375.5 mg (89%). Elemental Analysis Calculated for $[UO_2(NO_3)_2\{C_5H_{10}NCON(CH_3)_2\}_2]$, $C_{16}H_{32}N_6O_{10}U$ (%): Expected: C=27.2; H=4.5; N=11.9. Found: C= 26.7; H=4.2; N= 11.5. IR (Nujol, υ/cm^{-1}): 1525 (C=O), 925 ($U{=}O_{assy}$). ^1H NMR ($CDCl_3$, 25 ^oC, δ in ppm): 3.55 (br, 4H, 2,6-piperidyl CH_2), 3.14 (s, 6H, $N(CH_3)_2$), 1.63 (br, 6H, 3,4,5-piperidyl CH_2).

*2.2.3.2 Synthesis of $[UO_2(NO_3)_2\{C_5H_{10}NCON(C_2H_5)_2\}_2]$ (**2**)*

Compound **2** was prepared in a similar way as compound **1** by taking N,N-diethylpiperidine-1-carboxamide (240 mg, 1.3 mmol) and $UO_2(NO_3)_2.6H_2O$ (300 mg, 0.59 mmol). Yield: 418.9 mg (92%). Elemental Analysis Calculated for $[UO_2(NO_3)_2\{C_5H_{10}NCON(C_2H_5)_2\}_2]$, $C_{20}H_{40}N_6O_{10}U$ (%): Expected: C=31.5; H=5.2; N=11.0. Found: C= 31.1; H=4.8; N= 10.7. IR

(Nujol, υ/cm^{-1}): 1521 (C=O), 928 (U=O$_{assy}$). ^{1}H NMR (CDCl$_3$, 25 ^{o}C, δ in ppm): 3.52 (br, 8H, 2,6-piperidyl CH$_2$ and N(C$_2$H$_5$)$_2$ CH$_2$), 1.63 (br, 6H, 3,4,5-piperidyl CH$_2$), 1.26 (s, 6H, N(C$_2$H$_5$)$_2$ CH$_3$).

*2.2.3.3 Synthesis of [$UO_2(NO_3)_2\{C_5H_{10}NCON(^iC_3H_7)_2\}_2$] (**3**)*

Compound **3** was prepared in a similar way as compound **1** by taking N,N-diisopropylpiperidine-1-carboxamide (270 mg, 1.27 mmol) and $UO_2(NO_3)_2.6H_2O$ (300 mg, 0.59 mmol). Yield: 415.5 mg (85%). Elemental Analysis Calculated for [$UO_2(NO_3)_2\{C_5H_{10}NCON(^iC_3H_7)_2\}_2$], $C_{24}H_{48}N_6O_{10}U$ (%): Expected: C=35.2; H=5.9; N=10.2. Found: C= 35.1; H=5.8; N= 10.1. IR (Nujol, υ/cm^{-1}): 1522 (C=O), 932 (U=O$_{assy}$). ^{1}H NMR (CDCl$_3$, 25 ^{o}C, δ in ppm): 3.90 (br, 2H, N(^{i}Pr$_2$) CH), 3.40 (br, 4H, 2,6-piperidyl CH$_2$), 1.56 (br, 6H, 3,4,5-piperidyl CH$_2$), 1.41 (d, J = 6.0 Hz, 12H, N(^{i}Pr$_2$) CH$_3$).

*2.2.3.4 Synthesis of [$UO_2(C_6H_5COCHCOC_6H_5)_2\{C_5H_{10}NCON(CH_3)_2\}$] (**4**)*

To a solution of N,N-dimethylpiperidine-1-carboxamide (80 mg, 0.51 mmol) in dichloromethane, solid $UO_2(C_6H_5COCHCOC_6H_5)_2.2H_2O$ (350 mg, 0.47 mmol) was added and the resulting mixture was refluxed for 2 h with constant stirring. The solution was filtered and layered with dodecane. This on slow evaporation yielded an orange red crystalline solid product. Yield: 373.4 mg (92%). Elemental Analysis Calculated for [$UO_2(C_6H_5COCHCOC_6H_5)_2\{C_5H_{10}NCON(CH_3)_2\}$], $C_{38}H_{38}N_2O_7U$ (%): Expected: C=52.3; H=4.4; N=3.2. Found: C= 51.8; H=3.9; N= 3.0. IR (Nujol, υ/cm^{-1}): 1591 (C=O, DBM), 1542 (C=O, Ligand), 907 (U=O$_{assy}$). ^{1}H NMR (CDCl$_3$, 25 ^{o}C, δ in ppm): 8.46 (d, 8H, Ph, DBM), 8.0 (d, 4H, Ph, DBM), 7.58 (br, 8H, Ph, DBM), 7.24 (s, 2H, CH, DBM), 3.53 (br, 4H, piperidyl CH$_2$), 3.14 (br, 6H, N(CH$_3$)$_2$), 1.55 (br, 6H, piperidyl CH$_2$).

*2.2.3.5 Synthesis of [$UO_2(C_6H_5COCHCOC_6H_5)_2\{C_5H_{10}NCON(C_2H_5)_2\}$] (**5**)*

Compound **5** was prepared in a similar way as compound **4** by taking N,N-diethylpiperidine-1-carboxamide (90 mg, 0.49 mmol) and $UO_2(C_6H_5COCHCOC_6H_5)_2.2H_2O$ (350 mg, 0.47

mmol). Yield: 393.8 mg (94%). Elemental Analysis Calculated for $[UO_2(C_6H_5COCHCOC_6H_5)_2\{C_5H_{10}NCON(C_2H_5)_2\}]$, $C_{40}H_{42}N_2O_7U$ (%): Expected: C=53.3; H=4.7; N=3.1. Found: C= 52.8; H=4.5; N= 3.0. IR (Nujol, υ/cm^{-1}): 1591 (C=O, DBM), 1542 (C=O, Ligand), 905 ($U=O_{assy}$). ^{1}H NMR ($CDCl_3$, 25 ^{o}C, δ in ppm): 8.49 (br, 8H, DBM Ph), 8.0 (d, 4H, DBM Ph), 7.58 (s, 8H, DBM Ph), 7.25 (s, 2H, DBM CH), 3.53 (br, 8H, piperidyl CH_2 and $N(C_2H_5)_2$ CH_2), 1.52 (s, 6H, piperidyl CH_2), 1.23 (t, J = 6.6 Hz, 6H, $N(C_2H_5)_2$ CH_3).

*2.2.3.6 Synthesis of $[UO_2(C_6H_5COCHCOC_6H_5)_2\{C_5H_{10}NCON(^iC_3H_7)_2\}]$ (**6**)*

Compound **6** was prepared in a similar way as compound **4** by taking N,N-diisopropylpiperidine-1-carboxamide (105 mg, 0.5 mmol) and $UO_2(C_6H_5COCHCOC_6H_5)_2.2H_2O$ (350 mg, 0.47 mmol). Yield: 384.4 mg (89%). Elemental Analysis Calculated for $[UO_2(C_6H_5COCHCOC_6H_5)_2\{C_5H_{10}NCON(^iC_3H_7)_2\}]$, $C_{42}H_{46}N_2O_7U$ (%): Expected: C=54.3; H=4.9; N=3.0. Found: C= 53.9; H=4.5; N= 2.8. IR (Nujol, υ/cm^{-1}): 1592 (C=O, DBM), 1541 (C=O, Ligand), 901 ($U=O_{assy}$). ^{1}H NMR ($CDCl_3$, 25 ^{o}C, δ in ppm): 8.61 (br, 4H, DBM Ph), 8.40 (br, 4H, DBM Ph), 8.0 (d, 4H, DBM Ph), 7.59 (s, 8H, DBM Ph), 7.27 (s, 2H, DBM CH), 3.94 (s, 2H, $N(^iPr_2)$ CH), 3.42 (s, 4H, piperidyl CH_2), 1.49 (s, 18H, piperidyl CH_2 and $N(^iPr_2)$ CH_3).

*2.2.3.7 Synthesis of $[UO_2(C_4H_3SCOCHCOCF_3)_2\{C_5H_{10}NCON(CH_3)_2\}]$ (**7**)*

To a dichloromethane solution of N,N-dimethylpiperidine-1-carboxamide (70 mg, 0.44 mmol), solid $UO_2(C_4H_3SCOCHCOCF_3)_2.2H_2O$ (300 mg, 0.4 mmol) was added and refluxed for 2 h with constant stirring. This solution was filtered and layered with isooctane. This solution on slow evaporation yielded bright yellow colored needle shaped crystals. Yield: 327.2 mg (94%). Elemental Analysis Calculated for $[UO_2(C_4H_3SCOCHCOCF_3)_2\{C_5H_{10}NCON(CH_3)_2\}]$, $C_{24}H_{24}N_2O_7F_6S_2U$ (%): Expected: C=33.2; H=2.8; N=3.2. Found: C= 32.8; H=2.7; N= 3.1. IR (Nujol, υ/cm^{-1}): 1618 (C=O, TTA), 1540 (C=O, Ligand), 919 ($U=O_{assy}$). ^{1}H NMR ($CDCl_3$, 25 ^{o}C, δ in ppm): 8.26 (s, 2H, thiophene CH), 7.83 (t, J = 6.6 Hz, 2H, thiophene CH), 7.28 (q, J = 4.5 Hz, 2H, thiophene CH), 6.79 (s, 2H, TTA CH), 3.59 (br, 4H, piperidyl CH_2), 3.22 (s, 6H, $N(CH_3)_2$), 1.63 (br, 6H, piperidyl CH_2).

*2.2.3.8 Synthesis of $[UO_2(C_4H_3SCOCHCOCF_3)_2\{C_5H_{10}NCON(C_2H_5)_2\}]$ (**8**)*

Compound **8** was prepared in a similar way as compound **7** by taking N,N-diethylpiperidine-1-carboxamide (80 mg, 0.43 mmol) and $UO_2(C_4H_3SCOCHCOCF_3)_2.2H_2O$ (300 mg, 0.4 mmol). Yield: 319.8 mg (89%). Elemental Analysis Calculated for $[UO_2(C_4H_3SCOCHCOCF_3)_2\{C_5H_{10}NCON(C_2H_5)_2\}]$, $C_{26}H_{28}N_2O_7F_6S_2U$ (%): Expected: C=34.8; H=3.1; N=3.1. Found: C= 34.6; H=2.9; N= 3.0. IR (Nujol, υ/cm^{-1}): 1591 (C=O, TTA), 1539 (C=O, Ligand), 922 ($U=O_{assy}$). ^1H NMR ($CDCl_3$, 25 °C, δ in ppm): 8.26 (br, 2H, thiophene CH), 7.84 (br, 2H, thiophene CH), 7.28 (d, J = 4.7 Hz, 2H, thiophene CH), 6.79 (s, 2H, TTA CH), 3.52 (br, 8H, piperidyl CH_2 and $N(C_2H_5)_2$ CH_2), 1.61 (br, 6H, piperidyl CH_2), 1.23 (br, 6H, $N(C_2H_5)_2$ CH_3).

*2.2.3.9 Synthesis of $[UO_2(C_4H_3SCOCHCOCF_3)_2\{C_5H_{10}NCON(^iC_3H_7)_2\}]$ (**9**)*

Compound **9** was prepared in a similar way as compound **7** by taking N,N-diisopropyl piperidine-1-carboxamide (90mg, 0.42mmol) and $UO_2(C_4H_3SCOCHCOCF_3)_2.2H_2O$ (300 mg, 0.4 mmol). Yield: 326.1 mg (88%). Elemental Analysis Calculated for $[UO_2(C_4H_3SCOCHCOCF_3)_2\{C_5H_{10}NCON(^iC_3H_7)_2\}]$, $C_{28}H_{32}N_2O_7F_6S_2U$ (%): Expected: C=36.4; H=3.5; N=3.0. Found: C= 35.8; H=3.0; N= 3.0. IR (Nujol, υ/cm^{-1}): 1618 (C=O, TTA), 1540 (C=O, Ligand), 922 ($U=O_{assy}$). ^1H NMR ($CDCl_3$, 25 °C, δ in ppm): 8.25 (t, 2H, thiophene CH), 7.82 (d, 2H, thiophene CH), 7.29 (br, 2H, thiophene CH), 6.79 (s, 2H, TTA CH), 3.91 (s, 2H, $N(^iPr_2)$ CH), 3.46 (s, 4H, piperidyl CH_2), 1.56 (s, 6H, piperidyl CH_2), 1.46 (d, J = 6.6 Hz, 12H, $N(^iPr_2)$ CH_3).

*2.2.3.10 Synthesis of [$UO_2Cl_2\{C_5H_{10}NCON(^iC_3H_7)_2\}_2$] (**10**)*

Solid UO_3 (300 mg) was dissolved in 4 mL of concentrated HCl and the volume of the solution was reduced completely to dryness on a hot plate. The orange colored solid thus obtained was dissolved in 10 mL of methanol to give a clear solution. To this solution N,N-diisopropylpiperidine-1-carboxamide was added and heated for 2 min. The volume of the solution was reduced to 2mL, and 20 mL of diethyl ether was added into it with stirring. The yellow product formed was filtered, washed with ether and dried in air. This product was recrystallized from a chloroform/isooctane mixture to give a crystalline solid. Yield: 714.2 mg (89%). Elemental Analysis Calculated for [$UO_2Cl_2\{C_5H_{10}NCON(^iC_3H_7)_2\}_2$], $C_{24}H_{48}N_4O_4Cl_2U$ (%): Expected: C=37.6; H=6.3; N=7.3. Found: C= 37.2; H=6.0; N= 7.2. IR (Nujol, υ/cm^{-1}): 1524 (C=O), 924 (U=O_{assy}).

*2.2.3.11 Synthesis of [$UO_2Br_2\{C_5H_{10}NCON(^iC_3H_7)_2\}_2$] (**11**)*

This was synthesized similar to **10**, by taking concentrated HBr instead of HCl. Yield 85%. Elemental Analysis Calculated for [$UO_2Br_2\{C_5H_{10}NCON(^iC_3H_7)_2\}_2$], $C_{24}H_{48}N_4O_4Br_2U$ (%): Expected: C=33.7; H=5.6; N=6.6. Found: C= 33.2; H=5.2; N= 6.2. IR (Nujol, υ/cm^{-1}): 1525 (C=O), 928 (U=O_{assy}).

*2.2.3.12 Synthesis of [$UO_2(NO_3)_2\{C_4H_{10}NCON(^iC_4H_9)_2\}_2$] (**12**)*

$UO_2(NO_3)_2\cdot6H_2O$ (200 mg, 0.4 mmol) and ligand $C_4H_{10}NCON(^iC_4H_9)_2\}_2$ (182 mg, 0.8 mmol) were taken in dichloromethane (DCM) and stirred for 2 hours and all the uranyl nitrate was dissolved. The solution was filtered and the filtrate is layered with isooctane to get obtain yellow crystals of the compound. Yield: 331.9 mg (98%). Elemental Analysis Calculated for [$UO_2(NO_3)_2\{C_4H_{10}NCON(^iC_4H_9)_2\}_2$], $C_{26}H_{56}N_6O_{10}U$ (%): Expected: C=36.7; H=6.6; N=9.9. Found: C= 36.2; H=6.9; N= 9.1. IR (υ/cm^{-1}): 1540 (C=O). ^{1}H NMR ($CDCl_3$, 25 ^oC, δ in ppm): 0.879 (d, 12H, CH_3, ^{i}Bu), 1.252 (t, 6H, CH_3, Et), 2.042 (m, 2H, –CH–, ^{i}Bu), 3.272 (d, 2H, –CH_2N–, ^{i}Bu), 3.053 (m, br, 4H, –CH_2N–, Et).

2.2.3.13 Synthesis of $[UO_2Cl_2\{C_4H_{10}NCON(^iC_4H_9)_2\}_2]$ ***(13)***

Solid UO_3 (114 mg, 0.4 mmol) was dissolved in 4 mL of concentrated HCl and the volume of the solution was reduced completely to dryness on a hot plate to get orange powder of $UO_2Cl_2{\cdot}XH_2O$. To a DCM solution of $C_4H_{10}NCON(^iC_4H_9)_2\}_2$ (182 mg, 0.8 mmol), $UO_2Cl_2{\cdot}XH_2O$ was added and stirred for 2 hours. The solution was filtered and the filtrate was layered with isooctane to obtain yellow crystals of the compound. Yield: 311.3 mg (98%). Elemental Analysis Calculated for $[UO_2Cl_2\{C_4H_{10}NCON(^iC_4H_9)_2\}_2]$, $C_{26}H_{56}N_4O_4Cl_2U$ (%): Expected: C=39.1; H=7.0; N=7.0. Found: C= 38.6; H=7.9; N= 6.9. IR (υ/cm^{-1}): 1523 (C=O). ^{1}H NMR: ($CDCl_3$, 25 ^{o}C, δ in ppm): 0.910 (d, 12H, CH_3, ^{i}Bu), 1.290 (br, 6H, CH_3, Et), 2.058 (m, 2H, –CH–, ^{i}Bu), 3.429 (br, 2H, –CH_2N–, ^{i}Bu), 3.673 (br, 4H, –CH_2N–, Et).

2.2.3.14 Synthesis of $[UO_2Br_2\{C_4H_{10}NCON(^iC_4H_9)_2\}_2]$ ***(14)***

This was synthesized similar to **13**, by taking concentrated HBr instead of HCl. Yield 97%. Elemental Analysis Calculated for $[UO_2Br_2\{C_4H_{10}NCON(^iC_4H_9)_2\}_2]$, $C_{26}H_{56}N_4O_4Br_2U$ (%): Expected: C=35.2; H=6.3; N=6.3. Found: C= 34.7; H=6.8; N= 6.2. IR (Nujol, υ/cm^{-1}): 1522 (C=O). ^{1}H NMR ($CDCl_3$, 25 ^{o}C, δ in ppm): 0.910 (d, 12H, CH_3, ^{i}Bu), 1.282 (t, 6H, CH_3, Et), 2.057 (m, 2H, –CH–, ^{i}Bu), 3.424 (d, 2H, –CH_2N–, ^{i}Bu), 3.676 (d, 4H, –CH_2N–, Et).

2.2.4 Solvent extraction studies

Solvent extraction studies were performed by using a solution of N, N-diethyl-N’,N’-dioctyl urea in dodecane (0.2 M) with the required aqueous phase spiked with ^{233}U or ^{239}Pu tracers in a thermostat water bath for 1 h at 25 ± 0.1 ^{o}C. Assay of organic and aqueous phases were done in duplicate by alpha counting using a dioxane based liquid scintillator for ^{233}U and ^{239}Pu. The distribution ratio (D) is defined as the ratio of the concentration of uranium and plutonium in the organic phase to that of the aqueous phase.

2.2.5 Separation studies

Stock solutions containing 5 g of [$Th(NO_3)_4 . 6H_2O$], 200 mg of [$La(NO_3)_3 .6H_2O$], 200 mg of [$Sm(NO_3)_3 .6H_2O$], 200 mg of [$Eu(NO_3)_3 .6H_2O$] and 200 mg of [$UO_2(NO_3)_2 .6H_2O$] were prepared in 20 ml of 3 M HNO_3. This solution was layered with 1 ml of N, N-diethyl-N',N'-diisobutyl urea and allowed to stand for overnight. This process deposited yellow crystalline solid material (Fig. 2.1), which was filtered, washed with water and then with hexane and dried. The supernatants and the solutions of yellow solid in ethanol were used for the elemental analysis using the total reflection X-ray fluorescence (TXRF) method.

Fig. 2.1 Stock solution of La, Sm, Eu, Th and U layered without (left) and with the ligand (right)

2.2.6 X-ray diffraction studies of compounds 3, 9, 10, 11, 12, 13 and 14

Selected crystallographic data for compounds **3, 9, 10, 11, 12, 13** and **14** are summarized in Table 2.1.

Table 2.1 Crystallographic data for compounds **3, 9, 10, 11, 12, 13** and **14**

	3	**9**	**10**	**11**	**12**	**13**	**14**
Empirical formula	$C_{24}H_{48}N_6O_{10}U$	$C_{28}H_{34}N_2O_7S_2F_6U$	$C_{24}H_{48}N_4O_4Cl_2U$	$C_{24}H_{48}N_4O_4Br_2U$	$C_{26}H_{56}N_6O_{10}U$	$C_{26}H_{56}N_4O_4Cl_2U$	$C_{26}H_{56}N_4O_4Br_2U$
Formula weight	818.7	926.73	765.60	854.50	850.79	797.68	886.58
Crystal system	Monoclinic	Monoclinic	Orthorhombic	Orthorhombic	Triclinic	Monoclinic	Monoclinic
Space group	$P\ 2_1/n$	$P\ 2_1/n$	Pbca	Pbca	$P\bar{1}$	$P12_1/n1$	$P12_1/n1$
a (Å)	8.9696(2)	16.0316(3)	15.2149(6)	15.2003(4)	9.4988(7)	9.1746(2)	8.9803(4)
b (Å)	18.2161(4)	9.03822(19)	12.2538(7)	12.3726(3)	10.8674(9)	14.7815(3)	13.5484(4)
c(Å)	10.2600(3)	23.4060(4)	16.9457(8)	16.9049(4)	18.8816(12)	13.3902(3)	15.0855(5)
α (°)	------	------	------	------	88.045(6)	------	------
β (°)	102.403(3)	94.8813(18)	------	------	79.572(6)	98.738(2)	99.086(4)
γ (°)	------	------	------	------	76.641(7)	------	------
Volume (Å^3)	1637.26	3379.16(12)	3159.4(3)	3179.24(13)	1865.0(2)	1794.84(7)	1812.40(11)
Z (formula unit)	2	4	4	4	2	2	2
Calculated density (g/cm^3)	1.661	1.822	1.610	1.785	1.515	1.476	1.625

μ (mm^{-1})	14.447	15.382	16.279	17.576	12.703	14.348	15.436
Reflections collected/unique	3088/2010	6283/4965	2957/1360	2981/1769	6875/3820	3347/2238	3428/2394
Data/restrains/ parameters	3088/36/202	6283/138/457	2957/0/165	2981/72/165	3820/108/401	2238/0/175	2394/0/175
Goodness of fit on F^2	1.060	1.007	1.050	1.000	1.109	1.065	1.040
Final R_1 indices [$I > 2\sigma(I)$]	0.0425	0.0416	0.0798	0.0452	0.0785	0.0567	0.0487
wR_2 indices (all data)	0.0688	0.0559	0.1308	0.0789	0.1825	0.1491	0.1185

$w = 1/[\sigma^2(F_o^2)+(0.0649P)^2]$ for **3**, $w = 1/[\sigma^2(F_o^2)+(0.0643P)^2\ ]$ for **9**, $w = 1/[\sigma^2(F_o^2)+(0.1805P)^2 + 0.8529P]$ for **10**, $w = 1/[\sigma^2(F_o^2)+(0.0646P)^2 +1.6221P]$ for **11**, $w = 1/[\sigma^2(F_o^2) + (0.0833P)^2 + 1.1877P]$ for **12**, $w = 1/[\sigma^2(F_o^2) + (0.0971P)^2]$ for **13** and $w = 1/[\sigma^2(F_o^2) + (0.0809P)^2]$ for **14**, where, $P=(F_o^2+2F_c^2)/3$

2.2.7 Theoretical study

Experimentally derived crystal structures of $UO_2(NO_3)_2(L^1)_2$ and $Th(NO_3)_4(L^1)_2$ are further subjected to gas phase optimizations with generalized-gradient approximated BP86 [30-31] functional. For O and N atoms triple ζ-TZVP basis set [32-33] and for C and H, def2-SV(P) basis set [34] are used in conjugation with their corresponding auxiliary basis sets. Resolution of Identity (RI) approximations are imposed to speed up the optimizations [35-39]. Single point calculations on the optimized structures are carried out with meta-GGA M06-2X functional. using TZVP basis set. We have benchmarked previously that M06-2X [40] is good for predicting energetics for a series of actinyl complexes [41]. For both the actinides, def-TZVP basis set is used to describe their valance orbitals while core orbitals (60 electrons) are modelled with small-core effective core potential (SC-ECP). The effect of solvation media (water) was incorporated during energy minimization using COSMO continuum salvation model [42] setting dielectric constant values to 80. Further, analytical frequency calculations are performed to verify the optimized structures (Table 2.2) as their potential minima and to derive the free energy of formation of actinide complexes (ΔG). Zero point energy and thermal corrections are incorporated for 298.15 K. In addition, Mülliken population analysis (MPA) [43] (Table 2.3) is also carried out to gauge on the charge distribution over the complexes. All the above calculations are carried out using TURBOMOLE v 6.3.1 [44].

To decipher the nature of metal-ligand binding, energy decomposition analysis (EDA) [45-46] (Table 2.4) is carried out at B3LYP/TZP level using pre-optimized structure as implemented in ADF2013 programme package [47-48]. The total bonding energy (ΔE_{bond}) between the two fragments is calculated using following equation:

$$\Delta E_{bond} = \Delta E_{pauli} + \Delta E_{elast} + \Delta E_{orb}$$

where, ΔE_{pauli} is destabilizing in nature and related to the exchange energy contributions. The attractive electrostatic component, ΔE_{elast} in combination with ΔE_{pauli} gives the total steric interaction in bonding. ΔE_{orb} accounts for the orbital interactions between the fragments which originates during relaxation and mixing of fragmented molecular orbitals. Scalar relativistic corrections are incorporated into these calculations using Zeroth Order Regular Approximation (ZORA) at integration level 4.5.

Finally, In order to scrutinize the percentage of metallic character and the atomic hybrid decompositions of metal-carbonyl, we further performed natural localized molecular orbital (NLMO) analysis (Table 2.5) on the pre-optimized structures at B3LYP/TZP level within the framework of NBO 6.0 version [49] as implemented in ADF 2013 programme package. Natural Population Analysis (Table 2.6) of the actinide-amide complexes was carried out to get an idea about the involvement of valence orbitals in the bonding of the said complexes.

Separation factor (S.F) is calculated using the following equation,

$$S.F = \sim\exp(-\Delta\Delta G_{U/Th}/RT) \text{ for U/Th separation with } \mathbf{L^1} \text{ at 298.15K.}$$

Table 2.2 Optimized structural parameters of actinide-amide complexes

	U=O (Å)	U/Th-O_{L1} (Å)	C=O (Å)	∠(U/Th)-O=C_{L1}	U/Th-NO_3 (Å)	∠O=U=O
$UO_2(NO_3)_2(L^1)_2$	1.803, 1.804 (1.742, 1.746)	2.375, 2.396 (2.327, 2.350)	1.265, 1.268 (1.247, 1.282)	178.6, 153.2 (168.8, 153.8)	2.521-2.543 (2.532-2.545)	179.2 (179.6)
$Th(NO_3)_4(L^1)_2$	---	2.379, 2.380	1.281, 1.281	174.4	2.519-2.551	---

Table 2.3 Net charge transfer from Mülliken Population Analysis of actinide-amide complexes.

Complex	Net Charge Δq, a.u		
	UO_2/Th	Ligand	Nitrate
$[UO_2(NO_3)_2.2L^1]$	0.397	+1.106	-1.503
$[Th(NO_3)_4.2L^1]$	1.205	+0.517	-1.722

Table 2.4 Energy decomposition analysis of actinide-amide complexes at TZP/B3LYP/ZORA level.

Complex	Pauli repulsion $\Delta E_{\mathrm{pauli}}$	Electrostatic interaction $\Delta E_{\mathrm{elstat}}{}^{a}$	Total steric interaction	Orbital interactions $\Delta E_{\mathrm{orb}}{}^{a}$	Total bonding energy
$UO_2(NO_3)_2(L^1)_2$	115.07	-107.75 (61.40%)	7.33	-67.72 (38.60%)	-60.40
$Th(NO_3)_4(L^1)_2$	135.50	-130.14 (59.54%)	5.36	-88.47 (40.46%)	-83.11

[a] Values in the parenthesis represent the percentage contribution of $\Delta E_{\mathrm{elstat}}$ and ΔE_{orb} in total attractive energy ($\Delta E_{\mathrm{elstat}} + \Delta E_{\mathrm{orb}}$).

Table 2.5 Natural Localized Molecular Orbital (NLMO) analysis of actinide-amide complexes.[a]

Complex	NLMO decomposition (%)		Atomic hybrid decomposition (%)	
	NBO[a]	M : O=C_{L1}	M s/p/d/f	O=$C_{L/L}$ s/p/d
$[UO_2(NO_3)_2.2\ L^1]$	BD U-$O_1(L^1)$	8.3:90.5	11.4/0/54.4/34.2	61/39/0
	BD U-$O_2(L^1)$	8.4:90.6	11.3/0/55.3/33.3	60.9/39.1/0
	LP O_1 (L^1)	2.6:92.2	0.3/0.9/29.3/69.6	0/100/0
	LP O_2 (L^1)	3.0:91.8	0/0.6/29.7/69.7	0/100/0
$[Th(NO_3)_4.2L^1]$	BD Th-$O_1(L^1)$	7.4:91.5	11.3/0/54.5/ 34.1	56.3/ 43.7/0
	BD Th-$O_2(L^1)$	7.6:91.5	11.9/0.1/55.2/32.8	60.1/39.1/0
	LP O_1 (L^1)	3.3:92.7	2.3/0.2/47.8/50.0	1/95.7/3.3
	LP O_2 (L^1)	3.1:92.6	0.9/0.3/45.1/53.8	2/98.1/0.1

[a] BD and LP correspond to 2 center valence bond and 1 center lone pair, respectively.

Table 2.6 Natural Population Analysis of actinide-amide complexes.

M	Natural Orbital populations			
	5f	*6d*	*7s*	*7p*
U(VI)	2.63	1.55	0.18	0.01
Th(IV)	0.86	1.12	0.18	0.01

2.3 Results and discussion

2.3.1 Complexation study of piperidine carboxamide ligands with the uranyl nitrate

The complexing ability of $C_5H_{10}NCON(CH_3)_2$, $C_5H_{10}NCON(C_2H_5)_2$ and $C_5H_{10}NCON(^iC_3H_7)_2$ with uranyl nitrate was studied by using elemental analysis, IR and NMR spectroscopic techniques. The reaction of $[UO_2(NO_3)_2.6H_2O]$ with the piperidine carboxamide ligands yielded the compounds **1** to **3** (Scheme 2). The C, H and N analysis revealed that the ratio of ligand to uranyl nitrate is 2:1 in all these compounds.

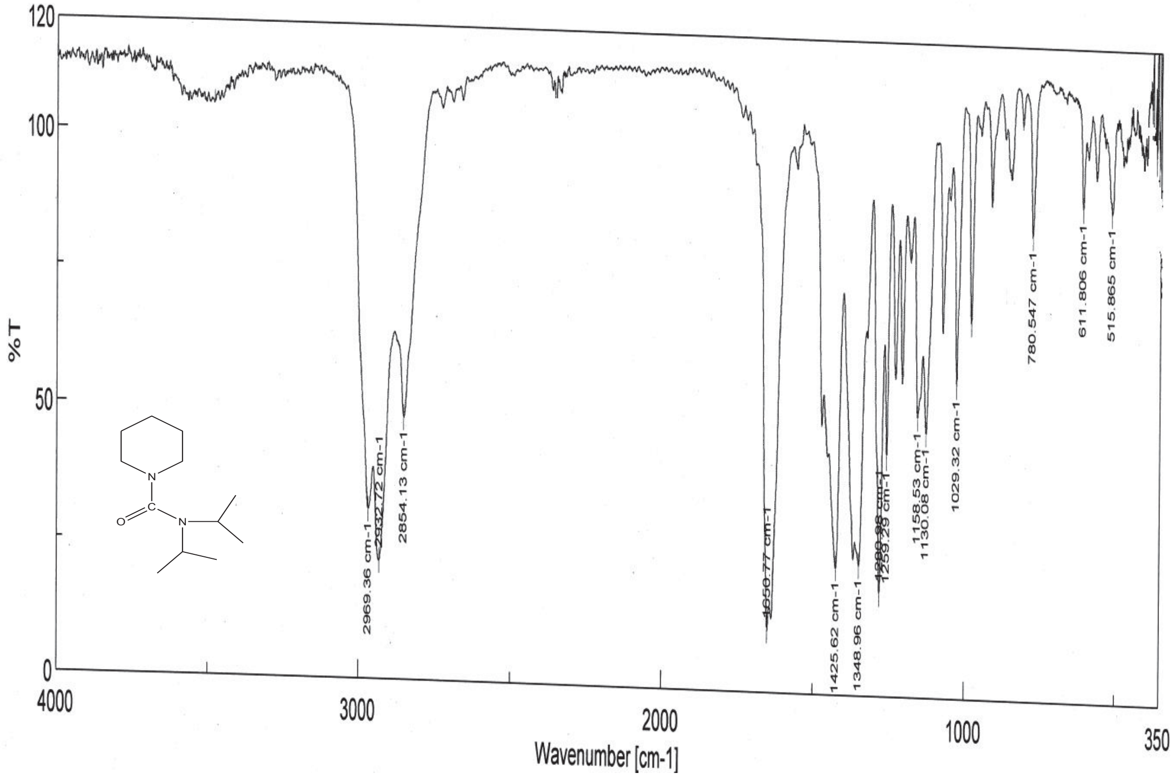

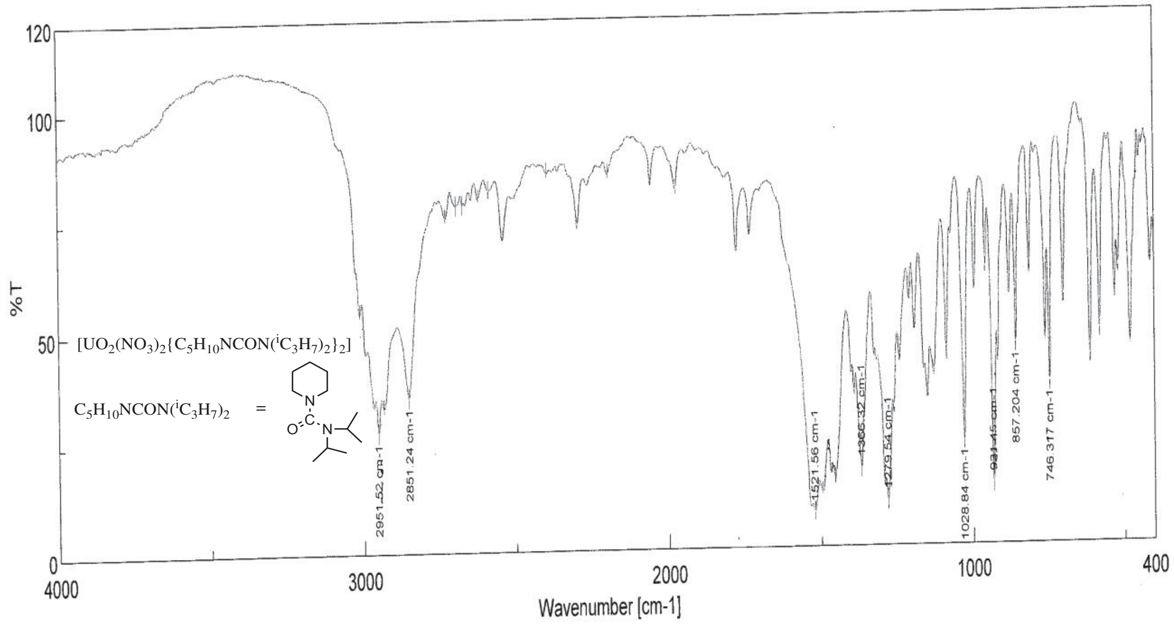

Fig. 2.2 IR spectra of the free ligand $\mathbf{L^3}$ (above) and compound **3** (below)

The IR spectra of the compounds **1–3** show that the water molecules from the starting compound $[UO_2(NO_3)_2 .6H_2O]$ are completely replaced by the ligand and that the ligand is bonded through the carbamoyl oxygen atom to the uranyl group (Fig. 2.2). The observed frequency differences for a carbamoyl ($\Delta\upsilon_{CO}$ = 101-129 cm^{-1}, where $\Delta\upsilon_{CO} = \upsilon_{CO\ (free\ ligand)} - \upsilon_{CO\ (coordinated)}$ group are consistent with the supposition that the carbamoyl group is bonded to the uranyl group directly in the reported compounds. These differences are comparable in magnitude with those of the, $[UO_2(NO_3)_2$ (N-cyclohexyl,2-pyrrolidone)$_2]$ [27], $[UO_2(NO_3)_2$ (1,3-dimethyl,2-imidazolidone)$_2]$ [28], $[UO_2(NO_3)_2\{{}^iC_3H_7CON({}^iC_4H_9)_2\}_2]$ [50] and $[UO_2(NO_3)_2({}^iC_3H_7)_2NCOCH_2CON({}^iC_3H_7)_2]$ [51].

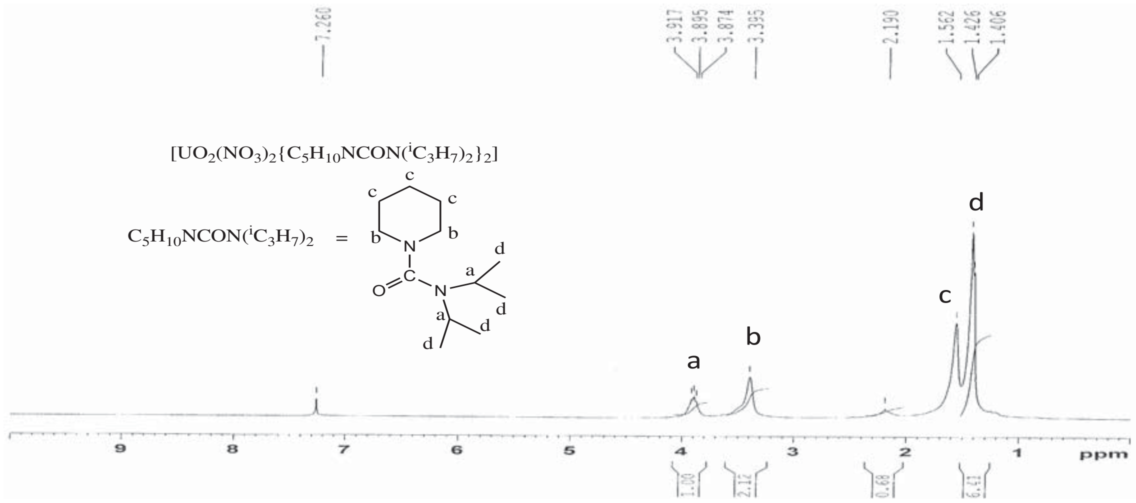

Fig. 2.3 ^{1}H NMR spectrum of compound **3**

Fig 2.3 showed the ^{1}H NMR spectrum of complex **3**. The multiplet at 3.90 ppm is attributed to two CH protons (chemically equivalent due to C-N(diisopropyl) bond rotation at room temperature) of the isopropyl groups in the ligand L^3. These are the most deshielded protons because the CH groups are attached with electronegetive N-atom. Next, the broad peak at 3.40 ppm is due to the four CH_2 protons (chemically equivalent due to C-N(piperidine) bond rotation at room temperature) of the piperidine ring at 2 and 6 position. This peak is broad rather than well resolved multiplet because of quadrapolar effect of ^{14}N-atom adjacent to the carbon atoms at 2 and 6 position. The six CH_2 protons of the piperidine ring at 3, 4 and 5 position resonate together as a singlet at 1.56 ppm. At 1.41 ppm, the doublet is assigned to the twelve CH_3 protons of the isopropyl groups of the ligand. The methyl groups are adjacent to the CH groups of the isopropyl groups, so the signal split into a doublet (n+1 rule, n=1). The spectrum also shows that the protons of the piperidine carboxamide ligands are deshielded by ca. 0.5–0.8 ppm with respect to the free ligand, indicating that the ligand is coordinated to the uranyl group in solution also. It is apparent from the elemental analysis and IR spectral results that ligands are acting as monodentate ligand in compounds **1–3** in the solid state to give similar structures to those observed in the compounds of pyrrolidone [27,28] or other monodentate amides [19–21] with the uranyl nitrate. Interestingly, all these complexes are air and moisture stable crystalline solids, having good solubility in $CHCl_3$ and CH_2Cl_2, and can be used as a starting compound for further reactions. The structure of **3** has been determined by single crystal X-ray diffraction methods, which confirms the IR and elemental analysis results.

2.3.2 Molecular structure of compound ***3***

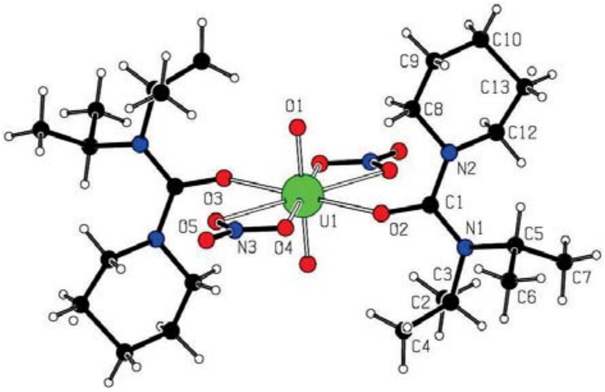

Fig. 2.4 Molecular structure of compound **3**

The molecular structure of the compound **3** is shown in Fig.2.4 and the selected interatomic bond distances and angles for are given in Table 2.7. The structure contains a crystallographic center of symmetry with the uranium atom surrounded by eight oxygen atoms in a hexagonal bi-pyramidal geometry. Two uranyl oxygen atoms occupy the axial positions. There are two bidentate nitrate ligands in the hexagonal equatorial plane together with two carbamoyl oxygen atoms from the two monodentate piperidine carboxamide ligands.

This type of co-ordination is similar to that observed in the compounds of the monofunctional ligands, phosphine oxide, phosphates and amides or pyrrolidones with uranyl nitrate such as: $[UO_2(NO_3)_2$(N-cyclohexylmethyl,2-pyrrolidone)$_2]$ [28], $[UO_2(NO_3)_2$(1,3-dimethyl,2-imidazolidone)$_2]$ [28], $[UO_2(NO_3)_2\{{}^iC_3H_7CON({}^iC_4H_9)_2\}_2]$ [50], $[UO_2(NO_3)(DMF)_2]$ [19], $[UO_2(NO_3)_2$(tetrabutylglutaramide)$_2]$, $[UO_2(NO_3)_2$(tetrabutylglutaramide)$_2]$ [21] and $[UO_2(NO_3)_2(PhN(CH_3)CO(CH_3)NPh)_2]$ [52]. The U–O(amide) distance (2.378(6) Å) in **3** is comparable in magnitude with those of earlier reported uranyl nitrate-amide compounds, such as

$UO_2(NO_3)_2$(N-cyclohexylmethyl,2-pyrrolidone)$_2$] (2.374(2)Å) [28], [$UO_2(NO_3)_2$(1,3-dimethyl,2-imidazolidone)$_2$] (2.383(2)Å) [28], [$UO_2(NO_3)_2\{^iC_3H_7CON(^iC_4H_9)_2\}_2$] (2.349(6)Å) [50], [$UO_2(NO_3)(DMF)_2$] (2.397(6) Å) [19], [$UO_2(NO_3)_2$(tetrabutylglutaramide)$_2$] (2.378(6) Å), [$UO_2(NO_3)_2$(dibutyldecanamide)$_2$] (2.37(2) Å) [21] and [$UO_2(NO_3)_2$ $(PhN(CH_3)CO(CH_3)NPh)_2$] (2.381(2) Å) [52]. The observed average U–O(NO_3) bond distance of 2.527(9) Å is normal. The angles subtended at the metal atom show that the uranium atom has a slightly distorted hexagonal bipyramidal geometry.

The shorter bond lengths observed in this compound can be explained on the basis of a strong pi bonding interaction between the filled 'p' orbitals of oxygen atom with those of the vacant d/f orbitals of the uranyl group, which lead to the opening of the U–O–C bond angle to 149.3(6)° (normally observed in number of metal–amide compounds [53]) to 171.2(6)°. The observed bond lengths and the U–O–C bond angles are compatible with the earlier reported correlation diagram for the uranyl nitrate–amide compounds [28]. In particular, the characteristic of shorter bond distances and wider bond angles are reported for the iso-butyramide based ligands in the compounds of [$Th(NCS)_4(^iC_3H_7CON\{^iC_3H_7\}_2)_3$] [54], [$UO_2Cl_2(^iC_3H_7CON\{^iC_3H_7\}_2)_2$], [$UO_2Br_2(^iC_3H_7CON\{^{sec}C_4H_9\}_2)_2$] [17] and [$UO_2(C_6H_3Cl_2S)_2$ $(^iC_3H_7CON\{^iC_4H_9\}_2)_2$] [18].

Table 2.7 Important bond distances (Å) and angles (°) for the compound **3**

U1–O1	1.762(6)	O1–U1–O2	87.4(2)
U1–O2	2.378(6)	O3–U1–O4	50.0(2)
U1–O3	2.517(6)	O2–U1–O4	65.2(2)
U1–O4	2.538(6)	U1–O2–C1	149.3(6)
C1–O2	1.253(9)		

2.3.3 Complexation study of piperidine carboxamide with the uranyl bis(β-diketonates)

The reactions of $\mathbf{L^1}$–$\mathbf{L^3}$ with [$UO_2(OO)_2.2H_2O$] (OO = $C_4H_3SCOCHCOCF_3$ or $C_6H_5COCHCOC_6H_5$) yielded the compounds **4–9** (Scheme 2). C, H and N analyses revealed that the ratio of ligand to uranyl bis(β-diketonate) is 1:1 in all the compounds. The IR spectra (Fig. 2.5) of **4–9** show that the water molecules from the starting compound [$UO_2(OO)_2.2H_2O$] are completely replaced by the ligand and furthermore the observed frequency difference for the carbamoyl group ($\Delta\nu_{CO}$ = 100–120 cm^{-1}, where $\Delta\nu_{CO} = \nu_{CO\ (free\ ligand)} - \nu_{CO\ (coordinated)}$) is consistent with the supposition that the carbamoyl group is bonded to the uranyl group directly. This difference is comparable in magnitude with those observed in $[UO_2(DBM)_2\{^iC_3H_7CON(^iC_3H_7)_2\}_2]$ [50], $[UO_2(NO_3)_2$(N-cyclohexyl,2-pyrrolidone)$_2]$ [28] and $[UO_2(NO_3)_2$(1,3-dimethyl,2-imidazolidone)$_2]$ [28].

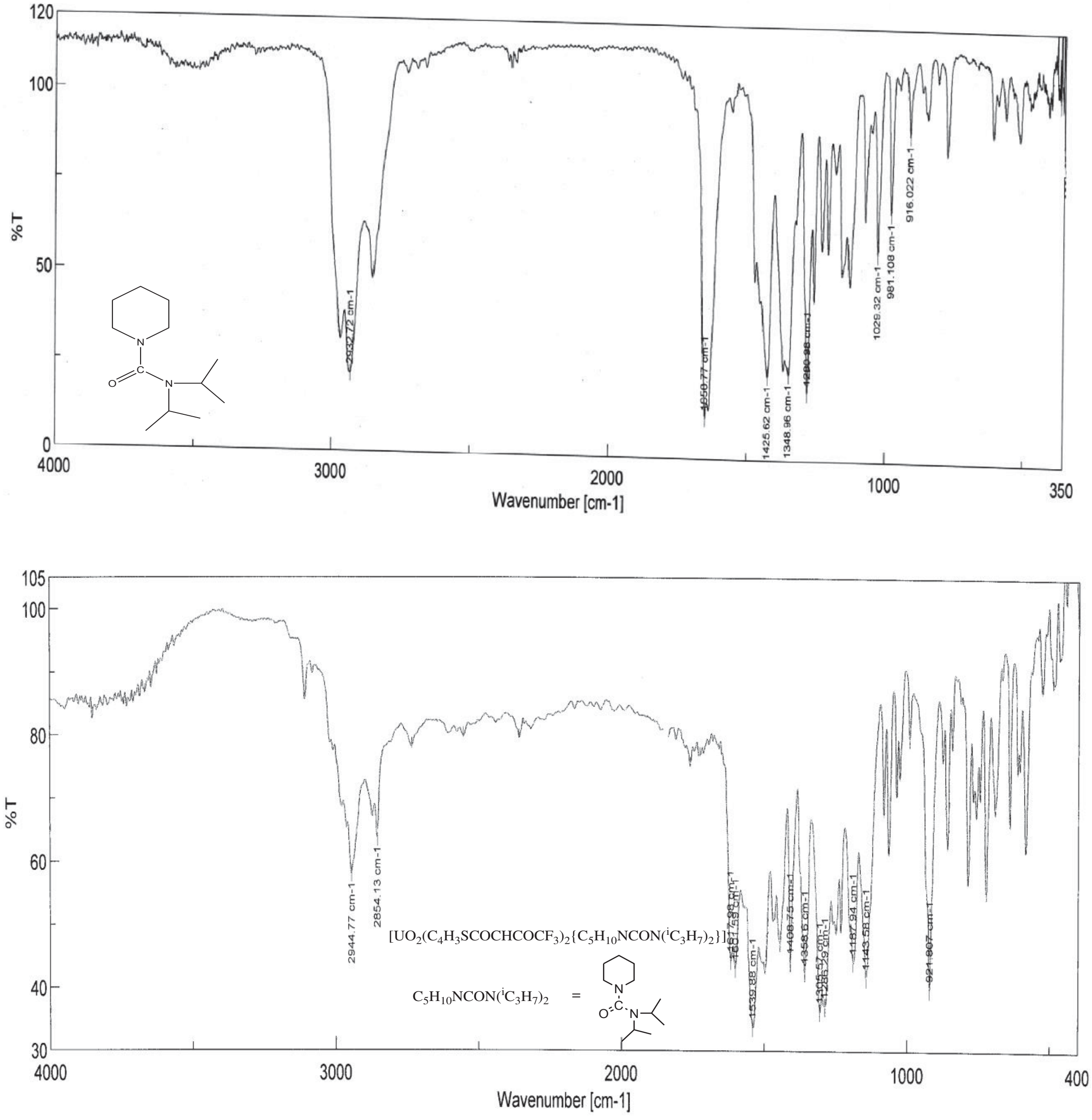

Fig. 2.5 IR spectra of $\mathbf{L^3}$ (above) and the compound **9** (below)

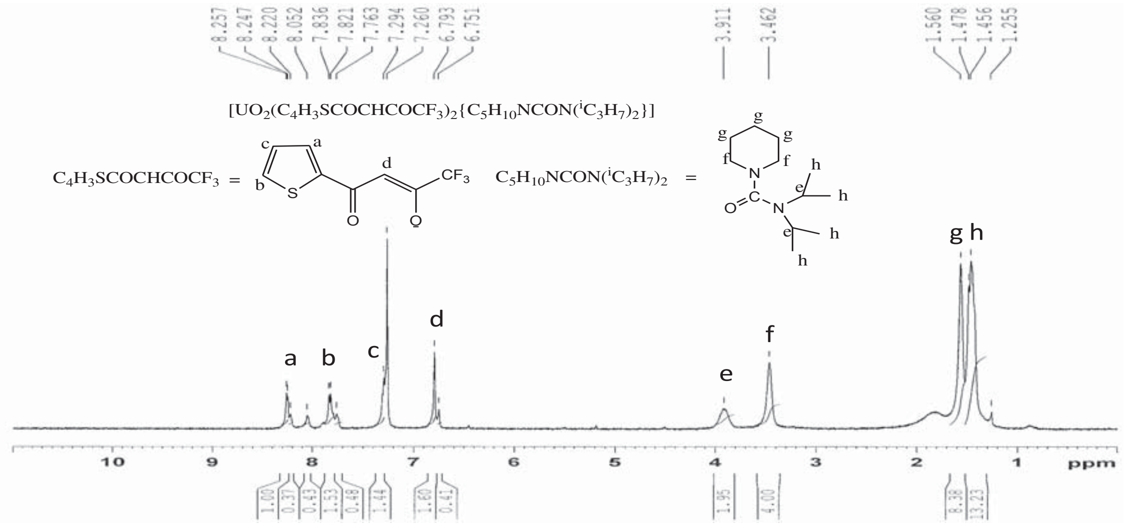

Fig. 2.6 ^{1}HNMR spectrum of compound **9**

Fig 2.6 showed the ^{1}H NMR spectrum of complex **9**. The triplet at 8.25 ppm, the doublet at 7.82 ppm and the broad peak at 7.29 ppm are attributed to the ring protons (two from two TTA ligands) of the thiophene ring at 3, 5 and 4 position respectively. These protons are deshielded because all are aromatic protons. At 6.79 ppm, the singlet is assigned to the CH protons (two from two TTA ligands) adjacent to the keto/enol groups of the TTA ligand. Two CH protons (chemically equivalent due to C-N(diisopropyl) bond rotation at room temperature) of the isopropyl groups of the ligand L^3 resonate as a broad peak at 3.91 ppm. This peak is broad rather than well resolved multiplet because of quadrapolar effect of ^{14}N-atom. Next, the broad peak at 3.46 ppm is due to the four ring protons (chemically equivalent due to C-N(piperidine) bond rotation at room temperature) of the piperidine ring at 2 and 6 position. The six ring protons of the piperidine ring at 3, 4 and 5 position together resonate as a singlet at 1.56 ppm. At 1.46 ppm, the doublet is attributed to the twelve CH_3 protons of the isopropyl groups of the ligand. The methyl groups are adjacent to the CH groups of the isopropyl groups, so the signal split into a doublet. The piperidine carboxamide protons are deshielded by ca. 0.5 ppm with respect to the free ligand, indicating that the bonding between the ligand and uranyl group persists in solution.

The structure of **9** has been determined by the single crystal X-ray diffraction method and confirms the spectral and analysis results.

*2.3.4 Molecular structure of compound **9***

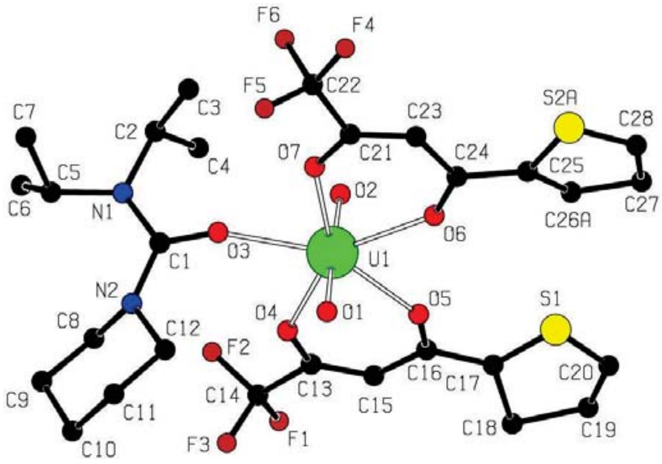

Fig.2.7 The molecular structure of compound **9** (hydrogen atoms omitted for the clarity)

The structure of **9** is shown in Fig. 2.7 together with the numbering scheme, and selected bond distances and angles are given in Table 2.8. The structure shows that the uranyl group is bonded to two $C_4H_3SCOCHCOCF_3$ groups and one piperidine carboxamide ligand to give a coordination number of seven. The piperidine carboxamide ligand acts as a monodentate ligand and is bonded through the carbamoyl oxygen to the uranyl group. Four oxygen from two bidentate $C_4H_3SCOCHCOCF_3$ groups and one oxygen from the piperidine carboxamide ligand form the equatorial plane, which together with two oxygen atoms of the uranyl group form a pentagonal bipyramidal geometry around the uranium(VI) ion. The thiophene ring is disordered due to 180° rotation of this ring about the C16-C17 and C24-C25 bonds. A hybrid scattering factor consisting of 50% sulphur and 50% carbon was used to model this disorder.

Table 2.8 Important bond distances (Å) and angles (°) for compound **9**

U1–O1	1.754(5)	O1–U1–O2	178.2(2)
U1–O2	1.757(5)	O6 – U1 – O7	70.06(17)
U1–O3	2.375(5)	O4 – U1 – O3	73.97(17)
U1–O4	2.387(5)	U1 – O3 – C1	155.6(5)
U1–O5	2.393(5)	O4 – U1 – O5	70.29(18)
U1–O6	2.379(5)	O5 – U1 – O6	71.18(18)
U1–O7	2.383(5)	O3 – U1 – O7	74.60(17)
C1–O3	1.256(8)		

Similar structures are also observed in the compounds of phosphine oxides, sulfoxides, ketones, N-oxides and amides with uranyl bis(β-diketoantes), viz., $[UO_2(DBM)_2(OPPh_3)]$ [55], $[UO_2(DBM)_2(C_6H_5CH_2SOCH_3)]$ [56], $[UO_2(TTA)_2(DBA)]$ [57], $[UO_2(TTA)_2(C_5H_5NO)]$ [58], $[UO_2(TTA)_2(camphor)]$ [59] and $[UO_2(DBM)_2({}^iC_3H_7CON\{{}^iC_3H_7)_2)]$ [50]. The observed U-O amide bond distance (2.375(5) Å) is comparable in magnitude with that reported in $[UO_2(DBM)_2({}^iC_3H_7CON\{{}^iC_3H_7)_2)]$ (2.379(5) Å) [50].

2.3.5 Complexation study of piperidine carboxamide ligands with the uranyl dihalides

The reaction of $[UO_2X_2.\ nH_2O]$ (X = Cl or Br) with the ligand $\mathbf{L^3}$ yielded compounds **10** and **11** (Scheme 2). However, similar reactions with $\mathbf{L^1}$ and $\mathbf{L^2}$ yielded hydroscopic products which were therefore not characterized. C, H and N analyses of **10** and **11** revealed that the ratio of ligand to uranyl halide is 2:1 in both compounds. The IR spectra (Fig. 2.8) of **10** and **11** show that the water molecules from the starting compounds $[UO_2X_2.nH_2O]$ are replaced completely by the ligand. The observed frequency difference for the carbamoyl group ($\Delta\nu_{CO}$ = 125 cm^{-1}, where $\Delta\nu_{CO} = \nu_{CO\ (free\ ligand)} - \nu_{CO\ (coordinated)}$) shows that the carbamoyl group is bonded to the uranyl group directly. This difference is comparable/greater in magnitude than those observed in $[UO_2X_2\{{}^iC_3H_7CON({}^iC_4H_9)_2\}_2]$ (X = Cl or Br) [17], $[UO_2(NO_3)_2\{{}^iC_3H_7CON({}^iC_4H_9)_2\}_2]$ [50] $UO_2(NO_3)_2$(N-cyclohexyl,2-pyrrolidone)$_2$] [28], $[UO_2(NO_3)_2$(1,3-dimethyl,2-imidazolidone)$_2$] [28] and $[UO_2(NO_3)_2({}^iC_3H_7)_2NCOCH_2CON({}^iC_3H_7)_2]$ [51].

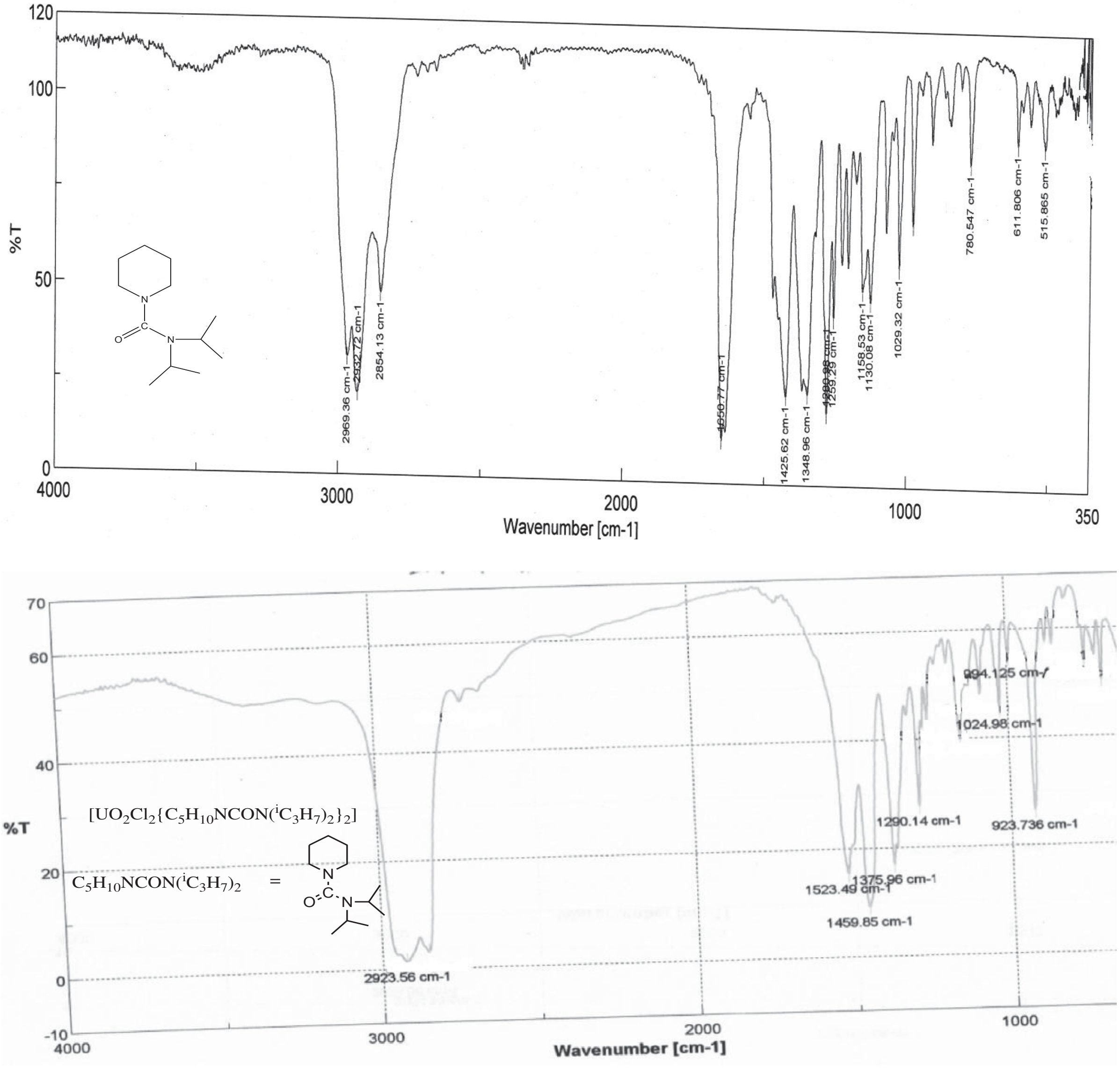

Fig. 2.8 IR spectra of **L^3** (above) and the compound **10** (below)

The ^{1}H NMR spectra of **10** and **11** are very similar to that of compound **3** (already discussed in details earlier) since these complexes are derived from the same ligand (L^3). The proton peaks of the ligand in the spectrum of complexes **10** and **11** are deshielded with respect to the free ligand indicating the bonding between the ligand and uranyl group persists in solution. It is apparent from the IR and NMR spectra that the ligand bonds through the carbamoyl groups to the uranyl group. The structures of **10** and **11** have been determined by the single crystal X-ray diffraction method, which confirms these spectral results.

*2.3.6 Molecular structure of compounds **10** and **11***

The structures of **10** and **11** are shown in Fig, 2.9 and 2.10, respectively, and selected bond distances and angles are given in Table 2.9. The structures of both **10** and **11** show a centrosymmetric uranium(VI) ion surrounded by four oxygen atoms and two halogen atoms in an octahedral geometry. The two uranyl oxygen atoms occupy the axial positions. Two oxygen atoms of the two piperidine carboxamide ligands together with two halogen atoms form the equatorial square plane. This type of coordination is similar to that observed in the compounds of uranyl chloro or bromo compounds such as $[UO_2X_2\{^iC_3H_7CON(^iC_4H_9)_2\}_2]$ (X = Cl or Br) [17] and $[UO_2Cl_2(OPPh_3)_2]$ [60] with monodentate ligand. The average U-O(amide) distance of 2.322(10) Å in **10** and 2.317(5) Å in **11** are comparable in magnitude with those of earlier reported uranyl halide-amide compounds $[UO_2X_2\{^iC_3H_7CON(^iC_4H_9)_2\}_2]$ (2.3151(18) Å for X = Cl and 2.281(4) Å for X = Br) [17]. The observed average U-Cl bond distance 2.683(5) Å in **10** and U-Br distance 2.8073(10) Å in **11** are normal [50, 60]. The angles subtended at the metal atom show that the uranium atom has a slightly distorted octahedral geometry.

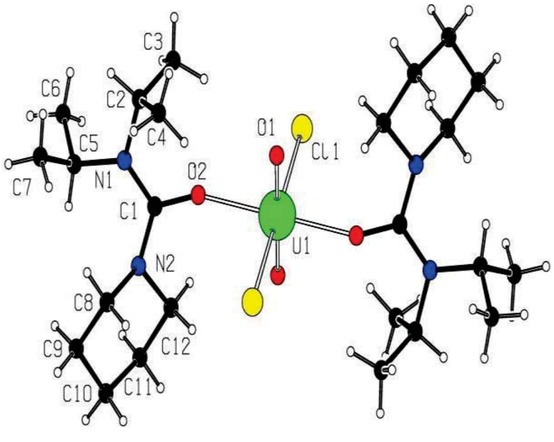

Fig.2.9 The molecular structure of compound **10**

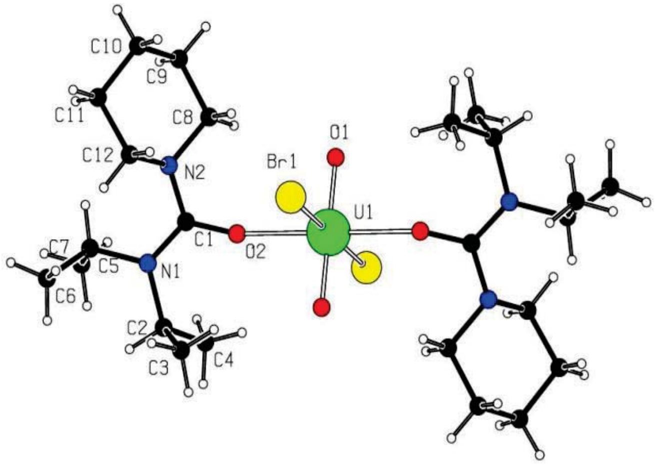

Fig. 2.10 The molecular structure of compound **11**

Table 2.9 Important bond distances (Å) and angles (^{o}) for compound **10** and **11**

10			
U1–O1	1.754(5)	O1–U1–O2	178.2(2)
U1–O2	1.757(5)	O1 – U1 – Cl1	70.06(17)
U1–Cl1	2.375(5)	O2 – U1 – Cl1	73.97(17)
C1–O2	2.387(5)	U1 – O2 – C1	155.6(5)
11			
U1–O1	1.754(6)	O1–U1–O2	91.4(2)
U1–O2	2.317(5)	O1 – U1 – Br1	89.99(19)
U1–Br1	2.8073(10)	O2 – U1 – Br1	88.10(14)
C1–O2	1.263(9)	U1 – O2 – C1	155.2(5)

2.3.7 Complexation study of N,N-diethyl-N′,N′-di-isobutyl urea with the uranyl nitrate

The complexing ability of $C_4H_{10}NCON({}^iC_4H_9)_2\}_2$ with uranyl nitrate was studied by using elemental analysis, IR and NMR spectroscopic techniques. The reaction of $[UO_2(NO_3)_2.6H_2O]$ with the tetraalkyl urea ligand $\mathbf{L^1}$ yielded the compounds **12** (Scheme 2). The C, H and N analysis revealed that the ratio of uranyl nitrate to ligand is 1:2 in the compound.

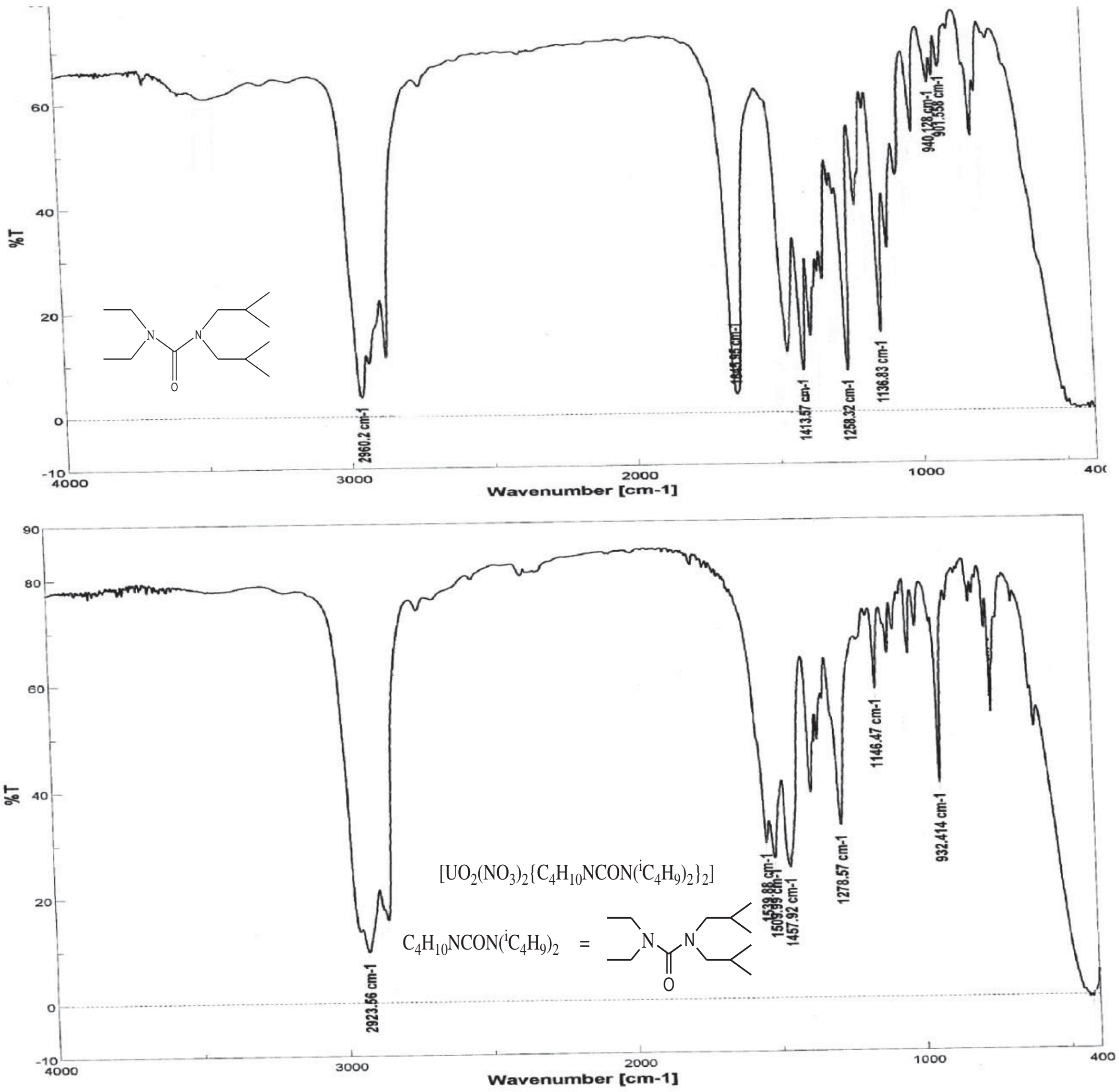

Fig. 2.11 IR spectra of the **L^4** (above) and compound **12** (below)

The IR spectrum of the compound **12** show that the water molecules from the starting compound $[UO_2(NO_3)_2 .6H_2O]$ are completely replaced by the ligand and that the ligand is bonded through the carbamoyl oxygen atom to the uranyl group (Fig. 2.11). The observed frequency difference for a carbamoyl ($\Delta\upsilon_{CO}$ = 106 cm^{-1}, where $\Delta\upsilon_{CO} = \upsilon_{CO\ (free\ ligand)} - \upsilon_{CO\ (coordinated)}$ group are consistent with the supposition that the carbamoyl group is bonded to the uranyl group directly in the reported compounds. These differences are comparable in magnitude with those of the, $[UO_2(NO_3)_2$ (N-cyclohexyl,2-pyrrolidone$)_2]$ [27], $[UO_2(NO_3)_2$ (1,3-dimethyl,2-imidazolidone$)_2]$

[28], $[UO_2(NO_3)_2\{^iC_3H_7CON(^iC_4H_9)_2\}_2]$ [50] and $[UO_2(NO_3)_2(^iC_3H_7)_2NCOCH_2CON(^iC_3H_7)_2]$ [51].

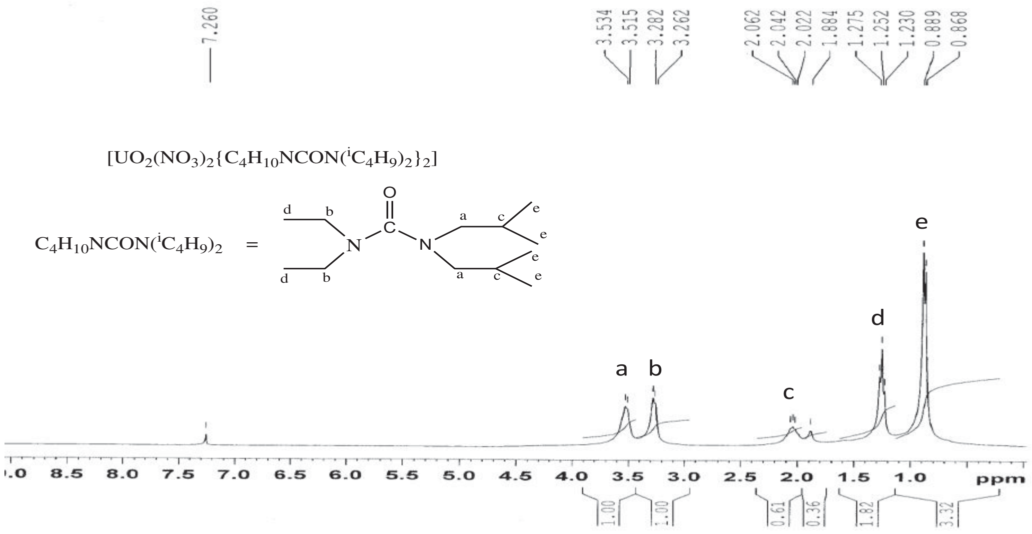

Fig. 2.12 ^1H NMR spectrum of compound **12**

Fig 2.12 showed the ^1H NMR spectrum of complex **12**. The broad multiplet at 3.53 ppm is assigned to four CH_2 protons (chemically equivalent due to C-N(diisobutyl) bond rotation at room temperature) of the isobutyl groups of the ligand L^4. Next, four CH_2 protons (chemically equivalent due to C-N(diethyl) bond rotation at room temperature) of the ethyl groups resonate as the broad multiplet at 3.27 ppm. These two peaks are broad because of quadrapolar effect of ^{14}N-atom adjacent to the CH_2 group protons. These are the deshielded protons in the spectrum because they are attached with electronegative N-atom via one carbon atom. The multiplet at 2.04 ppm is attributed to two CH protons (chemically equivalent due to C-N(diisobutyl) bond rotation at room temperature) of the isobutyl groups. Next, the six CH_3 protons of the ethyl groups of the ligand resonate as a triplet at 1.25 ppm. The signal is split into a triplet, because the methyl group protons are coupled with two adjacent CH_2 protons. At 0.88 ppm, the doublet is due to the twelve CH_3 protons of the isobutyl groups of the ligand. Here, the signal is split into a doublet, because the methyl group protons are coupled with one adjacent CH protons. The spectrum also shows that all the protons of the ligand are deshielded with respect to the free ligand, indicating that the ligand is coordinated to the uranyl group in solution also. It is apparent from the elemental analysis and IR spectral results that ligand is acting as monodentate ligand in compounds **12** in the solid state to give similar structures to those observed in the compounds of pyrrolidone [27,28] or other monodentate amides [19–21] with the uranyl nitrate. Interestingly, the complex is air and moisture stable crystalline solids, having good solubility in $CHCl_3$ and CH_2Cl_2, and can be used as a starting compound for further reactions. The structure of **12** has been determined by single crystal X-ray diffraction methods, which confirms the IR and elemental analysis results.

*2.3.8 Molecular structure of compound **12***

The molecular structure of the compound **12** is shown in Fig. 2.13 and the selected interatomic bond distances and angles for are given in Table 2.10. The structure contains a crystallographic centre of symmetry with the uranium atom surrounded by eight oxygen atoms in a hexagonal bi-pyramidal geometry. Two uranyl oxygen atoms occupy the axial positions. There are two bidentate nitrate ligands in the hexagonal equatorial plane together with two carbamoyl oxygen atoms from two monodentate tetraalkyl urea ligands. The $U–O_{amide}$ bond distances are 2.327(14) Å (U1–O2) and 2.350(13) Å (U1–O7), which are comparable to the previously reported uranyl nitrate complexes of the isobutyramide ligand [17].

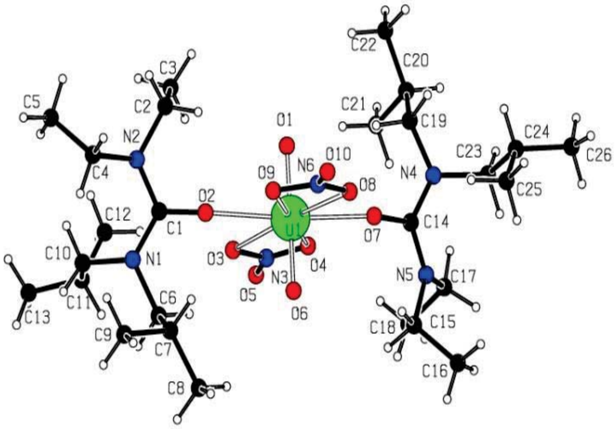

Fig. 2.13 The molecular structure of compound **12**

The observed U–O$_{amide}$ bond distances are shorter in length when compared to the corresponding uranyl nitrate complexes with phosphine oxide ligands $[UO_2(NO_3)_2(Ph_3PO)_2]$ (2.327(14) and 2.350(13) Å vs. 2.359 (7) Å) [22]. The bond angles C1–O2–U1 and C14–O7–U1 are 168.8 (1)° and 153.9 (1)°, respectively and further confirm the inverse relationship between the bond angles (C–O–U) and bond distance (O–U) in the amide–uranyl system as described earlier [28]. However, such a short U–O$_{amide}$ bond distance and nearly linear bond angle 168.8(1)° is rare in uranyl amide chemistry [17] and the presence of the short U–ligand bond lengths and almost linear bond angle indicates very strong bonding between the ligand and uranyl.

Table 2.10 Important bond distances (Å) and angles (^{o}) for the compound **12**

U1–O1	1.742(10)	C1–O2–U1	168.8(14)
U1–O2	2.350(13)	C14–O7–U1	153.9(12)
U1–O3	2.545(14)	O1–U1–O6	179.6(5)
U1–O4	2.532(12)	O1–U1–O7	87.8(5)
U1–O6	1.746 (9)	O1–U1–O2	87.8(5)
U1–O7	2.327(14)	O6–U1–O7	92.4(5)
U1–O8	2.534(14)	O6–U1–O2	92.0(4)
U1–O9	2.541(14)		

2.3.9 Complexation study of N,N-diethyl-N',N'-di-isobutyl urea with the uranyl dihalides

The reaction of $[UO_2X_2.nH_2O]$ (X = Cl or Br) with the ligand $\mathbf{L^1}$ yielded compounds **13** and **14** (Scheme 2). Compounds **13** and **14** are soluble in most organic solvents and all are stable towards moisture and air (in general the chloro and bromo compounds are moisture sensitive). C, H and N analyses of **13** and **14** revealed that the ratio of ligand to uranyl halide is 2:1 in both compounds. The IR spectra (Fig. 2.14) of **13** and **14** show that the water molecules from the starting compounds $[UO_2X_2.nH_2O]$ are replaced completely by the ligand. The observed frequency difference for the carbamoyl group ($\Delta\nu_{CO}$ = 123-124 cm^{-1}, where $\Delta\nu_{CO} = \nu_{CO\ \text{(free ligand)}} - \nu_{CO\ \text{(coordinated)}}$) shows that the carbamoyl group is bonded to the uranyl group directly. This difference is comparable/greater in magnitude than those observed in $[UO_2X_2\{^iC_3H_7CON(^iC_4H_9)_2\}_2]$ (X = Cl or Br) [17], $[UO_2(NO_3)_2\{^iC_3H_7CON(^iC_4H_9)_2\}_2]$ [50]

$UO_2(NO_3)_2$(N-cyclohexyl,2-pyrrolidone)$_2$] [28], [$UO_2(NO_3)_2$(1,3-dimethyl,2-imidazolidone)$_2$] [28] and [$UO_2(NO_3)_2(^iC_3H_7)_2NCOCH_2CON(^iC_3H_7)_2$] [51].

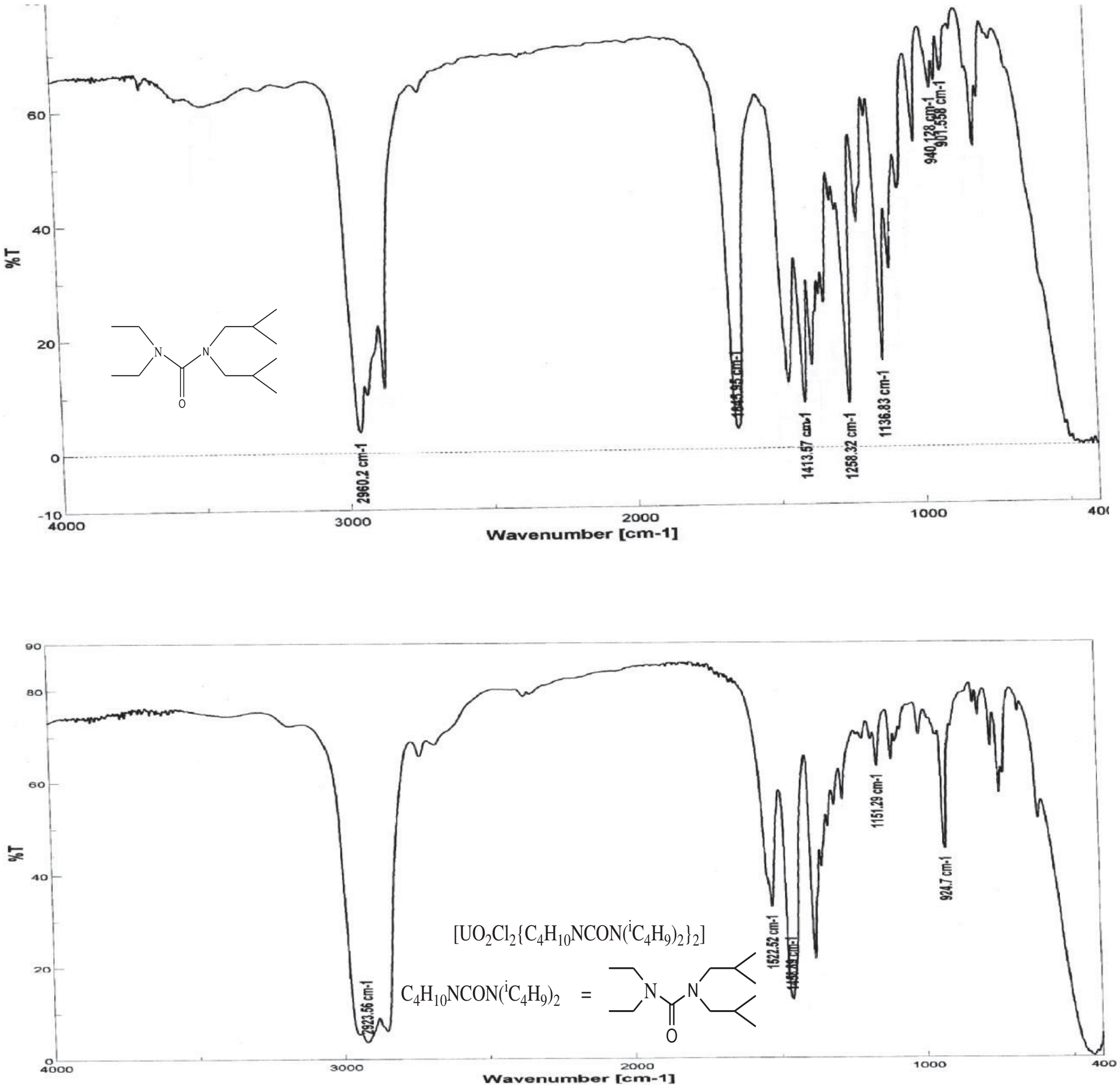

Fig. 2.14 IR spectra of **L^4** (above) and the compound **13** (below)

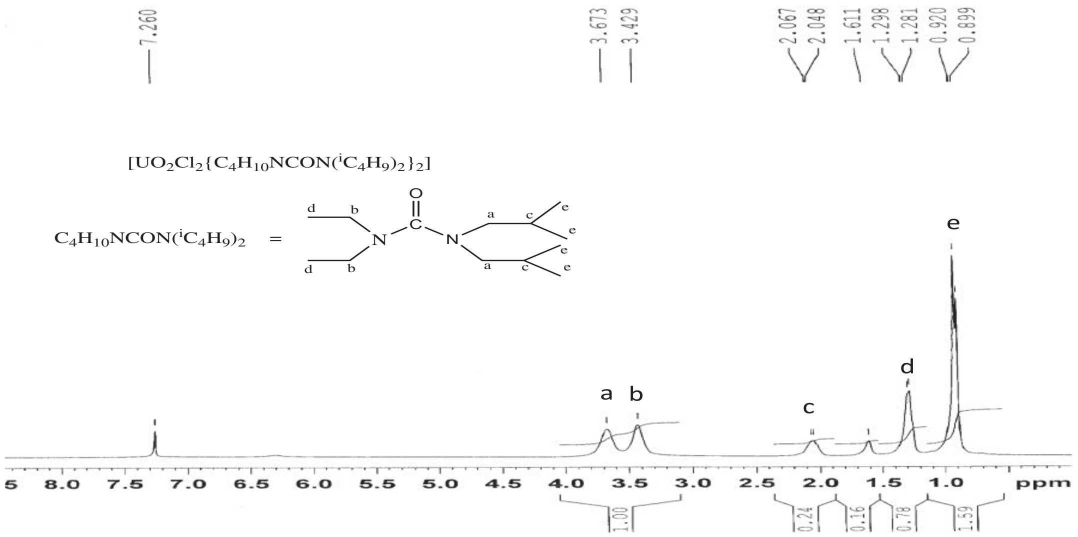

Fig. 2.15 ^{1}H NMR spectrum of compound **13**

Fig 2.15 showed the ^{1}H NMR spectrum of complex **13**. The broad peak at 3.67 ppm is assigned to four CH_2 protons (chemically equivalent due to C-N(diisobutyl) bond rotation at room temperature) of the isobutyl groups of the ligand L^4. Next, at 3.43 ppm, the broad peak is due to four CH_2 protons (chemically equivalent due to C-N(diethyl) bond rotation at room temperature) of the ethyl groups. These two peaks are broad because of quadrapolar effect of ^{14}N-atom adjacent to the CH_2 group protons. These are the deshielded protons in the spectrum because they are attached with electronegative N-atom via one carbon atom. The multiplet at 2.06 ppm is attributed to two CH protons (chemically equivalent due to C-N(diisobutyl) bond rotation at room temperature) of the isobutyl groups. The six CH_3 protons of the ethyl groups of the ligand resonate as a triplet at 1.29 ppm. The signal is split into a triplet, because the methyl group protons are coupled with two adjacent CH_2 protons. At 0.91 ppm, the doublet is due to the twelve CH_3 protons of two isobutyl groups of the ligand. The signal is split into a doublet, because the methyl group protons are coupled with one adjacent CH protons. All the protons are deshielded with respect to the free ligand indicating that the bonding between the ligand and uranyl group persists in solution. It is apparent from the IR and NMR spectra that the ligand bonds through the carbamoyl groups to the uranyl group. The structures of **13** and **14** have been determined by the single crystal X-ray diffraction method, which confirms these spectral results.

*2.3.10 Molecular structure of compounds **13** and **14***

The structures of **13** and **14** are shown in Fig. 2.16 and 2.17, respectively, and selected bond distances and angles are given in Table 2.11. Complex **13** and **14** [$UO_2X_2 \cdot 2L^1$ where X = Cl^- and Br^-] show a distorted octahedral geometry around the uranium centre. The two halide ions and two ligands are trans to each other. The U–O_{amide} bond distances are 2.264 (6) Å and 2.288 (6) Å in **13** and **14**, respectively, which are very close to the reported uranyl chloride (2.315 (3) Å) and uranyl bromide (2.281 (4) Å) isobutyramide complexes [17]. Again, these bond distances are shorter when compared to the reported [$UO_2Cl_2(Ph_3PO)_2$] complexes [60(a)] (2.264 Å vs. 2.300 (8) Å) showing the strong bonding to uranyl compared to the phosphine oxide donor. The C1–O2–U bond angles are 167.7 (6) and 167.3 (6) for complex **13** and **14**, respectively, which are in line with the previously reported isobutyramide complexes with uranyl halide (2.281–2.315(18) Å) [17]. From the abovementioned structural discussion it is evident that ligand L^1 forms a stronger complex with uranyl dihalides when compared to that of phosphine oxide based ligands, as well as having similar structural features as the isobutyramide ligands. Therefore, the selectivity for uranyl has been explored as isobutyramide type ligands are known to be selective for the uranyl over plutonium and thorium from nitric acid medium [13, 50].

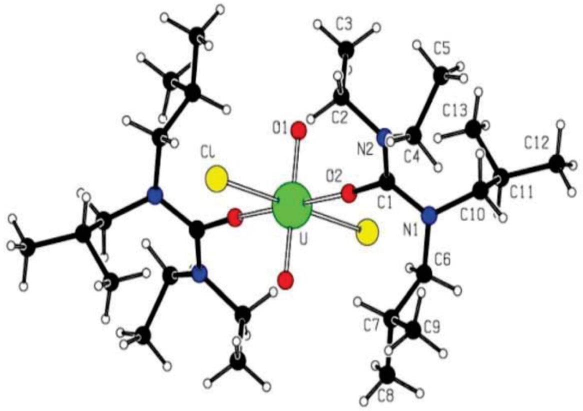

Fig. 2.16 The molecular structure of compound **13**

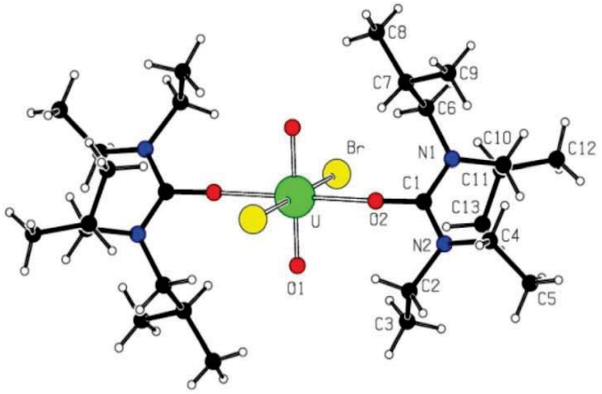

Fig. 2.17 The molecular structure of compound **14**

Table 2.11 Important bond distances (Å) and angles (°) for compound **13** and **14**

13			
U1–O1	1.762(6)	C1–O2–U	167.7(6)
U1–O2	2.264(6)	O1–U–O2	90.9(3)
U1–Cl	2.663(3)	O1–U–Cl	88.6(3)
14			
U1–O1	1.763(6)	C1–O2–U	167.3(6)
U1–O2	2.288(6)	O1–U–O2	90.2(3)
U1–Br	2.8118(12)	O1–U–Br	89.2(2)

2.3.11 Comparison of ligand (L^1-L^4) donor strength in the uranyl complexes by comparing the uranyl stretching frequency in the vibrational spectroscopy

The symmetric stretching frequency (ν_1) of the linear uranyl group (U=O$_{axial}$) is infra-red inactive but Raman active. On the other hand, the reverse response is true for the asymmetric bond stretching frequency (ν_3) of the same. This is due to the mutual exclusion principle of any molecule or group having centre of inversion akin to linear uranyl ($O=U=O^{2+}$) group.

The central uranium atom in the uranyl complexes generally adopts six to eight coordination number with two linear oxygen atoms at the axial positions and four to six donor atoms in the equatorial positions. It is well proven that, the donor atoms at the equatorial positions form more strong bond with the uranium atom, the bond strength of the equatorial bonds is increased which ultimately weakens the axial bonds and decreases the axial bond strength and vice versa. Thus the donor ability of the ligands can be compared indirectly by comparing either the symmetric stretching frequency (ν_1) of the axial uranyl bond in the Raman spectroscopy or the asymmetric stretching frequency (ν_3) of the same in the infra-red spectroscopy. Here, we have recorded the infra-red spectra of the uranyl nitrate, halides and β-diketonate complexes with four newly synthesized ligands (**L^1-L^4**) and systematically tabulated in table 2.12.

Table 2.12 Comparison of IR frequencies of uranyl complexes

Complex	$C{=}O_{str}$ frequency of free ligands (cm^{-1})	$C{=}O_{str}$ frequency of the bonded ligands (cm^{-1})	$\Delta\nu_{CO}$ (cm^{-1})	$U{=}O_{asy}$ frequency of the axial bond (cm^{-1})
$[UO_2(NO_3)_2\{C_5H_{10}NCON(CH_3)_2\}_2]$ (1)	1653	1525	128	925
$[UO_2(NO_3)_2\{C_5H_{10}NCON(C_2H_5)_2\}_2]$ (2)	1622	1521	101	928
$[UO_2(NO_3)_2\{C_5H_{10}NCON(^iC_3H_7)_2\}_2]$ (3)	1651	1522	129	931
$[UO_2(C_6H_5COCHCOC_6H_5)_2\{C_5H_{10}NCON(CH_3)_2\}]$ (4)	1653	1542	111	907
$[UO_2(C_6H_5COCHCOC_6H_5)_2\{C_5H_{10}NCON(C_2H_5)_2\}]$ (5)	1622	1542	80	905
$[UO_2(C_6H_5COCHCOC_6H_5)_2\{C_5H_{10}NCON(^iC_3H_7)_2\}]$ (6)	1651	1541	110	901
$[UO_2(C_4H_3SCOCHCOCF_3)_2\{C_5H_{10}NCON(CH_3)_2\}]$ (7)	1653	1540	113	919
$[UO_2(C_4H_3SCOCHCOCF_3)_2\{C_5H_{10}NCON(C_2H_5)_2\}]$ (8)	1622	1539	83	922
$[UO_2(C_4H_3SCOCHCOCF_3)_2\{C_5H_{10}NCON(^iC_3H_7)_2\}]$ (9)	1651	1540	111	922
$[UO_2Cl_2\{C_5H_{10}NCON(^iC_3H_7)_2\}_2]$ (10)	1651	1524	127	924
$[UO_2Br_2\{C_5H_{10}NCON(^iC_3H_7)_2\}_2]$ (11)	1651	1525	126	928
$[UO_2(NO_3)_2\{C_4H_{10}NCON(^iC_4H_9)_2\}_2]$ (12)	1646	1540	106	932
$[UO_2Cl_2\{C_4H_{10}NCON(^iC_4H_9)_2\}_2]$ (13)	1646	1523	123	925

$[UO_2Br_2\{C_4H_{10}NCON(^iC_4H_9)_2\}_2]$ (14)	1646	1522	124	927

From the table it can be observed that, in the $[UO_2(NO_3)_2.6H_2O]$, $[UO_2(C_6H_5COCHCOC_6H_5)_2.2H_2O]$, $[UO_2(C_4H_3SCOCHCOCF_3)_2.2H_2O]$ complexes of piperidine carboxamide ligands, the order of $U{=}O_{asy}$ frequency is (3) > (2) > (1), (4) > (5) > (6) and (9) = (8) > (7) respectively, which signifies that donor strength order of the ligands is $L^1 > L^2 > L^3$ in these complexes. This can be explained on the basis of decreasing basicity of the ligands with increasing bulkiness of the ligands since the electronic property is almost same for all the ligands. Similarly, In the $[UO_2(NO_3)_2.6H_2O]$ and uranyl dihalide complexes of tetraalkyl urea complexes the order of $U{=}O_{asy}$ frequency is (12) > (13) ~ (14), which signifies that donor strength order of L^4 ligand in these complexes is (13) ~ (14) > (12). This is as expected because the ligands encounter lesser steric effect in the halide complexes (six coordinated) with respect to the nitrate complexes (eight coordinated) when approaches toward the metal centre, hence the basicity is decreased in the nitrate complexes with respect to the halide complexes where the ligands get more chance to approach the metal centre closely.

2.3.12. Precipitation studies of U(VI) ions from the bulk of Th(IV) and Ln(III) ions

The EDXRF spectra of the initial solution, supernatant and precipitate are shown in Fig. 2.18. From the EDXRF spectrum, it is clear that there is only thorium present in the supernatant solution and no trace of uranium was detected. Similarly, the EDXRF spectrum of the precipitate shows only the presence uranium and no thorium. This study clearly revealed that the ligand is selective for uranium and precipitate uranium from the solution containing a large excess of thorium. The observed UV-Vis spectra of the initial and supernatant (Fig. 2.19) solutions also supported the abovementioned observations. This experiment was repeated with a nitric acid solution containing a mixture of uranyl, thorium and lanthanide (La^{3+}, Sm^{3+} and Eu^{3+}) ions to ascertain the selectivity of the ligand towards uranyl ions over lanthanide and thorium ions. This process also selectively deposited uranyl ions from the solution containing a bulk of thorium and lanthanide ions as confirmed by EDXRF analysis (Fig. 2.20).

Similarly, in the supernatant no traces of uranium are observed in the EDXRF spectra (Fig. 2.20(a)) and all the lanthanides are present in the supernatant as observed in the EDXRF spectra (Fig. 2.20(b)). From the above mentioned precipitation studies, it is observed that the ligand $\mathbf{L^1}$ can be used to selectively precipitate uranium from a solution containing thorium and lanthanides from a nitric acid medium.

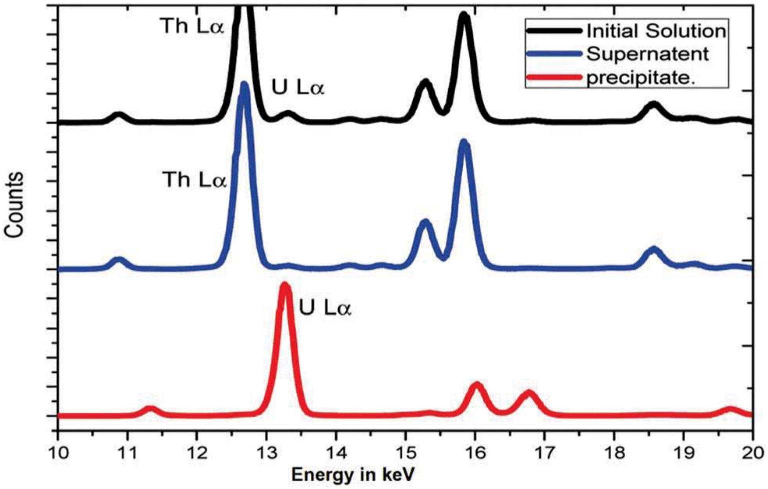

Fig. 2.18 The EDXRF spectra of the precipitate, supernatant and initial solution.

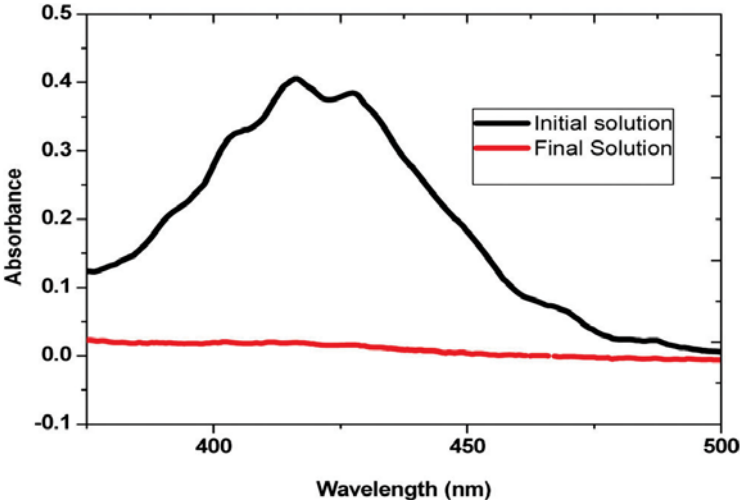

Fig. 2.19 The UV-Vis spectra of the initial and supernatant solutions

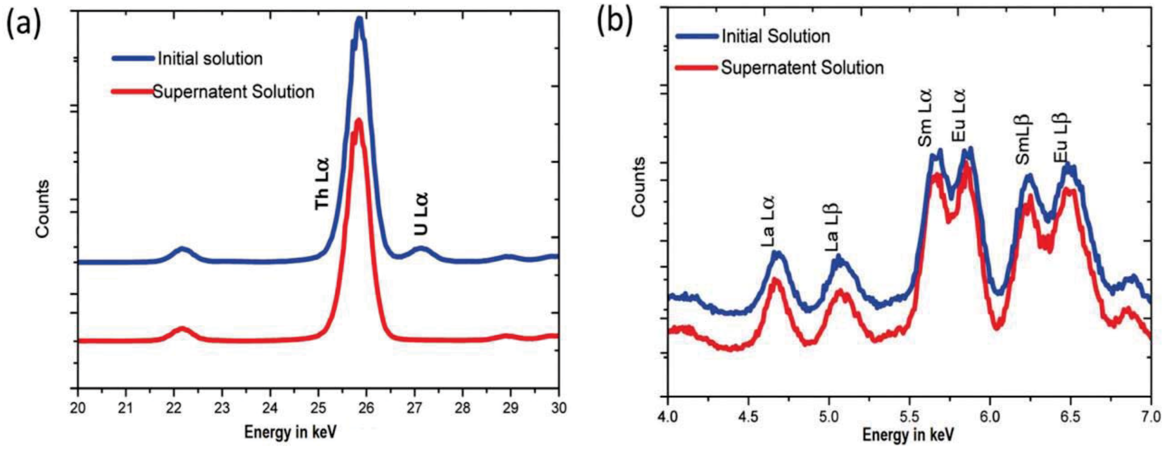

Fig. 2.20 (a) EDXRF spectra of the initial and supernatant solutions containing a Rh source and (b) EDXRF spectra of the initial and supernatant solution containing a Ge secondary target.

2.3.13. Extraction studies of U(VI) and Pu(IV) with $C_4H_{10}NCON(C_8H_{17})_2$ from nitric acid

The extraction studies were carried out by using the ligand $C_4H_{10}NCON(C_8H_{17})_2$ in dodecane with the U(VI) and Pu(IV) ions in tracer level (using the 233U and 239Pu) from nitric acid medium to assess the feasibility of using this ligand for the extraction purpose. Distribution ratios (D) for U(VI) and Pu(IV) as a function of nitric acid concentrations (Fig.2.21) shows clearly that observed distribution values are very low for both the U(VI) and Pu(IV) under the acid concentrations of 1–10 M. However, under any acid concentration, the D for Pu(IV) is much smaller than those of U(VI). This observation is completely contradictory to the data reported for any of the extractants (either mono-functional or bi- functional) with that of Pu(IV) ($D_{Pu(IV)} >> D_{U(VI)}$ always) [6-9] and agrees well with the result reported for the isobutyramide based extractant [13-15]. This shows clearly that the uranium can be selectively separated from plutonium or vice versa.

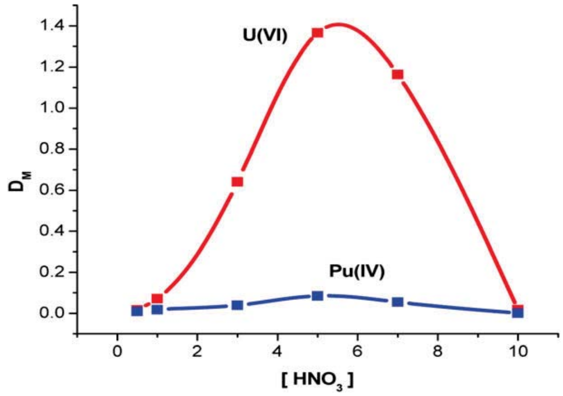

Fig. 2.21 Variation of distribution ratio for U(VI) and Pu(IV) with HNO_3

2.3.14 Theoretical studies

The molecular level insights on the origin of selectivity of ligand $\mathbf{L^1}$ obtained in experiments can be understood through density functional theory (DFT) based calculations. The geometries predicted using the BP86 functional of compound **1** are fairly comparable with that of the experimental data (Fig. 2.22). The ligand $\mathbf{L^1}$ binds strongly to uranyl U–$O_L{}^1$, which in turn weakens the axial U=O_{yl} bond by a similar margin. The computed bond angle of one U–O=$C_L{}^1$ is akin to the experimental value, whereas the second bond angle is overestimated by 10 degrees. The U–O_{NO3} bond lengths are very accurately predicted within 0.01 Å to the X-ray data. Furthermore, the computed bond angle (O=U=O) is also predicted to be linear, which corroborates well with our experimental data. Upon complexation, the computed C=O vibrational frequency of the bound species is red-shifted by ~100 cm^{-1}, which is in line with our experimental IR shifts and thus consistent with the elongation of the C=O bond distance (by ~0.02 Å) upon metal binding. Similarly, the U=O stretching frequency is also red-shifted by 30 cm^{-1} with respect to the bare uranyl nitrate hexahydrate (the experimentally observed shift is 14 cm^{-1}). However, for Th(IV) bound complexes we find this shift is somewhat larger (no complex formation occur experimentally), which is reflected in the elongated C=O bond length (by 0.02 Å) when compared to the uranium species. To ascertain the thermodynamic favourability of these metal complexation reactions, we have calculated the formation free energies for the two actinide ions using the M06-2X functional and BP86 optimized structures (Table 2.13). Furthermore, the computed separation factor of uranyl in the presence of Th(IV) with $\mathbf{L^1}$ is very high (110.4), which explains the unavailability of uranium in the supernatant and the absence of thorium precipitation in the observed complexation processes. The large negative entropy for Th(IV) originates from the overcrowded coordination centre when compared to the uranium centre. Energy decomposition analysis (EDA) was performed (TZP/B3LYP/ZORA) on the metal bound species to segregate the contributions of the various repulsive-attractive energy components from the total bonding energy. For both metal ions, favourable electrostatic interactions (~60%) contributed more to the total bonding energy. However, orbital interactions, originating from the orbital relaxation of fragmented orbitals from the excited to ground state also seems to contribute an extent of ~40% with respect to the total attractive term. It can be noted that for both actinides, the positive Pauli repulsion term cancels the attractive electrostatic interaction resulting in a positive value for the total steric repulsion. The prominent electrostatic interactions between $\mathbf{L^1}$ and the actinides arise from the net charge transfer from the ligand to the metal (derived from Mülliken population analysis). When compared to Th bound complex, the uranyl complex has higher ligand to uranyl charge transfer. Furthermore, the net charge on nitrates is involved in neutralizing the tetra-positive thorium than uranium, which implies the relatively stronger binding with nitrate for the former. A detailed molecular orbital analysis was carried out through natural localized molecular orbital (NLMO) theory to understand the binding behavior of $\mathbf{L^1}$ with the metal ions. We found that the lone pair of the carbonyl oxygen in the ligand is strongly delocalized (~3%) in the U–$O_L{}^1$ antibond wherein the f-orbital of U majorly acts as the acceptor orbital (69%). However, for Th, both the d and f orbitals equally participate as the acceptor orbital for the delocalization of the carbonyl lone pair electrons. The sigma bond between U/Th and the carbonyl oxygen is formed by the involvement of ~8% uranium and ~92% carbonyl oxygen orbitals. In this bond, the metal orbitals have a contribution of roughly

11% s, 54% d and 34% f orbitals. In line with the NLMO results, the natural orbital population shows lesser involvement of the 7s and 7p orbitals in ligand binding. In addition, between 6d and 5f, greater participation of the 5f orbital is noticed for uranium, whereas the 6d orbital contributes more for thorium.

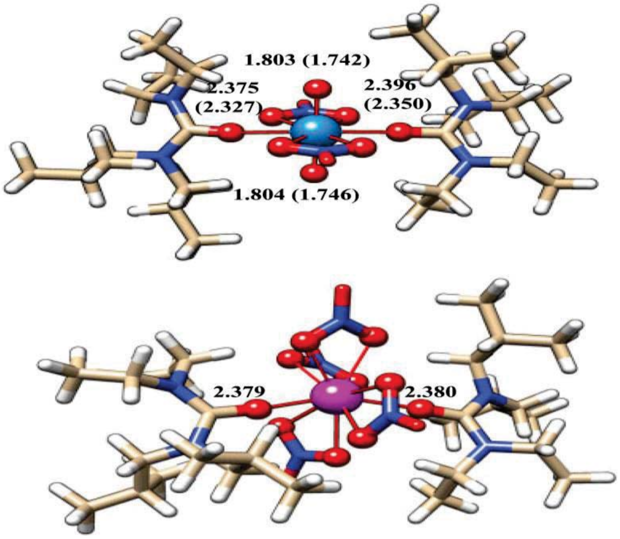

Fig. 2.22 The optimized structures (bond length in Å) of the actinide–amide complexes. The values in the brackets correspond to the X-ray structure data.

Table 2.13 The computed formation free energies and separation factor (S.F) using the M06-2X functional (kcal mol^{-1})

	ΔG	ΔΔG[a]	S.F (UO_2/Th)
UO_2	−6.47	−2.79	110.4
Th	−3.68	—	

[a] $\Delta\Delta G = \Delta G(UO_2) - \Delta G(Th)$.

2.4 Conclusions

The piperidine based amide ligands form 2:1 complexes with uranyl chloride, bromide and nitrate and 1:1 complexes with the uranyl bis(β-diketonates). The uranyl chloro and bromo compounds are air and moisture stable and soluble in common organic solvents. The structures of the chloro and bromo complexes show that the uranium(VI) ion is surrounded by two halogen, two uranyl and two amido oxygen atoms in an octahedral geometry. The structures of the uranyl nitrate and uranyl bis (β-diketonates) complexes show hexagonal bipyramidal and pentagonal bipyramidal geometries respectively around the uranium(VI) ion.

The selective recognition of one useful metal ion in the presence of other interfering ions is one of the most important research areas in the field of nuclear waste management processes. In this study, we have carried out combined experimental and electronic structure calculations to understand the origin of selectivity of a structurally known but unexplored extractant, N,N-diethyl-N′,N′-diisobutyl urea. We have characterized the structure of the uranyl bound complexes through X-ray crystallography. Furthermore, the extractant selectivity towards uranyl ion in the presence of Th(IV) and other interfering lanthanide ions in a nitric acid medium was explored using several spectroscopic techniques. Based on electronic structure calculations at the DFT level of theory, we found that the preferential binding of uranyl ion to Th(IV) is modulated by both steric and electronic factors. Thus, the combined experimental and theoretical studies are extremely useful to understand the selectivity of heavy metal ions, which is relevant to the backend of the nuclear fuel cycle.

2.5 References

1. L.R. Morss, N.M. Edelstein, J. Fuger, J.J. Katz, ‘The Chemistry of the Actinide and Transactinide Elements, Springer’, Netherlands (2006).
2. C.J. Burns, M.P. Neu, H. Boukhalfa, K.E. Gutowshi, N.J. Bridges, R.D. Rogers, J.A. McCleverty, T.J. Meyer, G.F.R. Parkin, (Eds.), ‘Comprehensive Coordination Chemistry II’, Elsevier, Oxford, 3 (2004) 189.
3. M. Ephritikhine, Dalton Trans. (2006) 2501.
4. S. Kant, Int. J. Nucl. Ener. Sci. Tech. 1 (2005) 204.
5. R. K. Sinha, A. Kakodkar, Nucl. Eng. Des. 236 (2006) 683.
6. C. Musikas, Inorg. Chim. Acta 140 (1987) 197.
7. C. Madic, M.J. Hudson, ‘High Level Liquid Waste Partitioning by Means of Completely Incinerable Extractants’, European Commission, Nuclear Science and Technology, EU18038EN, Luxembourg (1998).
8. L. Nigond, C. Musikas, C.C. Cullerdier, Solv. Extr. Ion Exch. 12 (1994) 261.

9. L. Nigond, N. Condamines, P.Y. Cordier, J. Livert, C. Madic, C.C. Cullerdier, C. Musikas, Sep. Sci. Technol. 30 (1995) 2075.
10. Y. Sasaki, Y. Sugo, S. Suzuki, S. Tachimori, Solv. Extr. Ion Exch. 19 (2001) 91.
11. S. Tachimori, Y. Sasaki, S. Suzuki, Solv. Extr. Ion Exch. 20 (2002) 687.
12. Z. Zhu, Y. Sasaki, H. Suzuki, S. Suzuki, T. Kimura, Anal. Chim. Acta 527 (2004) 163.
13. P.N. Pathak, R. Veeraraghavan, D.R. Prabhu, G.R. Mahajan, V.K. Manchanda, Sep. Sci. Technol. 34 (1999) 2601.
14. P.N. Pathak, L.B. Kumbhare, V.K. Manchanda, Solv. Extr. Ion Exch. 19 (2001) 105.
15. V.K. Manchanda, P.N. Pathak, Sep. Purif. Technol. 35 (2004) 85.
16. T.R. Varga, M. Sato, Zs. Fazekas, M. Harada, Y. Ikeda, H. Tomiyasu, Inorg. Chem. Commun. 3 (2000) 637.
17. S. Kannan, C.L. Barnes, P.B. Duval, Chem. Commun. (2005) 5997.
18. S. Kannan, C.L. Barnes, P.B. Duval, Inorg. Chem. 44 (2005) 9137.
19. J.M. Gil, F.J.M. Gil, A. Perales, J. Fayos, M.M. Ripoll, Acta Crystallogr. Sect. C 39 (1983) 44.
20. P. Charpin, M. Lance, M. Nierlich, D. Vigner, Acta Crystallogr. Sect. C 43 (1987) 442.
21. P. Charpin, M. Lance, M. Nierlich, D. Vigner, Acta Crystallogr. Sect. C 42 (1986) 560.
22. N.W. Alcock, M.M. Roberts, D. Brown, J. Chem. Soc., Dalton Trans. (1982) 25.
23. B. Kanellakopulos, E. Dornberger, R. Maier, B. Nuber, H.G. Stammler, M.L. Ziegler, Z. An org. Allg. Chem. 619 (1993) 593.
24. J.H. Burns, Inorg. Chem. 20 (1981) 3868.
25. A.R. de Aquino, G. Bombieri, P.C. Isolani, G. Vicentini, J.Z. Schpector, Inorg. Chim. Acta 306 (2000) 101.
26. G. Agostini, G. Giacometti, D.A. Clemente, M. Vicentini, Inorg. Chim. Acta 62 (1982) 237.
27. T.R. Varga, A.C. Benyei, Z. Fazekas, H. Tomiyasu, Y. Ikeda, Inorg. Chim. Acta 342 (2003) 291.
28. N. Koshino, M. Harada, M. Nogami, Y. Morita, T. Kikuchi, Y. Ikeda, Inorg. Chim. Acta 358 (2005) 1857.
29. K.M. Abubacker, N.S.K. Prasad, J. Inorg. Nucl. Chem. 16 (1961) 296.
30. A.D. Becke, Phys. Rev. A 38 (1988) 3098.
31. J.P. Perdew, Phys. Rev. B 33 (1986) 8822.
32. A. Schäfer, C. Huber, R. Ahlrichs, J. Chem. Phys. 100 (1994) 5829.
33. F. Weigend, R. Ahlrichs, Phys. Chem. Chem. Phys. 7 (2005) 3297.

34. A. Schäfer, H. Horn, R. Ahlrichs, J. Chem. Phys. 97 (1992) 2571.
35. J.L. Whitten, J. Chem. Phys. 58 (1973) 4496.
36. E.J. Baerends, D.E. Ellis, P. Ros, Chem. Phys. 2 (1973) 41.
37. B.I. Dunlap, J.W.D. Connolly, J.R. Sabin, J. Chem. Phys. 71 (1979) 3396.
38. C. Van Alsenoy, J. Comp. Chem. 9 (1988) 620.
39. K. Eichkorn, O. Treutler, H. Öhm, M. Häser, R. Ahlrichs, Chem. Phys. Letters. 40 (1995) 283.
40. Y. Zhao, D.G. Truhlar, Acc. Chem. Res. 41 (2008) 157.
41. J.P. Austin, N.A. Burton, I.H. Hillier, M. Sundararajan, M.A. Vincent, Phys. Chem. Chem. Phys. 11 (2009) 1143.
42. A. Klamt, G. Schüürmann, J. Chem. Soc., Perkin Trans. 2 (1993) 799.
43. R. S. Mülliken, J. Chem. Phys. 23 (1955) 1833.
44. R. Ahlrichs, M. Bar, H. P. Baron, R. Bauernschmitt, S. Bocker, M. Ehrig, K. Eichkorn, S. Elliot, F. Furche, F. Haase, M.Haser, H. Horn, C. Huber, U. Huniar, M. Kattannek, C. Kolmel, M. Koolwitz, K. May, C. Ochsenfeld, H. Ohm, A. Schafer, U. Schneider, O. Treutler, M. von Arnim, F. Weigend, P. Weis, H. Weiss, TURBOMOLE V6.3.1 2011, a development of University of Karlsruhe and Forschungszentrum Karlsruhe GmbH, 1989-2007, TURBOMOLE GmbH, since 2007; available from http://www.turbomole.com.
45. K. Morokuma, J. Chem. Phys. 55 (1971) 1236.
46. T. Ziegler, A. Rauk, Theor. Chim. Acta 46 (1977) 1.
47. G. te Velve, F.M. Bickelhaupt, E.J. Baerends, S.J.A. Gisbergen, van C.F. Guerra, J.G. Snijders, T. Ziegler, J. Comput. Chem. 22 (2001) 931.
48. C. Fonseca Guerra, J.G. Snijders, G. teVelde, E. Baerends, J. Theor. Chem. Acc. 99 (1998) 391.
49. E.D. Glendening, C.R. Landis, F. Weinhold, J. comp.chem. 34 (2013) 1429.
50. S. Kannan, S.B. Deb, J.S. Gamare, M.G.B. Drew, Polyhedron 27 (2008) 2557.
51. G.J. Lumetta, B.K. McNamara, B.M. Rapko, R.L. Sell, R.D. Rogers, G. Broker, J.E. Hutchison, Inorg. Chim. Acta 309 (2000) 103.
52. L.M. Zhu, B.L. Li, Z.B. Cao, Y. Zhang, Chin. J. Struct. Chem. 5 (2003) 521.
53. O. Clements, B.M. Rapko, B.P. Hay, Coord. Chem. Rev. 170 (1998) 203.
54. K.W. Bagnall, F. Benetollo, E. Forsellini, G. Bombieri, Polyhedron 11 (1992) 1765.
55. S. Alagar, K. Rajagopal, R.V. Krishnakumar, M. Subha Nandhini, S. Kannan, S. Natarajan, Acta Crystallogr. E 59 (2003) m1-m3.

56. S. Kannan, M.R.A. Pillai, V. Venugopal, P.A. Droege, C.L. Barnes, Polyhedron 15 (1996) 97.
57. S. Kannan, M.R.A. Pillai, V. Venugopal, P.A. Droege, C.L. Barnes, E.O. chlemper, Polyhedron 15 (1996) 465.
58. S. Kannan, A. Usman, H.K. Fun, Polyhedron 21 (2002) 2403.
59. S. Kannan, M.R.A. Pillai, V. Venugopal, P.A. Droege, C.L. Barnes, Inorg. Chim. Acta 254 (1997) 113.
60. (a) G. Bombieri, E. Forsellini, J.P. Day, W.I. Azeez, Dalton Trans. (1978) 677. (b) S.B. Akona, J. Fawcett, J.H. Holloway, D.R. Russel, I. Leban, Acta Crystallogr. C 47 (1991) 45.

CHAPTER 3

Synthesis, structural and coordination studies of N-oxo pyridine2-carboxamide ligands with uranyl(VI) and lanthanide (III) ions

3.1 Introduction

Different groups around the world have developed many extractants which showed good extraction properties for trivalent actinides. These processes are always associated with the co-extraction of trivalent lanthanides present at large proportion in Purex raffinate [1-4]. This is because of the chemical similarity of trivalent actinides with trivalent lanthanides. Several bifunctional neutral extractants with various combinations of functional groups were synthesized and tested for this purpose, sometimes known as 'Actinide Partitioning'. The TRUEX process, employed octyl(phenyl)-N,N-diisobutylcarbamoyl methyl phosphine oxide (CMPO) as extractant (similarly carbamoyl methyl phosphonates (CMP)), in which C=O and P=O functional groups are involved in bonding and it acts as a bidentate chelating ligand [5-6]. In DIAMEX process, substituted malonamides such as, dimethyl-dibutyl-tetradecylmalonamide (DMDBTDMA) and N,N'-dimethyl-N,N'-dioctylhexylethoxymalonamide (DMDOHEMA) were used as extractants which contain two C=O functional groups in combination and these also act as bidentate chelating ligands [7-9]. Apart from these, some acidic organophosphorus extractants like di-isodecyl phosphoric acid (DIDPA) [10], Di-(2-ethylhexyl)phosphoric acid (DEHPA or HDEHP) [11-12], di-nonyl phenyl phosphoric acid (DNPPA) [13-14], di-octyl phenyl phosphoric acid (DOPPA) [15-16], were used to separate uranium or trivalent actinides from lower acidic solution. All these extractants are composed of PO(OH) functional groups and bonded with the metal ions through both P=O and P-O groups. Apart from these conventional extractants, so many other bifunctional neutral extractants were synthesized and studied for the coordination and extraction properties in the laboratory scale. For example, carbamoyl methyl sulfoxide (CMSO) (combination of C=O and S=O functional groups) [17-18], β-sulfoxo phosphine oxide (combination of P=O and S=O functional groups), β-N-oxo phosphine oxide (combination of P=O and N-O functional groups) [19], bis(diphenylphosphino)methane dioxide (combination of two P=O functional groups) have also been studied previously [20]. Solid state structural analyses of the coordination complexes of these ligands with actinides and lanthanides reveal that, they can act either as bidentate chelating, bidentate bridging (in dimeric or polymeric structure) or monodentate ligands. The mode of bonding for these ligands are controlled both by steric as well as electronic properties. However, in this series, the study of the coordination and extraction chemistry of bifunctional ligands containing the NO–CO groups is very limited [21], though the extraction and coordination chemistry of monofunctional N-oxide and amides are well established [22-26]. 4-(5-nonyl) pyridine oxide and trioctylamine oxide were tested for the extraction of uranium from different mineral acid solutions, which showed that the former acts as a better extractant in dilute HNO_3 and HCl media than that of TBP [22]. Structural studies on the complexes of a mixed hydroxy N-oxo amide ligand, 2-hydroxy-2-(1-oxy-pyridin-2-yl)-N,N-diphenylacetamide with $La(NO_3)_3$ showed that the ligand bonds through the hydroxyl and amide O-atoms to metal centre and leaving the N-oxide group free (uncoordinated) [27]. In another report, the N,N-di(pyridine N-oxide-2-yl)pyridine-2,6-dicarboxamide ligand forms 1:1 complex with lanthanide nitrate and is bonded through both the N-oxide groups as bidentate chelating mode, while both the amidic O atoms of the ligand are free [28]. These studies promoted us to synthesize NO–CO based ligands, N-oxo picolinamides and study their complex chemistry with uranyl nitrate and lanthanide (La, Sm, Eu) nitrates to see the mode of bonding in solid state and their potential for the separation of actinides.

3.2 Experimental

3.2.1 Synthesis of N-oxo pyridine 2-carboxamide ligands

3.2.1.1 Synthesis of $C_5H_4NOCON(^iC_3H_7)_2$ ($\boldsymbol{L^1}$)

A solution of 3-chloroperoxybenzoic acid (1.9 g, 70%, 11mmol) in dichloromethane (20 ml) was added drop wise to a solution of N,N-diisopropyl 2-pyridine carboxamide (2.06 g, 10mmol) in dichloromethane (15 ml) at 5–10 °C. After 16 h at room temperature, the reaction mixture was cooled on an ice bath and sodium hydroxide (2 M solution in water, 14.5 ml, 29 mmol) was added into it. After 15 min, the reaction mixture was diluted with chloroform (25 ml). The organic layer was separated and washed with 2M NaOH solution, dried over sodium carbonateand evaporated under reduced pressure. The residue was purified bysilica gel column chromatography to give the final product (86% yield). Dichloromethane solution on slow evaporation yielded colourless plate type crystals which was analysed by single crystal XRD method. Anal.Calcd.for $C_{12}H_{18}N_2O_2$: C, 64.86; H, 8.11; N, 12.61. Found: C, 64.22; H, 8.42; N, 12.26. IR (ATR, ν/cm^{-1}): 1628(s) (C=O), 1249(s) (N-O).^{1}H NMR (25°C, 300 MHz, $CDCl_3$) 8.25 (s, 1H), 7.36 (s, 3H), 3.56(t, *J*= 6.3 Hz, 2H), 1.55 (d, J= 6.6 Hz, 6H), 1.36 (s, 6H).

*3.2.1.2 Synthesis of $C_5H_4NOCON(^iC_4H_9)_2$ (**L^2**)*

This was prepared similar to that of **L^1** by taking N,N-diisobutyl 2-pyridine carboxamide instead of N,N-diisopropyl 2-pyridine carboxamide. Yield: 82%. Anal.Calcd.for $C_{14}H_{22}N_2O_2$: C, 67.20; H, 8.80; N, 11.20. Found: C, 67.12; H, 8.98; N, 11.01. IR spectrum (ATR, ν/cm^{-1}): 1639(s) (C=O), 1207(s) (N-O).^{1}H NMR (25°C,500 MHz, $CDCl_3$) 8.06 (d, J= 3.0 Hz, 1H), 7.25 (t, J= 4.5 Hz, 1H), 7.21 (d, *J*= 3.0 Hz, 2H), 3.78 (dd, J= 13.25 Hz, J= 8.5 Hz, 1H), 3.07 (dd, *J*= 14.25 Hz, *J*= 5.5 Hz, 1H), 2.77 (q, J= 5.5Hz, 1H), 2.68 (t, J= 10.0 Hz, 1H), 2.07 (t, J= 7.0 Hz, 1H), 1.76 (s, 1H), 0.92 (d, J= 6.5 Hz, 6H), 0.72 (d, J= 6.5 Hz, 3H), 0.62 (d, J= 6.0 Hz, 3H).

*3.2.1.3 Synthesis of $C_5H_4NOCONH(^tC_4H_9)$ (**L^3**)*

This was prepared similar to that of **L^1** by taking N-^{t}butyl 2-pyridine carboxamide instead of N,N-diisopropyl 2-pyridine carboxamide. Yield: 81%. Anal.Calcd.for $C_{10}H_{14}N_2O_2$: C, 61.86; H, 7.22; N, 14.43. Found: C, 61.67; H, 7.69; N, 14.31. IR (ATR, ν/cm^{-1}): 1669(s) (C=O), 1227(s) (N-O). ^{1}H NMR (25°C,300 MHz, $CDCl_3$) 11.2 (s, 1H),8.39 (d, J= 7.5 Hz, 1H), 8.22 (d, J= 6.0 Hz, 1H), 7.45 (t, J= 7.5 Hz, 1H), 7.37 (d, J= 6.0Hz, 1H), 1.45 (s, 9H).

3.2.2 Synthesis of uranyl complexes of N-oxo pyridine 2-carboxamide ligands

*3.2.2.1 Synthesis of $[UO_2(NO_3)_2\{C_5H_4NOCON(^iC_3H_7)_2\}]$ (**1**)*

To a solution of **L^1** (280 mg, 1.26mmol) in $CHCl_3$ (20 mL), solid $[UO_2(NO_3)_2{\cdot}6H_2O]$ (318 mg, 0.63mmol) was added and stirred for one hour at room temperature and then at reflux condition for 3-4 hours. This produces yellow precipitate at the bottom of the round bottom flask. It was filtered, washed with $CHCl_3$ and then dissolved in acetonitrile.The solution on slow evaporation yielded yellow crystalline solid, which was filtered, washed with hexane, dried and analysed by single crystal XRD method.Yield:91%. ^{1}H NMR (25°C, 300 MHz,CD_3COCD_3): δ = 8.81 [d, J= 5.7 Hz, 1H], 8.06 [s, 1H], 7.97 [t, J= 6.3 Hz, 1H], 7.85 [t, J= 6.3 Hz, 1H], 3.93 [sep, J= 6.9 Hz, 1H], 1.70 [d, J= 6.6 Hz, 3H], 1.46 [d, J= 6.6 Hz, 3H], 1.39 [d, J= 6.6 Hz, 3H], 1.35 [d, J= 6.6 Hz, 3H]. IR (cm^{-1}): ν = 1510(s) (C=O), 1215(s) (N-O),924(s) (U=O). Analysis Calcd for $C_{12}H_{18}N_4O_{10}U$: C, 23.38; H, 2.92; N, 9.09. Found: C, 23.52; H, 3.06; N, 9.26.

*3.2.2.2 Synthesis of $[UO_2(NO_3)_2\{C_5H_4NOCON(^iC_4H_9)_2\}]$ (**2**)*

This was prepared similarly to **1** by taking **L^2** (343 mg, 1.37 mmol) and $[UO_2(NO_3)_2{\cdot}6H_2O]$ (341 mg, 0.68mmol) in 87% yield. ^{1}H NMR (25°C, 300 MHz,CD_3COCD_3): δ = 8.65 [d, J= 5.4 Hz, 1H], 7.94 [s, 1H], 7.87 [d, J= 6.9 Hz, 1H], 7.81 [t, J= 6.6 Hz, 1H], 3.32 [br, 2H], 2.23[m, 2H], 0.99 [d, J= 6.6 Hz, 6H], 0.82 [d, J= 6.6 Hz, 6H]. IR (cm^{-1}): ν = 1594(s) (C=O), 1219(s) (N-O),931(s) (U=O). Analysis Calcd for $C_{14}H_{22}N_4O_{10}U$: C, 26.09; H, 3.42; N, 8.70. Found: C, 26.21; H, 3.52; N, 8.47.

*3.2.2.3 Synthesis of $[UO_2(NO_3)_2\{C_5H_4NOCONH(^tC_4H_9)\}]$ (**3**)*

This was prepared similarly to **1** by taking **L^3** (249 mg, 1.28 mmol) and $[UO_2(NO_3)_2{\cdot}6H_2O]$ (322 mg, 0.64mmol) in 86% yield. The acetonitrile solution on slow evaporation yielded yellow crystalline solid, which was filtered, washed with hexane, dried and analysed by single crystal XRD method. ^{1}H NMR (25°C, 300 MHz,CD_3COCD_3): δ = 8.66 [s, 1H], 8.41 [m, 1H], 7.82 [d, J= 4.8 Hz, 2H], 1.52 [s, 9H]. IR (cm^{-1}): ν = 1641(s) (C=O), 1205(s) (N-O), 930(s) (U=O). Analysis Calcd for $C_{10}H_{14}N_4O_{10}U$: C, 20.41; H, 2.38; N, 9.52. Found: C, 20.21; H, 2.47; N, 9.46.

3.2.3 Synthesis of lanthanide complexes of N-oxo pyridine 2-carboxamide ligands

3.2.3.1 Lanthanum complexes

*3.2.3.1.1 Synthesis of $[La(NO_3)_3(H_2O)\{C_5H_4NOCON(^iC_3H_7)_2\}_2]$ (**4**)*

To a solution of $\mathbf{L^1}$ (411 mg, 1.85mmol) in CH_2Cl_2 (20 mL), solid $[La(NO_3)_3{\cdot}6H_2O]$ (267 mg, 0.62mmol) was added and stirred at room temperature for one hour which produces white precipitate at the bottom of the flask. It was filtered, washed with $CHCl_3$dried. Yield: 89%. ^1H NMR (25°C, 300 MHz, CD_3COCD_3): δ = 8.22 [m, 1H], 7.45 [m, 3H], 3.61 [sep, J= 6.9 Hz, 1H], 3.43 [sep, J= 6.9 Hz, 1H], 1.47 [d, J= 6.6 Hz, 6H], 1.28 [d, J= 6.6 Hz, 6H]. IR (cm^{-1}): ν = 1594(s) (C=O), 1220(s) (N-O). Analysis Calcd for $C_{24}H_{38}N_7O_{14}La$: C, 36.60; H, 4.83; N, 12.45. Found: C, 36.49; H, 4.96; N, 12.56.

*3.2.3.1.2 Synthesis of $[La(NO_3)_3(H_2O)\{C_5H_4NOCON(^iC_4H_9)_2\}_2]$ (**5**)*

This was prepared by taking solid $\mathbf{L^2}$ (480 mg, 1.92mmol) and $[La(NO_3)_3{\cdot}6H_2O]$ (277 mg, 0.64mmol) in CH_2Cl_2 and under reflux condition all solid $[La(NO_3)_2{\cdot}6H_2O]$ slowly got disappeared and white product was precipitated. Yield: 86%. IR (cm^{-1}): ν = 1596(s) (C=O), 1227(s) (N-O). Analysis Calcd for $C_{28}H_{46}N_7O_{14}La$: C, 39.86; H, 5.46; N, 11.63. Found: C, 39.67; H, 5.62; N, 11.79.

3.2.3.2 Samarium complexes

*3.2.3.2.1 Synthesis of $[Sm(NO_3)_2(H_2O)\{C_5H_4NOCON(^iC_3H_7)_2\}_2]$ (**6**)*

To a solution of $\mathbf{L^1}$ (400 mg, 1.80mmol) in CH_2Cl_2 (20 mL), solid $[Sm(NO_3)_2{\cdot}6H_2O]$ (267 mg, 0.60mmol) was added and stirred at reflux condition which dissolves all solid $[Sm(NO_3)_2{\cdot}6H_2O]$ and clear solution was obtained. Then the solvent was evaporated, washed with $CHCl_3$and dried.Yield: 88%. ^1H NMR (25°C, 300 MHz, CD_3COCD_3): δ = 8.31 [s, 1H], 7.50 [s, 3H], 3.62 [s, 1H], 1.45 [d, J= 4.8 Hz, 6H], 1.26 [s, 3H], 1.10 [d, J= 5.4 Hz, 3H]. IR (cm^{-1}): ν = 1638(s)

(C=O), 1215(s) (N-O). Analysis Calcd for $C_{24}H_{38}N_7O_{14}Sm$: C, 36.07; H, 4.76; N, 12.28. Found: C, 36.02; H, 4.85; N, 12.39.

*3.2.3.2.2 Synthesis of [Sm(NO$_3$)$_2$(H$_2$O){C$_5$H$_4$NOCON(^{i}C$_4$H$_9$)$_2$}$_2$] (**7**)*

This was prepared similarly to **6** by taking **L^2** (533 mg, 2.13mmol) and $[Sm(NO_3)_2\cdot 6H_2O]$ (316 mg, 0.71mmol) in 86% yield. IR (cm^{-1}): ν = 1593(s) (C=O), 1222(s) (N-O). Analysis Calcd for $C_{28}H_{46}N_7O_{14}Sm$: C, 39.33; H, 5.38; N, 11.47. Found: C, 39.54; H, 5.42; N, 11.62.

3.2.3.3 Europium complexes

*3.2.3.3.1 Synthesis of [Eu(NO$_3$)$_3$(H$_2$O){C$_5$H$_4$NOCON(^{i}C$_3$H$_7$)$_2$}$_2$] (**8**)*

To a solution of **L^1** (433 mg, 1.95mmol) in CH_2Cl_2 (20 mL), solid $[Eu(NO_3)_3\cdot 6H_2O]$ (290 mg, 0.65mmol) was added and stirred at reflux condition for one hour which produces white precipitate at the bottom of the flask. It was filtered, washed with $CHCl_3$ and then dissolved in dichloromethane. Dichloromethane solution on slow evaporation yielded white needle type crystals which was analysed by single crystal XRD method.Yield: 91%. ^{1}H NMR (25°C, 300 MHz,CD_3COCD_3): δ = 8.03 [d,J= 6.0 Hz, 1H], 7.49 [m, 1H], 7.40 [m, 2H], 3.67 [sep, J= 6.9 Hz, 1H], 1.61 [d, J= 6.6 Hz, 3H], 1.53 [d, J= 6.6 Hz, 3H], 1.28 [d, J= 6.6 Hz, 3H], 1.09 [d, J= 6.9 Hz, 3H]. IR (cm^{-1}): ν = 1621(s) (C=O), 1219(s) (N-O). Analysis Calcd for $C_{24}H_{38}N_7O_{14}Eu$: C, 36.0; H, 4.75; N, 12.25. Found: C, 36.08; H, 4.91; N, 12.38.

*3.2.3.3.2 Synthesis of [Eu(NO$_3$)$_3$(H$_2$O){C$_5$H$_4$NOCON(^{i}C$_4$H$_9$)$_2$}$_2$] (**9**)*

This was prepared by taking solid **L^2** (473 mg, 1.89mmol) and $[Eu(NO_3)_3\cdot 6H_2O]$ (281 mg, 0.63mmol) in CH_2Cl_2 and under reflux condition all solid $[Eu(NO_3)_2\cdot 6H_2O]$ slowly got disappeared and white product was precipitated. Yield: 87%. IR (cm^{-1}): ν = 1594(s) (C=O), 1220(s) (N-O). AnalysisCalcd for $C_{28}H_{46}N_7O_{14}Eu$: C, 39.25; H, 5.37; N, 11.45. Found: C, 39.13; H, 5.49; N, 11.61.

3.2.4 X-ray crystallography

Selected crystallographic data for the compounds $\mathbf{L^1}$, **3** and **8** are summarized in Table 3.1.

Table 3.1 Crystallographic data for compounds $\mathbf{L^1}$, **3** and **8**

	$\mathbf{L^1}$	**3**	**8**
Empirical formula	$C_{12}H_{18}N_2O_2$	$C_{10}H_{14}N_4O_{10}U$	$C_{24}H_{38}N_7O_{14}Eu$
Formula weight	222.28	588.28	799.96
Crystal system	Monoclinic	Monoclinic	triclinic
Space group	P 1 21/c 1	P 1 21/c 1	P -1
a (Å)	6.3595(4)	15.8049(4)	9.0106(5)
b (Å)	7.4334(4)	10.4286(2)	12.8895(9)
c(Å)	26.7575(14)	10.2359(3)	15.6708(7)
α (°)	90	90	107.570(5)
β (°)	89.779(5)	98.514(2)	90.619(4)
γ (°)	90	90	90.415(5)
Volume (Å^3)	1264.89(13)	1668.52(7)	1734.92(18)
Z (formula unit)	4	4	2
Density (g/cm^3)	1.167	2.342	1.532
μ (mm^{-1})	0.647	27.962	13.562
Reflections collected/unique	2381/1639	3241/2152	6640/4510
Data/restrains/parameters	2381/0/149	3241/0/230	6640/0/424
Goodness of fit on F^2	1.105	1.070	1.146
Final R$_1$ indices[$I > 2\sigma(I)$]	0.0985	0.1105	0.1099
wR$_2$ indices (all data)	0.1357	0.1329	0.1491

$w = 1/[\sigma^2(F_o^2) + (0.1132P)^2 + 2.0722P]$ for $\mathbf{L^1}$, $w = 1/[\sigma^2(F_o^2) + (0.2000P)^2]$ for **3** and $w = 1/[\sigma^2(F_o^2)+(0.2000P)^2]$ for **8**, where $P = (F_o^2 + 2F_c^2)/3$.

3.3 Results and discussion

3.3.1 Complexation study of N-oxo pyridine2-carboxamide ligands with uranyl nitrate

The complexing ability of $C_5H_4NOCON(^iC_3H_7)_2$, $C_5H_4NOCON(^iC_4H_9)_2$ and $C_5H_4NOCONH(^tC_4H_9)$ with uranyl nitrate was studied by using elemental analysis, IR and NMR spectroscopic techniques. The reaction of $[UO_2(NO_3)_2.6H_2O]$ with the N-oxo pyridine 2-carboxamide ligands yielded the compounds **1** to **3**. The C, H and N analysis revealed that the ratio of uranyl nitrate to ligand is 1:1 in all these compounds.

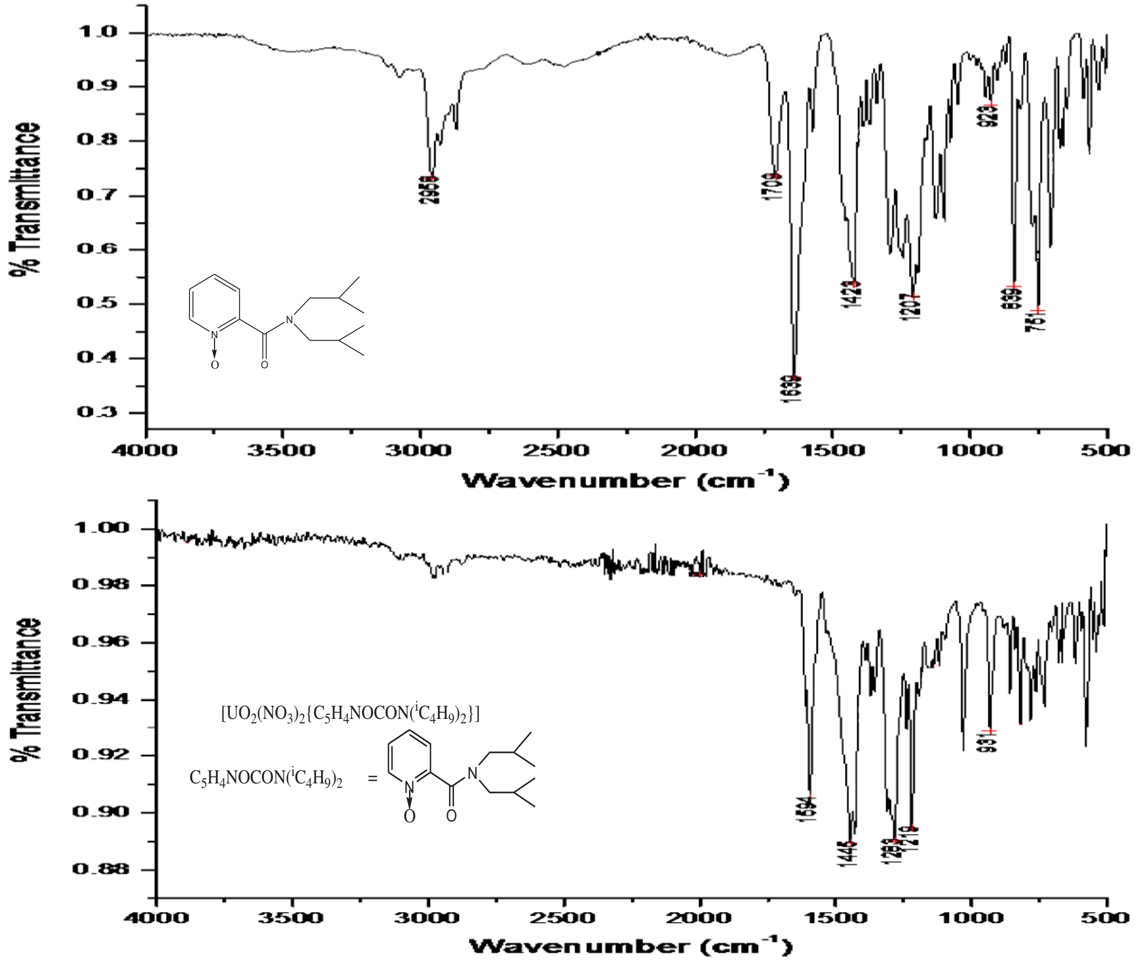

Fig. 3.1 IR spectra of the free ligand $\mathbf{L^2}$ (above) and compound **2** (below)

The IR spectra of the compounds **1–3** show that the water molecules from the starting compound $[UO_2(NO_3)_2.6H_2O]$ are completely replaced by the ligand and that the ligand is bonded through both the carboxyl oxygen and N-oxo oxygen atom to the uranyl group (Fig. 3.1). The observed frequency differences for the carboxyl ($\Delta\upsilon_{CO}$ = 28-118 cm^{-1}, where $\Delta\upsilon_{CO}$= $\upsilon_{CO(free\ ligand)}$ - $\upsilon_{CO(coordinated)}$) group and the N-oxide ($\Delta\upsilon_{NO}$ = 22-34 cm^{-1}, where $\Delta\upsilon_{NO}$ = $\upsilon_{NO(free\ ligand)}$ - $\upsilon_{NO(coordinated)}$) group are consistent with the supposition that both the carbamoyl and N-oxo groups are bonded to the uranyl group directly in the reported compounds [21]. These differences are comparable in magnitude with those of the $[UO_2(NO_3)_2(C_5H_4NOSCH_2CON(^iC_4H_9)_2)]$ [21], $[UO_2$(2,2'-bipyridine-N-oxide)$(OH)(NO_3)]_2.H_2O$ [29], $[UO_2$(quinoline oxide)$_2(NO_3)_2]$ [30], UO_2(Bis(2-pyridyl-N-oxide)disulphide)$_2$(NO$_3$)$_2$ [31], [UO$_2$(NO$_3$)$_2$ (N-cyclohexyl,2-pyrrolidone)$_2$] [32], [UO$_2$(NO$_3$)$_2$ (1,3-dimethyl,2-imidazolidone)$_2$] [33], [UO$_2$(NO$_3$)$_2${^{i}C$_3$H$_7$CON(^{i}C$_4$H$_9$)$_2$}$_2$] [34] and [UO$_2$(NO$_3$)$_2$(^{i}C$_3$H$_7$)$_2$NCOCH$_2$CON(^{i}C$_3$H$_7$)$_2$] [35] complexes.

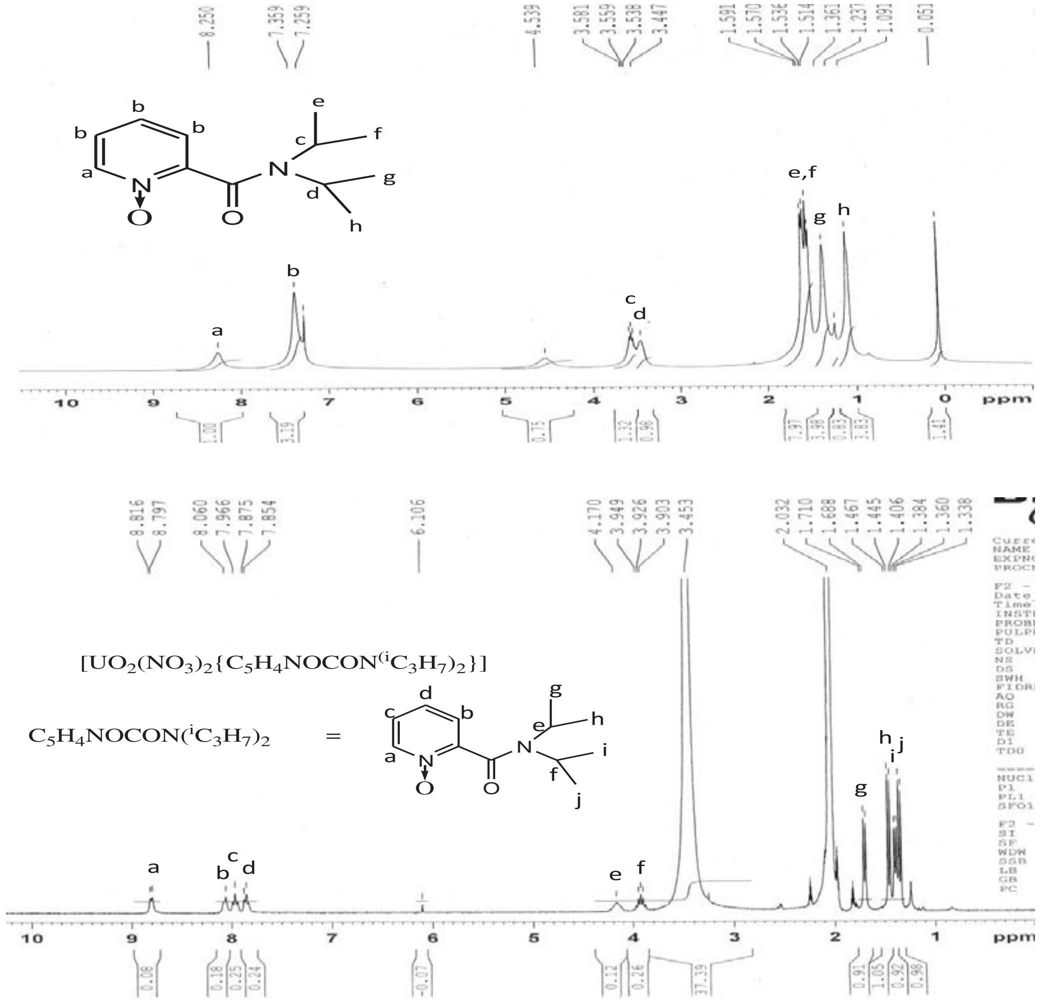

Fig. 3.2 ^{1}H NMR spectrum of compound **L^1** (above) and **1** (below)

Fig 3.2 showed the ^{1}H NMR spectrum of ligand L^1 and complex **3** together. In the ligand spectrum, two singlet at 8.25 ppm and 7.36 ppm are attributed to the ring protons of the pyridine ring at 6 (one proton) position and at 3, 4, 5 (three protons altogether) position respectively. These are the deshielded protons because these are the aromatic pyridine ring protons. Next, two broad peaks at 3.56 and 3.45 ppm are assigned to two CH protons (chemically non-equivalent at room temperature) of two isopropyl groups. These peaks are broad because of quadrapolar effect of ^{14}N-atom adjacent to the CH groups of the isopropyl groups. Six CH_3 protons (chemically non-equivalent at room temperature) of one substituted isopropyl groups resonate as doublets at 1.58 and 1.52 ppm. Both the signals are split into a doublet, because the methyl group protons are coupled with one adjacent CH proton. Two singlet peaks at 1.36 and 1.09 ppm are due to six CH_3 protons (chemically non-equivalent at room temperature) of the other substituted isopropyl groups. Spectrum of the complex 3 is also similar to the ligand L^1 except two additional peaks are appeared at 3.45 and 2.03 ppm due to the residual water impurity and CH_3COCH_3 molecule in the solvent acetone-d_6. All the proton peaks of the ligand in the spectrum of complex 3 are deshielded by ca. 0.2-0.6 ppm with respect to the free ligand, indicating that the ligand is coordinated to the uranyl group in solution also. It is apparent from the IR spectral analysis that ligands are acting as bidentate ligand and bonded through both carboxyl oxygen and N-oxo oxygen (both the $C{=}O_{str}$ and $N\text{-}O_{str}$ frequencies are reduced in the compounds with respect to the free ligands) to the uranyl group in compounds **1–3** in the solid state to give similar structures to those observed in the compounds of (N,N-dialkylcarbamoyl methyl) (2-pyridyl-N-oxide) sulfide [21] with the uranyl nitrate. The structure of **3** has been determined by single crystal X-ray diffraction method, which confirms the IR and elemental analysis results.

3.3.2 Molecular structure of ***3***

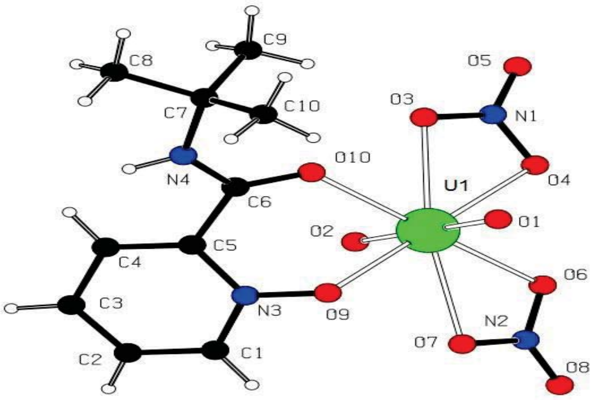

Fig. 3.3 Molecular structure of $[UO_2(NO_3)_2\{C_5H_4NOCONH(^tC_4H_9)\}]$

The molecular structure of the compound **3** is shown in Fig. 3.3 and the selected interatomic bond distances and angles for are given in Table 3.2. The uranium atom is surrounded by eight oxygen atoms in a distorted hexagonal bi-pyramidal geometry. Two uranyl oxygen atoms occupy the axial positions. The four oxygen atoms of the two nitrate groups and the two oxygen atoms of the ligand forms the equatorial hexagonal plane. The ligand acts as a bidentate chelating ligand and is bonded through both the N-oxo and amido oxygen atoms to the uranyl group.

This type of co-ordination is similar to that observed in the complexes of the bifunctional ligands with uranyl nitrate such as, carbamoyl methyl phosphonate complexes $[UO_2(NO_3)_2\{Ph(EtO)POCH_2CONEt_2\}]$, $[UO_2(NO_3)_2(Ph_2POCH_2CONEt_2)]$ [36], malonamide complex $[UO_2(NO_3)_2(^iC_3H_7)_2NCOCH_2CON(^iC_3H_7)_2]$ [35], β-sulfoxo phosphine oxide complex $[UO_2(NO_3)_2\{(^iPrO)_2POCH_2SO(p\text{-}MeC_6H_4)\}]$ [37] or bis(carbamoylmethyl) sulphide complex $UO_2(NO_3)_2(^iBu_2NCOCH_2SCH_2CON^iBu_2)]$ [38] etc. The observed bond distance for $U–O_{(amide)}$ (2.430(9) Å) in **3** is close to the values observed in earlier reported uranyl nitrate-amide complexes, such as $[UO_2(NO_3)_2(C_5H_4NOSCH_2CON(^iC_4H_9)_2)]$ (2.393 (12)Å) [21], $UO_2(NO_3)_2$(N-cyclohexylmethyl,2-pyrrolidone)$_2$] (2.374(2)Å) [32], $[UO_2(NO_3)_2$(1,3-dimethyl,2-imidazolidone)$_2$] (2.383(2)Å) [33], $[UO_2(NO_3)_2$(tetrabutylglutaramide)$_2$] (2.378(6) Å) [39], $[UO_2(NO_3)_2$(dibutyldecanamide)$_2$] (2.37(2) Å) [39] and $[UO_2(NO_3)_2(PhN(CH_3)CO(CH_3)NPh)_2]$ (2.381(2) Å) [40]. The $U–O_{(N\text{-}oxide)}$ distance (2.360(12) Å) in **3** is comparable in magnitude with those of earlier reported uranyl nitrate-N-oxide complex, such as $[UO_2(NO_3)_2(C_5H_4NOSCH_2CON(^iC_4H_9)_2)]$ (2.389 (12)Å) [21]. The observed average $U–O(NO_3)$ bond distance of 2.498(14) Å is normal. The angles subtended at the metal atom show that the uranium atom has a slightly distorted hexagonal bipyramidal geometry.

Table 3.2 Important bond distances (Å) and angles (°) for the compound **3**

U1–O1	1.761(12)	O1–U1–O2	178.1(6)
U1–O2	1.762(11)	O3–U1–O4	50.5(4)
U1–O3	2.479(17)	O6–U1–O7	50.8(4)
U1–O9	2.360(12)	O9–U1–O10	66.0(4)
U1–O10	2.430(9)	U1–O10–C1	131.4(9)
C1–O10	1.23(2)	U1–O9–N4	117.0(10)

The preliminary structural studies of compound **1** also confirms the chelating mode bonding for the ligand with uranyl nitrate and confirms the connectivity between ligand and metal ion.

3.3.3 Comparison of ligand (L^1-L^3) donor strength in the uranyl complexes by comparing the uranyl stretching frequency in the vibrational spectroscopy

Here, we have recorded the infra-red spectra of the uranyl nitrate, halides and β-diketonate complexes with three newly synthesized ligands (**L^1-L^3**) and systematically tabulated in table 3.3.

Table 3.3 Comparison of IR frequencies of uranyl complexes

Complex	C=O$_{str}$ frequency of free ligands (cm^{-1})	C=O$_{str}$ frequency of the bonded ligands (cm^{-1})	Δν$_{CO}$ (cm^{-1})	Δν$_{NO}$ (cm^{-1})	U=O$_{asy}$ frequency of the axial bond (cm^{-1})
$[UO_2(NO_3)_2\{C_5H_4NOCON(^iC_3H_7)_2\}]$ (1)	1628	1510	128	34	924
$[UO_2(NO_3)_2\{C_5H_4NOCON(^iC_4H_9)_2\}]$ (2)	1639	1594	101	12	931
$[UO_2(NO_3)_2\{C_5H_4NOCONH(^tC_4H_9)\}]$ (3)	1669	1641	129	22	930

From the table it can be observed that, in the $[UO_2(NO_3)_2.6H_2O]$ complexes of N-Oxo pyridine 2-carboxamide ligands, the order of U=O$_{asy}$ frequency is (2) > (3) > (1), which signifies that donor strength order of the ligands is $L^1 > L^3 > L^2$ in these complexes. The increase in donor strength of ligand L^1 with respect to the ligand L^2 can be explained on the basis of increase in steric bulkiness of the later with respect to the former since the electronic property is almost same for both the ligands. The decrease in basicity of the amidic oxygen atom in ligand L^3 due to mono N-alkyl substituted nature may be the reason behind the less donor strength of this ligand with respect to ligand L^1, here ligand basicity is the dominating factor. But the lesser donor capacity of the ligand L^2 can be explained on the basis of more steric bulkiness of the ligand L^2 (N, N-disubstituition) with respect to the ligand L^3 (N-mono substituition), here steric factor is the dominating factor.

3.3.4 Complexation study of N-oxo pyridine2-carboxamide ligands with lanthanide nitrates

The reaction of ligands $\mathbf{L^1}$–$\mathbf{L^3}$ with lanthanide nitrate hexahydrate $[Ln(NO_3)_3 \cdot 6H_2O]$ (where, Ln = La, Sm, Eu) yielded compounds **4–9**. C, H, and N analyses revealed that the ratio of lanthanide nitrate to ligand is 1:2 in all compounds. The IR spectra of **4–9** (Fig. 3.4 for **4, 6** and **8**) show that the water molecules from the starting compound $[Ln(NO_3)_3 \cdot 6H_2O]$ are not completely replaced by the ligand and that the ligand is bonded only through the N-oxo oxygen atom to the lanthanide ions. The observed frequency differences for the N-oxide ($\Delta\upsilon_{NO}$ = 29-34 cm^{-1}, where $\Delta\upsilon_{NO} = \upsilon_{NO(\text{free ligand})} - \upsilon_{NO(\text{coordinated})}$) group are consistent with the supposition that only the N-oxo group is bonded to the lanthanide ions directly in the reported compounds.

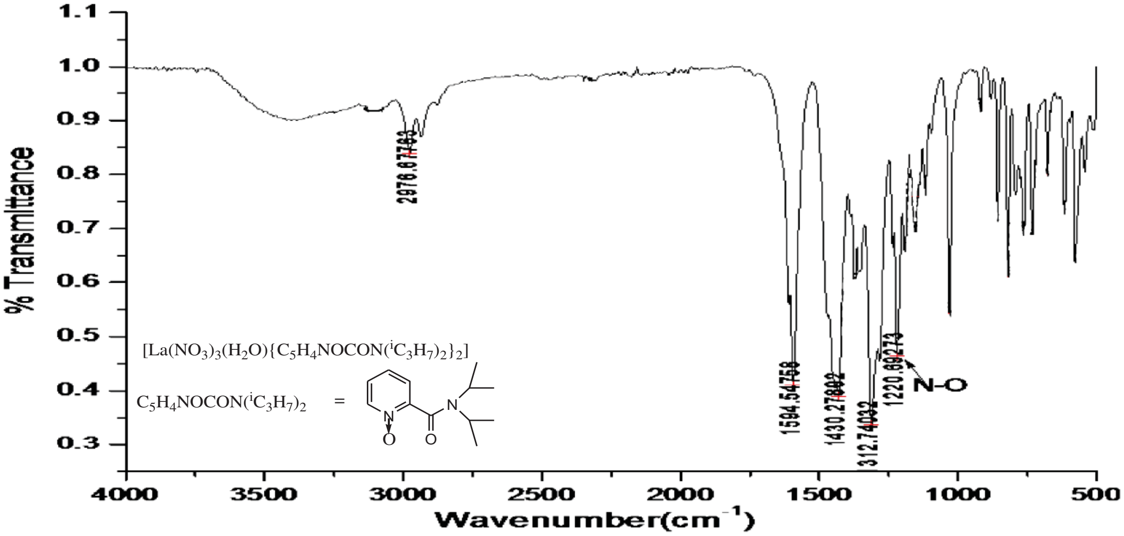

(a)

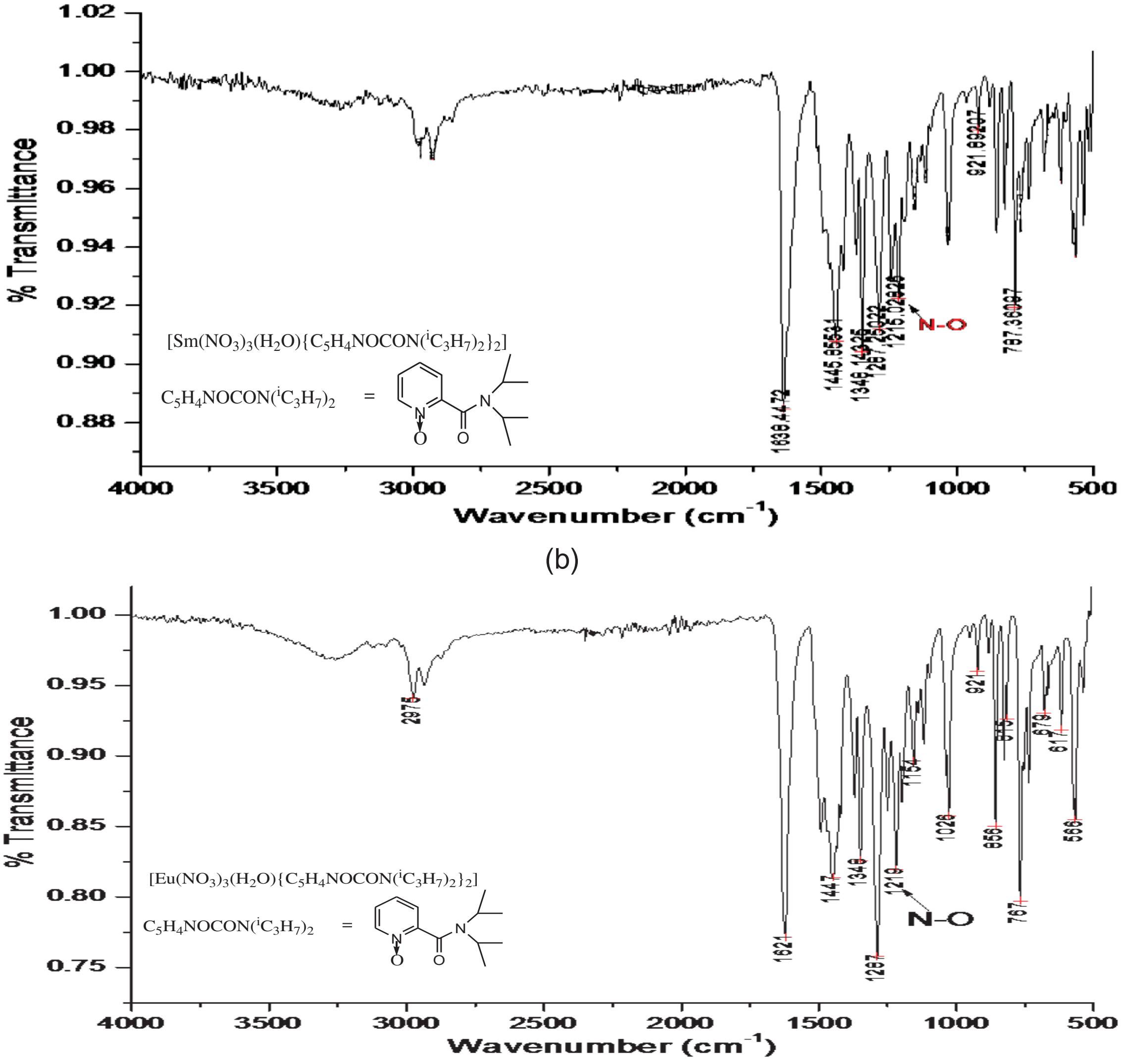

(b)

(c)

Fig. 3.4 IR spectra of (a) compound **4,** (b) compound **6,** (c) compound **8**

Fig 3.5 showed the ^{1}H NMR spectrum of (a) complex **4,** (b) complex **6** and (c) complex **8** together. These spectra are exactly similar to that of ligand L^1 (already discussed in details earlier) since these complexes are derived from the same ligand. The proton peaks of the ligand in the spectrum of all complexes are deshielded by ca. 0.2-0.3 ppm with respect to the free ligand, indicating that the ligand is coordinated to the lanthanide ions in solution also. It is apparent from the IR spectral analysis that ligands are acting as monodentate ligand and bonded only through N-oxo oxygen (only the N-O$_{\mathrm{str}}$ frequencies are reduced in the compounds with respect to the free ligands) to the lanthanide ions in compounds **4–9** in the solid state. The structure of **8** has been determined by single crystal X-ray diffraction methods, which confirms the IR and elemental analysis results.

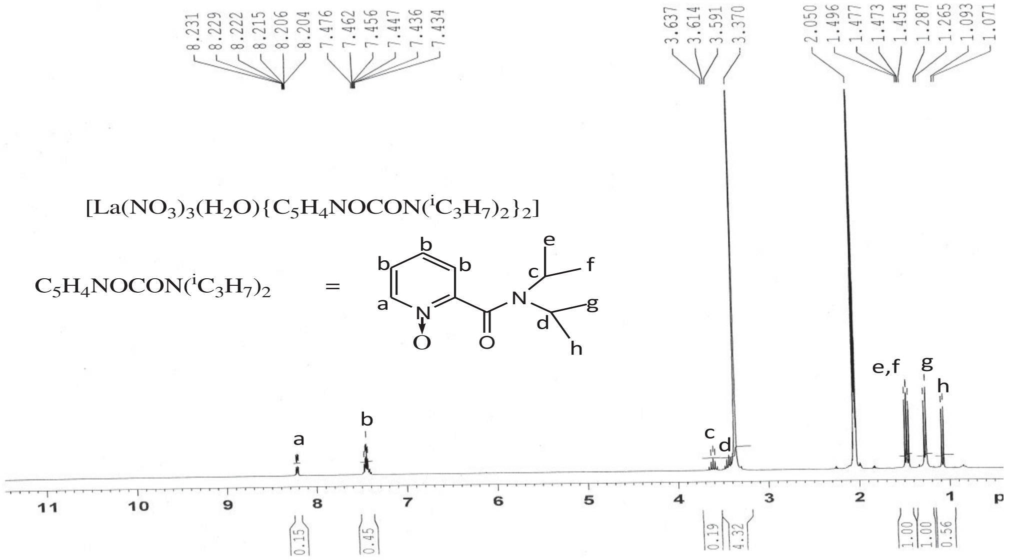

(a)

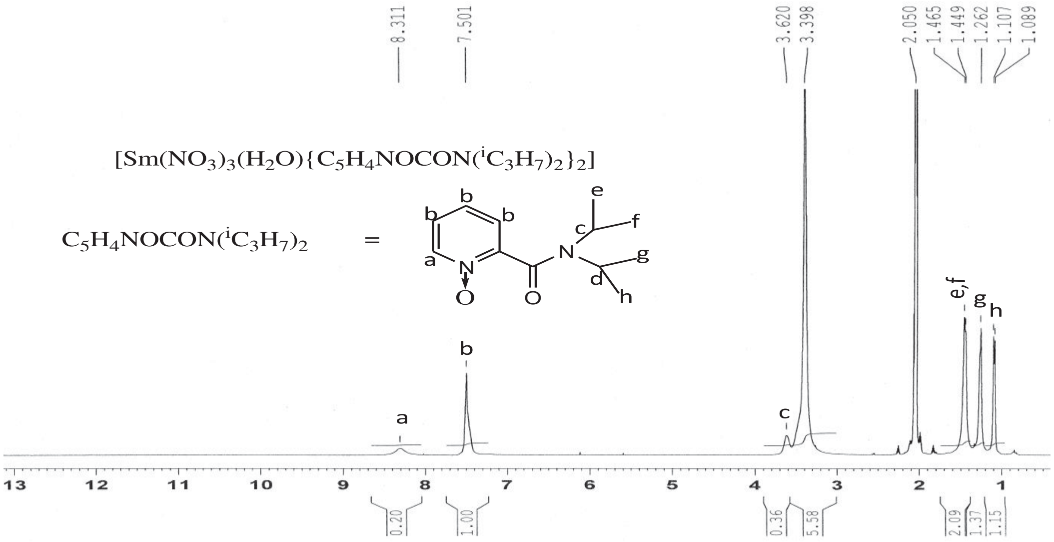

(b)

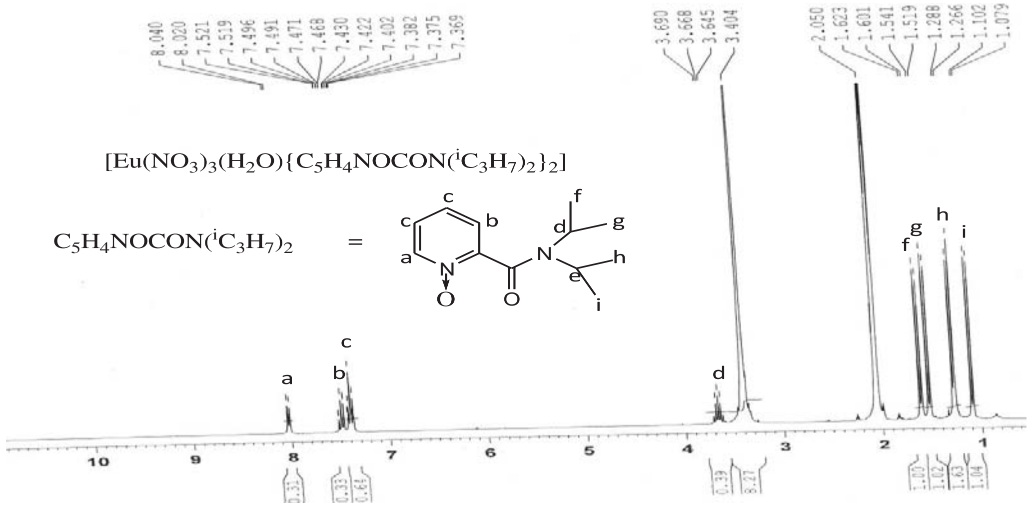

(c)

Fig. 3.5 ^{1}H NMR spectrum of (a) compound **4,** (b) compound **6,** (c) compound **8**

*3.3.5 Molecular structure of compound **8***

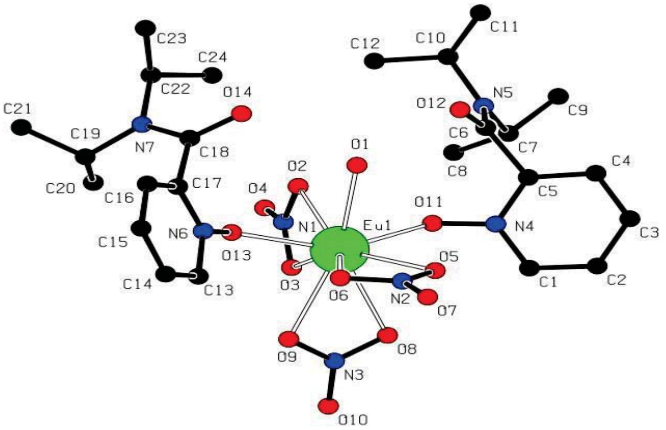

Fig. 3.6 Molecular structure of [Eu$(NO_3)_3(H_2O)\{C_5H_4NOCON(^iC_3H_7)_2\}_2$]

The molecular structure of the compound **8** is shown in Fig. 3.6 and the selected interatomic bond distances and angles for are given in Table 3.4. The europium atom is surrounded by nine oxygen atoms in a distorted tricapped trigonal prismatic geometry. Six oxygen atoms from three bidentate nitrate groups, two oxygen atoms from two N-oxo group of the ligands and one oxygen atom from one water molecule satisfy the coordination number of nine. The ligand acts as a monodentate ligand and is bonded only through the N-oxo oxygen atom to the europium atom while amide group is free. Two ligands are placed mutually syn to each other. The pyridyl rings of both the ligands are essentially non coplanar with the tortion angle of 72.37^{o}.

The observed bond distance for Eu–O$_{(N\text{-oxide})}$ (2.345(8) Å) in **8** is close to the values observed in earlier reported lanthanide nitrate-N-oxide complexes, such as [Eu(nicotinic acid N-oxide)$_3$(H$_2$O)$_2$]$_n$. 4n H$_2$O (2.379 (5)Å) [41], [Eu(2,6-bis((1H-pyrazol-1-yl)methyl)pyridine 1-oxide)$_2$(NO$_3$)$_3$] (2.376(13) Å) [42], {[Eu(2,6-Bis(diphenyl-N,N-diethylcarbamoylmethylphosphine oxide)-pyridine N-Oxide)(NO$_3$)$_3$]·(Me$_2$CO)$_{0.75}$·(H$_2$O)$_{0.3}$}$_4$ (2.467 (3)Å) [43], Eu(2,6-Bis[bis(2-(trifluoromethyl)phenyl)phosphinoylmethyl]pyridine N-Oxide)(NO$_3$)$_3$ (2.424(2) Å) [44]. The observed average Eu–O(NO$_3$) bond distance of 2.496(11) Å is normal.

Table 3.4 Important bond distances (Å) and angles (^{o}) for the compound **8**

Eu1-O11	2.335(8)	O11-Eu1-O13	149.1(4)
Eu1-O13	2.355(8)	O6-Eu1-O5	50.3(3)
Eu1-O8	2.507(10)	O9-Eu1-O8	51.1(3)
Eu1-O6	2.486(11)	O3-Eu1-O2	51.0(5)
Eu1-O2	2.496(11)	N4-O11-Eu1	133.9(8)
Eu1-O1	2.418(11)	N6-O13-Eu1	133.7(8)
		N1-O3-Eu1	97.4(11)

3.4 Conclusions

N-oxo pyridine 2-carboxamide ligands showed coordination diversity towards uranyl nitrate and lanthanide nitrates. The reaction between uranyl nitrate and N-oxo pyridine 2-carboxamide yielded complexes with 1:1 stoichiometry. In these complexes, the ligands are bonded with the uranyl group in a bidentate chelating fashion through both the amidic oxygen and N-oxide oxygen atoms. The geometry around the uranium is distorted hexagonal bipyramid. On the other hand, the lanthanide nitrates (Ln = La, Sm, Eu) form 1:2 complexes with N-oxo pyridine 2-carboxamide ligands. The ligands act as monodetate ligands and bond through the N-oxide oxygen atom with metal centre and leaving the amido oxygen atom free. The geometry around the europium(III) ion is distorted tricapped trigonal prism.

3.5 References

1. J.N. Mathur, M.S.Murali, K.L. Nash, Solvent Extr. Ion Exch. 19 (2001) 357-390.
2. Seraj A. Ansari, Priyanath Pathak, Prasanta K. Mohapatra, Vijay K. Manchanda, Chem. Rev. 112 (2012) 1751–1772.
3. G.R. Mahajan, D.R. Prabhu, V.K. Manchanda, L.P. Badheka, Waste Manage. 18 (1998) 125-133.
4. Henk H. Dam, David N. Reinhoudt, Willem Verboom, New J. Chem. 31 (2007) 1620-1632.
5. E. Philip Horwitz , Dale C. Kalina , Herbert Diamond , George F. Vandegrift, Wallace W. Schulz, Solvent Extr. Ion Exch. 3 (1985) 75-109.
6. W.W. Schulz, E.P. Horwitz, Sep. Sci. Technol. 23 (1988) 1191-1210.
7. A.B Patil, P. Pathak, V.S Shinde, S.V Godbole, P.K Mohapatra, Dalton Trans. 42 (2013) 1519-1529.
8. Eil-Hee Lee, Jae-Gwan Lim, Dong-Yong Chung, Jae-Hyung Yoo, Kwang-Wook Kim, Nucl. Eng. Technol. 41 (2009) 319-326.
9. Benoît Gannaz, Mark R. Antonio, Renato Chiarizia, Clément Hill, Gérard Cote, Dalton Trans. (2006) 4553-4562.
10. Sujoy Biswas, D.K. Singh, K.N. Hareendran, J.N. Sharma, S.B. Roy, J. Radioanal. Nucl. Chem. 284 (2010) 201–205.
11. Taichi Sato, J. Inorg. Nucl. Chem. 24 (1962) 699-706.
12. F.E. Kosinski, H. Bostian, J. Inorg. Nucl. Chem. 31 (1969) 3623-3631.
13. Ahmed F. Abdel-Magied, Mostafa I. Amin, Int. J. Ind. Chem. 7 (2016) 21–28.
14. S. Biswas, P.N. Pathak, D.K. Singh, S.B. Roy, V.K. Manchanda, Int. J. Miner. Process. 104-105 (2012) 17–23.
15. F.J. Hurst, D.J. Crouse, Ind. Eng. Chem., Process Des. Develop. 13 (1974) 286-291.
16. P.D. Mithapara, V.K. Manchanda, P.R. Natarajan, J. Radioanal. Nucl. Chem. Art. 83/2 (1984) 301-307.
17. Shanmugaperumal Kannan, Kuna Venugopal Chetty, Venkatarama Venugopal, Michael G.B. Drew, Dalton Trans. (2004) 3604–3610.
18. S.B. Deb, S. Kannan, M.G.B. Drew, J. Coord. Chem. 63 (2010) 3620-3626.
19. Sabrina Ouizem, Daniel Rosario-Amorin, Diane A. Dickie, Benjamin P. Hay, Robert T. Paine, Polyhedron 101 (2015) 37–47.
20. Anthony M.J. Lees, Andrew W.G. Platt, Inorg. Chem. 42 (2003) 4673−4679.

21. Bal Govind Vats, Jayashree S. Gamare, S. Kannan, I.C. Pius, D.M. Noronha, M. Kumar, Inorg. Chim. Acta 467 (2017) 1–6.
22. M. Ejaz, Sep. Sci. 10 (1975) 425-446.
23. Z.B. Maksimović, R.G. Puzić, J. Inorg. Nucl. Chem. 34 (1972) 1031-1038.
24. Neelam Kumari, D.R. Prabhu, A.S. Kanekar, P.N. Pathak, Ind. Eng. Chem. Res. 51 (2012) 14535–14542.
25. Kevin McCann, Bruce J. Mincher, Nicholas C. Schmitt, Jenifer C. Braley, Ind. Eng. Chem. Res. 56 (2017) 6515−6519.
26. Kevin McCann, Jessica A. Drader, Jenifer C. Braley, Sep. Purif. Rev. doi.org/10.1080/15422119.2017.1321018.
27. Sylvie Pailloux, Iris Binyamin, Lorraine M. Deck, Benjamin P. Hay, Eileen N. Duesler, Lev N. Zakharov, W. Scott Kassel, Arnold L. Rheingold, Robert T. Pain, Polyhedron 28 (2009) 3979–3984.
28. Hai-Jun Zhang, Ru-Hu Gou, Lan Yan, Ru-Dong Yang, Spectrochim. Acta, Part A 66 (2007) 289–294.
29. Zbigniew Hnatejko, Stefan Lis, Przemysław Starynowicz, Zdzisław Stryła, Polyhedron 30 (2011) 880–885.
30. Zbigniew Hnatejko, J. Rare Earths 30 (2012) 552.
31. I.S. Ahuja , C.L. Yadava, Shailendra Tripathi, Synth. React. Inorg. Met.-Org. Chem. 18 (1988) 953-963.
32. T.R. Varga, A.C. Benyei, Z. Fazekas, H. Tomiyasu, Y. Ikeda, Inorg. Chim. Acta 342 (2003) 291.
33. N. Koshino, M. Harada, M. Nogami, Y. Morita, T. Kikuchi, Y. Ikeda, Inorg. Chim. Acta 358 (2005) 1857.
34. S. Kannan, S.B. Deb, J.S. Gamare, M.G.B. Drew, Polyhedron 27 (2008) 2557.
35. G.J. Lumetta, B.K. McNamara, B.M. Rapko, R.L. Sell, R.D. Rogers, G. Broker, J.E. Hutchison, Inorg. Chim. Acta 309 (2000) 103.
36. L.J. Caudle, E.N. Duesler, R.T. Paine, Inorg. Chim. Acta 110 (1985) 91–100.
37. D.T. Cromer, R.R. Ryan, S. Karthikeyan, R.T. Paine, Inorg. Chim. Acta 172 (1990) 165–172.
38. S.B. Deb, J.S. Gamare, S. Kannan, M.G.B. Drew, Polyhedron 28 (2009) 2673–2678.
39. P. Charpin, M. Lance, M. Nierlich, D. Vigner, Acta Crystallogr. Sect. C 42 (1986) 560.
40. O. Clements, B.M. Rapko, B.P. Hay, Coord. Chem. Rev. 170 (1998) 203.

41. Jiang-Gao Mao, Hong-Jie Zhang, Jia-Zuan Ni, Shu-Bin Wang, Thomas C.W Mak, Polyhedron 17 (1998) 3999–4009.
42. Sabrina Ouizema, Daniel Rosario-Amorina, Diane A. Dickiea, Benjamin P. Hay, Robert T. Paine, Polyhedron 101 (2015) 37–47.
43. Daniel Rosario-Amorin, Sabrina Ouizem, Diane A. Dickie, Yufeng Wen, Robert T. Paine, Jian Gao, John K. Grey, Ana de Bettencourt-Dias, Benjamin P. Hay, Lætitia H. Delmau, Inorg. Chem. 52 (2013) 3063–3083.
44. Sylvie Pailloux, Cornel Edicome Shirima, Alisha D. Ray, Eileen N. Duesler, Robert T. Paine, John R. Klaehn, Michael E. McIlwain, Benjamin P. Hay, Inorg. Chem. 48 (2009) 3104–3113.

CHAPTER 4

Synthesis, structural and theoretical studies of carbamoyl pyrazole compounds of the uranyl(VI) and Pd(II) ions

4.1 Introduction

The speciality of actinide coordination chemistry is their high coordination number and their structures depend on the steric effect provided by the bonded ligands like main group metal atoms [1-3]. It also modulates the mode of bonding of the bonded ligands and stoichiometry of the metal ligand complexes. Like other actinides, uranium also forms stable complexes with ligands consist of hard donor atoms like O, N, etc, which often form five or six membered cyclic chelates. It is evident from the previous studies that, five membered chelating ligands are more sterically controlled than six or higher membered chelating ligands [4]. In past, we had synthesized two types of carbamoyl methyl pyrazole based ligands (Fig. 1a, b) which form six membered chelating ring with uranyl nitrate irrespective to the steric demand of the respective ligands and relative orientation of the donor atoms in the ground state [5].

In continuation of our interest on the complex chemistry of uranyl and other metal ions with newly synthesized ligands [6], we report herein the synthesis, characterization, and complex chemistry of the analogous carbamoyl pyrazole based ligands (Fig. 1c, d) with uranyl as well as palladium (II) ions. Since these ligands are having a soft pyrazolyl nitrogen atom apart from hard amidic oxygen atom, they can form stable complexes with soft metal ion like palladium. These ligands can act as monodentate or bidentate ligands while bonding with palladium ions. Comparison of the complex chemistry between these two types (carbamoyl methyl pyrazole and carbamoyl pyrazole) of ligands is also done to understand the effect of ring size on complex formation. Density functional theory is done to validate and explain our experimental observation.

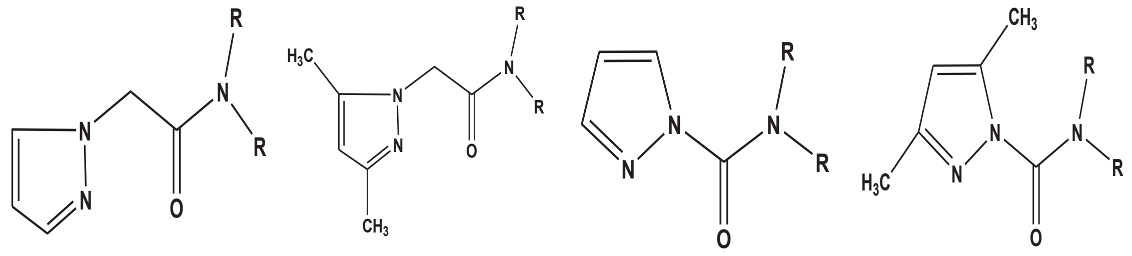

(a) (b) (c) (d)

Fig. 1 (a) Carbamoyl methyl pyrazole, (b) carbamoyl methyl (3,5-dimethyl pyrazole), (c) carbamoyl pyrazole, (d) carbamoyl (3,5-dimethyl pyrazole)

4.2 Experimental

4.2.1 Synthesis of the carbamoyl pyrazole ligands

*4.2.1.1 Synthesis of $C_3H_3N_2CON(CH_3)_2$ (**L^1**)*

A solution of pyrazole (10 g, 0.14 mol) and triethyl amine (17.5 g, 0.17 mol) in benzene (50 mL) was added slowly to a solution of N,N-dimethyl carbamoyl chloride (15.8 g, 0.14 mol) in benzene (50 mL) with stirring. The reaction mixture was refluxed for 6 h and treated with 100 mL of 5% HCl solution. The organic layer was separated, dried over anhydrous sodium sulfate, and filtered. Removal of the solvent in vacuum yielded a colorless solution of L^1 in 59% yield. ^{1}H NMR (25 ^{o}C, $CDCl_3$): $\delta = 3.23$ [s, 6H, NCH_3], 6.35 [q, 1H, pz], 7.64 [d, 1H, pz], 8.12 [q, 1H, pz]. IR (cm^{-1}): $\nu = 1693$ (C=O). Analysis Calcd for $C_6H_9N_3O$: C, 51.8; H, 6.5; N, 30.2. Found: C, 51.1; H, 6.1; N, 29.7.

*4.2.1.2 Synthesis of $C_3H_3N_2CON(C_2H_5)_2$ (**L^2**)*

This was prepared similarly as for L^1 by taking N,N-diethyl carbamoyl chloride (20 g, 0.14 mol) and pyrazole (10 g, 0.14 mol) in 73% yield. ^{1}H NMR (25 °C, $CDCl_3$): $\delta = 1.27$ [t, 6H, CH_3], 3.61 [br, 4H, NCH_2], 6.34 [q, 1H, pz], 7.62 [d, 1H, pz], 8.13 [q, 1H, pz]. IR (cm^{-1}): $\nu =$

1687(C=O). Analysis Calcd for $C_8H_{13}N_3O$: C, 57.5; H, 7.8; N, 25.1. Found: C, 56.9; H, 7.4; N, 24.7.

4.2.1.3 Synthesis of $C_3H_3N_2CON(^iC_3H_7)_2$ ($\mathbf{L^3}$)

This was prepared similarly to L^1 by taking N,N-diisopropyl carbamoyl chloride (25 g, 0.15 mol) and pyrazole (10 g, 0.14 mol) in 90% yield. ^{1}H NMR (25 °C, $CDCl_3$): $\delta = 1.38$ [d, 12H, CH_3], 4.09 [m, 2H, CH, ^{i}Pr], 6.33 [q, 1H, pz], 7.60 [d, 1H, pz], 8.03 [q, 1H, pz]. IR (cm^{-1}): $\nu = 1687$(C=O). Analysis Calcd for $C_{10}H_{17}N_3O$: C, 61.5; H, 8.7; N, 21.5. Found: C, 61.2; H, 8.4; N, 21.1.

4.2.1.4 Synthesis of $C_5H_7N_2CON(CH_3)_2$ ($\mathbf{L^4}$)

This was prepared similarly to L^1 by taking N,N-dimethyl carbamoyl chloride (12 g, 0.11 mol) and dimethyl pyrazole (10 g, 0.11 mol) in 80% yield. ^{1}H NMR (25 °C, $CDCl_3$): $\delta = 2.23$ [s, 3H, CH_3, dmpz], 2.39 [s, 3H, CH_3, dmpz], 3.09 [s, 6H, NCH_3], 5.89 [s, 1H, dmpz]. IR (cm^{-1}): $\nu = 1697$(C=O). Analysis Calcd for $C_8H_{13}N_3O$: C, 57.5; H, 7.8; N, 25.1. Found: C, 57.1; H, 7.2; N, 24.8.

4.2.1.5 Synthesis of $C_5H_7N_2CON(C_2H_5)_2$ ($\mathbf{L^5}$)

This was prepared similarly to L^1 by taking N,N-diethyl carbamoyl chloride (15 g, 0.11 mol) and dimethyl pyrazole (10 g, 0.11 mol) in 84% yield. ^{1}H NMR (25 °C, $CDCl_3$): $\delta = 1.23$ [t, 6H, CH_3, C_2H_5], 2.21 [s, 3H, CH_3, dmpz], 2.37 [s, 3H, CH_3, dmpz], 3.45 [s, 4H, NCH_2], 5.87 [s, 1H, dmpz]. IR (cm^{-1}): $\nu = 1691$ (C=O). Analysis Calcd for $C_{10}H_{17}N_3O$: C, 61.5; H, 8.7; N, 21.5. Found: C, 60.9; H, 8.5; N, 21.0.

4.2.1.6 Synthesis of $C_5H_7N_2CON(^iC_3H_7)_2$ ($\mathbf{L^6}$)

This was prepared similarly to L^1 by taking N,N-diisopropyl carbamoyl chloride (17 g, 0.11 mol) and dimethyl pyrazole (10 g, 0.11 mol) in 86% yield. ^{1}H NMR (25 °C, $CDCl_3$): $\delta = 1.31$ [d, 12H, CH_3, ^{i}Pr], 2.16 [2, 3H, CH_3, dmpz], 2.28 [s, 3H, CH_3, dmpz], 3.66 [m, 2H, CH, ^{i}Pr], 5.81 [s, 1H, dmpz]. IR (cm^{-1}): ν = 1693 (C=O). Analysis Calcd for $C_{12}H_{21}N_3O$: C, 64.6; H, 9.4; N, 18.8. Found: C, 64.3; H, 9.1; N, 18.5.

4.2.2 Synthesis of uranyl complexes of carbamoyl pyrazole ligands

*4.2.2.1 Synthesis of $[UO_2(NO_3)_2\{C_3H_3N_2CON(CH_3)_2\}]$ (**1**)*

To a solution of **L^1** (200 mg, 1.44 mmol) in CH_2Cl_2 (20 mL), solid $[UO_2(NO_3)_2{\cdot}6H_2O]$ (300 mg, 0.59 mmol) was added and stirred for few minutes until all $[UO_2(NO_3)_2{\cdot}6H_2O]$ dissolved to give a clear solution. This solution was filtered and layered with iso-octane. The solution on slow evaporation yielded yellow crystalline solid, which was filtered, washed with hexane, and dried. Yield: 85%. ^1H NMR (25°C, CD_3COCD_3): δ = 3.82 [br, 3H, NCH_3], 3.98 [br, 3H, NCH_3], 7.22 [br, 1H, pz], 9.26 [br, 2H, pz]. IR (cm^{-1}): ν = 1653(C=O), 935(U=O). Analysis Calcd for $C_6H_9N_5O_9U$: C, 13.5; H, 1.7; N, 13.5. Found: C, 13.4; H, 1.6; N, 13.2.

*4.2.2.2 Synthesis of $[UO_2(NO_3)_2\{C_3H_3N_2CON(C_2H_5)_2\}]$ (**2**)*

This was prepared similarly to **1** by taking **L^2** (220 mg, 1.37 mmol) and $[UO_2(NO_3)_2{\cdot}6H_2O]$ (300 mg, 0.59 mmol) in 91% yield. ^1H NMR (25°C, CD_3COCD_3): δ = 1.56 [br, 6H, CH_3], 4.15 [br, 4H, NCH_2], 7.4 [s, 1H, pz], 8.98 [s, 1H, pz], 9.24 [s, 2H, pz]. ^1H NMR (25°C, $CDCl_3$): δ 1.25 [br, 6H, CH_3], 4.06 [br, 4H, NCH_2], 7.12 [s, 1H, pz], 8.44 [s, 1H, pz], 9.4 [s, 2H, pz]. IR (cm^{-1}): ν = 1654 (C=O), 941 (U=O) 941. ES-MS (CH_2Cl_2): m/z = 666 $[UO_2(NO_3)(L^2)_2]^+$, 517 $[UO_2(NO_3)(L^2)H_2O]^+$, 499 $[UO_2(NO_3)(L^2)]^+$. Analysis Calcd for $C_8H_{13}N_5O_9U$: C, 17.1; H, 2.3; N, 12.5. Found: C, 17.0; H, 2.3; N, 12.4.

*4.2.2.3 Synthesis of $[UO_2(NO_3)_2\{C_3H_3N_2CON(^iC_3H_7)_2\}]$ (**3**)*

This was prepared similarly to **1** by taking **L^3** (250 mg, 1.28 mmol) and $[UO_2(NO_3)_2{\cdot}6H_2O]$ (300 mg, 0.59 mmol) in 86% yield. ^1H NMR (25°C, CD_3COCD_3): δ = 1.35 [s, 3H, CH_3], 1.80 [s, 3H, CH_3], 4.42 [m, 2H, CH, ^{i}Pr], 7.21 [s, 1H, pz], 8.95 [s, 1H, pz], 9.2 [s, 2H, pz]. ^1H NMR (25°C, $CDCl_3$): δ 1.25 [br, 6H, CH_3], 4.06 [br, 4H, NCH_2], 7.12 [br 1H, pz], 8.44 [br, 1H, pz], 9.4 [br, 2H, pz]. IR (cm^{-1}): ν = 1643(C=O), 939 (U=O). Analysis Calcd for $C_{10}H_{17}N_5O_9U$: C, 20.4; H, 2.9; N, 11.9. Found: C, 20.2; H, 2.7; N, 11.8.

*4.2.2.4 Synthesis of [$UO_2(NO_3)_2(H_2O)_2\{C_5H_7N_2CON(CH_3)_2\}_2$] (**4**)*

This was prepared similarly to **1** by taking **L^4** (220 mg, 1.37 mmol) and [$UO_2(NO_3)_2\cdot 6H_2O$] (300 mg, 0.59 mmol) in acetone. The acetone solution on slow evaporation yielded yellow crystalline solid, which was filtered, washed with ether, and dried. Yield: 96%. ^{1}H NMR (25 °C, CD_3COCD_3): δ = 2.14 [s, 3H, CH_3, dmpz], 2.31 [s, 3H, CH_3, dmpz], 3.05 [s, 6H, NCH_3], 5.94 [s, 1H, dmpz]. IR(cm^{-1}): ν = 3400−3200(H_2O), 1690 (C=O), 935 (U=O). Analysis Calcd for $C_{16}H_{30}N_8O_{12}U$: C, 25.1; H, 3.9; N, 14.6. Found: C, 25.0; H, 3.7; N, 14.9.

*4.2.2.5 Synthesis of [$UO_2(NO_3)_2(H_2O)_2\{C_5H_7N_2CON(C_2H_5)_2\}_2$] (**5**)*

This was prepared similarly to **4** by taking **L^5** (250 mg, 1.28 mmol) and [$UO_2(NO_3)_2\cdot 6H_2O$] (300 mg, 0.59 mmol) in 92% yield. ^{1}H NMR (25°C, CD_3COCD_3): δ = 1.17 (t, 6H, CH_3, C_2H_5], 2.13 [s, 3H, CH_3, dmpz], 2.30 [s, 3H, CH_3, dmpz], 3.41 [s, 4H, NCH_2], 5.92 [s, 1H, dmpz]. IR (cm^{-1}): ν = 3500−3200 (H_2O), 1691 (C=O), 941 (U=O). Analysis Calcd for $C_{20}H_{38}N_8O_{12}U$: C, 29.3; H, 4.6; N, 13.6. Found: C, 29.1; H, 4.5; N, 13.3.

*4.2.2.6 Synthesis of [$UO_2(NO_3)_2(H_2O)_2\{C_5H_7N_2CON(^iC_3H_7)_2\}_2$] (**6**)*

This was prepared similarly to **4** by taking **L^6** (280 mg, 1.25 mmol) and [$UO_2(NO_3)_2\cdot 6H_2O$] (300 mg, 0.59 mmol) in 93% yield. ^{1}H NMR (25 °C, CD_3COCD_3): δ = 1.31 [d, 12H, CH_3, ^{i}Pr], 2.12 [2, 3H, CH_3, dmpz], 2.27 [s, 3H, CH_3, dmpz], 3.74 [m, 2H, CH, ^{i}Pr], 5.91 [s, 1H, dmpz]. IR (cm^{-1}): ν = 3500−3200 (H_2O), 1687 (C=O), 941 (U=O). Analysis Calcd for $C_{24}H_{46}N_8O_{12}U$: C, 32.9; H, 5.3; N, 12.8. Found: C, 32.7; H, 5.2; N, 12.7.

*4.2.2.7 Synthesis of [$UO_2(C_6H_5COCHCOC_6H_5)_2\{C_3H_3N_2CON(CH_3)_2\}$] (**7**)*

To a hot chloroform (30 mL) solution of **L^1** (70 mg, 0.5 mmol), solid [$UO_2(C_6H_5COCHCOC_6H_5)_2\cdot 2H_2O$] (350 mg, 0.47 mmol) was added and refluxed for 2 h. The clear solution was filtered and layered with iso-octane. The solution on slow evaporation yielded an orange colored product in 86% yield. ^{1}H NMR (25°C, $CDCl_3$): δ = 4.24 [s, 6H, NCH_3], 6.91 [s, 1H, pz], 7.37 [s, 2H, DBM], 7.53 (t, 1H, pz), 7.61 [m, 12H, C_6H_5, DBM], 8.0 [d, 1H, pz], 8.46 [m, 8H, C_6H_5, DBM]. IR (cm^{-1}): ν = 1656 (C=O) (L^1), 1591 (C=O) (DBM), 904 (U-O). Analysis Calcd for $C_{36}H_{31}N_3O_7U$: C, 50.5; H,3.6; N, 4.9. Found: C, 49.7; H, 3.4; N, 4.7.

*4.2.2.8 Synthesis of [$UO_2(C_6H_5COCHCOC_6H_5)_2\{C_3H_3N_2CON(C_2H_5)_2\}$] (**8**)*

This was prepared similarly to **7** by taking **L^2** (80 mg, 0.48 mmol) and [$UO_2(C_6H_5COCHCOC_6H_5).2H_2O$] (350 mg, 0.47 mmol) in 90% yield. ^{1}H NMR (25°C, CD_3COCD_3): δ = 1.18 [t, 6H, CH_3], 3.55 [m, 4H, NCH_2], 6.37 [s, 1H, pz], 7.40 [s, 2H, DBM], 7.65 [m, 13H, C_6H_5 + pz], 8.6 [m, 8H, C_6H_5]. IR (cm^{-1}): ν = 1650 (C=O) (L^2), 1591 (C=O) (DBM), 902 (U=O). ES-MS (CH_2Cl_2): m/z = 678 [UO_2(DBM)(L^2)(H_2O)]$^+$, 660 [UO_2(DBM)(L^2)]$^+$. Analysis Calcd for $C_{38}H_{35}N_3O_7U$: C, 51.6; H, 3.9; N, 4.8. Found: C, 51.0; H, 3.7; N, 4.5.

4.2.3 Synthesis of palladium complexes of carbamoyl pyrazole ligands

*4.2.3.1 Synthesis of [$PdCl_2\{C_3H_3N_2CON(CH_3)_2\}_2$] (**9**)*

To an acetonitrile solution of $PdCl_2$ (200 mg, 1.1 mmol), $C_3H_3N_2CON\{CH_3\}_2$ (314 mg, 2.25 mmol) was added and refluxed for 2 h. This solution was evaporated to dryness completely, washed with hexane and dried. The resulting residue was extracted in CH_2Cl_2 and filtered to remove insoluble materials. The solution was layered with 5 ml of iso-octane and allowed to evaporate slowly. This process deposited brownish yellow colored product in 91% yield. ^{1}H NMR (25°C, $CDCl_3$): δ 3.27 [s, 6H, NCH_3], 6.45 [q, 1H, pz], 7.63 [d, 1H, pz], 8.12 [q, 1H, pz]. IR (cm^{-1}): ν = 1716 (C=O). Anal. Calc. for [$PdCl_2\{C_6H_9N_3O\}_2$]: C, 31.6; H, 4.0; N, 18.4. Found: C, 31.1; H, 3.8; N, 18.1%.

*4.2.3.2 Synthesis of [PdCl$_2${C$_5$H$_7$N$_2$CON(C$_2$H$_5$)$_2$}$_2$] (**10**)*

This was prepared similarly to 1 by taking PdCl$_2$ (200 mg, 1.1 mmol) and C$_3$H$_3$N$_2$CON{C$_2$H$_5$}$_2$ (377 mg, 2.24 mmol) in 88% yield. ^{1}H NMR (25^{o}C, CDCl$_3$): δ = 1.31 [br, 6H, CH$_3$], 3.61 [q, 4H, NCH$_2$], 6.42 [q, 1H, pz], 7.29(d, 1H, pz], 7.99 [q, 1H, pz]. IR (cm^{-1}): ν = 1714 (C=O). ESI-MS (CH$_3$CN): 475 (100%,) [PdL$_2$Cl$^+$]: Anal. Calc. for [PdCl$_2${C$_8$H$_{13}$N$_3$O}$_2$]: C, 37.5; H, 5.1; N, 16.4. Found: C, 37.2; H, 4.7; N, 16.3%.

*4.2.3.3 Synthesis of [PdCl$_2${C$_3$H$_3$N$_2$CON(^{i}C$_3$H$_7$)$_2$}$_2$] (**11**)*

This was prepared similarly to 1 by taking PdCl$_2$ (200 mg, 1.1 mmol) and C$_3$H$_3$N$_2$CON{^{i}C$_3$H$_7$}$_2$ (440 mg, 2.25 mmol) in 91% yield. ^{1}H NMR (25^{o}C, CDCl$_3$): δ = 1.48 [d, 12H, CH$_3$], 3.77 [m, 2H, CH, ^{i}Pr], 6.37 [q, 1H, pz], 7.60 (d, 1H, pz], 8.02 [q, 1H, pz]. IR (cm^{-1}): ν = 1709 (C=O). Anal. Calc. for [PdCl$_2${C$_{10}$H$_{17}$N$_3$O}$_2$]: C, 42.3; H, 6.0; N, 14.8. Found: C, 41.9; H, 6.2; N, 14.4%.

*4.2.3.4 Synthesis of [PdCl$_2${C$_5$H$_7$N$_2$CON(CH$_3$)$_2$}$_2$] (**12**)*

This was prepared similarly to 1 by taking PdCl$_2$ (200 mg, 1.1 mmol) and C$_5$H$_7$N$_2$CON{CH$_3$}$_2$ (377 mg, 2.25 mmol) in 90% yield. ^{1}H NMR (25^{o}C, CDCl$_3$): δ = 2.31 [s, 3H, CH$_3$, dmpz], 2.87 [d, 3H, CH$_3$, dmpz], 2.98 [br, 3H, NCH$_3$], 3.34 [br, 3H, NCH$_3$], 5.97 [s, 1H, dmpz]. IR (cm^{-1}): ν = 1711 (C=O). Anal. Calc. for [PdCl$_2${C$_8$H$_{13}$N$_3$O}$_2$]: C, 37.5; H, 5.1; N, 16.4. Found: C, 37.4; H, 4.9; N, 16.1%.

*4.2.3.5 Synthesis of [PdCl$_2${C$_5$H$_7$N$_2$CON(C$_2$H$_5$)$_2$}$_2$] (**13**)*

This was prepared similarly to 1 by taking PdCl$_2$ (200 mg, 1.1 mmol) and C$_5$H$_7$N$_2$CON{C$_2$H$_5$}$_2$ (440 mg, 2.24 mmol) in 89% yield. ^{1}H NMR (25^{o}C, CDCl$_3$): δ = 1.15 [br, 3H, CH$_3$, C$_2$H$_5$], 1.47 [br, 3H, CH$_3$, C$_2$H$_5$], 2.31 [s, 3H, CH$_3$, dmpz], 2.86[s, 3H, CH$_3$, dmpz], 3.43 [br, 2H, NCH$_2$], 3.73 [br, 2H, NCH$_2$], 5.95 [s, 1H, dmpz]. IR (cm^{-1}): ν = 1695 (C=O). ESI-MS (CH$_3$CN): 573 (100%,) [PdL$_2$Cl$^+$]: Anal. Calc. for [PdCl$_2${C$_{10}$H$_{17}$N$_3$O}$_2$]: C, 42.3; H, 6.0; N, 14.8. Found: C, 42.0; H, 6.1; N, 14.6%.

4.2.3.6 *Synthesis of* $[PdCl_2\{C_5H_7N_2CON(^iC_3H_7)_2\}_2]$ *(**14**)*

This was prepared similarly to 1 by taking $PdCl_2$ (200 mg, 1.1 mmol) and $C_5H_7N_2CON\{^iC_3H_7\}_2$ (504 mg, 2.24 mmol) in 91% yield. ^1H NMR (25°C, $CDCl_3$): $\delta = 1.53$ [d, 12H, CH_3, ^{i}Pr], 2.31 [2, 3H, CH_3, dmpz], 2.93 [s, 3H, CH_3, dmpz], 3.67 [m, 2H, CH, ^{i}Pr], 5.93 [s, 1H, dmpz]. IR (cm^{-1}): $\nu = 1703$ (C=O). Anal. Calc. for $[PdCl_2\{C_{12}H_{21}N_3O\}_2]$: C, 46.2; H, 6.8; N, 13.5. Found: C, 46.0; H, 6.6; N, 13.2%.

4.2.4 X-ray crystallography

Selected crystallographic data for the compounds **2, 5, 8, 10,** and **13** are summarized in Tables 4.1.

Table 4.1 Crystallographic data for compounds **2, 5, 8, 10,** and **13**

	2	**5**	**8**	**10**	**13**
Empirical formula	$C_8H_{13}N_5O_9U$	$C_{20}H_{38}N_8O_{12}U$	$C_{38}H_{35}N_3O_7U$	$C_{16}H_{26}N_6O_2Cl_2Pd$	$C_{20}H_{34}N_6O_2Cl_2Pd$
Formula weight	561.25	820.59	883.73	511.74	567.85
Crystal system	Monoclinic	Monoclinic	Monoclinic	Monoclinic	Monoclinic
Space group	$P2_1/c$	$P2_1/n$	$P2_1/n$	C2/c	$P2_1/c$
a (Å)	8.3229(6)	10.207(2)	10.2750(5)	22.3590(7)	7.1517(4)
b (Å)	18.0208(11)	8.5355(17)	21.6295(10)	7.2273(2)	11.4886(5)
c(Å)	10.6066(8)	18.095(4)	15.8792(7)	13.6515(4)	14.8111(6)
β (^{o})	100.902(8)	95.74(2)	100.913(4)	111.791(3)	92.600(4)
Volume (Å^3)	1562.12(19)	1568.6(6)	3465.2(3)	2048.37(10)	1215.67(9)
Z (formula unit)	4	2	4	4	2
Density (g/cm^3)	2.386	1.737	1.694	1.659	1.551
μ (mm^{-1})	10.445	5.240	4.738	1.191	1.012
Reflections collected/unique	9807/4518	9787/4376	17433/9611	5722/2904	7036/3384
Data/restrains/parameters	4518/0/210	4376/31/202	9611/0/444	2904/0/126	3384/0/146
Goodness of fit on F^2	1.038	1.010	1.073	1.041	1.087
Final R_1 indices[$I > 2\sigma(I)$]	0.0755	0.0658	0.0639	0.0256	0.0243
wR_2 indices (all data)	0.1855	0.1496	0.1133	0.0577	0.0578

$w = 1/[\sigma^2(F_o^2) + (0.1166P)^2 + 0.000P]$ for **2**, $w = 1/[\sigma^2(F_o^2) + (0.0667P)^2 + 0.000P]$ for **5**, $w = 1/[\sigma^2(F_o^2) + (0.0378P)^2 + 3.2432P]$ for **8**, $w = 1/[\sigma^2(F_o^2)+(0.0231P)^2 + 0.7398P]$ for **10** and $w = 1/[\sigma^2(F_o^2)+(0.0251P)^2 + 0.5630P]$ for **13**, where $P = (F_o^2 + 2F_c^2)/3$.

4.2.5 Theoretical calculations

For uranium complexes, full geometry optimization for the N,N-dimethyl analog of the ligands a−d and complexes (A−D) has been carried out applying a popular nonlocal correlated hybrid density functional, namely, B3LYP. Gaussian type atomic basis functions, 6-31+G(d), are adopted for H, C, N, and O atoms, and for U atom, a very recently suggested basis set, SARC-ZORA [7a], is used for all the calculations. SARC-ZORA basis sets are segmented all-electron scalar relativistic basis sets in which the coefficients of contracted GTOs have been optimized for use with the ZORA scalar relativistic Hamiltonian. These particular basis sets for U are obtained from Extensible Computational Chemistry Environment Basis Set Database, Pacific Northwest National Laboratory [7b]. The quasi-Newton−Raphson based algorithm has been applied to carry out geometry optimization to locate the minimum energy structure in each case. Hessian calculations have also been carried out to check the nature of the equilibrium geometry. Macroscopic solvation effect of solvent water has been incorporated in energy calculation through polarizable continuum model (PCM). All these calculations have been carried out applying GAMESS suit of ab initio program on a LINUX cluster platform [7c].

For palladium complexes, full geometry optimization of the ligands (**L**^{2} and **L**^{5}) and complexes (**10** and **13**) has been carried out applying a recently developed density functional with empirical dispersion correction, namely, ωB97XD. Gaussian type atomic basis functions, 6-31+G(d) are adopted for H, C, N, O and Cl atoms and for Pd atom 3-21G basis sets are used for all the calculations. Recently, it has been reported that for transition metal complexes the ωB97XD functional performs best among functionals accounting for dispersion corrections as well as other popular DFT functionals not including dispersion. The functional adopted is observed to offer relatively small statistical errors when considering the overall structure as well as selected distances [8]. It is worthwhile mentioning that basis sets like LANL2DZ ECP and aug-cc-pVDZ-pp were also used for palladium, but such calculations were unsuccessful due to SCF convergence failure or optimization to unreasonable geometries.

4.3 Results and discussion

4.3.1. Synthesis of carbamoyl pyrazole and carbamoyl 3,5-dimethyl pyrazole ligands

Reaction of pyrazole and 3,5-dimethyl pyrazole with corresponding N,N-dialkyl carbamoyl chloride in benzene in presence of triethyl amine as base yielded the corresponding ligands (**L^1** to **L^6**)**.** The IR spectra of all ligands (Fig. 4.1) show the presence of the carbamoyl group in the synthesized compounds.

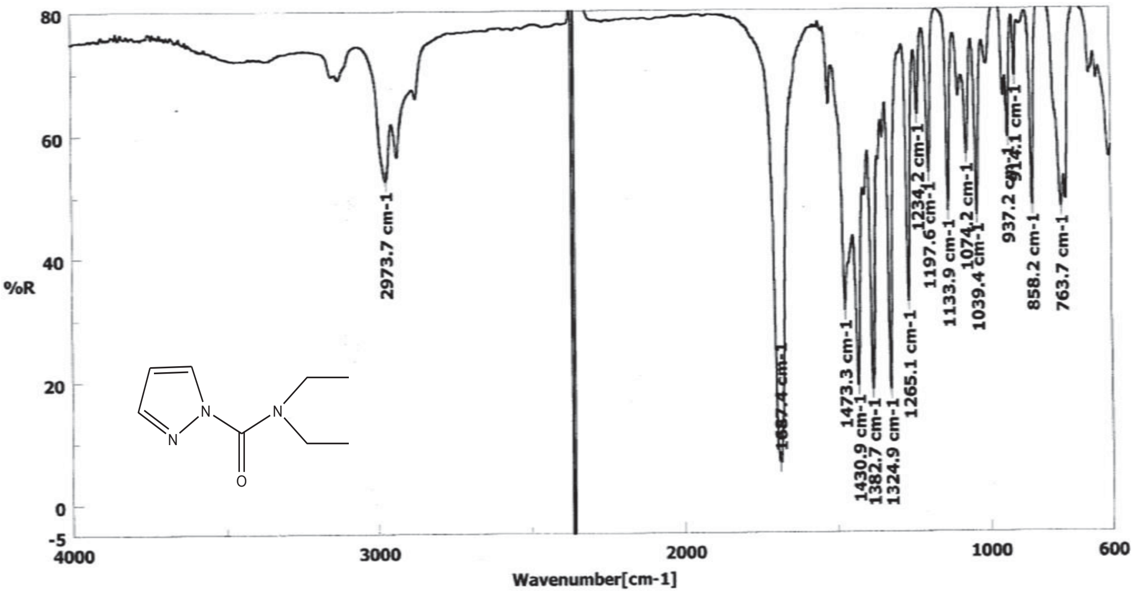

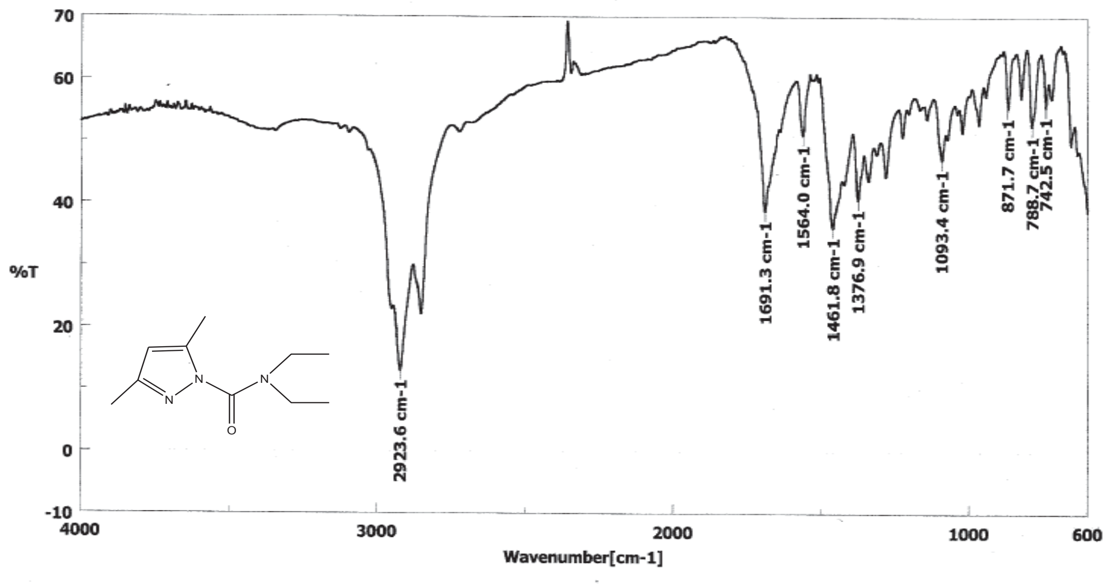

Fig. 4.1 IR spectra of ligand **L^2** (above) and **L^5** (below)

Fig 4.2 showed the ^{1}H NMR spectrum of ligand L^2. The three singlet peaks at 8.13, 7.62 and 6.34 ppm are due to each ring proton of the pyrazole ring at 5, 3 and 4 position respectively. Next, at 3.61 ppm, the broad peak is assigned to four CH_2 protons (chemically equivalent due to C-N(diethyl) bond rotation at room temperature) of the ethyl groups. This peak is broad because of quadrapolar effect of ^{14}N-atom adjacent to the CH_2 group protons. Six CH_3 protons (chemically equivalent due to C-N(diethyl) bond rotation at room temperature) of two ethyl groups of the ligand resonate as a triplet at 1.27 ppm. The signal is split into a triplet, because the methyl group protons are coupled with two adjacent CH_2 protons. The C, H, N analysis supports the expected stoichiometry for the compounds.

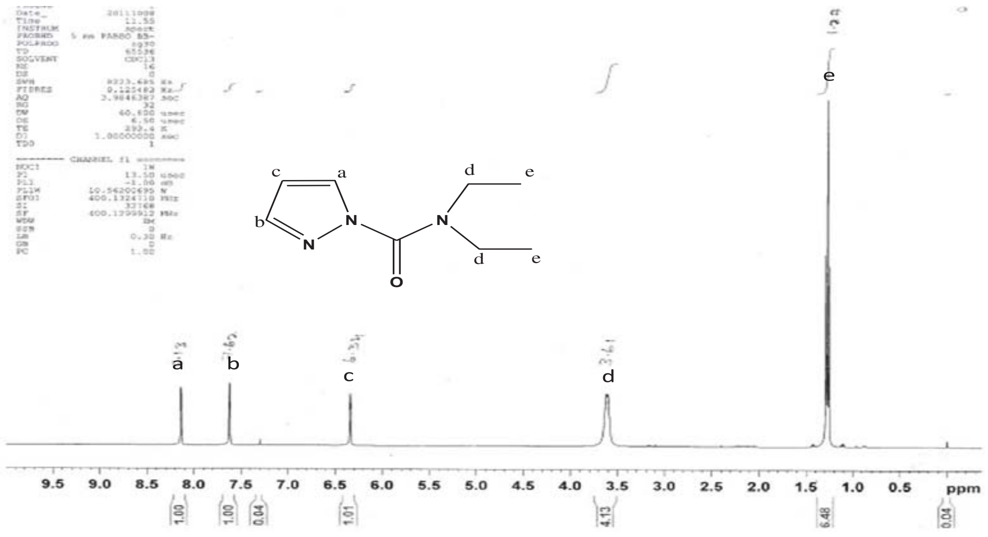

Fig. 4.2 ^{1}H NMR spectrum of ligand **L^2**

4.3.2 Synthesis and structural studies of uranyl complexes

4.3.2.1 Synthesis and complexation studies of carbamoyl pyrazole ligands with uranyl nitrate

The reaction of ligands **L^1–L^3** with $[UO_2(NO_3)_2{\cdot}6H_2O]$ yielded compounds **1–3**. C, H, and N analyses revealed that the ratio of ligand to uranyl nitrate is 1:1 in all compounds. The IR spectra of **1–3** (Fig. 4.3 for **2**) show that the water molecules from the starting compound $[UO_2(NO_3)_2{\cdot}6H_2O]$ are completely replaced by the ligand and that the ligand is bonded through the carbamoyl oxygen atom to the uranyl group. The observed frequency difference for a carbamoyl ($\Delta\nu_{CO}$ = 20–40 cm^{-1}, where $\Delta\nu_{CO} = \nu_{CO(\text{free ligand})} - \nu_{CO(\text{coordinated})}$) group is consistent with the supposition that the carbamoyl group is bonded to the uranyl group directly. This difference is comparable in magnitude with those observed in $[UO_2(NO_3)_2$(N-cyclohexyl-2-pyrrolidone)$_2]$ [9a], $[UO_2(NO_3)_2$(1,3-dimethyl-2-imidazolidone)$_2]$ [9b], $[UO_2(NO_3)_2\{^iC_3H_7CON(^iC_4H_9)_2\}_2]$ [10], $[UO_2(NO_3)_2(^iC_3H_7)_2NCOCH_2CON(^iC_3H_7)_2]$ [11] and $[UO_2(NO_3)_2(C_{15}H_{27}N_3O)]$ [5].

Fig 4.4 showed the ^{1}H NMR spectrum of complex **2**. The spectrum is exactly similar to that of ligand L^2 (already discussed in details earlier) since these complexes are derived from the same ligand. Some of the proton peaks of the ligand in the spectrum of the complex are deshielded (maximum up to 1.3 ppm) with respect to the free ligand, indicating that the bonding between pyrazolyl nitrogen and uranyl group persists in solution [5]. It is apparent from IR and NMR spectral results that the ligand acts as a bidentate chelating ligand and bonds through the carbamoyl and pyrazolyl nitrogen to uranyl group. The structure of **2** has been determined by single crystal X-ray diffraction methods and confirms the spectral and analysis results.

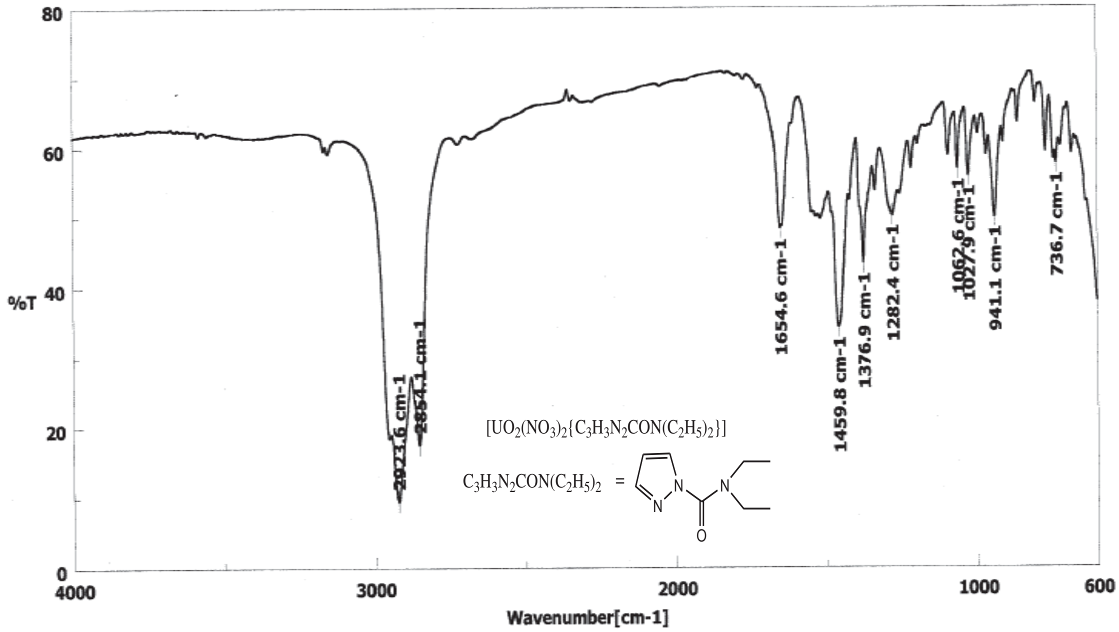

Fig. 4.3 IR spectrum of complex **2**

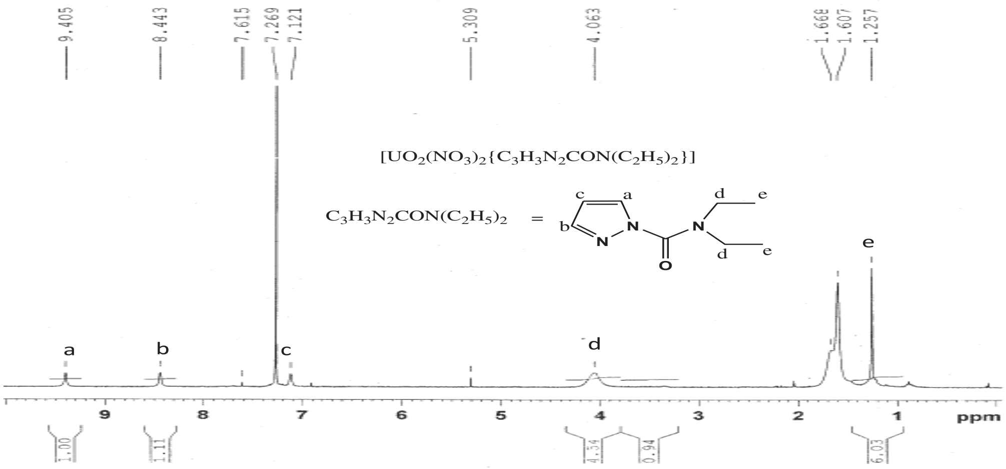

Fig. 4.4 ^{1}H NMR spectrum of complex **2**

Electrospray ionization mass spectrometric detection of positive ions for **2** (Fig. 4.5) in CH_2Cl_2 shows three intense peaks at the m/z values of 499.1 (61%), 517.15 (63%), and 666.24 (100%). These peaks are assigned to the species $[UO_2(NO_3)L]^+$ (69%), $[UO_2(NO_3)(H_2O)L]^+$ (71%), and $[UO_2(NO_3)L_2]^+$ (100%) (where, L = $C_3H_3N_2CON(C_2H_5)_2$), respectively. This study shows clearly that the ligand retains its bonding with the metal ion in solution and also that the compound undergoes disproportionation to give a mixture of 1:1 and 1:2 complexes [6a].

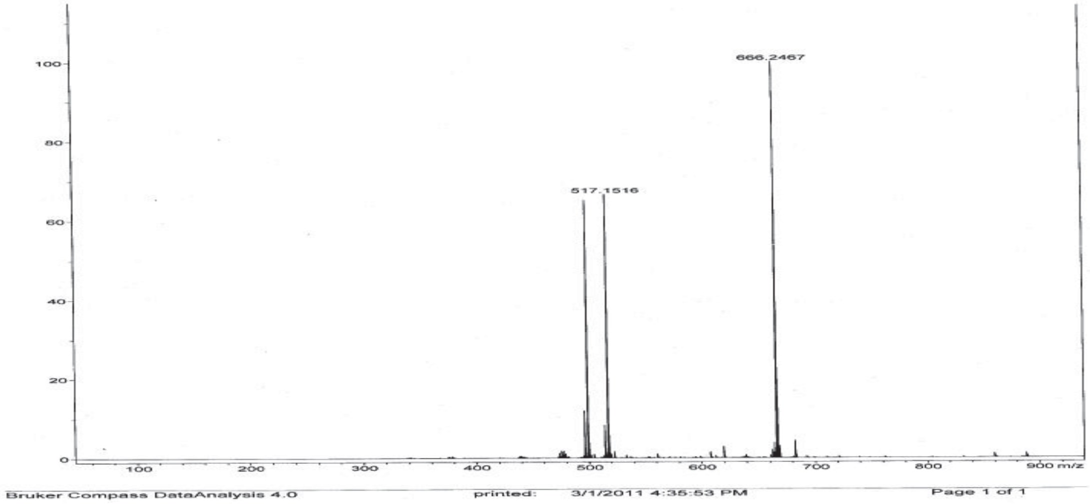

Fig. 4.5 ESI-MS spectrum of complex **2**

*4.3.2.2 Molecular structure of compound **2***

The structure of **2** is shown in Fig. 4.6, and selected bond distances and angles are given in Table 4.2. The structure of **2** shows that the uranium atom is surrounded by one nitrogen and seven oxygen atoms in a hexagonal bipyramidal geometry. Four oxygen atoms of the two bidentate nitrate groups, together with one oxygen and one nitrogen atom of bidentate carbamoyl pyrazole ligand, form the equatorial hexagonal plane. The UO_5N atoms in the equatorial plane show a root mean square (rms) deviation of 0.082 Å. The two uranyl oxygen atoms occupy the axial positions.

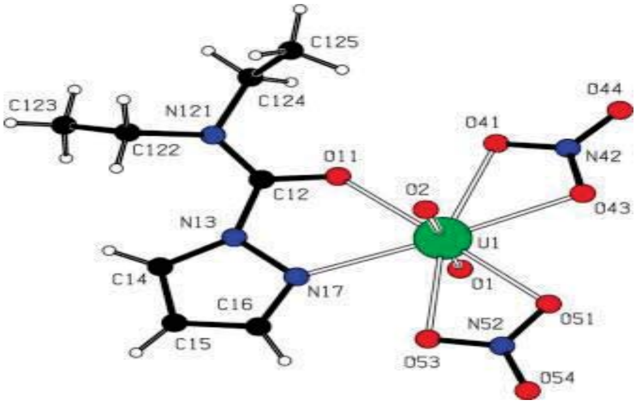

Fig. 4.6 The molecular structure of compound **2**

This type of coordination is similar to that observed in the compounds of the bifunctional ligands, malonamide, carbamoyl methyl phosphonate, carbamoyl methyl phosphine oxide, and carbamoyl methyl pyrazole with uranyl nitrate, such as $[UO_2(NO_3)_2(\{^iC_3H_7)_2NCO\}_2]$ [11], $[UO_2(NO_3)_2(^iC_3H_7O)_2POCH_2CONEt_2]$ [12a], $[UO_2(NO_3)_2(C_6H_5)_2POCH_2CONEt_2]$ [12b], $[UO_2(NO_3)_2.C_6H_5SOCH_2CONBu_2]$ [6a] and $[UO_2(NO_3)_2(C_{15}H_{27}N_3O)]$ [5]. The U−O(amide) distance (2.392(8) Å) in **2** is comparable in magnitude with those of earlier reported uranyl nitrate-amide compounds, such as $[UO_2(NO_3)_2$(N,N-dimethylformamide)$_2]$ (2.397(6) Å) [13], $[UO_2(NO_3)_2$(tetrabutylglutaramide)$_2]$ (2.378(6)Å [14], $[UO_2(NO_3)_2$(dibutyldecanamide)$_2]$ (2.37(2) Å) [15] and $[UO_2(NO_3)_2(C_{15}H_{27}N_3O)]$ (2.364(7) Å) [5]. The U−N(pyrazole) distance (2.544(9) Å) is very close to the values observed in

$[UO_2(NO_3)_2(C_{15}H_{27}N_3O)]$ (2.554(9)Å) [5], $[UO_2(NO_3)_2$(phenanthroline)] (2.556(2)Å) [16] and $[UO_2$(terpyridine)](OTf)$_2$ ((2.567(6), 2.592(6) Å) [17]. The observed average U−O(NO_3) bond distance 2.485(9) Å is normal [6,9,11−15]. The angles subtended at the metal atom show that the uranium atom has a slightly distorted hexagonal bipyramidal geometry.

Table 4.2 Important bond distances (Å) and angles (°) for the compound **2**

U1–O1	1.775(9)	U1−O51	2.467(9)
U1–O2	1.778(9)	U1−O53	2.494(9)
U1–O11	2.392(8)	U1−O43	2.513(9)
U1–O41	2.466(8)	U1−N17	2.544(9)
O1−U1−O2	178.4(4)	O51−U1−O53	50.7(3)
O41−U1−O43	50.7(3)	O11−U1−N17	61.7(3)
O53−U1−N17	66.3(3)	C12−O11−U1	127.4(7)

4.3.2.3 Synthesis and complexation studies of carbamoyl 3,5-dimethyl pyrazole ligands with uranyl nitrate

The reaction of ligands $\mathbf{L^4}$–$\mathbf{L^6}$ with $[UO_2(NO_3)_2\cdot 6H_2O]$ yielded the compounds **4−6**. The C, H, and N analysis revealed that the ratio of ligand to uranyl nitrate is 2:1 in all compounds. The IR spectra of **4−6** (Fig. 4.7 for **5**) show that the water molecules from the starting compound $[UO_2(NO_3)_2\cdot 6H_2O]$ have not been completely replaced by the ligand and that the ligand is uncoordinated in the complex [18].

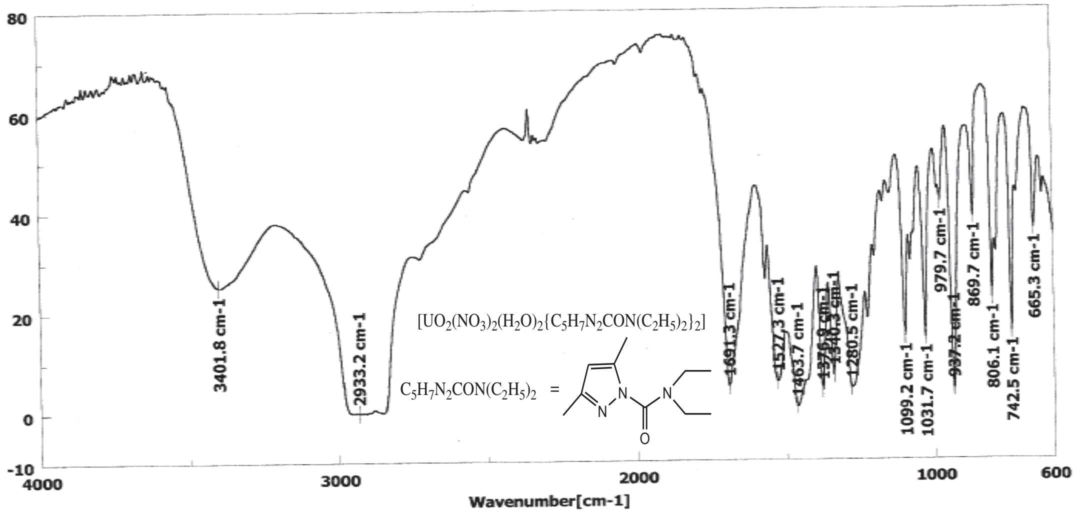

Fig. 4.7 IR spectrum of complex **5**

Fig 4.8 showed the ^{1}H NMR spectrum of complex **5**. The singlet peak at 5.93 ppm is attributed to the ring proton of the pyrazole ring at 4-position. Next, at 3.42 ppm, the doublet is assigned to four CH_2 protons (chemically equivalent due to C-N(diethyl) bond rotation at room temperature) of two ethyl groups. Two singlet peaks at 2.30 and 2.14 ppm are due to six CH_3 protons attached with the pyrazole ring at 3 and 5 position. Finally, six CH_3 protons (chemically equivalent due to C-N(diethyl) bond rotation at room temperature) of two ethyl groups of the ligand resonate as a singlet at 1.18 ppm. The spectrum also shows that the peaks are broadened and their positions are very similar to those of free ligands. This indicates clearly that there is no bonding between ligand and metal in solution. In order to find out the nature of bonding between the carbamoyl 3,5-dimethyl pyrazole ligand and uranyl nitrate in solid state, the structure of **5** has been determined by single crystal X-ray diffraction methods.

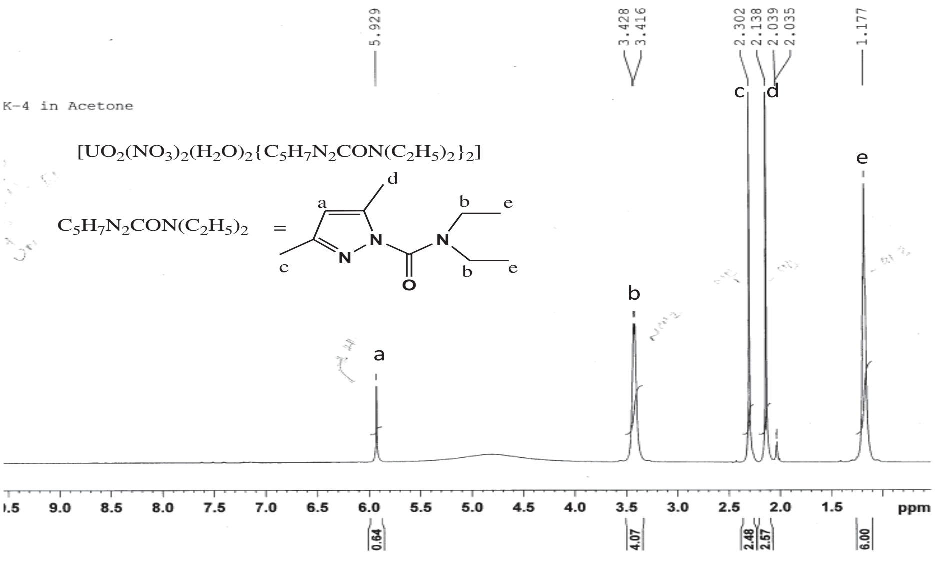

Fig. 4.8 ^{1}H NMR spectrum of complex **5**

*4.3.2.4 Molecular structure of compound **5***

The structure of **5** is shown in Fig. 4.9, and selected bond distances and angles are given in Table 4.3. The structure consists of centrosymmetric [$UO_2(NO_3)_2 \cdot 2H_2O$] groups, bridged by carbamoyl, dimethyl pyrazole ligand via O−H···O and O−H···N hydrogen bonds. The structure shows that there is no direct bonding between ligand and that the uranyl ion and the uranium(VI) ion are surrounded by eight oxygen atoms to give hexagonal bipyramidal geometry. The ligand forms a second sphere coordination [19] compound with [$UO_2(NO_3)_2 \cdot 2H_2O$]. Such types of second sphere compounds with uranyl nitrate are known previously for the weak donor ligands, such as crown ethers [18] or alcohols [20] but not with a strong donor ligand amide. However, some compounds of phosphine oxide with the transition metal ions show second sphere coordination [20b,c]. The average distances for $U{-}O_{uranyl}$ (1.711(7) Å) [6,9,11-17], $U{-}O_{H2O}$ (2.434(7)Å) [18,20] and $U{-}O_{NO3}$ (2.488(7)Å) [6,9,11−15] agree well with the values reported earlier. The hydrogen bonding $O_{water} \cdots O_{carbonyl}$ and $O_{water} \cdots N$ distances and angles are within the accepted values. Thus, O(1)−H(1)···O(7) (x − 1, y, z) has dimensions O···O, 2.760(9) Å, O−H···O, 155°, and H···O, 1.98 Å while O(1)−H(2)···N (2) (0.5 − x, y + 0.5, 0.5 − z) has dimensions O···N, 2.691(10) Å, O−H··N, 152°, and H···N, 1.92 Å.

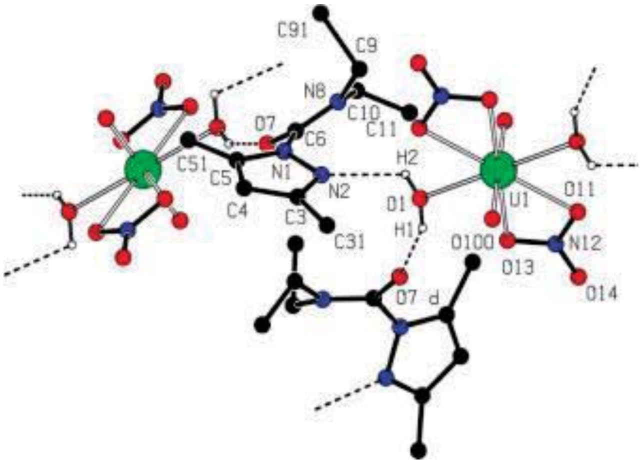

Fig. 4.9 The molecular structure of compound **5**

It is noteworthy that the analogous pyrazole ligands $\mathbf{L^1}$–$\mathbf{L^3}$ form inner sphere complexes with uranyl nitrate and directly bond to the metal center in the bidentate fashion via the carbamoyl oxygen and pyrazolyl nitrogen atoms. However, such type of bonding is not seen with the ligands $\mathbf{L^4}$–$\mathbf{L^6}$. It is interesting to note further that the analogous carbamoyl methyl pyrazole and carbamoyl methyl, 3,5-dimethyl pyrazole ligands form an inner sphere complex with the uranyl nitrate [5] and also act as bidentate chelating ligands. These observations could be explained purely on the basis of a steric effect due to the interaction between the methyl groups at the 3 and 5 positions of the pyrazole group with the carbamoyl oxygen and pyrazolyl nitrogen atoms of the ligands during metal ligand bond formation. However, the analogous carbamoyl methyl pyrazole type of ligands form a six member metallocyclic ring with the uranyl ion [6a] and here, the methyl groups at the 3 and 5 positions are positioned well away from the donor groups. These differences are consistent with the earlier reports that the steric effects play an important role during complex formation when ligands form a five member metallocyclic ring [4].

Table 4.3 Important bond distances (Å) and angles (^{o}) for the compound **5**

U1–O100	1.711(7)	U1–O1	2.434(7)
U1–O11	2.484(7)	U1–O13	2.492(6)
O1–H1	0.838(10)	O1–H2	0.841(10)
O100–U1–O100	179.999(1)	O1–U1–O1	180.0
O1–U1–O13	63.7(2)	O11–U1–O13	128.9(2)

4.3.2.5 Synthesis and complexation studies of carbamoyl pyrazole ligands with uranyl bis(dibenzoylmethanate)

The reaction of $\mathbf{L^1}$–$\mathbf{L^2}$ with [$UO_2(C_6H_5COCHCOC_6H_5)_2 \cdot 2H_2O$] yielded the compounds **7** and **8**. C, H, and N analyses revealed that the ratio of ligand to uranyl bis(dibenzoylmethanate) is 1:1 in both compounds. The IR spectra of **7** and **8** show that the water molecules from the starting compound [$UO_2(C_6H_5COCHCOC_6H_5)_2 \cdot 2H_2O$] are completely replaced by the ligand,

and furthermore, the observed frequency difference for a carbamoyl ($\Delta\nu_{CO} = 35$ cm^{-1}, where $\Delta\nu_{CO} = \nu_{CO(free\ ligand)} - \nu_{CO(coordinated)}$) group is consistent with the supposition that the carbamoyl group is bonded to the uranyl group directly. This difference is comparable in magnitude with those observed in $[UO_2(DBM)_2\{^iC_3H_7CON(^iC_3H_7)_2\}_2]$ (where DBM = $C_6H_5COCHCOC_6H_5$) [10], $[UO_2(NO_3)_2$(N-cyclohexyl-2-pyrrolidone)$_2]$ [9a], $[UO_2(NO_3)_2$(1, 3-dimethyl-2-imidazolidone)$_2]$ [9b], $[UO_2(NO_3)_2(^iC_3H_7)_2NCOCH_2CON\ (^iC_3H_7)_2]$ [11] and $[UO_2(NO_3)_2(C_{15}H_{27}N_3O)]$ [13].

The ^{1}H NMR spectra of **7–8** show the expected peaks and integrations. The pyrazolyl protons are deshielded by ca. 0.5 ppm with respect to the free ligand indicating that the bonding between ligand and uranyl group persists in solution [6a]. The structure of **8** has been determined by single crystal X-ray diffraction methods and confirms the spectral and analysis results. The ES-MS spectrum of **8** (Fig. 4.10) in CH_2Cl_2 shows peaks at the m/z values of 660.2 (100%), 678.2 (24%), and 849(18%). The peaks at 660.2 and 678.2 could be assigned to the species $[UO_2(DBM)L]^+$ and $[UO_2(DBM)L(H_2O)]^+$, respectively, thus showing clearly that the ligand retains bonding with the metal ion in solution.

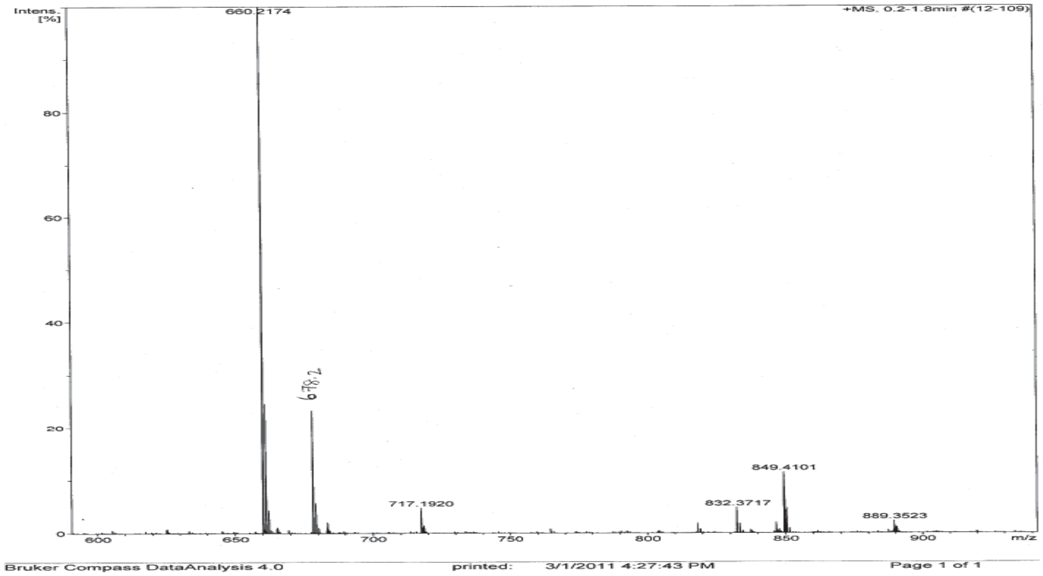

Fig. 4.10 ESI-MS spectrum of complex **8**

*4.3.2.6 Molecular structure of compound **8***

The structure of **8** is shown in Fig. 4.11 together with the numbering scheme, and selected bond distances and angles are given in Table 4.4. The structure shows that the uranyl group is bonded to two $C_6H_5COCHCOC_6H_5$ groups and a carbamoyl pyrazole ligand to give a coordination number of seven. The pyrazole ligand acts as a monodentate ligand and is bonded through the carbamoyl oxygen atom to the uranyl group. Four oxygens from two bidentate $C_6H_5COCHCOC_6H_5$ groups and one oxygen from the carbamoyl pyrazole ligand form the equatorial plane, and together with two oxygen atoms of the uranyl group form a pentagonal bipyramidal geometry around the uranium(VI) ion. The five oxygen atoms in the equatorial plane show an rms deviation of 0.062 Å. Similar structures are also observed in the compounds of phosphine oxides, sulfoxides, ketones, N-oxides, and amides with the uranyl bis(β-diketoantes), viz, $[UO_2(DBM)_2(OPPh_3)]$ [21a], $[UO_2(DBM)_2(C_6H_5SOCH_3)]$ [21b], $[UO_2(TTA)_2(C_5H_5NO)]$ [21c], $[UO_2(DBM)_2(camphor]$ [21d], $[UO_2(DBM)_2(iC_3H_7CON\{iC_3H_7\}_2)]$ [6], and $[UO_2(DBM)_2(C_4H_9CON\{C_4H_9\}_2)]$ [21e]. The observed U−O amide bond distance (2.437(5)Å) is much longer in length compared to any of the amide−uranyl bond distances reported, and the U−O−C angle is very close to linear (177.8(5)°). These dimensions are unusual in metal amide chemistry [22] with $U-O_{(amide)}$ distance being longer and the U−O−C angle being larger than usual. The inverse relation between the M−O bond distance and M−O−C bond angle is reported in the literature [9b] and could be explained on the basis of π donation of electron from the filled p orbitals of oxygen to the vacant f/d orbitals of metal center thereby shortening of M−O bond distance with the opening in M−O−C bond angle [10, 23a,b]. However, the observed dimensions in **8** could be explained purely on the basis of steric effects caused by the interaction between the pyrazole group and the bulky phenyl groups of the diketonate units, which may lead to the formation of a longer M−O bond with larger M−O−C bond angle.

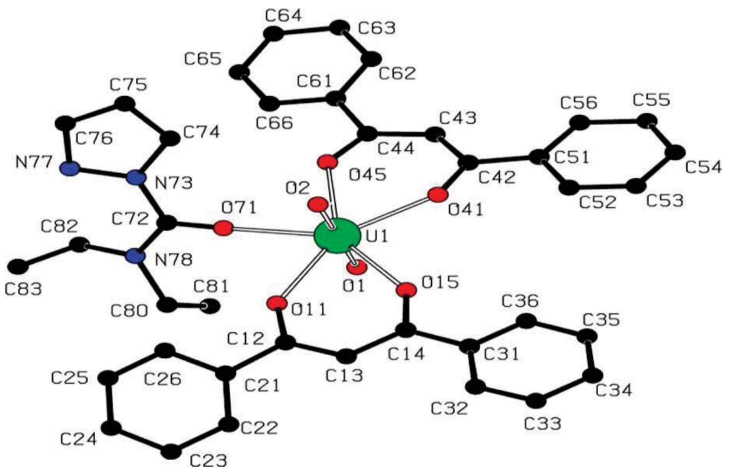

Fig. 4.11 The molecular structure of compound **8**

Table 4.4 Important bond distances (Å) and angles (°) for the compound **8**

U1−O1	1.772(4)	U1−O2	1.774(4)
U1−O11	2.350(5)	U1−O15	2.318(5)
U1−O41	2.326(5)	U1−O45	2.358(5)
U1−O71	2.437(5)	C72−O71	1.221(8)
O1−U1−O2	179.6(2)	O15−U1−O41	77.07(16)
O15−U1−O11	69.88(16)	O41−U1−O45	70.72(16)
O45−U1−O71	71.93(16)	C72−O71−U1	177.8(5)

4.3.2.7 Comparison of ligand (L^1-L^6) donor strength in the uranyl complexes by comparing the uranyl stretching frequency in the vibrational spectroscopy

Here, we have recorded the infra-red spectra of the uranyl nitrate and β-diketonate complexes with six newly synthesized ligands ($\mathbf{L^1}$-$\mathbf{L^6}$) and systematically tabulated in table 4.5.

Table 4.5 Comparison of IR frequencies of uranyl complexes

Complex	C=O$_{str}$ frequency of free ligands (cm^{-1})	C=O$_{str}$ frequency of the bonded ligands (cm^{-1})	Δν$_{CO}$ (cm^{-1})	U=O$_{asy}$ frequency of the axial bond (cm^{-1})
$[UO_2(NO_3)_2\{C_3H_3N_2CON(CH_3)_2\}]$ *(1)*	1693	1653	40	935
$[UO_2(NO_3)_2\{C_3H_3N_2CON(C_2H_5)_2\}]$ *(2)*	1687	1654	33	941
$[UO_2(NO_3)_2\{C_3H_3N_2CON(^iC_3H_7)_2\}]$ *(3)*	1687	1643	44	939

$[UO_2(NO_3)_2(H_2O)_2\{C_5H_7N_2CON(CH_3)_2\}_2]$ (4)	1697	1690	7	935
$[UO_2(NO_3)_2(H_2O)_2\{C_5H_7N_2CON(C_2H_5)_2\}_2]$ (5)	1691	1691	0	941
$[UO_2(NO_3)_2(H_2O)_2\{C_5H_7N_2CON(^iC_3H_7)_2\}_2]$ (6)	1693	1687	6	941
$[UO_2(C_6H_5COCHCOC_6H_5)_2\{C_3H_3N_2CON(CH_3)_2\}]$ (7)	1693	1656	37	904
$[UO_2(C_6H_5COCHCOC_6H_5)_2\{C_3H_3N_2CON(C_2H_5)_2\}]$ (8)	1687	1650	37	902

From the table it can be observed that, in the $[UO_2(NO_3)_2.6H_2O]$ complexes of carbamoyl pyrazole ligands (L^1-L^3), the order of U=O_{asy} frequency is (2) > (3) > (1), which signifies that donor strength order of the ligands is L^1 > L^3 > L^2 in these complexes. The increase of donor strength of ligand L^1 with respect to the ligand L^2 and L^3 can be explained on the basis of increase in steric bulkiness (more alkyl group) of L^2 and L^3 with respect to L^1, since the electronic property is almost same for all the ligands. Between L^2 and L^3, the ethyl group is a poor donor as compare to isopropyl group, which leads to a slight difference in the frequency.

4.3.2.8 Theoretical study

Full geometry optimization of carbamoyl pyrazole and carbamoyl methyl pyrazole ligands has been carried out applying a correlated nonlocal hybrid density functional, namely, B3LYP. SARC-ZORA basis sets for U and Gaussian type atomic basis functions 6-31+G(d) for H, C, N, and O atoms are applied for all the calculations. Table 4.6 displays the calculated atomic charge density over N1 and O1 atoms of the corresponding ligands and O atoms of H_2O molecule. It is clearly observed that charge density increases over N1 and O1 atoms (Fig. 4.12) on putting $-CH_3$ groups as expected. This indicates the formation of coordinated complexes to be facilitated in case of methylated ligands. Geometry of the complexes A−D (Fig. 4.12) has been optimized, adopting the same level of theory, and selected geometrical parameters are listed in the same Table 4.6. It is observed that, in case of complex B, the distance between U and N1 is longer than that in other cases by ~0.15 Å. The calculated distance suggests that due to steric factor N1 atom fails to approach U ion close in comparison to other complexes making the binding of this ligand weak to make the complex. This is reflected in the calculated binding energy (BE) of the complexes as displayed in Table 4.6. Binding energy has been calculated from the theoretical BE curve as shown in Fig. 4.13. This curve has been generated by calculating the total energy of the complex, keeping the ligand at different distances from the central ion of the complex until it goes to dissociation limit. The calculated binding energy has been refined, considering PCM macroscopic solvent model, and the results do show a similar trend as reflected in the table. To form a stable complex, a suitable geometry and proper orbital orientation of the central ion and chelating sites of the ligand is essential. In the present case, the chelating atoms of the ligand and the central ion should be in a plane to have a good orbital overlap to result in a stable complex. Calculated angle between N1−O1−U and O1−U−O(NO_2) planes are also listed in Table 4.6. It suggests that, in case of complex B, chelating site of the ligand N1 is out of plane from the remaining atoms by ~14°. This configuration may not allow good overlap between N1 and U ion orbitals. As a result, this complex is expected to be weaker compared to the other complexes. In fact, X-ray crystallography data suggests that two H_2O molecules stay in the first solvation layer and this ligand stays in the second solvation layer. This should make the complex more stable due to additional four H-bonding between four H atoms of two H_2O molecules and the ligands as shown in Fig. 4.9. Binding energy curve of the complex E with two H_2O molecules in place of the ligand (complex B) is depicted in Fig. 4.14, which suggests complex E to be more stable than complex B by 1.9 kcal/mol.

Table 4.6 Selected Geometrical and Other Parameters of the Complex Calculated Applying B3LYP/6-31+G(d) Level of Theory[a]

	Mulliken atomic charge density in the corresponding ligands (au)		selected bond distances (Å) in the complex				
complex	N1	O1	U−N1	U−N2	U−O1	δ(N1−O1−U−O(NO_2)) (degree)	binding energy (kcal/mol)[b]
A	−0.13	−0.24	2.91	3.75	2.77	1.7	27.8 (17.0)
B	−0.20	−0.28	3.06	3.80	2.75	14.1	24.7 (14.6)
C	−0.19	−0.30	2.92	3.84	2.69	7.6	28.8 (18.0)
D	−0.20	−0.29	2.93	3.81	2.73	9.4	28.5 (17.6)
E					2.75	0.6	27.6 (16.9)

[a]For U atom, SARC-ZORA basis function has been considered.

[b]Binding energy has been calculated in gas phase as well as in water medium applying a macroscopic solvent model, namely, PCM. Binding energy has been calculated by moving away the ligand from U ion to a distance of 2.5 times of the equilibrium distance of U−N2 as shown in Figure 4.12 or U−O1 (in case of complex E). The values in parentheses show the calculated binding energy including solvent effect (water).

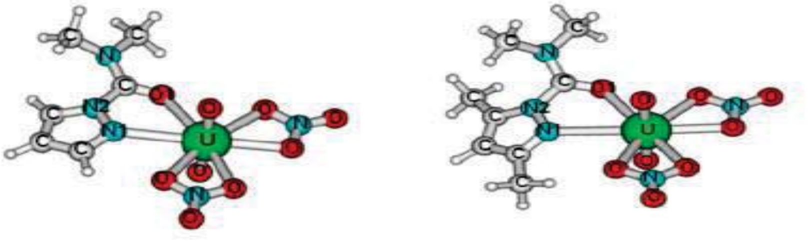

Complex **A** Complex **B**

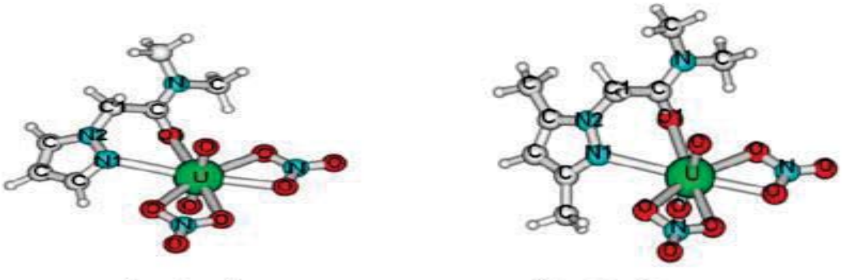

Complex **C** Complex **D**

Fig. 4.12 Fully optimized minimum energy structure for the $[UO_2(NO_3)_2]$ complex with the N,N-dimethyl analog of the ligands (A−D).

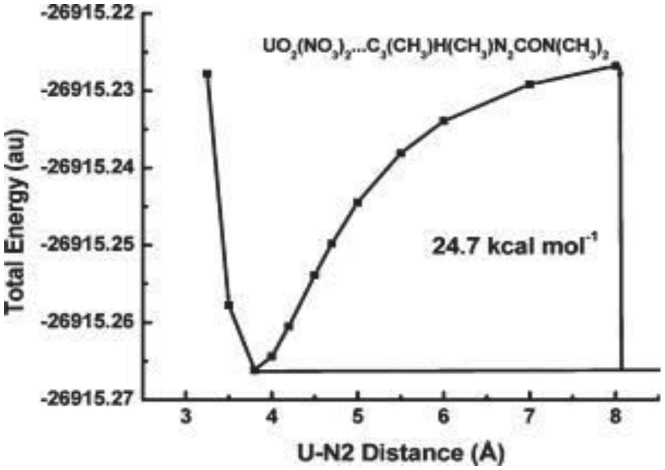

Fig. 4.13 Binding energy curve for the complex B

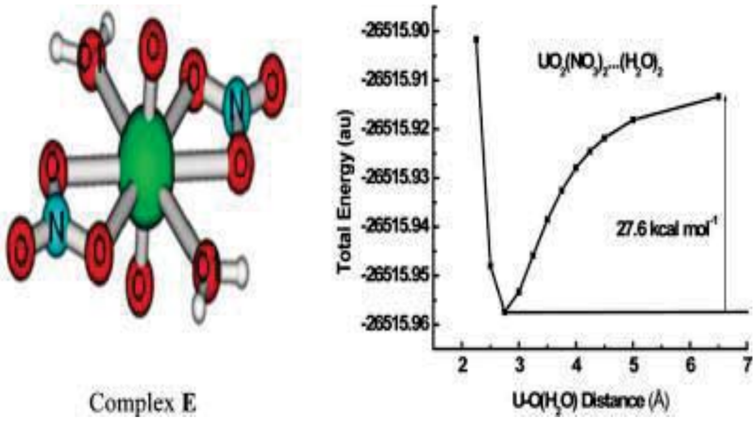

Complex **E**

Fig. 4.14 Minimum energy structure and binding energy curve for $[UO_2(NO_3)_2\cdot 2H_2O]$

4.3.3 Synthesis and structural studies of palladium complexes

4.3.3.1 Synthesis and complexation studies of carbamoyl pyrazole and carbamoyl 3,5-dimethyl pyrazole ligands with palladium chloride

The reaction of ligands $C_3H_3N_2CON\{CH_3\}_2$ (**L^1**), $C_3H_3N_2CON\{C_2H_5\}_2$ (**L^2**), $C_3H_3N_2CON\{^iC_3H_7\}_2$ (**L^3**), $C_5H_7N_2CON\{CH_3\}_2$ (**L^4**), $C_5H_7N_2CON\{C_2H_5\}_2$ (**L^5**), and $C_5H_7N_2CON\{^iC_3H_7\}$ (**L^6**) with $PdCl_2(CH_3CN)_2$ yielded the compounds $[PdCl_2L_2]$ (where L = **L^1**, **9**; **L^2**, **10**; **L^3**, **11**; **L^4**, **12**; **L^5**, **13**; **L^6**, **14**). The C, H and N analyses revealed that the ratio of ligand to metal ratio is 2:1 in all these compounds **9-14**. The IR spectra of **9-14** (Fig. 4.15 for **10**) show that the absorption frequency for the carbamoyl groups in all compounds is ca.

3–27 cm^{-1} more than that of the corresponding free ligands. It clearly shows that the carbamoyl group is un-coordinated in all the compounds and that the ligand bonds through the pyrazole nitrogen atom to the metal centre. The IR data further show that the ν_{CO} frequency difference (between free and coordinated) is more for the pyrazole based ligands (22–27 cm^{-1}) than the dimethyl pyrazole based ligands (3–14 cm^{-1}), which indicates that the pyrazole ligands are more strongly bonded to the metal centre than the dimethyl pyrazole ligands.

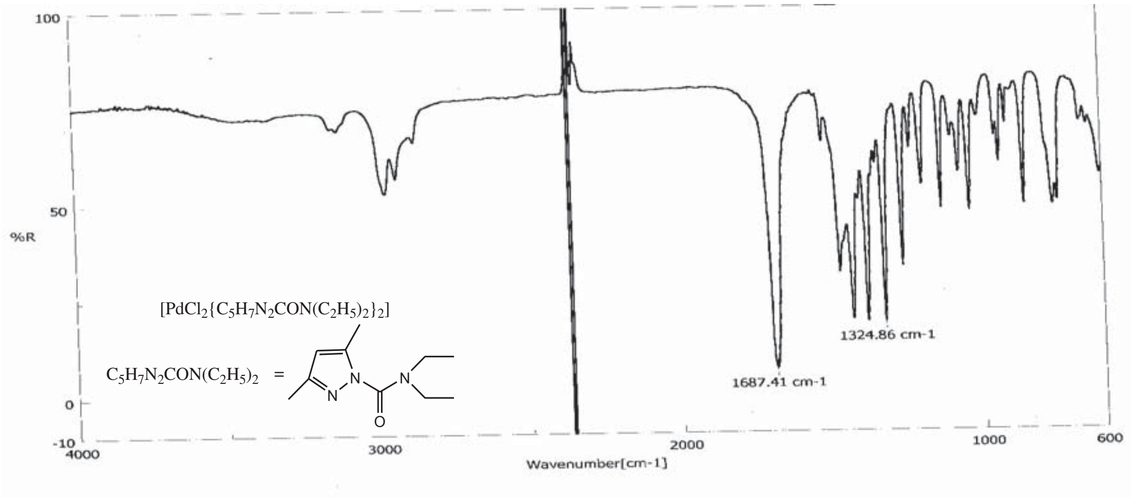

Fig. 4.15 IR spectrum of complex **10**

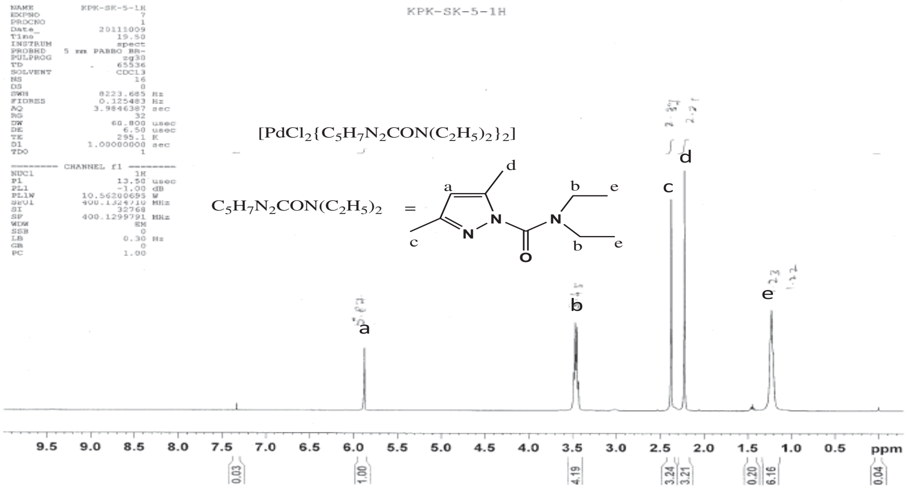

Fig. 4.16 ^{1}H NMR spectrum of complex **13**

Fig 4.16 showed the ^{1}H NMR spectrum of complex **13**. The spectrum is exactly similar to that of complex **5** (already discussed in details earlier) since both these complexes are derived from the same ligand L^5. The spectrum shows that the pyrazole protons are deshielded with respect to the free ligands proving further evidence for the coordination of the ligand to the metal ion. The CH_2 and CH_3 groups attached to the nitrogen atom show a broad line indicating that the complexes exhibit a syn-anti type isomerization in solution. This type of isomerisation was also observed in previously reported palladium(II) chloride pyrazole compounds such as [trans-$PdCl_2(C_5H_7N_2CH_2OCH_2CH_2OCH_3)_2$] [24], [trans-$PdCl_2(C_3H_3NCH_2CON\{^iC_4H_9\}_2)_2$] [6b], [trans-$PdCl_2(C_5H_7N_2CH_2OH)_2$] [25], [trans-$PdCl_2(C_3H_3N_2CH_2CH_2OH)_2$] [26] and [trans-$PdCl_2(C_{10}H_9N_2CH_2OH)_2$] [27]. The structures for compounds **10** and **13** have been determined by single crystal X-ray diffraction methods and confirm our interpretation of the spectral data.

*4.3.3.2 Molecular structure of compound **10***

The molecular structure of **10** which contains a crystallographic centre of symmetry is shown in Fig. 4.17, together with the atom numbering scheme. The important bond lengths and angles are given in Table 4.6. The structure shows that the palladium(II) ion is bonded to two trans-$C_3H_3N_2CON\{C_2H_5\}_2$ and two trans-chloride ligands to give a square planar coordination geometry. This agrees well with the earlier reported palladium(II) chloride pyrazole compounds. Both the ligands act as monodentate ligands and are bonded through the pyrazole nitrogen atom to the palladium(II) chloride. The observed Pd–Cl (2.2905(4) Å) and Pd–N (2.0114(5) Å) distances agree well with previously reported values [28,24,6b,25–27]. The position of the $NCONC_2H_5$ groups show that the molecule exists in the anti-conformation, similar to those reported for [trans-$PdCl_2(C_5H_7N_2CH_2OCH_2CH_2OCH_3)_2$] [24], [trans-$PdCl_2(C_5H_7N_2CH_2OH)_2$] [25], [trans-$PdCl_2(C_3H_3N_2CH_2CH_2OH)_2$] [26] [trans-$PdCl_2(C_{10}H_9N_2CH_2OH)_2$] [27] and [trans-$PdCl_2(C_3H_3NCH_2CON\{^iC_4H_9\}_2)_2$] [6b]. The structure of **10** shows further that the carbonyl group of the ligands are trans to the Pd–N bond giving rise to a trans-anti–anti conformation equivalent to that reported in [trans-$PdCl_2(C_3H_3NCH_2CON\{^{i}C_4H_9\}_2)_2$] [6b]. The structure also shows that the carbamoyl group is oriented (N11–N15–C16–O17, torsion angle ca. 49.2°) in such a way that the carbonyl oxygen atoms point away from the palladium(II) centre, and the shortest contacts to palladium centre are formed by the N18 atom with the Pd···N distance of 3.45(1) Å. These interaction can be viewed to complete a highly distorted octahedral coordination geometry around the palladium (II) centre.

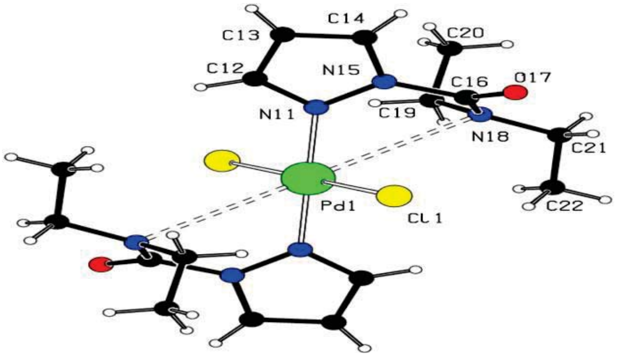

Fig. 4.17 The molecular structure of compound **10**

Table 4.6 Important bond distances (Å) and angles (°) for the compound **10**

Pd1–N11	2.0114(15)	Pd1–Cl1	2.2905(4)
N11–N15	1.362(2)	C16–O17	1.212(2)
C12–N11	1.328(2)	C14–N15	1.355(2)
Pd1–N18	3.449(1)	O17–C16–N15	117.19(15)
O17–C16–N18	127.78(18)	N11–Pd1–Cl1	89.49(4)

*4.3.3.3 Molecular structure of compound **13***

The molecular structure of **13** which also contains a crystallographic centre of symmetry is shown in Fig. 4.18, together with atom numbering scheme. The important bond lengths and angles are given in Table 4.7. The structure shows that the palladium(II) ion is bonded to two trans-$C_5H_7N_2CON\{C_2H_5\}_2$ and two trans-chloride ligands to give a square planar coordination geometry similar to **10**. These ligands are monodentate and bonded through the pyrazole nitrogen atom to the palladium(II) chloride. The observed Pd–Cl (2.3115(4) Å) and Pd–N (2.0217(13) Å) distances agree well with those of previously reported values [6b, 24, 25-27, 28]. The observed Pd–N distance (2.0217(13) Å) in **13** is slightly longer that in **10** (2.0114(5) Å), and supports our conclusion from the IR spectra that the pyrazole ligands form stronger bonds with palladium(II) than dimethyl pyrazole ligands. The position of the $NCONC_2H_5$ groups show that the molecule exists in the anti-conformation, similar to that reported for [trans-$PdCl_2(C_5H_7N_2CH_2OCH_2CH_2OCH_3)_2$] [24], [trans-$PdCl_2(C_3H_3NCH_2CON\{^iC_4H_9\}_2)_2$] [6b], [trans-$PdCl_2(C_5H_7N_2CH_2OH)_2$] [25], [trans-$PdCl_2(C_3H_3N_2CH_2CH_2OH)_2$] [26], and [trans-$PdCl_2(C_{10}H_9N_2CH_2OH)_2$] [27]. This structure also shows that the carbonyl group of the ligand is cis to the Pd–N bond, thus giving rise to a trans-anti–syn conformation. The structure also shows that the carbamoyl group is oriented (N11–N15–C16–O16, torsion angle ca. 132.8^o) in such a way that the carbonyl oxygen atoms point towards the palladium(II) centre, with a Pd┈O distance of 3.226(1) Å. These interaction can be viewed to complete a highly distorted octahedral coordination geometry around the palladium(II) centre. This type of weak Pd┈O interaction with distorted octahedral geometry around palladium(II) ion is by no means unknown and has been reported previously in compounds in which the bond lengths are as follows: 2.651 Å in [{(2,4,6-trimethoxyphenyl)$_3$P}$_2$Pd(BF_4)$_2$] [29], 3.09 Å in [trans-$PdCl_2(C_5H_7N_2CH_2OCH_2CH_2OCH_3)_2$] [24], 2.95 Å in [trans-$PdCl_2(Me_2NNC_{10}H_{14}O)_2$] [30], 2.92–3.03 Å in [trans-$PdBr_2(Me_2NNC_{10}H_{14}O)_2$] [31], 3.476 Å in [trans-$PdCl_2(\{\eta^5\text{-}C_5H_5\}\text{-}Fe\{\eta^5\text{-}C_5H_4\}CHN(C_6H_4OH))_2$] [32] and 3.232–3.548 Å in [trans-$PdCl_2$(Me-AcGIcN)$_2$] (where Me-AcGIcN = methyl, 3,4,6-tri O-acetyl, 2-amino, 2-deoxy, β-D glucopyranoside) [33], 2.708 Å in [$PdCl_2$(8-(2-pyridyl methyl) quinoline] [34] and 2.630–2.673 Å in [$PdCl_2$ hexakis(8-quinolyoxymethyl)benzene] [35]. The structural studies clearly reveal that the methyl group at position **13** of the pyrazole group plays an important role in determining the conformation around the palladium(II) chloride.

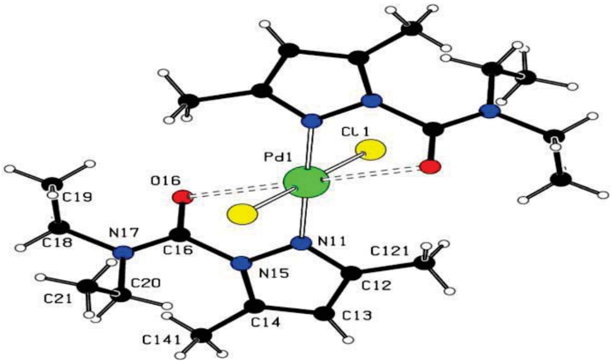

Fig. 4.18 The molecular structure of compound **13**

Table 4.7 Important bond distances (Å) and angles (^{o}) for the compound **13**

Pd1–N11	2.0217(13)	Pd1–Cl1	2.3115(4)
N11–N15	1.3747(16)	C16–O17	1.2182(19)
Pd1–O16	3.226(1)	O16–C16–N15	118.88(14)
O16–C16–N17	125.65(15)	N11–Pd1–Cl1	90.15(4)

4.3.3.4 Theoretical studies

Geometry of the two ligands (**L^{2}** and **L^{5}**) and the corresponding Pd(II) chloride complexes (**10** and **13**) has been fully optimized to obtain the most stable structures applying the ωB97XD density functional which includes an empirical dispersion correction. Geometry optimization has been carried out with different possible conformations as the initial structure for the ligands. Both ligands have an anti conformation with respect to carbonyl O and ring N (N11) in their most stable structure under isolated condition as shown in Fig. 4.19. For the two complexes, X-ray structures have been used as the input structures for optimization. Geometrical parameters of both the complexes in the most stable structures have been observed to be very close (bond length ±0.1 Å and bond angle ±1^{o}) to the X-ray crystallography data. Calculated Mulliken atomic charges for both the ligands are listed in Table 4.8. Based on these values, ligand **L^{5}** is expected to be a better donor than ligand **L^{2}** as the negative charge over the N11 atom is predicted to be greater in **L^{5}** (-0.28 a.u.) than that in

L^2 (0.13 a.u.). The most stable structures of the Pd(II) chloride complexes with these two ligands are also displayed in Fig. 4.19. Complex **10** does show the ligand **L^2** to retain its conformation. However in complex **13**, the two ligands **L^5** undergo rotation along the N15–C16 bond and as a result carbamoyl O and ring N (N11) makes a syn conformation in the most stable structure. This produces a distorted octahedral Pd(II) chloride complex with this simple ligand, **L^5**. Due to the presence of –CH_3 groups in ligand **L^5**, two ligands may feel steric hindrance to approach Pd(II)Cl_2 moiety in its original anti conformation. To reduce steric repulsion, the ligands undergo rotation along N15–C16 bond to form the complex in the syn conformation. This is supported by the calculated dihedral angle δ(Cl1–Pd1–N11–N15) which is 73.0^o in complex **13** compared to 50.2^o in complex **10**. Note that the respective dihedral angles in the X-ray crystal structures are 60.8^o and 45.2^o. It can be concluded that the larger dihedral angle in **13** reduces the steric repulsion between the CH_3 group of one ligand and the C_2H_5 group of the other. Calculated Mulliken atomic charges over selected atoms of these complexes are supplied in Table 4.8. In the case of **10**, the central Pd atom is highly negative (-1.61 a.u.) in contrast to complex **13** where the central Pd atom is hardly negative (-0.10 a.u.). This suggests that the pyrazole based ligand **L^2** is the better donor and thus forms a stronger Pd–N bond than the dimethyl pyrazole based ligand **L^5**. This prediction is supported by IR results where the shift in carbonyl frequency is larger for the pyrazol based ligand than for the dimethyl pyrazole based ligands as discussed in the above section. The binding energy of these ligands with Pd(II)Cl_2 to form respective complexes has been calculated via dissociation energy curves as shown in Fig. 4.20a. Potential energy curves have been calculated by keeping the two ligands symmetrically away from the central Pd atom at a fixed distance till the potential energy curve reaches the dissociation limit. From these curves, the binding energy (BE) per ligand of **13** is predicted to be larger by 5.5 kcal/mol than that of **10**. It will be noted that these BE values apparently contradict our previous conclusion that the pyrazole based ligand **L^2** forms a stronger Pd–N bond than the dimethyl pyrazole based ligand **L^5**. However, in case of **13** the stability due interaction between carbamoyl O with Pd is very small as they are far off (3.226 Å). In fact, visualization of specific frontier molecular orbital (FMO) in **13** suggests an interaction between the p_z orbital of O and the d_{xz} orbital of Pd atom as depicted in Fig. 4.20b, particularly as the spatial orientation of the two orbitals which have the same symmetry (shown by color) is favorable for the interaction. This additional interaction in complex 5 may be the reason for the extra stability of complex 5 over 2. The geometry of the complex formed between the Pd(II)Cl2 unit and ligand L^2 keeping the N11 and O atoms in the syn conformation by rotating along the N15–C16 bond as shown in Fig. 4.20b, has also been optimized at the same level of theory. The complex thus formed has been observed to be less stable than **10** by 6.0 kcal/mol. The calculated dihedral angle δ(Cl–Pd–N1–N2) is larger by 1.2^{o} than that in complex **10**. To examine the other structural possibility for **13**, geometry of the complex formed between Pd(II)Cl$_2$ unit and ligand **L^5** keeping N11 and O atoms the in anti conformation has also been optimized. This complex has been predicted to be less stable than complex **13** by 2.2 kcal/mol. The calculated dihedral angle δ(Cl–Pd–N1–N2) in the new complex is smaller by 11.3^{o} than that in complex **13**.

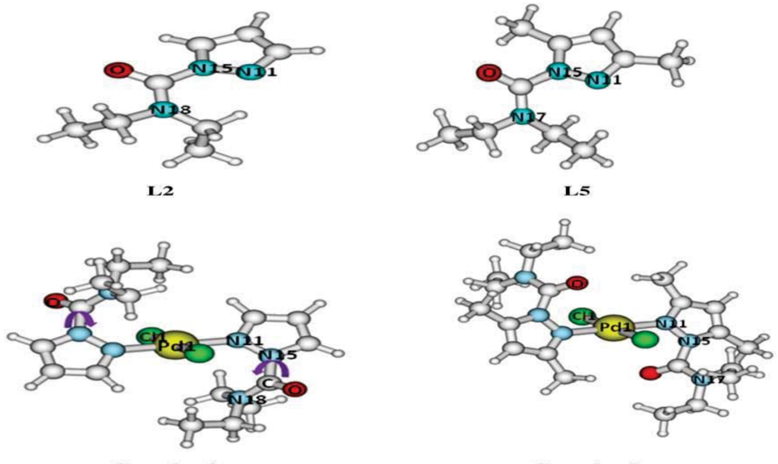

Fig. 4.19 Minimum energy structures of two ligands (**L^2** and **L^5**) and their complexes (**10** and **13**) optimized with DFT.

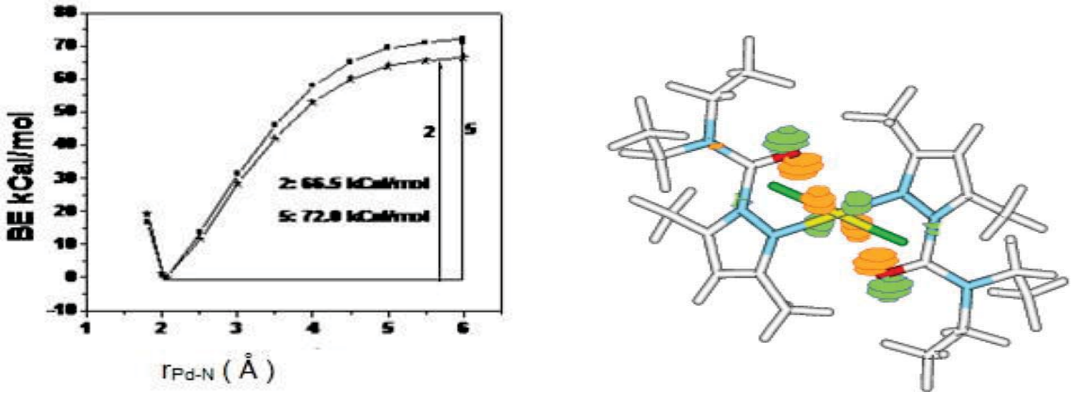

Fig. 4.20 (a) Dissociation energy curves of Pd(II)Cl_2 complexes **10** and **13** calculated applying the ωB97XD DFT functional. (b) A frontier molecular orbital (FMO) of complex **13** showing the interaction between of O and Pd atoms.

Table 4.8 Calculated Mulliken atomic charges (in a.u.) for selected atoms in **L**$^{\mathbf{2}}$, **L**$^{\mathbf{5}}$, **10** and **13** (Fig. 4.19 for atom numbering).

Atom	**L**$^{\mathbf{2}}$	**L**$^{\mathbf{5}}$	**10**	**13**
Pd	–	–	-1.61	-0.10
Cl	–	–	-0.23	-0.32
N11	-0.13	-0.28	+0.33	+0.30
N15	-0.10	-0.07	-0.04	+0.02
N18/N17	-0.24	-0.23	+0.01	+0.15
O	-0.51	-0.48	-0.36	-0.28

4.4 Conclusions

The coordination chemistry of the bifunctional ligand, carbamoyl pyrazole with uranyl nitrate, shows that it acts as a bidentate chelating ligand bonding through both the carbamoyl oxygen and pyrazolyl nitrogen atoms. However, the analogous carbamoyl 3,5-dimethyl pyrazole ligand forms a second sphere complex with the uranyl nitrate. The complex chemistry of carbamoyl pyrazole ligands could be explained on the basis of steric effect, and this effect controls the complexation reaction.

Whereas both the carbamoyl pyrazole and carbamoyl 3,5-dimethyl pyrazole ligands act as monodentate ligands and bonded through the N atom with the palladium (II) chloride. The complex chemistry of substituted pyrazole with palladium(II) chloride shows that geometry around the palladium(II) chloride is sterically controlled to give a highly distorted octahedral geometry around palladium(II) ion. Theoretical studies revealed that the orientation of the carbonyl group attached to the nitrogen atom is also sterically controlled by the methyl group at position 5 of the pyrazolyl ring during complexation to give different conformations.

4.5 References

1. Anne E.V. Gorden, Michael A. DeVore, Branson A. Maynard, Inorg. Chem. 52 (2013) 3445−3458.
2. Gabriella Bombieri, Inorg. Chim. Acta 139 (1987) 21-32.
3. Simon Cotton; Lanthanide and Actinide Chemistry, John Wiley & Sons Ltd, 2006.
4. (a) R.D. Hancock, A.E. Martell, Chem. Rev. 89 (1989) 1875−1914. (b) A.E. Martell, R.D. Hancock, Metal complexes in aqueous solution; Plenum Press: New York, 1996.
5. S. Kannan, J.S. Gamare, K.V. Chetty, M.G.B. Drew, Polyhedron 26 (2007) 3810−3816.
6. (a) S. Kannan, K.V. Chetty, V. Venugopal, M.G.B. Drew, Dalton Trans. (2004) 3604−3610. (b) S. Kannan, M.G.B. Drew, Inorg. Chim. Acta (2007) 3647−3649. (c) S.B. Deb, J.S. Gamare, S. Kannan, M.G.B. Drew, Polyhedron 28 (2009) 2673−2678.
7. (a) A.P. Dimitrios, N. Frank, J. Chem. Theory Comput. 7 (2011) 677−684. (b) K.L. Schuchardt, B.T. Didier, T. Elsethagen, L. Sun, V. Gurumoorthi, J. Chase, J. Li, T.L. Windus, J. Chem. Inf. Model. 47 (2007) 1045−1052. (c) W. Schmidt, K.K. Baldridge, J.A. Boatz, S.T. Elbert, M.S. Gordon, J.H. Jensen, S. Koseki, N. Matsunaga, K.A. Nguyen, S.J. Su, T.L. Windus, M. Dupuis, J.A. Montgomery, J. Comput. Chem. 14 (1993) 1347−1363.
8. Y. Minenkov, A. Singstad, G. Occhipinti, V.R. Jensen, Dalton Trans. 41 (2012) 5526.
9. (a) T.R. Varga, A.C. Benyei, Z. Fazekas, H. Tomiyasu, Y. Ikeda, Inorg. Chim. Acta 342 (2003) 291−294. (b) N. Koshino, M. Harada, M. Nogami, Y. Morita, T. Kikuchi, Y. Ikeda, Inorg. Chim. Acta 358 (2005) 1857−1864.
10. S. Kannan, S.B. Deb, J.S. Gamare, M.G.B. Drew, Polyhedron 27 (2008) 2557−2562.
11. A.R. de Aquino, G. Bombieri, P.C. Isolani, G. Vicentini, Zukerman Schpector, J. Inorg. Chim. Acta 306 (2000) 101−106.
12. (a) S.M. Bowen, E.N. Duesler, R.T. Paine, Inorg. Chem. 21 (1982) 261−265. (b) J. Caudle, E.N. Duesler, R.T. Paine, Inorg. Chim. Acta 110 (1985) 91−100.
13. J.M. Gil, F.J.M. Gil, A. Perales, J. Fayos, M.M. Ripoll, Acta Crystallogr. C 39 (1983) 44−45.
14. P. Charpin, M. Lance, M. Nierlich, D. Vigner, Acta Crystallogr. C 43 (1987) 442−445.
15. P. Charpin, M. Lance, M. Nierlich, D. Vigner, Acta Crystallogr. C 42 (1986) 560−563.

16. (a) J.C. Berthet, M. Nierlich, M. Ephritikhine, Chem. Commun. (2003) 1660−1661. (b) J.C. Berthet, M. Nierlich, M. Ephritikhine, Dalton Trans. (2004) 2814−2821.
17. (a) N.W. Alcock, D.J. Flanders, D. Brown, Dalton Trans. (1985) 1001−1007. (b) N.W. Alcock, D.J. Flanders, M. Pennington, D. Brown, Acta Crystallogr. C 44 (1988) 247−250.
18. (a) R.D. Rogers, A.H. Bond, W.G. Hipple, A.N. Rollins, R.F. Henry, Inorg. Chem. 30 (1991) 2671−2679. (b) G. Bombieri, G. De Paoli, A. Cassol, A. Immirzi, Inorg. Chim. Acta 18 (1976) L23−L24. (c) P.G. Eller, R.A. Penneman, Inorg. Chem. 15 (1976) 2439−2442. (d) S. Kannan, S.S. Raj, H.K. Fun, Polyhedron 20 (2001) 2145−2150.
19. H.M. Colquhoun, J.F. Stoddart, D.J. Williams, Angew. Chem., Int. Ed. Engl. 25 (1986) 487−507.
20. (a) C. Villiers, P. Thuery, M. Ephritikhine, Polyhedron 23 (2004) 1613−1618. (b) A.M.J. Lees, A.W.G. Platt, Acta Crystallogr. C 65 (2009) m10−m13. (c) M. Pourayoubi, J.A. Golen, M.R. Chaijan, V. Divjakovic, M. Negari, A.L. Rheingold, Acta Crystallogr. C 67 (2011) m160−m164.
21. (a) S. Alagar, M. Subha Nandhini, R.V. Krishnakumar, S. Kannan, S. Natarajan, Acta Crystallogr. E 59 (2003) m524−m526. (b) S. Kannan, V. Venugopal, M.R.A. Pillai, P.A. Droege, C.L. Barnes, Polyhedron 15 (1996) 97−101. (c) S. Kannan, A. Usman, H.K. Fun, Polyhedron 21 (2002) 2403−2407. (d) S. Kannan, M.R.A. Pillai, V. Venugopal, P.A. Droege, C.L.Barnes, Inorg. Chim. Acta 254 (1997) 113−117. (e) S. Rajagopal, S. Kannan, V. Venugopal, R.V. Krishnakumar, M. Subha Nandhini, S.J. Natarajan, Chem. Res. (2003) 468−469.
22. O. Clement, B.M. Rapko, B.P. Hay, Coord. Chem. Rev. 170 (1998) 203−243.
23. (a) S. Kannan, C.L. Banes, P.B. Duval, Chem. Commun. (2005) 5997−5998. (b) S. Kannan, C.L. Barnes, P.B. Duval, Inorg. Chem. 44 (2005) 9137−9139.
24. A. Boixassa, J. Pons, X. Solans, M.F. Bardia, J. Ros, Inorg. Chim. Acta 346 (2003) 151.
25. A. Boixassa, J. Pons, A. Virgili, X. Solans, M.F. Bardia, J. Ros, Inorg. Chim. Acta 340 (2002) 49.
26. A. Boixassa, J. Pons, X. Solans, M.F. Bardia, J. Ros, Inorg. Chim. Acta 357 (2004) 733.
27. J.A. Perez, V. Montoya, J.A. Ayllon, M.F. Bardia, T. Calvet, J. Pons, Inorg. Chim. Acta 394 (2013) 21.
28. K. Li, J. Darkwa, I.A. Guzei, S.F. Mapolie, J. Organomet. Chem. 660 (2000) 108.
29. K.R. Dunbar, J.S. Sun, Chem. Commun. (1994) 2387.

30. M.F.N.N. Carvalho, M.T. Duarte, R. Herrmann, Collect. Czech. Chem. Commun. 71 (2003) 302.
31. M.F.N.N. Carvalho, A.M. Galvao, A.S.D. Ferreira, J. Organomet. Chem. 694 (2009) 2061.
32. S. Perez, C. Lopez, A. Caubet, X. Solans, M.F. Bardia, M. Gich, E. Molins, J. Organomet. Chem. 692 (2007) 2402.
33. S.A. Johannesen, B.O. Petersen, J.O. Duus, T. Skrydstrup, Inorg. Chem. 46 (2007) 4326.
34. M.R.A. Al-Mandhary, P.J. Steel, Inorg. Chim. Acta 351 (2003) 7.
35. M.R.A. Al-Mandhary, C.M. Fitchett, P.J. Steel, Aust. J. Chem. 59 (2006) 307.

CHAPTER 5

Synthesis, structural and theoretical Studies of picolinamide complexes with palladium(II) and uranyl (VI) ions

5.1 Introduction

The separation of the metal ions from high level liquid waste after spent fuel reprocessing is very challenging [1-2] and an important step in the back end of fuel cycle in nuclear industry to reduce the long term radiotoxicity of the waste and further utilization of the precious elements. N-substituted amides are proposed to be very promising extractants for the solvent extraction removal of actinides from nitric acid medium [3-5]. In this respect, N-heterocyclic amide ligands are found to be a potential candidate to form stable complex with actinides and show structural variety in the solid state [6]. This type of ligands has an additional advantage compared to the simple N-substituted amide ligands. These ligands contain both hard oxygen and soft nitrogen donors in combination, which can help to extract both hard actinides as well as soft fission product elements during solvent extraction from the high level liquid waste solution [7].

N-heterocyclic amides such as picolinamide or pyrazole 2-carboxamide show a great tenability in bonding while forming complexes with different type of metal ions. In few cases, it acts as a chelating bidentate ligand with either pyridine-N and amido-O or pyridine-N and amido-N as donors to the metal center [8-12], while in other cases, it acts as a monodentate ligand with either pyridine N or amido O atom as donor centers [13-14]. The type of metal ions and electronic as well as steric factor of the ligands are the reason behind the bonding diversity in the coordination complexes. These findings clearly indicate that by tuning the alkyl group of the amides, it is possible to extract/separate metal ions of interest from any mixture of metal ions which is directly relevant to nuclear-waste management processes.

Although many structures of picolinic acid with metal complexes including palladium are known [15-19], the corresponding picolinamide complexes with palladium are reported here for the first time. In fact, to the best of our knowledge, only one X-ray structure of Pd(II) with picolinamide is reported to date [20], where the coordination is with methyl palladium and not simple Pd(II) ion. Since this ligands have hard donor group (carbamoyl) in addition to soft nitrogen group, it is expected to form complexes with actinides/lanthanides during separation process. So, the understanding of complexes chemistry of this ligands with actinides is also important.

We report the synthesis, characterization and structural studies of Pd(II) and uranyl (VI) complexes derived from picolinamide based ligands. The Pd/ U complexes synthesized and characterized herein are aimed to find the bonding mode for these ligands with palladium(II)/uranyl(VI) ions. This study will be useful for designing new ligands for the separation of palladium from high level liquid waste in solution. Particularly, we are very much interested in understanding the crucial role played by increasing the bulkiness of the ligand upon complexation with Pd(II) ion.

5.2 Experimental

5.2.1 Synthesis of pyridine 2-carboxamide ligands

5.2.1.1 Synthesis of $C_5H_4NCON({}^iC_3H_7)_2$ *(* $\boldsymbol{L^1}$ *)*

A solution of 2-Pyridine carbonyl chloride (2.12 g, 15 mmol) in CH_2Cl_2 (30 mL) was slowly added to a solution of di-isopropyl amine (1.52 g, 15 mmol) and triethyl amine (4.2 mL, 30 mmol) in CH_2Cl_2 (15 mL) at 0°C. After the addition, the mixture was slowly brought to room temperature and stirred for about 24 h. The solution was treated with 50 ml of 10% HCl and the organic layer was separated. The separated organic solution was dried over Na_2SO_4, filtered and the solvent was evaporated *in vacuo* to give the final product (69% yield). Anal. Calcd. for $C_{12}H_{18}N_2O$: C, 69.90; H, 8.73; N, 13.59. Found: C, 69.22; H, 8.99; N, 13.26. IR (ATR, ν/cm^{-1}): 1624(s) (C=O). ^{1}H NMR (300 MHz, $CDCl_3$) 8.62 (s, 1H), 7.88 (s, 1H), 7.48 (d, *J*= 9.3Hz, 1H), 7.30 (d, J= 5.1Hz, 1H), 3.78 (q, *J*= 6.3Hz, 1H), 3.56 (d, J= 6.3Hz, 1H), 1.55 (t, J= 6.3Hz, 6H), 1.19 (s, 6H).

5.2.1.2 Synthesis of $C_5H_4NCON(^iC_4H_9)_2$ (L^2)

This was prepared similar to that of $\mathbf{L^1}$ by taking di-isobutyl amine instead of di-isopropyl amine. Yield: 72%. Anal. Calcd. for $C_{14}H_{22}N_2O$: C, 71.79; H, 9.40; N, 11.97. Found: C, 71.42; H, 9.68; N, 12.11. IR spectrum (ATR, *ν*/cm^{-1}): 1628(s) (C=O). ^{1}H NMR (300 MHz, $CDCl_3$) 8.60 (s, 1H), 7.82 (t, J= 7.2Hz, 1H), 7.57 (d, *J*= 7.5Hz, 1H), 7.36 (d, J= 4.5Hz, 1H), 3.37 (d, *J*= 7.5Hz, 2H), 3.28 (d, J= 7.5Hz, 2H), 2.15 (p, J= 6.6Hz, 1H), 1.77 (p, J= 6.3Hz, 1H), 1.00 (d, J= 6.6Hz, 6H), 0.73 (s, 6H).

5.2.1.3 Synthesis of $C_5H_4NCONH(^tC_4H_9)$ (L^3)

This was prepared similar to that of $\mathbf{L^1}$ by taking tert-butylamine. Yield: 65%. Anal. Calcd. for $C_{10}H_{14}N_2O$: C, 67.42; H, 7.87; N, 15.73. Found: C, 67.07; H, 7.99; N, 15.41. IR (ATR, *ν*/cm^{-1}): 1675(s) (C=O), 3373(m) (-NH). ^{1}H NMR (300 MHz, $CDCl_3$) 8.51 (d, J= 3.9Hz, 1H), 8.17 (d, J= 7.8Hz, 1H), 8.04 (s, 1H, NH), 7.84 (t, *J*= 7.5Hz, 1H), 7.40 (t, J= 6.0Hz, 1H), 1.48 (s, 9H).

5.2.2 Synthesis of uranyl complexes of pyridine 2-carboxamide ligands

5.2.2.1 Synthesis of $[UO_2(NO_3)_2\{C_5H_4NCON(^iC_3H_7)_2\}]$ (1)

To a solution of N,N-diisopropyl pyridine-2-carboxamide (300 mg, 1.46 mmol) ($\mathbf{L^1}$) in chloroform, solid $UO_2(NO_3)_2.6H_2O$ (365 mg, 0.71 mmol) was added with stirring. The solution was allowed to stir until all uranyl nitrate dissolved to give a clear solution. This solution was filtered and layered with isooctane. This solution on slow evaporation yielded a yellow crystalline solid. This was filtered, washed with hexane and air dried. Yield: 89%. Anal. Calc. for $C_{12}H_{18}N_4O_9U$: C, 24.0; H, 3.0; N, 9.33. Found: C, 24.21; H, 3.38; N, 9.52. IR (ν/cm^{-1}) : 1590 (C=O), 935 (U=O$_{assy}$). ^{1}HNMR (300 MHz, CD_3COCD_3) 8.56 (d, J= 4.8Hz, 1H), 7.95 (t, J= 6.9Hz, 1H), 7.53 (t, *J*= 8.4Hz, 2H), 1.54 (t, J= 8.1Hz, 6H), 1.22 (s, 6H).

*5.2.2.2 Synthesis of [$UO_2(NO_3)_2\{C_5H_4NCON(^iC_4H_9)_2\}$] (**2**)*

This was prepared similarly to **1** by taking $UO_2(NO_3)_2.6H_2O$ (300 mg, 0.60 mmol) and **L^2** (293 mg, 1.25 mmol). Yield 87%. Anal. Calc. For $C_{14}H_{22}N_4O_9U$: C, 26.75; H, 3.50; N, 8.92. Found: C, 26.29; H, 3.81; N, 8.79. IR (ν/cm^{-1}) 1590 (C=O), 934 ($U{=}O_{assy}$). : ^1H NMR (300 MHz, CD_3COCD_3) 8.59 (s, 1H), 7.91 (s, 1H), 7.57 (s, 1H), 7.45 (s, 1H), 3.38 (d, *J*= 6.9Hz, 2H), 3.31 (d, *J*= 6.3Hz, 2H), 1.79 (d, J= 5.1Hz, 1H), 1.26 (s, 1H), 0.95 (d, J= 5.7Hz, 6H), 0.69 (d, J= 5.7Hz, 6H).

*5.2.2.3 Synthesis of [$UO_2(NO_3)_2\{C_5H_4NCONH(^tC_4H_9)\}$] (**3**)*

This was prepared similarly to **1** by taking $UO_2(NO_3)_2.6H_2O$ (300 mg, 0.60 mmol) and **L^3** (240 mg, 1.3 mmol). Yield 86%. Anal. Calc. For $C_{10}H_{14}N_4O_9U$: C, 20.98; H, 2.45; N, 9.79. Found: C, 20.71; H, 2.88; N, 10.07. . IR (ν/cm^{-1}) : 1620 (C=O), 899 ($U{=}O_{assy}$). ^1H NMR (300 MHz, CD_3COCD_3) 8.67 (d, J= 18.3Hz, 1H), 8.13 (s, 2H), 7.72 (s, 1H), 1.56 (s, 9H).

5.2.3 Synthesis of palladium complexes of pyridine 2-carboxamide ligands

*5.2.3.1 Synthesis of [$PdCl_2\{C_5H_4NCON(^iC_3H_7)_2\}_2$] (**4**)*

To an acetonitrile solution of $PdCl_2$ (200 mg, 1.13 mmol), **L^1** (466 mg, 2.26 mmol) was added and refluxed for 2 h. This solution was evaporated to dryness completely, washed with hexane and dried. The resulting residue was extracted in CH_2Cl_2 and filtered to remove insoluble materials. The solution was layered with 5 ml of iso-octane and allowed to evaporate slowly. This process deposited brownish yellow colored product (yield. 91%). Anal. Calc. For $C_{24}H_{36}N_4O_2Cl_2Pd$: C, 48.86; H, 6.11; N, 9.50. Found: C, 48.71; H, 6.48; N, 10.67. IR (ν/cm^{-1}) 1621 (C=O). ^1H NMR (300 MHz, DMSO-d6): 8.54 (s, 1H), 7.88 (t, *J*= 8.1Hz, 1H), 7.61 (q, *J*= 6.9Hz, 2H), 3.60 (d, *J*= 6.0Hz, 2H), 1.43 (d, J= 3.3Hz, 6H), 1.11 (s, 6H).

5.2.3.2 Synthesis of $[PdCl_2\{C_5H_4NCON({}^iC_4H_9)_2\}_2]$ *(**5**)*

This was prepared similarly to **4** by taking $PdCl_2$ (200 mg, 1.1 mmol) and $\mathbf{L^2}$ (524 mg, 2.24 mmol) in 88% yield. Anal. Calc. For $C_{28}H_{44}N_4O_2Cl_2Pd$: C, 52.06; H, 6.82; N, 8.68. Found: C, 52.31; H, 6.99; N, 8.57. (ν/cm^{-1}) 1638 (C=O). ^1H NMR (300 MHz, $CDCl_3$) 9.07 (d, J= 5.4Hz, 1H), 7.78 (t, J= 7.2Hz, 1H), 7.39 (d, *J*= 7.5Hz, 1H), 7.32 (t, J= 6.6Hz, 1H), 3.54 (s, 2H), 3.24 (s, 2H), 2.34 (t, J= 6.3Hz, 1H), 1.97 (p, J= 6.9Hz, 1H), 1.21 (d, J= 6.3Hz, 6H), 0.84 (d, J= 6.3Hz, 6H).

5.2.3.3 Synthesis of $[PdCl_2\{C_5H_4NCONH({}^tC_4H_9)\}]$ *(**6**)*

This was prepared similarly to **4** by taking $PdCl_2$ (220 mg, 1.24 mmol) and $\mathbf{L^3}$ (445 mg, 2.5 mmol) in 90% yield. Anal. Calc. For $C_{10}H_{14}N_2OCl_2Pd$: C, 33.76; H, 3.94; N, 7.88. Found: C, 33.70; H, 4.08; N, 7.67.). IR (ν/cm^{-1}) 1619 (C=O). ^1H NMR (300 MHz, CD_3COCD_3) 8.94 (d, J= 5.4Hz, 1H), 8.53 (d, J= 8.1Hz, 1H), 8.38 (t, J= 7.5Hz, 1H), 7.94 (t, *J*= 6.3Hz, 1H), 1.51 (d, *J*= 10.5Hz, 9H).

5.2.4 X-ray crystallography

Selected crystallographic data for the compounds **1, 4** and **6** are summarized in Tables 5.1.

Table 5.1 Crystallographic data for compounds **1, 4** and **6**

	1	**4**	**6**
Empirical formula	$C_{12}H_{18}N_4O_9U$	$C_{28}H_{42}N_5O_2Cl_2Pd$	$C_{12}H_{17}N_3OCl_2Pd$
Formula weight	600.32	657.99	396.61
Crystal system	monoclinic	triclinic	monoclinic
Space group	P 1 21/n 1	P -1	P 1 21/a 1
a (Å)	10.9779(9)	7.5131(10)	19.631(5)
b (Å)	14.6010(4)	9.7076(12)	10.5763(8)
c(Å)	12.4580(9)	12.2336(17)	12.855(3)
β (°)	111.894(8)	76.728(12)	141.81(5)
Volume (Å^3)	1852.9(2)	836.2(2)	1650.3(13)
Z (formula unit)	4	1	4
Calculated density (g/cm^3)	2.152	1.334	1.596
μ (mm^{-1})	25.154	6.203	12.021
Reflections collected/unique	3442/2304	3003/2803	3075/2127
Data/restrains/ parameters	3442/0/240	3003/48/184	3075/0/176
Goodness of fit on F^2	0.983	1.128	1.096
Final R$_1$ indices [I > 2σ(I)]	0.0824	0.0790	0.1021
wR$_2$ indices (all data)	0.1141	0.0878	0.1239

$w=1/[\sigma^2(F_o^2) + (0.1516P)^2]$ for **1**, $w=1/[\sigma^2(F_o^2) + (0.1690P)^2 + 1.3617P]$ for **4**, $w=1/[\sigma^2(F_o^2) + (0.2000P)^2]$ for **6**, where $P = (F_o^2 + 2F_c^2)/3$.

5.3 Results and discussion

5.3.1. Synthesis and characterization of N-substituted pyridine 2-carboxamide ligands

Reaction of 2-pyridine carbonyl chloride with corresponding N-substituted amines in presence of triethylamine as base in benzene yielded the corresponding ligands (**L^1** to **L^3**). The IR spectra of all ligands (Fig. 5.1) show the presence of the carbamoyl group in the synthesized compounds.

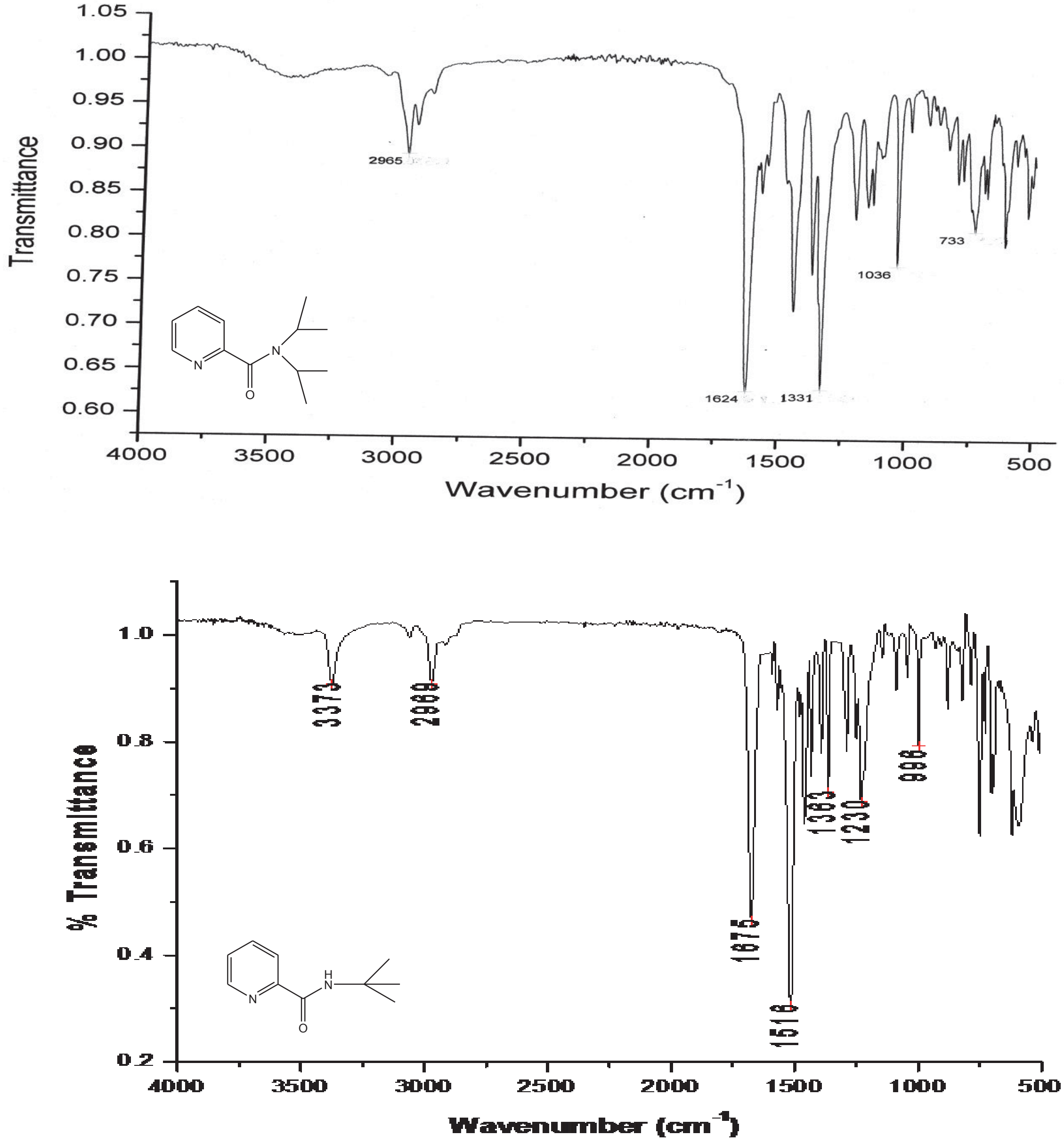

Fig. 5.1 IR spectra of ligand $\mathbf{L^1}$ (above) and $\mathbf{L^3}$ (below)

Fig 5.2 showed the ^{1}H NMR spectrum of ligand L^2. The singlet at 8.60 ppm, the triplet at 7.82 ppm, the doublet at 7.57 ppm and the doublet at 7.36 ppm are attributed to the ring protons of the pyridine ring at 6, 5, 3 and 4-position respectively. At 3.37 and 3.28 ppm, the doublets are assigned to four CH_2 protons (chemically non-equivalent at room temperature) of two isobutyl groups. Both the signals are split into a doublet, because the methylene group protons are coupled with one adjacent CH proton. Similarly, two multiplets at 2.15 and 1.77

ppm are attributed to two CH protons (chemically non-equivalent at room temperature) of two isobutyl groups. Finally, twelve CH_3 protons (chemically non-equivalent at room temperature) of two substituted isobutyl groups resonate as two doublets at 1.00 and 0.71 ppm. Both the signals are split into a doublet, because the methyl group protons are coupled with one adjacent CH proton. The C, H, N analysis supports the expected stoichiometry for the compounds.

Fig. 5.2 ^{1}H NMR spectrum of ligand $\mathbf{L^2}$

5.3.2 Synthesis and structural studies of uranyl complexes

5.3.2.1 Synthesis and complexation studies of pyridine 2-carboxamide ligands with uranyl nitrate

The reaction of ligands $\mathbf{L^1}$–$\mathbf{L^3}$ with $[UO_2(NO_3)_2{\cdot}6H_2O]$ yielded compounds **1–3**. C, H, and N analyses revealed that the ratio of ligand to uranyl nitrate is 1:1 in all compounds. The IR spectra of **1–3** (Fig. 5.3 for **2**) show that the water molecules from the starting compound $[UO_2(NO_3)_2{\cdot}6H_2O]$ are completely replaced by the ligand and that the ligand is bonded through the amide oxygen atom to the uranyl group. The observed frequency difference for a carbamoyl ($\Delta\nu_{CO}$ = 34−55 cm^{-1}, where $\Delta\nu_{CO} = \nu_{CO(free\ ligand)} - \nu_{CO(coordinated)}$) group is consistent with the supposition that the carbamoyl group is bonded to the uranyl group directly. This difference is comparable in magnitude with those observed in $[UO_2(NO_3)_2$(N-cyclohexyl-2-pyrrolidone)$_2]$ [21], $[UO_2(NO_3)_2$(1,3-dimethyl-2-imidazolidone)$_2]$ [22] $[UO_2(NO_3)_2\{{}^iC_3H_7CON({}^iC_4H_9)_2\}_2]$ [23], $[UO_2(NO_3)_2({}^iC_3H_7)_2NCOCH_2CON({}^iC_3H_7)_2]$ [24], and $[UO_2(NO_3)_2(C_{15}H_{27}N_3O)]$ [25].

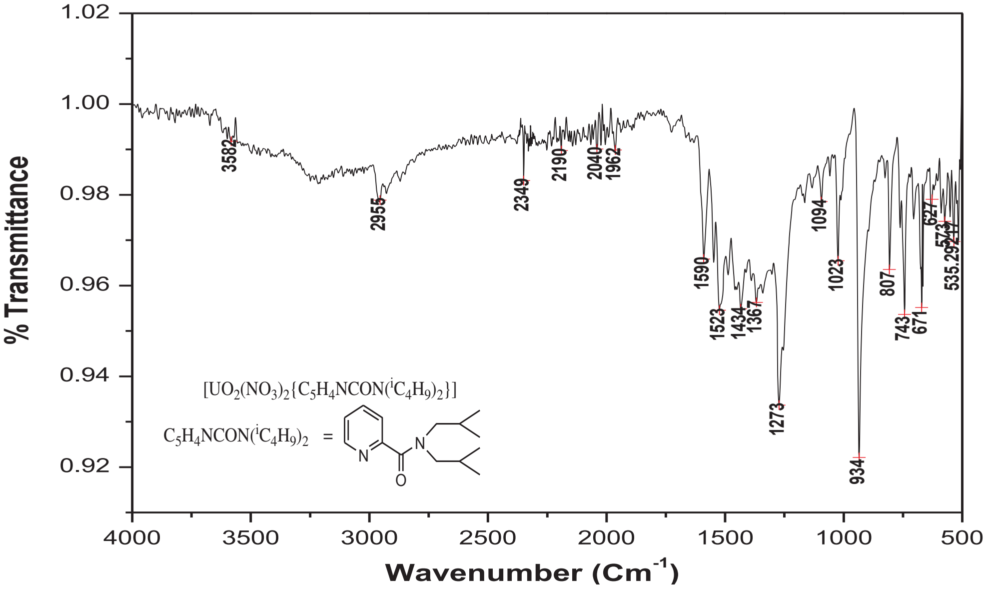

Fig. 5.3 IR spectrum of complex **2**

Fig 5.4 showed the ^{1}H NMR spectrum of complex **1**. The singlet at 8.65 ppm and the triplet at 7.95 ppm are assigned to the ring protons of the pyridine ring at 6 and 5 position respectively. The multiplet at 7.53 ppm is due to two ring protons of the pyridine ring at 3 and 4 position. Next, two doublets at 1.54 and 1.22 ppm are attributed to twelve CH_3 protons (chemically non-equivalent at room temperature) of two substituted isopropyl groups. Two additional peaks are appeared at 3.56 and 2.09 ppm due to the residual water impurity and CH_3COCH_3 molecule in the solvent acetone-d$_6$. The pyridyl protons are deshielded by ca. 0.2-0.3 ppm with respect to the free ligand indicating that the bonding between pyrazolyl nitrogen and uranyl group persists in solution. It is apparent from IR and NMR spectral results that the ligand acts as a bidentate chelating ligand and bonds through the carbamoyl and pyrazolyl nitrogen to uranyl group. The structure of **1** has been determined by single crystal X-ray diffraction methods and confirms the spectral and analysis results.

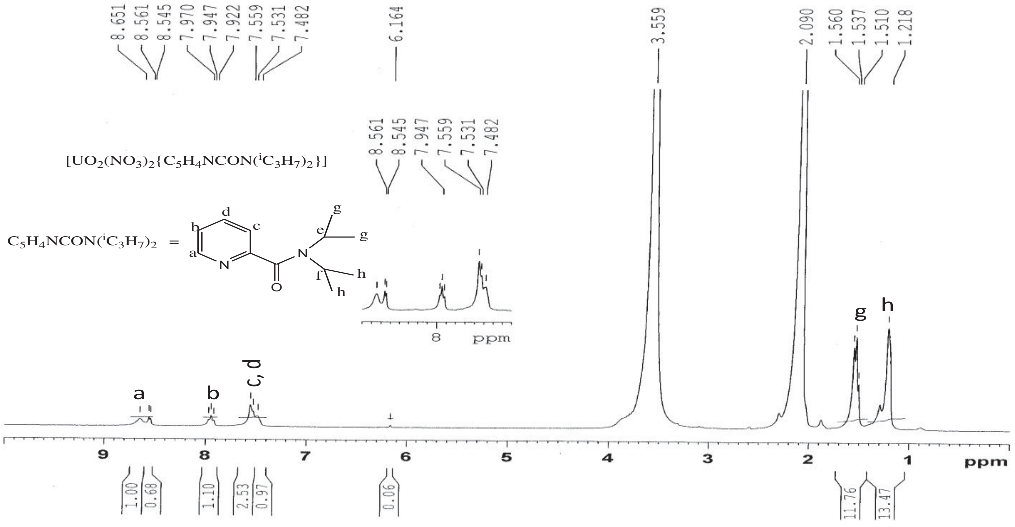

Fig. 5.4 ^{1}H NMR spectrum of complex **1**

*5.3.2.2 Molecular structure of compound **1***

The structure of 1 is shown in Fig. 5.5, and selected bond distances and angles are given in Table 5.2. The structure of **1** shows that the uranium atom is surrounded by one nitrogen and seven oxygen atoms in a slightly distorted hexagonal bipyramidal geometry. Four oxygen atoms of the two bidentate nitrate groups, together with one oxygen and one nitrogen atom of bidentate carboxamide ligand, form the equatorial hexagonal plane. The UO_5N atoms in the equatorial plane show a root mean square (rms) deviation of 0.082 Å. The two uranyl oxygen atoms occupy the axial positions. This type of coordination is similar to that observed in the compounds of the bifunctional ligands, malonamide, carbamoyl methyl phosphonate, carbamoyl methyl phosphine oxide, and carbamoyl methyl pyrazole with uranyl nitrate, such as $[UO_2(NO_3)_2\{(^iC_3H_7)_2NCO\}_2]$ [26], $[UO_2(NO_3)_2(^iC_3H_7O)_2POCH_2CONEt_2]$ [27a], $UO_2(NO_3)_2(C_6H_5)_2POCH_2CONEt_2]$ [27b] and $UO_2(NO_3)_2(C_{15}H_{27}N_3O)]$ [25]. The U−O$_{(amide)}$

distance (2.377(11) Å) in **1** is comparable in magnitude with those of earlier reported uranyl nitrate-amide compounds, such as [$UO_2(NO_3)_2$(N,N-dimethylformamide)$_2$] (2.397(6) Å) [28], [$UO_2(NO_3)_2$(tetrabutylglutaramide)$_2$] (2.378(6) Å) [29], [$UO_2(NO_3)_2$(dibutyldecanamide)$_2$] (2.37(2) Å) [30], and [$UO_2(NO_3)_2(C_{15}H_{27}N_3O)$] (2.364(7) Å) [25]. The U−N$_{(pyridyl)}$ distance (2.625(14) Å) is very close to the values observed in [$UO_2(NO_3)_2(C_{15}H_{27}N_3O)$] (2.554(9)Å) [25], [$UO_2(NO_3)_2$(phenanthroline)] (2.556(2)Å) [31], and [UO_2(terpyridine)](OTf)$_2$ ((2.567(6), 2.592(6) Å) [32]. The observed average U−O(NO_3) bond distance 2.493(14) Å is normal [21,22,25-30]. The angles subtended at the metal atom show that the uranium atom has slightly distorted hexagonal bipyramidal geometry.

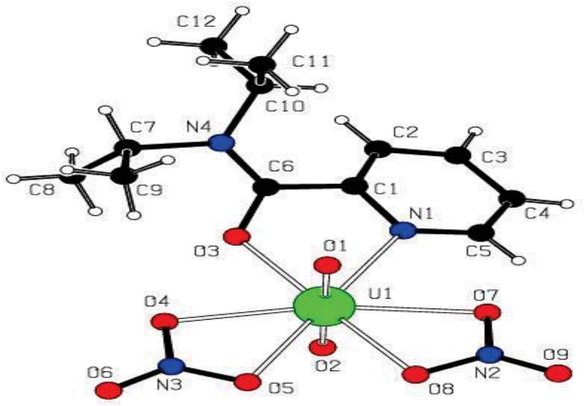

Fig. 5.5 The molecular structure of compound **1**

Table 5.2 Important bond distances (Å) and angles (°) for the compound **1**

U1-O1	1.727(17)	O3-U1-N1	62.6(5)
U1-O2	1.738(16)	O1-U1-O2	179.4(8)
U1-N1	2.615(15)	O8-U1-O7	50.8(5)
U1-O3	2.364(12)	O5-U1-O4	50.5(4)
U1-O5	2.499(15)	N1-U1-N3	154.7(5)
U1-O8	2.459(15)	N1-U1-N2	92.8(5)
U1-O4	2.501(14)	O5-U1-N1	176.5(5)
U1-O7	2.507(16)	O5-U1-N3	24.7(5)

5.3.2.3 Comparison of ligand (L^1-L^3) donor strength in the uranyl complexes by comparing the uranyl stretching frequency in the vibrational spectroscopy

Here, we have recorded the infra-red spectra of the uranyl nitrate complexes with three newly synthesized ligands (**L^1-L^3**) and systematically tabulated in table 5.3.

Table 5.3 Comparison of IR frequencies of uranyl complexes

Complex	$C=O_{str}$ frequency of free ligands (cm^{-1})	$C=O_{str}$ frequency of the bonded ligands (cm^{-1})	$\Delta\nu_{CO}$ (cm^{-1})	$U=O_{asy}$ frequency of the axial bond (cm^{-1})
$[UO_2(NO_3)_2\{C_5H_4NCON(^iC_3H_7)_2\}]$ (**1**)	1624	1590	34	935
$[UO_2(NO_3)_2\{C_5H_4NCON(^iC_4H_9)_2\}]$ (**2**)	1628	1590	38	934
$[UO_2(NO_3)_2\{C_5H_4NCONH(^tC_4H_9)\}]$ (**3**)	1675	1620	55	899

From the table it can be observed that, in the $[UO_2(NO_3)_2.6H_2O]$ complexes of pyridine 2-carboxamide ligands, the order of $U=O_{asy}$ frequency is (1) > (2) > (3), which signifies that donor strength order of the ligands is $L^3 > L^2 > L^1$ in these complexes. The increase of donor strength of ligand L^3 with respect to the ligand L^1 and L^2 can be explained on the basis of decrease in steric bulkiness (only one alkyl group is attached with amidic N-atom) of L^3 with respect to L^1 and L^2 (two alkyl group are attached with amidic N-atom), although the electronic property is different for the ligands. The L^1 is sterically more bulky as compare to L^2 as a result showing relatively poor donor ability of the former ligand.

5.3.3 Synthesis and structural studies of palladium complexes

5.3.3.1 Synthesis and complexation studies of pyridine 2-carboxamide ligands with palladium chloride

The reaction of the ligands $C_5H_4NCON\{^iC_3H_7\}_2$ (**L^1**) and $C_5H_4NCON\{^iC_4H_9\}_2$ (**L^2**) with $PdCl_2(CH_3CN)_2$ yielded the compounds $[PdCl_2L_2]$ (where L = **L^1**, **4**; **L^2**, **5**), whereas the similar reaction with $C_5H_4NCONH\{^tC_4H_9\}$ (**L^1**) yielded the compound [$PdCl_2L$] (where L = **L^3**, **6**). The IR spectra (Fig. 5.6 for **5**) of **4–5** show that the absorption frequencies of the C=O group in these compounds are almost unshifted with respect to the corresponding free ligands. It clearly shows that the C=O group is un-coordinated in these compounds and that the ligands are bonded through the pyridyl nitrogen atom to the metal centre. But the IR spectrum of compound **6** shows that the absorption frequency for the C=O groups in this compound is 56 cm^{-1} red shifted with respect to the corresponding free ligands, which clearly reveals that the amide group is directly coordinated to the Pd(II) centre in this compound. The IR data further show that the ν_{CO} frequency difference (between free and coordinated) is more for the pyrazole based ligands (22–27 cm^{-1}) than the dimethyl pyrazole based ligands (3–14 cm^{-1}), which indicates that the pyrazole ligands are more strongly bonded to the metal centre than the dimethyl pyrazole ligands. Fig 5.7 showed the ^1H NMR spectrum of complex **5**. The spectrum is exactly similar to that of ligand L^2 (already discussed in details earlier) since the complex is derived from the ligand L^2. However some of the proton peaks of the ligand in the spectrum of the complex are deshielded up to 0.5 ppm with respect to the free ligand proving further evidence for the coordination of the ligand to the metal ion. The structures for compounds **4** and **6** have been determined by single crystal X-ray diffraction methods and confirm our interpretation of the spectral data.

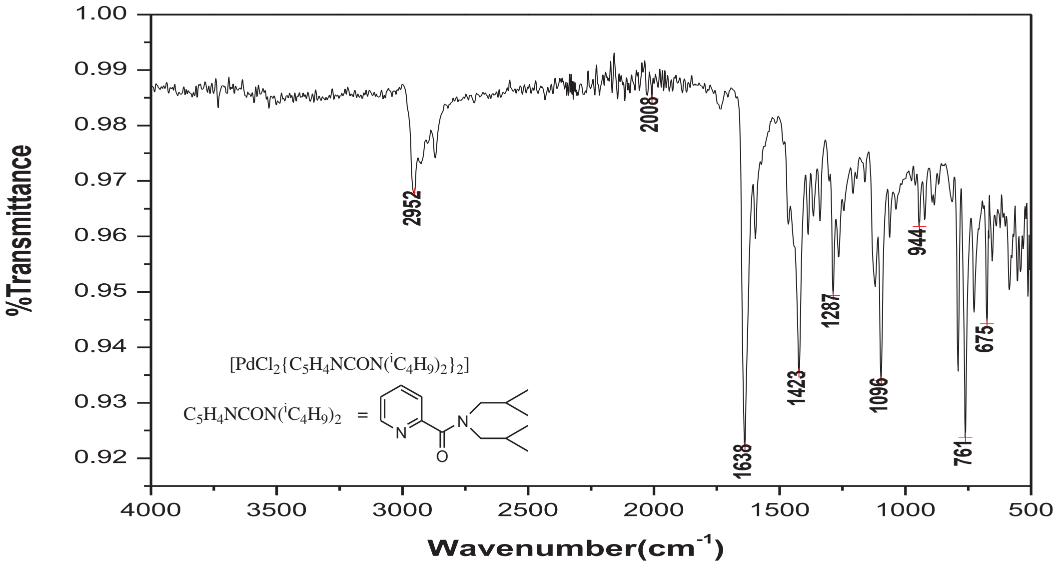

Fig. 5.6 IR spectrum of complex **5**

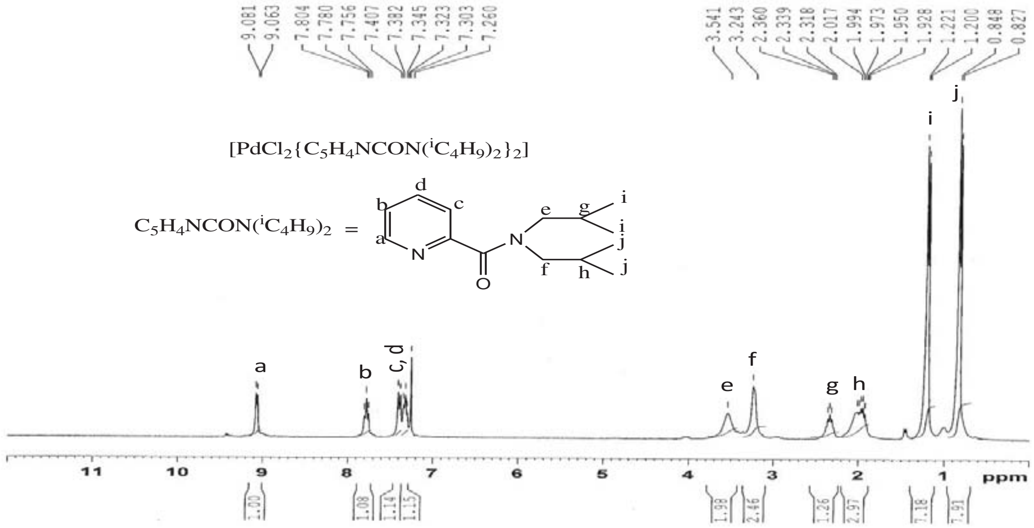

Fig. 5.7 ^{1}H NMR spectrum of complex **5**

*5.3.3.2 Molecular Structure of compound **4***

The molecular structure of **4** which contains a crystallographic centre of symmetry is shown in Fig. 5.8, together with the atom numbering scheme. The important bond lengths and angles are given in Table 5.4. The structure shows that the palladium(II) ion is bonded to two trans-C$_5$H$_4$NCON{^{i}C$_3$H$_7$}$_2$ ligands and two trans-chloride ligands to give a square planar coordination. The oxygen atom of the carbamoyl group shows week interaction (3.068 Å) with palladium centre, which can be viewed to complete a highly distorted octahedral coordination geometry around the palladium (II) centre. Similar type of coordination is observed in palladium(II) chloride compounds of carbamoyl methyl pyrazole [14] and carbamoyl pyrazole ligands [13]. Both the ligands act as monodentate ligands and are bonded through the pyridyl nitrogen atom to the palladium(II) chloride. The observed Pd–Cl (2.3043(19) Å) and Pd–N (2.005(6)Å) distances agree well with previously reported values [33-34].

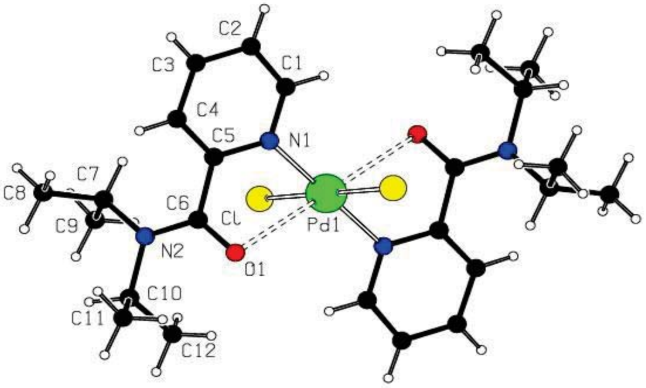

Fig. 5.8 The molecular structure of compound **4**

Table 5.4 Important bond distances (Å) and angles (°) for the compound **4**

Pd1-Cl	2.3043(19)	Cl-Pd1-Cl	180.0
Pd1-N1	2.005(6)	N1-Pd1-Cl	89.75(17)
N1-C1	1.327(11)	N1-Pd1-N1	180.0
N1-C5	1.356(10)	C1-N1-Pd1	118.8(6)
O1-C6	1.240(10)	C5-N1-Pd1	123.8(5)

*5.3.3.3 Molecular Structure of compound **6***

The molecular structure of **6** is shown in Fig. 5.9, together with the atom numbering scheme. The important bond lengths and angles are given in Table 5.5. The structure shows that the palladium(II) ion is bonded to one pyridine carboxamide $C_5H_4NCONH\{^tC_4H_9\}$ and two chloride ligands in cis fashion to give a square planar coordination geometry. The

$C_5H_4NCONH\{^tC_4H_9\}$ ligand acts as a bidentate chelating ligand and are bonds through both the pyridyl nitrogen and carbamoyl oxygen to the palladium(II) chloride. The observed Pd–Cl (2.279 (3) Å), Pd–N (2.015(9) Å) [35-36] and Pd-O (2.019(9) Å) [20] distances are normal agree well with previously reported values.

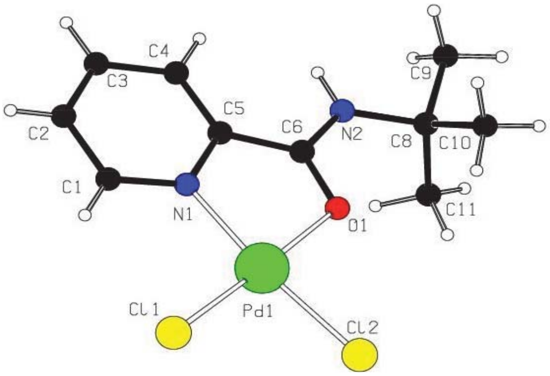

Fig. 5.9 The molecular structure of compound **6**

Table 5.5 Important bond distances (Å) and angles (^{o}) for the compound **6**

Pd1-Cl1	2.264(4)	Cl1-Pd1-Cl2	91.01(13)
Pd1-Cl2	2.279(3)	O1-Pd1-Cl2	91.1(2)
Pd1-O1	2.019(9)	O1-Pd1-Cl1	177.7(2)
Pd1-N1	2.015(9)	N1-Pd1-Cl2	172.1(3)
O1-C6	1.294(13)	N1-Pd1-Cl1	96.9(3)
		N1-Pd1-O1	81.0(3)

5.3.3.4 Computational studies

To gain valuable insights on the structure and coordination binding motifs of the picolinamide ligand to Pd, we have carried out electronic structure calculations at the density functional theory level. Our optimized structural parameters of species **4** and **6** are in good agreement with the experimental data (Fig. 5.10). Careful analysis reveals a large deviation in the structures between **4** and **6** depends on the binding modes of the ligand (i.e. monodentate vs chelation). In complex **4**, there are two $\mathbf{L^1}$ (*trans* to each other) each coordinating with Pd primarily through the nitrogens (Pd-N bonds are 2.04 Å) and the carbamoyl oxygens are weakly interacting with Pd (with a bond distance of 3.15 Å). Further, the computed Pd-N bond lengths in both **4** and **6** are within 0.04Å, which is in good agreement with the experimental estimates. The Pd-Cl bond lengths are also well reproduced within 0.05Å for both complexes against the experimental data. Further, in **4**, the C=O of the ligand is very weakly interacting with Pd (3.15Å) as compared to species **6**, whereas a direct strong coordination (Pd-O = 2.11Å) is noted. Although the Pd-O distance seems large to be considered as an interacting distance, a careful inspection of the optimized structure reveals that the oxygens are not rotated away and still facing the Pd centre, thus some weak electrostatic interaction is noted.

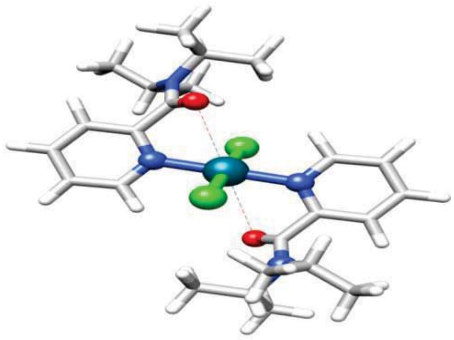

Fig. 5.10 Optimized structures (Å) of **4**.

The complexation energy for **4** (1:2) and **6** (1:1) are -63.4 kJ mol^{-1} and -77.3 kJ mol^{-1} respectively (Table 5.6) again suggesting both are facile processes with a preference for the **L^3** forming 1:1 complex over the **L^1** as 1:2. Further, we have also optimized structure of 1:1 complex with **L^3**. We find that this species is less favourable (by -59.8 kJ mol^{-1}) as compared to **6**. Due to the steric hindrance of the ligand **L^1**, a chelate binding motif is less preferable, thus this species is not experimentally observed. The C=O stretching frequency for **4** and **6** are 1643 cm^{-1} and 1594 cm^{-1} respectively which follows the experimental trends. It is very evident that there is a small blue shift in **4** and a red shift in **6** suggesting, in complex **4** the C=O oxygen is not bound to Pd and forms a distorted octahedral complex where as in **6** it is directly coordinated to Pd as a bidentate ligand forming a square planar complex.

Table 5.6 Complexation energies (in kJ mol^{-1}) of various reactions computed in this study.

Reaction	M:L	Complex	ΔG
$PdCl_2(CH_3CN)_2 + 2L^1 \rightarrow PdCl2(L^1)_2 + 2(CH_3CN)$	1:2	**4**	-63.4
$PdCl_2(CH_3CN)_2 + 1L^3 \rightarrow PdCl2(L^3)_1 + 2(CH_3CN)$	1:1	**6**	-77.3

5.4 Conclusions

A series of picolinamide based ligands of the type $C_5H_4NCONR_2$ (where, R= $^iC_3H_7$ (**L^1**), $^iC_4H_9$ (**L^2**) and $C_5H_4NCONHR$ (R= $^tC_4H_9$ (**L^3**)) have been synthesized and characterized. The coordination chemistry of these ligands with uranyl nitrate and palladium(II) chloride was studied using elemental analysis, FTIR, ^{1}H-NMR spectroscopy and single crystal X-ray diffraction methods. Crystal structures of uranyl complexes $[UO_2(NO_3)_2L^1]$ (**1**), $[UO_2(NO_3)_2L^3]$ (**3**) show that the ligands form 1:1 complex with uranyl nitrate in a bidentate chelation mode and bonds through both the pyridyl N and amido O atoms to the uranyl group. The structures of palladium complexes $[PdCl_2(L^1)_2]$ (**4**) and $[PdCl_2L^3]$ (**6**) indicate the structural diversity between the two complexes. In complex **4**, ligand **L^1** forms 2:1 complex with palladium(II) chloride, acts as a monodentate ligand and bonds only through pyridyl N atom to Pd(II) centre. However, in complex **6**, the ligand **L^3** forms 1:1 complex with palladium(II) chloride, acts as bidentate chelating ligand and bonds through both the pyridyl N and amido O atoms to the Pd(II) centre. Theoretical studies revealed that the steric effect is responsible for the observed structural diversity in the palladium complexes.

5.5 References

1. K.L. Nash, J.C. Braley, Challenges for Actinide Separations in Advanced Nuclear Fuel Cycles, ACS Symposium Series, 1046 (2010) 19 (Chapter 3).
2. Dominique Warin, IOP Conf. Series: Materials Science and Engineering 9 (2010) 012063.
3. Yuya Takahashi, Hiroyasu Hotokezaka, Kyoko Noda, Masanobu Nogami, Yasuhisa Ikeda, J. Nucl. Sci. Technol. 46 (2009) 787–792.

Table 5.6 Complexation energies (in kJ mol^{-1}) of various reactions computed in this study.

Reaction	M:L	Complex	ΔG
$PdCl_2(CH_3CN)_2 + 2L^1 \rightarrow PdCl2(L^1)_2 + 2(CH_3CN)$	1:2	**4**	-63.4
$PdCl_2(CH_3CN)_2 + 1L^3 \rightarrow PdCl2(L^3)_1 + 2(CH_3CN)$	1:1	**6**	-77.3

5.4 Conclusions

A series of picolinamide based ligands of the type $C_5H_4NCONR_2$ (where, R= $^iC_3H_7$ (**L^1**), $^iC_4H_9$ (**L^2**) and $C_5H_4NCONHR$ (R= $^tC_4H_9$ (**L^3**)) have been synthesized and characterized. The coordination chemistry of these ligands with uranyl nitrate and palladium(II) chloride was studied using elemental analysis, FTIR, ^{1}H-NMR spectroscopy and single crystal X-ray diffraction methods. Crystal structures of uranyl complexes $[UO_2(NO_3)_2L^1]$ (**1**), $[UO_2(NO_3)_2L^3]$ (**3**) show that the ligands form 1:1 complex with uranyl nitrate in a bidentate chelation mode and bonds through both the pyridyl N and amido O atoms to the uranyl group. The structures of palladium complexes $[PdCl_2(L^1)_2]$ (**4**) and $[PdCl_2L^3]$ (**6**) indicate the structural diversity between the two complexes. In complex **4**, ligand **L^1** forms 2:1 complex with palladium(II) chloride, acts as a monodentate ligand and bonds only through pyridyl N atom to Pd(II) centre. However, in complex **6**, the ligand **L^3** forms 1:1 complex with palladium(II) chloride, acts as bidentate chelating ligand and bonds through both the pyridyl N and amido O atoms to the Pd(II) centre. Theoretical studies revealed that the steric effect is responsible for the observed structural diversity in the palladium complexes.

5.5 References

1. K.L. Nash, J.C. Braley, Challenges for Actinide Separations in Advanced Nuclear Fuel Cycles, ACS Symposium Series, 1046 (2010) 19 (Chapter 3).
2. Dominique Warin, IOP Conf. Series: Materials Science and Engineering 9 (2010) 012063.
3. Yuya Takahashi, Hiroyasu Hotokezaka, Kyoko Noda, Masanobu Nogami, Yasuhisa Ikeda, J. Nucl. Sci. Technol. 46 (2009) 787–792.

4. Fa-tang Li, Biao Wu, Rui-hong Liu, Xiao-jing Wang, Lan-ju Chen, Di-shun Zhao, Chem. Eng. J. 274 (2015) 192–199.
5. P.N. Pathak, R. Veeraraghavan, D.R. Prabhu, G.R. Mahajan, V.K. Manchanda, Sep. Sci. Technol. 34 (1999) 2601.
6. Yingjie Zhang, Mohan Bhadbhade, Jiabin Gao, Inna Karatchevtseva, Jason R. Price, Gregory R. Lumpkin, Inorg. Chem. Commun. 37 (2013) 219–221.
7. Debasish Das, Bal Govind Vats, Shanmugaperumal Kannan, Dilip K. Maity, Michael G.B. Drew, Polyhedron 54 (2013) 104–109.
8. J. Qi, H. Ma, X. Li, Z. Zhou, M.C.K. Choi, A.S.C. Chan, Q. Yang, Chem. Commun. (2003) 1294.
9. H.R. Khavasi, A. Ghanbarpour, A.A. Tehrani, RSC Adv. 6 (2016) 2422.
10. L. Huang, B. Gu, W. Su, P. Yin, H. Li, RSC Adv. 5 (2015) 76296.
11. L. Kirsten, V.D. Schwade, L. Selter, A. Hagenbach, P.C. Piquini, E.S. Lang, U. Abram, Eur. J. Inorg. Chem. 21 (2015) 3748.
12. I. Lumb, M.S. Hundal, M. Corbella, V. Gómez, G. Hundal, Eur. J. Inorg. Chem. (2013) 4799.
13. D. Das, B.G. Vats, S. Kannan, D.K. Maity, M.G.B. Drew, Polyhedron 54 (2013) 104.
14. S. Kannan, M.G.B. Drew, Inorg. Chim. Acta 360 (2007) 3647.
15. M.K. Biswas, S.C. Patra, A.N. Maity, S. Ke, T. Weyhermuller, P. Ghosh, Chem. Commun. 49 (2013) 4522.
16. M. Roger, L.M.P. Lima, M. Frindel, C. Platas-Iglesias, J.F. Gestin, R. Delgado, V. Patinec, R. Tripier, Inorg. Chem. 52 (2013) 5246.
17. S. Yun, H. Seo, M. Song, S. Jin, S.K. Kang, Y. Kim, J. Organomet. Chem. 724 (2013) 244.
18. A.R. Rodríguez, Z. Garda, E. Ruscsák, D.E. Gómez, A. de Blas, T. Rodríguez-Blas, L.M.P. Lima, M. Beyler, R. Tripier, G. Tircsó, C. Platas-Iglesias, Dalton Trans. 44 (2015) 5017.
19. D.C. Zhao, Y.Y. Hu, H. Ding, H.Y. Guo, X.B. Cui, X. Zhang, Q.S. Huo, J.Q. Xu, Dalton Trans. 44 (2015) 8971.
20. M.J. Green, G.J.P. Britovsek, K.J. Cavell, F. Gerhards, B.F. Yates, K. Frankcombe, B.W. Skelton, A.H. White, J. Chem. Soc., Dalton Trans. (1998) 1137.
21. T.R. Varga, A.C. Benyei, Z. Fazekas, H. Tomiyasu, Y. Ikeda, Inorg. Chim. Acta 342 (2003) 291−294.

22. N. Koshino, M. Harada, M. Nogami, Y. Morita, T. Kikuchi, Y. Ikeda, Inorg. Chim. Acta 358 (2005) 1857−1864.
23. S. Kannan, S.B. Deb, J.S. Gamare, M.G.B. Drew, Polyhedron 27 (2008) 2557.
24. G.J. Lumetta, B.K. McNamara, B.M. Rapko, R.L. Sell, R.D. Rogers, G. Broker, J.E. Hutchison, Inorg. Chim. Acta 309 (2000) 103.
25. S. Kannan, J.S. Gamare, K.V. Chetty, M.G.B. Drew, Polyhedron 26 (2007) 3810−3816.
26. A.R. de Aquino, G. Bombieri, P.C. Isolani, G. Vicentini, Zukerman Schpector, J. Inorg. Chim. Acta 306 (2000) 101−106.
27. (a) S.M. Bowen, E.N. Duesler, R.T. Paine, Inorg. Chem. 21 (1982) 261−265. (b) J. Caudle, E.N. Duesler, R.T. Paine, Inorg. Chim. Acta 110 (1985) 91−100.
28. P. Charpin, M. Lance, M. Nierlich, D. Vigner, Acta Crystallogr. C 43 (1987) 442−445.
29. J. M. Gil, F.J.M. Gil, A. Perales, J. Fayos, M.M. Ripoll, Acta Crystallogr. C 39 (1983) 44−45.
30. P. Charpin, M. Lance, M. Nierlich, D. Vigner, Acta Crystallogr. C 42 (1986) 560−563.
31. (a) J.C. Berthet, M. Nierlich, M. Ephritikhine, Chem. Commun. (2003) 1660−1661. (b) J.C. Berthet, M. Nierlich, M. Ephritikhine, Dalton Trans. (2004) 2814−2821.
32. (a) N.W. Alcock, D.J. Flanders, D. Brown, Dalton Trans. (1985) 1001−1007. (b) N.W. Alcock, D.J. Flanders, M. Pennington, D. Brown, Acta Crystallogr. C 44 (1988) 247−250.
33. Maximilian N. Kopylovich, Jamal Lasri, M. Fatima C. Guedes da Silva´, Armando J. L. Pombeiro, Dalton Trans. (2009) 3074–3084.
34. Poulami Pattanayak, Jahar Lal Pratihar, Debprasad Patra, Paula Brandão, Vitor Felix, Surajit Chattopadhyay, Polyhedron 79 (2014) 43–51.
35. A.R. Balavardhana Rao, Samudranil Pal, J. Organomet. Chem. 731 (2013) 67-72.
36. Srinivasa Budagumpi, Yinshan Liu, Hongsuk Suh, Il Kim, J. Organomet. Chem. 696 (2011) 1887-1894.